



UNIVERSITAT  
POLITÈCNICA  
DE VALÈNCIA

# Analysis to support design for additive manufacturing with desktop 3D printing

(Análisis de las variables para el diseño y la fabricación de piezas con sistemas de  
impresión 3D de código abierto)

by

**Miguel Fernandez Vicente**

Doctoral thesis submitted for the award of  
PhD in Design, Manufacture and Management of Industrial Projects

Director:

**Andrés Conejero Rodilla**

July 2022

## **ACKNOWLEDGEMENTS**

I would like to thank my director Andres Conejero for the willingness to support me in this challenge and the encouragement to keep progressing. Your guidance has helped getting this in the right direction and find the support where needed.

Special thanks to prof. R. Ian Campbell for your key pills of DfAM knowledge that boosted my understanding of the topic and structuring this work. I could not have done it without your insights.

Thanks for the support, help, guidance, teamwork and feedback from:

Miquel C., Santi F., Wilson C., Juan S., Victor M., Rene H., Horacio M. P., Pedro A., Juan A.G., Manuel M., Miguel S., Ana E., Iñigo O., Andrew T., Lara B., Farhan K., Ollie H., Stuart W., Sandeep S., Llyr J., Utkarsha A., Alice W., Anthony J. and many others that helped shape this work and my understanding of DfAM.

Thank you to the external evaluators and tribunal for their time in this laborious process.

Thanks to my friends here and abroad for making life bearable when escaping from the computer.

Gracias a mi familia por el apoyo y aliento desde España.

Finally, thank you Estefania for always being there in this journey. Without your constant support and encouragement, this could not have happened.

## **ABSTRACT**

In recent years, Additive Manufacturing through material extrusion has experienced accelerated development and adoption thanks to the wide availability of low-cost machines and materials. The size of these machines has been reduced from shop floor to desktop size, enabling their usage in office setups or at home. This change has allowed the adoption of the technology by the broadest range of users than ever, with or without an engineering design background.

This new paradigm has created the challenge of how to enable these novel users to leverage the capabilities provided by this technology. This technology allows the creation of complex geometry and customised products with a cost lower than conventional manufacturing processes. Furthermore, the large number of users willing to share their designs allows finding design solutions from other designers. However, the wide range of machine configurations, parameters and materials requires providing support to obtain successful results under any combination.

This thesis addresses this challenge by identifying the design and manufacturing characteristics to be considered and investigating the mechanical and post-processing considerations. A new design framework that enables new users to leverage the capabilities and consider the limitations is proposed and evaluated.

This research finds that it is possible to create a design toolkit that enables untrained users to design products using the complexity enabled by the technology whilst ensuring the product's functionality and manufacturability.

## **RESUMEN**

En los últimos años, la fabricación aditiva a través de la extrusión de materiales ha experimentado un desarrollo y adopción acelerados gracias a la amplia disponibilidad de máquinas y materiales de bajo costo. El tamaño de estas máquinas se ha reducido del tamaño del taller al tamaño del escritorio, lo que permite su uso en configuraciones de oficina o en el hogar. Este cambio ha permitido la adopción de la tecnología por la gama más amplia de usuarios que nunca, con o sin experiencia en diseño de ingeniería.

Este nuevo paradigma ha creado el desafío de cómo habilitar que estos nuevos usuarios aprovechen las capacidades proporcionadas por esta tecnología. Esta tecnología permite la creación de geometrías complejas y productos personalizados con un coste inferior a los procesos de fabricación convencionales. Además, la gran cantidad de usuarios dispuestos a compartir sus diseños permite encontrar soluciones de diseño desde otros diseñadores. Sin embargo, la amplia gama de configuraciones de máquina, parámetros y materiales requiere brindar soporte para obtener resultados exitosos para cualquier combinación.

Esta tesis aborda este desafío identificando las características de diseño y fabricación a considerar e investigando las consideraciones mecánicas y de pos procesamiento. Se propone y evalúa un nuevo marco de diseño que permite a los nuevos usuarios aprovechar las capacidades y considerar las limitaciones.

Esta investigación encuentra que es posible crear un conjunto de herramientas de diseño que permita a los usuarios no capacitados diseñar productos utilizando la complejidad habilitada por la tecnología al tiempo que garantiza la funcionalidad y la capacidad de fabricación del producto.



## RESUM

En els últims anys, la fabricació additiva a través de l'extrusió de materials ha experimentat un desenvolupament i adopció accelerats gràcies a l'àmplia disponibilitat de màquines i materials de baix cost. La grandària d'aquestes màquines s'ha reduït de la grandària del taller a la grandària de l'escriptori, la qual cosa permet el seu ús en configuracions d'oficina o en a casa. Aquest canvi ha permès l'adopció de la tecnologia per la gamma més àmplia d'usuaris que mai, amb o sense experiència en disseny o enginyeria.

Aquest nou paradigma ha creat el desafiament de com habilitar que aquests nous usuaris aprofiten les capacitats proporcionades per aquesta tecnologia. Aquesta tecnologia permet la creació de geometries complexes i productes personalitzats amb un cost inferior als processos de fabricació convencionals. A més, la gran quantitat d'usuaris disposats a compartir els seus dissenys permet trobar solucions de disseny des d'altres dissenyadors. No obstant això, l'àmplia gamma de configuracions de màquina, paràmetres i materials requereix brindar suport per a obtindre resultats reeixits per a qualsevol combinació.

Aquesta tesi aborda aquest desafiament identificant les característiques de disseny i fabricació a considerar i investigant les consideracions mecàniques i de post processament. Es proposa i avalua un nou marc de disseny que permet als nous usuaris aprofitar les capacitats i considerar les limitacions.

Aquesta investigació troba que és possible crear un conjunt d'eines de disseny que permeti als usuaris no capacitats dissenyar productes utilitzant la complexitat habilitada per la tecnologia al mateix temps que garanteix la funcionalitat i la capacitat de fabricació del producte.

## LIST OF PUBLICATIONS

- Conejero, A., Ayala López, P., Martínez, M., **Fernández Vicente, M.** (2019). *Prototipado Industrial: Guía para diseñadores* (1st ed.). Parramón.
- Fernandez-Vicente, M.**, Escario Chust, A., & Conejero, A. (2017). Low cost digital fabrication approach for thumb orthoses. *Rapid Prototyping Journal*, 23(6), 1020–1031.
- Fernandez-Vicente, M.**, & Conejero, A. (2016). Suitability study of desktop 3d printing for concept design projects in engineering education. *10th International Technology, Education and Development Conference (INTED2016 Proceedings), Valencia, Spain, March 2016* (pp. 4485-4491) IATED.
- Corbaton, C. R., **Fernández-Vicente, M.**, & Conejero, A. (2016). Design and 3d printing of custom-fit products with free online software and low cost technologies. a study of viability for product design student projects. In: *10th International Technology, Education and Development Conference (INTED2016 Proceedings), Valencia, Spain, March 2016* (pp. 3906-3910). IATED.
- Fernandez-Vicente, M.**, Calle, W., Ferrandiz, S., & Conejero, A. (2016). Effect of infill parameters on tensile mechanical behavior in desktop 3D printing. *3D printing and additive manufacturing*, 3(3), 183-192.
- Fernandez-Vicente, M.**, Canyada, M., & Conejero, A. (2015). Identifying limitations for design for manufacturing with desktop FFF 3D printers. *International Journal of Rapid Manufacturing*, 5(1), 116-128.

# TABLE OF CONTENTS

Acknowledgements	II
Abstract	III
Resumen	IV
Resum	V
List of Publications	VI
Table of Contents	VII
List of figures	XI
List of tables	XXII
List of abbreviations and nomenclature	XXIII
<b>Chapter 1 Introduction</b>	<b>1</b>
1.1. Research Background	1
1.2. Scope of the work	3
1.1. Aims and Objectives	5
1.2. Research novelty	5
1.3. Thesis structure	7
<b>Chapter 2 3D Printing</b>	<b>11</b>
2.1. Introduction	11
2.2. History and purposes of use	11
2.3. Design possibilities	21
2.4. Overview of current technologies	27
2.5. Rise of desktop 3d printing	32
<b>Chapter 3 Fused Filament Fabrication</b>	<b>39</b>
3.1. Introduction	39
3.2. FFF 3D printers components	40
3.3. FFF Process	45
3.4. Summary	52
<b>Chapter 4 Design for Additive Manufacturing</b>	<b>53</b>
4.1. Introduction	53
4.2. Use of AM potentials	56
4.3. Design rules	59
4.4. Combined methods	64

4.5. Summary	66
<b>Chapter 5 Design Features determination</b>	<b>67</b>
5.1. Introduction	67
5.2. Prior work	68
5.3. Features identification	69
5.4. Overhangs, bridges and angles GBTAs study	73
5.5. Benchmarking geometries proposal	85
5.6. Results	91
5.7. Summary	93
<b>Chapter 6 Mechanical properties</b>	<b>95</b>
6.1. Introduction	95
6.2. Effect of infill parameters on tensile behaviour	98
6.2.1. Introduction	98
6.2.2. Literature review	99
6.2.3. Materials and methods	104
6.2.4. Results and discussion	108
6.2.5. Conclusions	115
6.3. Study: Determination of infill density and pattern influence in the bending behaviour	116
6.3.1. Materials and methods	119
6.3.2. Results and discussion	123
6.3.3. Conclusions	131
6.4. Mechanical properties studies. Conclusions	132
6.5. Summary	133
<b>Chapter 7 Post-processing of FFF parts</b>	<b>135</b>
7.1. Introduction	135
7.2. Support removal	137
7.3. Surface modification	140
7.3.1. Heat	143
7.3.2. Chemical solutions	145
7.3.3. Mechanical	150
7.3.4. Surface modification. Summary	162
7.4. Coating	162

7.5. Assembly	172
7.6. Summary	181
<b>Chapter 8 Perception of components due to surface quality</b>	<b>183</b>
8.1. Abstract	183
8.2. Introduction	184
8.3. Materials and methods	187
8.4. Results	190
8.5. Conclusions	192
<b>Chapter 9 Case study. Thumb orthosis</b>	<b>195</b>
9.1. Abstract	195
9.2. Introduction	196
9.2.1. Anatomical data acquisition	198
9.2.2. Additive Manufacturing of orthoses	199
9.2.3. Post-treatment of FFF parts	201
9.2.4. Open lattice structures in orthoses design	201
9.3. Aims and objectives	202
9.4. Method	202
9.4.1. 3D Scan data acquisition	203
9.4.2. CAD process	204
9.4.3. 3D Printing	207
9.4.4. Support removing	207
9.4.5. Surface treatment	208
9.4.6. Fastening	210
9.5. Cost analysis	210
9.6. Results and discussion	213
9.7. Conclusions and further research	215
<b>Chapter 10 Development of a DfAM toolkit</b>	<b>217</b>
10.1. Introduction	217
10.2. Toolkit structure	220
10.3. Identify requirements	221
10.4. Concept design. Ideation cards	222
10.5. Extract design solutions	226
10.6. Embodiment Design	230

10.6.1. Main design considerations	232
10.6.2. Design features	244
10.6.3. Assembly considerations.	253
10.7. Prototype	260
10.8. Deliver	262
10.9. Summary	262
<b>Chapter 11 Evaluation of the toolkit &amp; case studies</b>	<b>263</b>
11.1. Introduction	263
11.2. Methodology. Design of the trial	265
11.3. Results & discussion	267
11.3.1. Case study. Telescopic phone holder	270
11.3.2. Survey	274
11.4. Conclusions & future work	275
<b>Chapter 12 Discussion and Conclusions</b>	<b>277</b>
12.1. Introduction	277
12.2. Achievement of research objectives	278
12.3. Contribution to knowledge	280
12.4. Limitations of the research	282
12.5. Future work	283
<b>Bibliography</b>	<b>285</b>
<b>Appendix</b>	<b>315</b>

## LIST OF FIGURES

Figure 1.1. Network of FabLabs. Spaces with open access for novel users of digital manufacturing technologies, such as 3D printing. Source:fablabs.io	2
Figure 1.2. Generic AM Design considerations identified in ISO/ASTM 52910.	4
Figure 1.3. Post-processing workflow. From chapter 10.	6
Figure 1.4. 3D printed orthosis from chapter 9.	8
Figure 2.1. Illustration of the Photosculpture technique. Adapted from Willème (1864).	12
Figure 2.2. Two captures for the photosculpture process ca. 1865.	13
Figure 2.3. Two of the proposed configurations of the method described by Ciraud (1973)	14
Figure 2.4. Appearance model of a portable speaker. 3D printed with FFF. Workshop on Prototypes and Models subject. ETSID UPV.	17
Figure 2.5. Fit evaluation model for customised glasses.(Rodrigo Corbaton et al., 2016)	18
Figure 2.6. Areas where industrial AM is being used. Adapted from (Wohlers & Caffrey, 2015)	20
Figure 2.7. Percentage of direct-part AM production. Adapted from (Wohlers & Caffrey, 2015)	21
Figure 2.8. Part cost evolution with the increase of complexity. Comparison between conventional and additive manufacturing.	23
Figure 2.9. Seven AM technologies, the processes available and some machine manufacturers. Source: 3DHubs.com	32
Figure 2.10. Evolution of desktop 3D printers estimated sales. Adapted from (Wohlers, 2016b)	37
Figure 3.1, Extruder components in an FFF-based process. Source: Reprap.org	41
Figure 3.2. 3D Printer Extruder Filament Drive Gears: a) Plain Insert; b) Raptor Filament Drive Gear; c) MK8 Drive Gear; d) MK7 Drive Gear. Source: Airtripper.com	42
Figure 3.3. Thermal image capture to understand temperature behaviour in build adhesion.	43

Figure 3.4. The difference between Cartesian and Delta 3D printers, both types of FFF 3D printers. Source: 3D natives.com	44
Figure 3.5. Design and build workflow of FFF printing. A) Geometry to be manufactured, B) slicing in layers, C) Toolpath generation for each layer, and D) deposition.	45
Figure 3.6. Toolpath areas in a FFF part.	47
Figure 3.7. Polymer sintering in FFF: a) Contact, b)neck formation, c)diffusion.	48
Figure 3.8. Thermal image capture to understand temperature transfer with the environment.	49
Figure 3.9. Influencing factors in part quality & mechanical properties in FFF (Mohamed et al., 2015).	50
Figure 3.10. Fishbone diagram to illustrate the impacts of process parameters on part characteristics (Dey & Yodo, 2019).	51
Figure 4.1. Double Diamond design framework.	54
Figure 4.2. DWX and DFX in the innovation process. Adapted from Laverne et al. (2014)	55
Figure 4.3. Part consolidation workflow methods, adapted from Rodrigue and Rivette (2011) and Boyard et al. (2013)	57
Figure 4.4. Example of the Design Heuristics for AM cards (Blösch-Paidosh & Shea, 2017).	58
Figure 4.5. Standard elements and design rules. Adapted from Adam & Zimmer (2014)	61
Figure 4.6. Design for AM worksheet proposed by Booth et al. (2017)	62
Figure 4.7. Section of Design Rules for 3D Printing poster (Redwood et al., 2017)	63
Figure 4.8. Examples of AM Principle Cards (Lauff et al., 2019)	65
Figure 5.1. Illustration of someGBTAs from ISO/ASTM 52902. a) Linear dimensioning, b) resolution holes, c) resolution pins, d) resolution ribs, d) resolution slots.	69
Figure 5.2. AM Design considerations identified in ISO/ASTM 52910.	69
Figure 5.3. Distinct zones in angled walls (left) and an illustration of overhanging areas at the mesostructure level for various angles (right).	71



Figure 5.4. Characteristic geometries and variables studied for each a) Bridges b) Overhangs c) Angles	75
Figure 5.5. Top and side view of test specimens for the examination of different top-layer thickness possibilities; (a) 0.4 mm, (b) 0.8 mm, (c) 1.2 mm, and (d) 5 mm.	76
Figure 5.6. 0.5 to 2.2 Overhang test part.	77
Figure 5.7. Angles test part.	78
Figure 5.8. 5mm thickness bridges test part.	78
Figure 5.9. Overhangs chart results.	79
Figure 5.10. Detail of the 3x5mm overhang.	80
Figure 5.11. Overhangs detail pictures and simulation. a) 1.2 mm thickness. b) 5mm thickness. c) 5mm simulation.	81
Figure 5.12. Finish comparison between 55° angle specimens. $d_{\text{angle}}$ length: 30 mm on the left, 35 on the right.	82
Figure 5.13. Bridges diagram results.	83
Figure 5.14. Bridge feature measuring 5mm in thickness and 50mm in bridge length.	83
Figure 5.15. Comparison between the bottom layer (left) and the top layer (right) of the 1.2mm thickness bridge test.	84
Figure 5.16. Overhang benchmark from the study (left) and new version (right).	86
Figure 5.17. Chart of estimated printing times for each GBTA.	92
Figure 5.18. 5mm wide overhang GBTA produced in ABS (left) and PLA (right).	92
Figure 5.19. Angled walls GBTA. Concave (left), straight (centre) and convex (right) surface.	93
Figure 6.1. Issues with standard plastic tensile specimens. Adapted from Ahn et al. (2002)	96
Figure 6.2. Reported parameters and factors influencing the mechanical properties in FFF.	97
Figure 6.3 Section of the printed specimens. Characteristic areas	101
Figure 6.4 Density analysis on ImageJ software.	106
Figure 6.5 Infill patterns (a) rectilinear, (b) honeycomb, (c) line, and densities (d) 20%, (e) 50%, and (f) 100% used as variables.	106

Figure 6.6 Test specimen with the main dimensions in mm and print orientation	107
Figure 6.7 Tensile strength and Young modulus evolution with density change	109
Figure 6.8 Examples of tested specimens. A: Honeycomb 20%. B: Rectilinear 20%. C: Rectilinear 50%. D: Rectilinear 100%	110
Figure 6.9 Fracture detail of example tested specimens	111
Figure 6.10 Tensile strength box plot	112
Figure 6.11 Elastic modulus box plot	113
Figure 6.12 Strain-Stress diagram of the different mesostructures	114
Figure 6.13. Microstructure (left), adapted from (Azo materials, 2018), and mesostructure in FFF (right).	117
Figure 6.14. Beads mesostructure in a flexural test specimen SEM micrograph of the fracture surface.	118
Figure 6.15. Examples of various patterns that could be used to reduce the density of FFF components.	119
Figure 6.16, Dimensions, in mm, and orientation of the test specimens. Infill pattern for illustration purposes only.	120
Figure 6.17. Testing experimental setup.	122
Figure 6.18. Specimens prepared for SEM microscopy. 100% (left), 20% (top), and 50% (right) infill density.	123
Figure 6.19. Load vs displacement graph of the specimens with 20% rectilinear pattern (left) and 50% linear pattern (right).	123
Figure 6.20. Average strain-stress graphs, comparing patterns and infill densities. Left – different infill patterns at 50% density. Right – comparison between infill densities with the honeycomb pattern.	125
Figure 6.21. Flexural strength (left) and modulus (right) of FFF and injection moulded specimens.	125
Figure 6.22. Comparison of specimens weight.	126
Figure 6.23. Comparative graph of production times.	127
Figure 6.24. Specimen macro photography during fracture.	128

Figure 6.25. SEM micrograph of the fracture surface of 100% infill specimens with (a) Honeycomb, (b) Rectilinear, and (c) Line patterns.	129
Figure 6.26. 50% density SEM micrograph of the line (left) and honeycomb (right) specimens.	130
Figure 6.27. SEM micrograph of 50% dense specimens in the infill area of the rectilinear pattern (left) and perimeter area in the honeycomb pattern (right).	130
Figure 7.1. Post-processing steps of a functional FFF component.	136
Figure 7.2. Machining of the mounting areas of an FFF component. Source: <a href="http://stratasysdirect.com">stratasysdirect.com</a>	137
Figure 7.3. Different methods of supports structure generation: a) Manually in CAD, b) automatically generated in CAD, C) automatically generated by the print preparation software and B) the printed component after support removal.	138
Figure 7.4. Process of manual support removal.	140
Figure 7.5. Surface roughness parameters Ra, Rq and Rt (Castro-Casado, 2021)	141
Figure 7.6. Staircase effect in a component printed with FFF.	142
Figure 7.7. Approaches to remove the staircase effect to form a curved surface. Surface modification (left) and coating (right).	143
Figure 7.8. Dimensional change of PLA, PETG, ASA and ABS after thermal annealing. Source: <a href="http://Prusarinters.org">Prusarinters.org</a>	144
Figure 7.9. Surface finish in a PETG FFF component after thermal annealing embedded in salt. Source: <a href="http://cnckitchen.com">cnckitchen.com</a>	145
Figure 7.10. Methods of chemical post-processing by (a) natural evaporation, (b) forced evaporation and (c) immersion (Castro-Casado, 2021).	146
Figure 7.11. ABS Specimens that were used in the experiment of acetone dipping. Wall thickness (left) and cylindricity and tolerances (right).	147
Figure 7.12. Measurement setup for a) roughness, b) cylindricity, and c) planarity.	148
Figure 7.13. Roughness results of the acetone dipping experiment.	148

Figure 7.14. Effect of immersion in solvents on the surface of FFF PLA (Valerga et al., 2019).	149
Figure 7.15. Sanding tools, including a sanding paper attached to a customised curved wooden baking tool for sanding curved areas.	151
Figure 7.16. Effect of shot blasting on the surface of a PLA component (Bastian, 2013).	152
Figure 7.17. 3D Reconstructed 3D surface topography of ABS as-printed (a), and after alumina grit blasting (b) (Xu et al., 2018).	152
Figure 7.18. Engraved product logo with CNC in a finished FFF prototype of a portable Bluetooth speaker. Academic project from the Workshop on Prototypes and Models subject. ETSID UPV (Conejero Rodilla, 2018).	153
Figure 7.19. The rotary tool attached to the FFF machine.	154
Figure 7.20. Machining in the curved surface specimen (left) and datuming in the planar surfaces specimen (right).	155
Figure 7.21. Operations applied to the planar specimens: contouring (left), parallel facing (centre) and concentric facing (right).	156
Figure 7.22. Types of toolpaths used in the hemispherical specimens.	157
Figure 7.23. Comparison of hemisphere specimens during machining.	157
Figure 7.24. Composite mould tool being machined, produced by large-format additive material extrusion. Courtesy of The Manufacturing Technology Centre (UK).	159
Figure 7.25. Effect of tumbling smoothing (left) and polishing (right) media in a FFF component (Schneider, 2019)	160
Figure 7.26. Samples metallised by PVD after various surface modification treatments: (a) control, (b) atmospheric plasma (etched with an atmospheric hand-held plasma etcher), (c) 2000 grit sandpaper, (d) acetone vapour treatment, and (e) acetone dip treatment (White et al., 2018).	164
Figure 7.27. Prototype with a metallised component using vacuum PVD. Note that that the deposition lines are still visible due to not enough surface preparation. Academic project from the Workshop on Prototypes and Models subject. ETSID UPV.	165
Figure 7.28. FFF gear metallised by PVD. Courtesy of Fraunhofer IST.	166

Figure 7.29. Vacuum infiltration procedure (Mireles et al., 2011).	167
Figure 7.30. Brush application of epoxy resin to seal and smoothen the surface (BJB Enterprises, n.d.).	168
Figure 7.31. Cross-section of a sample with two layers of coating (Haidiezul et al., 2018).	169
Figure 7.32. Application of nitrocellulose putty to fill gaps in a FFF component. Workshop on Prototypes and Models subject. ETSID UPV.	170
Figure 7.33. Coating and material removal steps for an aesthetic evaluation prototype. The component was printed with the curved surface of the cylinder facing downwards.	171
Figure 7.34. Application of friction stir welding on a UAV. a) parts to be welded; b)welding movement schematic; c)welded parts; wing after spray painting; d) wing after assembly. Adapted from Tiwary et al. (2020).	173
Figure 7.35. Drilling a hole in a FFF component. A) layers of the component; B) cross-section with the infill visible and the planned drill in red; C) Drilling ; D) Misalignment of the bolt.	175
Figure 7.36. Self-tapping screw being inserted in a testing part.	176
Figure 7.37. Torque and clamp load curves in the forming process using self-tapping screws (Cumbicus et al., 2021).	177
Figure 7.38. Screen capture of the print preparation software (left); hardware embedding by press fit in a cavity on the top and side surfaces (right).	179
Figure 7.39. Steps of inserting a heat-setting insert. Alignment (left), heating and inserting (centre), and cooling down (right) (Giller, 2021).	180
Figure 8.1. FFF printing and stair-stepping effect.	186
Figure 8.2. Students sanding 3D printed bottle caps and thermoforming process.	188
Figure 8.3. From left to right: Original 3D printed part, acetone treated, XTC-3D treated and final appearance model with traditional post-processing techniques.	189
Figure 8.4. General initial questions answer distribution.	190
Figure 8.5. First specific question.	191

Figure 8.6. Second specific question.	191
Figure 8.7. Third specific question answers.	192
Figure 9.1. Long thumb CMIO made by MCS process.	197
Figure 9.2. Comparison between CMIO fabrication workflows. Left: Proposed workflow. Right: MCS traditional method.	203
Figure 9.3. From left to right: Mesh filling/zones to cut / final shape with the reduced mesh.	205
Figure 9.4. Different structures. From left to right: non-uniform Voronoi, regular cell, mesh edges pattern.	206
Figure 9.5. Final geometry ready for fabrication. Structure, border, and supports in different colours for better visualisation.	207
Figure 9.6. Manual removal of supports process.	208
Figure 9.7. Illustration and images of the two steps of the acetone treatment.	209
Figure 9.8. Hook-and-loop fastening.	210
Figure 9.9. Orthosis surface before (left) and after (right) acetone post-treatment.	214
Figure 9.10. Final orthosis fitted to the user.	215
Figure 10.1. Cause-and-effect diagram of the factors that could affect the outcome of desktop 3D printers. Source: (Sanchez et al., 2014)	219
Figure 10.2. The design process for the application of the proposed toolkit	220
Figure 10.3. Initial slides of the design toolkit indicating the design process and tools available	221
Figure 10.4. Design principles compilation method.	223
Figure 10.5. Some examples of the ideation cards.	225
Figure 10.6. The guidance that is provided in the design tool to utilise the cards.	225
Figure 10.7. Face shield design (left), in use (centre), the stacked version for production (right).	227
Figure 10.8. Some of face shield designs from thingiverse.com website.	228
Figure 10.9. AM Design considerations identified in ISO/ASTM 52910. Highlighted elements are included in this section.	230
Figure 10.10. Design for FFF worksheet table provided in the toolkit.	231

Figure 10.11. Staircase effect in 3D printed components. In SLS technology (left) and FFF (right).	233
Figure 10.12. Example of an irregular profile of the deposited strands, reducing the ability to determine dimensional tolerance.	235
Figure 10.13. CAD (left) and simulation (right) of a corner. The corners are rounded due to the roundness of the deposited bead.	236
Figure 10.14. Examples of various patterns that could be used to reduce the density of FFF components.	236
Figure 10.15. Part decomposition to avoid supports in sunken (a) and hollow (b) features (Oh et al., 2021).	237
Figure 10.16. Storyboard of assembly of a prototype. Academic project from the Workshop on Prototypes and Models subject. ETSID UPV.	239
Figure 10.17. Post-processing steps of a functional Bluetooth speaker prototype.	239
Figure 10.18. Customised 3D printed sanding block. Source: (Hsiao, 2018)	242
Figure 10.19. The three versions of the benchmark geometry for the overhanging angled wall feature.	245
Figure 10.20. Deformation in a horizontal overhang.	246
Figure 10.21. Toolpath simulation of the three overhang geometry test versions provided.	247
Figure 10.22. Geometric benchmarking test artefact provided for bridges.	248
Figure 10.23. Distortion force in the deposition of columns in FFF. In B) and C), the column deforms while the new layer is deposited due to the pressure applied by the extrusion. D) This new layer is bonded in the wrong location and fails to follow the CAD design.	250
Figure 10.24. Walls benchmarking geometry provided.	251
Figure 10.25. Testing parts provided to evaluate hole sizes (left) and illustration provided about hole modification (right). Ruler added for scale.	253
Figure 10.26. Tool for parametric automatic generation of lap joins in Solidworks (Dassault Systèmes, France).	255
Figure 10.27. Clearance and interference test geometry.	256

Figure 10.28. Top view of an example of clearance between moving components in a self-assembled mechanism. Source: (Clockspring3D, 2020a)	257
Figure 10.29. Bad (left) and good (right) orientations of a snap-fit joint. Adapted from Klahn et al. (2016)	258
Figure 10.30. Some examples of methods to add threads to FFF components. Inserts (A), Nut with side pocket (B), in-print cavity (C), and threading (D).	259
Figure 10.31. Example of FFF printed threads. Note the large size of the thread. Source: (Clockspring3D, 2020b)	260
Figure 11.1. Protocol of the study developed by Laverne et al. (2015)	264
Figure 11.2. Experimental procedure.	265
Figure 11.3. The early version of the ideation cards that were provided in the study.	266
Figure 11.4. Examples of design concepts created by the participants.	267
Figure 11.5. The design used as a reference in both cases (left) (Trentesous, 2018) and sketches from a group with mostly engineering background (centre) and product design (right).	269
Figure 11.6. Design iterations enabled by prototyping. Problem detected (left) and orientation of the parts in the print platform (centre) and reoriented in the second iteration (right).	269
Figure 11.7. Designs that were used as inspiration by the participants of this group.	270
Figure 11.8. Self-supporting leg assembly design solution extracted.	271
Figure 11.9. Post-processing considerations in the case study. Self-supporting feature in the telescopic feature (left) and print platform with most of the components without needing supports (right).	272
Figure 11.10. Dimensioning of the wall thickness in various features (left) and the size of the horizontal holes by the designers (right).	272
Figure 11.11. Assembly features in the design by the participant group. Annular press-fit joint (top) and printed thread (bottom).	273
Figure 11.12. Some challenges that the designers identified in the prototyping step. Not enough clearance (top) and too large pocket to stop the tripod legs aperture (bottom).	273



Figure 11.13. The case studied (left) and other example designs from the study.	274
Figure 11.14. Chart with a summary of the survey results.	275
Figure 12.1. The number of papers by year with FDM & FFF in the title or abstract. Source: Scopus.	282

## LIST OF TABLES

Table 2.1. Classification of AM processes and characteristics.	28
Table 5.1. Summary of design features found in the literature of design guidelines and benchmarking geometries.	70
Table 5.2. Angles deformation results.	81
Table 5.3. Geometrical test components.	87
Table 6.1 Values of the most characteristics fixed parameters	104
Table 6.2 Average tensile characteristics of the different mesostructures for ABS FFF 3D printed specimens	108
Table 6.3 Analysis of Variance with Lack-of-Fit of the squared-x model	115
Table 6.4. Values of some of the fixed parameters.	121
Table 6.5. Specimen designation and parameters setup.	121
Table 6.6. Results of the ANOVA of the flexural strength.	126
Table 7.1. Acetone dipping experiment parameters and values	147
Table 7.2. Roughness (Ra) comparison before and after machining.	157
Table 7.3. Advantages and limitations of the main surface modification techniques for FFF.	162
Table 7.4. Suitability of adhesives with different types of FFF materials according to literature. Source: (Espalin et al., 2009; Kovan et al., 2017; Lipina, Krys, et al., 2014; Suder et al., 2020)	174
Table 9.1. Cost calculations using the proposed workflow.	211
Table 9.2. Cost calculations using traditional MCS fabrication process.	213
Table 11.1 Questions of the toolkit evaluation survey.	267

## LIST OF ABBREVIATIONS AND NOMENCLATURE

- 3D: Three dimensional
- 3DP: Three Dimensional Printing
- ABS: Acrylonitrile Butadiene Styrene
- AM: Additive Manufacturing
- ANOVA: Analysis of Variance
- ANSI: American National Standards Institute
- ASA: Acrylonitrile styrene acrylate
- ASTM: American Society for Testing and Materials
- CAD: Computer-Aided Design
- CJP: ColorJet Printing
- CMIO: Custom-Made Orthoses
- CNC: Computer Numerical Control
- DFA: Design for Assembly
- DFA: Design for Assembly
- DfAM: Design for Additive Manufacturing
- DFM: Design for Manufacturing
- DFM: Design for Manufacturing
- DFMA: Design for Manufacturing and Assembly
- DFX: Design for X
- DIY: Do-It-Yourself
- DMLS: Direct Metal Laser Sintering
- DP: Design Principle
- DwAM: Design with AM
- DWX: Design With X
- EBM: Electron Beam Melting
- FDM: Fused Deposition Modelling
- FFF: Fused Filament Fabrication
- FS: Functional Surfaces
- GBTA: Geometric Benchmark Test Artefact
- HDPE: High Density Polyethylene
- IR: Infrared
- ISO: International Organization for Standardization
- KFP: Key Feature Parameters
- LOM: Laminated Object Manufacturing
- LTT: Low-Temperature Thermoplastic
- MCS: Mould Casting Splinting
- MIT: Massachusetts Institute of Technology
- MJF: Multi Jet Fusion
- MJP: MultiJet Printing
- MMP: Machine configuration, Material and Parameter
- PEEK: PolyEther Ether Ketone
- PEI: Polyetherimide
- PLA: Polylactide
- PPSF: Polyphenylsulfone
- PSF: Polyphenylsulfone
- PVA: PolyVinyl Alcohol
- RP: Rapid Prototyping
- RPM: Revolutions Per Minute
- RT: Rapid Tooling
- SEM: Scanning Electron Microscope
- SHS: Selective Heat Sintering
- SLA: Stereolithography
- SLA: Stereolithography

- SLM: Selective Laser Melting
- SLS: Selective Laser Sintering
- SLS: Selective Laser Sintering
- Tg: Glass Transition Temperature
- TMC: Trapeziometacarpal
- TPU: Thermoplastic polyurethane
- UAM: Ultrasonic Additive Manufacturing
- VDI: Association of German engineers
- VDR: Visual Design Representation

# Chapter 1

## Introduction

### 1.1. RESEARCH BACKGROUND

The ability to make tools has been a key characteristic of the human race since the prehistoric age. The tools help us to improve our lifestyle and to live more and better. This improvement increases the demand for better goods and consequently pushes the manufacturers to increase their ability to answer the market demand.

Since the first industrial revolution in the 18th century, manufacturers have been trying to find ways to improve their tasks. Such as the standardisation of the components to be able to combine them. Later was the redefinition of the process itself, with the creation of the manufacturing chain and the automation. This new approach has been referred to as the second industrial revolution (Heskett, 1980).

After a radical change in the way people can connect thanks to computers and especially to the internet, manufacturing has become a global process in which designers, engineers, and manufacturing facilities are in different locations. This change has been referred to as the third industrial revolution (Markillie, 2012). The global connection has also allowed collaboration between individuals, with the evolution of the consumer into *prosumers* and the emergence of new ways of manufacturing (Tapscott & Williams, 2008).



*Figure 1.1. Network of FabLabs. Spaces with open access for novel users of digital manufacturing technologies, such as 3D printing. Source:fablabs.io*

As opposed to forming or subtracting manufacturing methods, Additive Manufacturing (AM) methods comprise joining materials to make objects from 3D model data, usually layer upon layer (ISO/ASTM, 2015). In recent years, the AM through material extrusion has experienced accelerated development and adoption thanks to the wide availability of low-cost machines and materials. The size of some of these machines has been reduced from shop floor to desktop size, enabling their usage in office setups or at home. This type of technology, which uses material extrusion to build components and the material is provided in filament form, is usually referred to as desktop 3D printing technology or Fused Filament Fabrication (FFF).<sup>1</sup> This technology, merged with a global source of information, has empowered individuals, making them capable of carrying out the entire design and manufacturing process in a non-industrial setup (Markillie, 2012).

The cost barrier to acquiring a desktop 3D printing machine has been reduced to a level where users without engineering or design background are getting access to these machines and producing functional parts for everyday

---

<sup>1</sup> These two terms will be used across this thesis to refer to this technology

usage. Under this new scenario, the walls between the designer, the manufacturer, and the consumer are fuzzy.

These new users of the technology have some tools available for the design of parts, such as design tips on online websites (Hudson, n.d.) or books (Micallef, 2015), and designs available in repositories (Myminifactory, n.d.; Thingiverse, n.d.). There is no standard machine design or manufacturing parameters that modify the geometrical (Armillotta et al., 2013) and mechanical characteristics (Ahn et al., 2002). This gap renders the latter insufficient for a successful design, as these best tips do not provide specific geometry values. The designs from repositories have a similar issue; the design might work for the designer's machine but might fail if printed with the final user machine.

## **1.2. SCOPE OF THE WORK**

Even in conventional manufacturing processes, such as injection moulding, extrusion or casting, the manufacturing success relies on the designer's knowledge of the process capabilities and limitations (Boothroyd et al., 1998). In AM, this fits within the scope of Design for Additive Manufacturing (DfAM), which has been defined as the "*Synthesis of shapes, sizes, geometric mesostructures, and material compositions to best utilise manufacturing process capabilities to achieve desired performance and other lifecycle objectives*" (Gao et al., 2015).

As identified by Kumke et al. (2016), the analysis of DfAM in the context of VDI 2221 expose two overarching or primary limitations of existing DfAM approaches which provide, at the same time, promising research opportunities:

- Missing integration into a common framework
- Independence of DfAM approaches

In addition, according to this study, existing DfAM research possesses the following inherent or secondary limitations:

- Limited universal validity of AM design rules

- Focus on utilisation of single AM potentials
- Disproportionate attention to innovative designs

Therefore, for this task, it is necessary to develop design guidance for specific processes and materials (Bourell, Leu, et al., 2009) and be customisable to fit the user machine configuration, material and parameter (MMP) set. These needs were also identified as priority standardisation gaps by ANSI and the USA national additive manufacturing innovation institute, known as America Makes, in the Standardization Roadmap for Additive Manufacturing (ANSI, 2018).

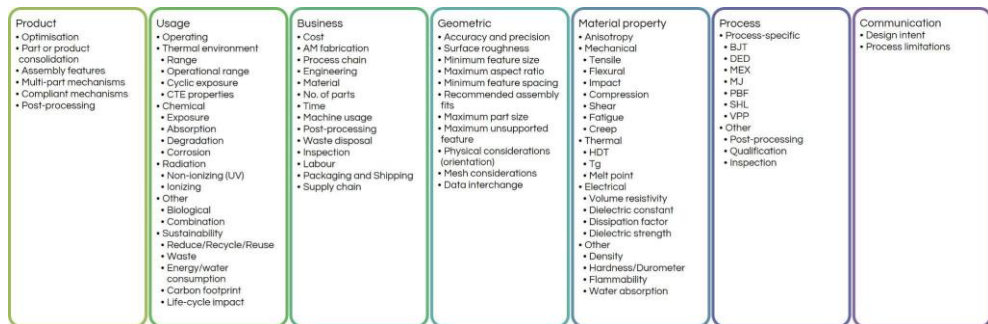


Figure 1.2. Generic AM Design considerations identified in ISO/ASTM 52910.

Therefore, this research scope is the DfAM support of novel extrusion-based desktop 3D printing technology users, with or without a design engineering background.

As Gao et al. (2015) stated:

*«The rapid proliferation of AM technologies is driven by the increase in the variety of materials, low-cost machines, and potential for new application areas. This has resulted in a lack of fundamental design guidelines or standardisation of best practices... As a result, designers' often waste building and support material due to the multiple trial-and-error iterations required for fixing unqualified feature requirements, surface resolution and clearances of mechanical parts and assemblies.»*



## **1.1. AIMS AND OBJECTIVES**

The motivation of this research comes from the necessities previously identified. The overall aim is to understand how novel users of desktop 3D printing can be supported to design components for this technology. Furthermore, it seeks to establish a framework for designing with AM that enables leveraging the advantages of the technology. For this purpose, a set of objectives can be defined:

- Understand the technology and social situation that define the ecosystem that frames this work.
- Define the design and manufacturing criteria that need to be considered for this technology, and analyse the process elements and characteristics that define the outcome.
- Review the current tools and methods and define an approach suitable for the scope.
- Identify the critical common geometrical elements between components.
- Complement the information available in literature by addressing the research gaps in the main areas to produce functional components.
- Develop a framework to leverage extrusion-based desktop 3D printing capabilities and evaluate their suitability. The wide range of machines and materials makes it necessary to specify a toolkit capable of being adapted to the variable performance.

## **1.2. RESEARCH NOVELTY**

The standardisation gaps described before are still not addressed by the standardisation bodies. The author participates in the ISO & ASTM joint working group defining the standard technical guide for material extrusion AM, but the scope of that document is to provide just some general considerations when designing for the process. While part of this thesis has served to develop the standard guide, this research scope is broader. It extends process and

application guidelines, allowing users to adapt further and specify to fit individual needs, as this was identified as a gap.

Much of the DfAM knowledge transfer research in literature has focused on the development of design rules (Adam & Zimmer, 2014), creativity methods (Laverne et al., 2014; Perez et al., 2019), theoretical global approaches (Kumke et al., 2016), or studying the best knowledge transfer format (Sinha et al., 2017). However, far too little attention has been paid to how to best support designers with direct access to desktop 3D printing machines.

In the non-academic or standardisation realms, there are some websites with design tips (Hudson, n.d.; Kočí, 2019a) or books that cover the technology and some sections on design guidance (Micallef, 2015; Redwood et al., 2017; Smyth, 2015). In both cases, this information is top-level and does not support the novel designer in leveraging the capabilities of the technology or how to apply this guidance to a specific machine and material.

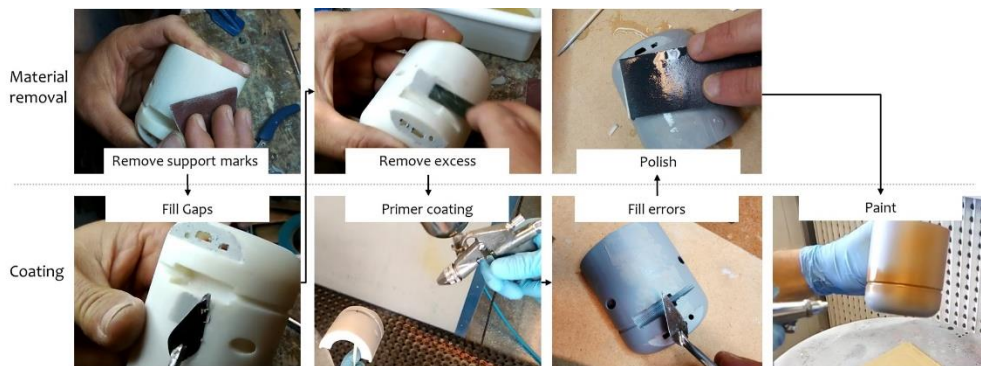


Figure 1.3. Post-processing workflow. From chapter 10.

This research novelty lies in supporting novel users with or without engineering background in the whole end to end journey, from the concept design to the finalised component. Therefore, the key novel elements of this research are:

- Consideration of the new ecosystem and non-professional background of the users.

- Identification of the key design features and development of generic benchmarking geometries.
- Identification of the impact of surface finish in the perception of 3D printed components.
- Integration of divergent and convergent design stages into a single toolkit framework.
- Define a design process considering the capabilities of the technology, the available design resources and repositories, and the limitations.
- Methodology to customise the design rules to the material, machine and parameters of the user. Rather than provide average values, which are continuously evolving thanks to the Open Source architecture of this technology and the wide range of systems, it seeks to be an unfixed tool able to adapt to almost every machine and configuration.
- Usage of different formats suitable for each of the tools provided.

### **1.3. THESIS STRUCTURE**

The chapters of this dissertation are structured as follows. Some of the studies developed were published and are integrated within the chapters or as standalone articles.

Chapter 2 reports the initial Literature Review and identifies the technology and social ecosystem in which the further chapters base their development. Based on this review, chapter 3 identifies the Fused Filament Fabrication process characteristics to serve as a reference for the further chapters.

Chapter 4 analyses the approaches proposed in the literature to support designers in DfAM tasks. This chapter helps find the gaps in current research and identify potential approaches to be integrated. These three chapters serve as the baseline for the following chapters.



*Figure 1.4. 3D printed orthosis from chapter 9.*

Chapter 5 aims to build knowledge in the geometrical features assessment by investigating the geometrical benchmarking artefacts in literature and proposing a set of these. The wider adoption of this technology for functional parts is still slowed down by limitations such as the surface finish quality (Boschetto et al., 2016a) and the reduced knowledge about their mechanical behaviour (Cuan-Urquizo et al., 2015). Chapter 6 investigates the latter, with particular attention to infill density and pattern effects in the mechanical behaviour. Chapter 7 examines the former, looking at the various methods available to modify the surface of FFF components to overcome one of the main reasons for dismissing this technology, the physical appearance. As the FFF components are often used as visual evaluation models, chapter 8 studies how the surface post-processing affects the perception of the components.

Chapter 9 describes an application case study using the knowledge developed in the previous studies by exploring a novel design workflow using low-cost design and manufacturing tools combined with non-manual finishing. The aim is to identify the element where the designer might need support in the various stages of the component development.

Chapter 10 proposes an approach to support novel designers using the outcome of the previous chapters and the information available in the literature. This approach consists of a set of multi-format tools that support

designers in every stage of ideation, concept, embodiment and detail stages of the design development.

Chapter 11 then evaluates the performance of the toolkit by a qualitative survey of users and evaluation of the outcome to find out how the toolkit was used. Finally, chapter 12 concludes the thesis by reflecting on the research findings, identifying weaknesses and suggesting areas for future investigation.



# Chapter 2

## 3D Printing

### 2.1. INTRODUCTION

A thorough review of the different aspects of 3D printing is needed to understand the ecosystem that requires the development of this work. For this purpose, first, is going to be identified the origins, the evolution and purposes of use from the initial steps of the technology to the nowadays mature Additive Manufacturing. Then, the unique capabilities of these fabrication methods are going to be described. Later are going to be described the different processes available in order to distinguish the technology purpose of this work from other processes. Finally, the different causes of the desktop 3D printing industry sector rising are identified and described.

### 2.2. HISTORY AND PURPOSES OF USE

Various terms have been used over the years to refer to the manufacturing of objects layer by layer. 3D Printing is the popular term used nowadays for what is called formally additive manufacturing, previously referred to as rapid prototyping (Chua & Leong, 2003), rapid manufacture (Hague et al., 2003; Hopkinson et al., 2006) or solid freeform fabrication (Malone & Lipson, 2007). Usually, the process includes the slicing of a digital model into 2D slices. These cross-sections are the layers of material that the machine adds sequentially (I. Gibson et al., 2015a). ASTM defines AM as “the process of joining materials to make objects from 3D model data, usually layer upon layer” (ISO/ASTM, 2015).

This process of direct addition has its roots in the 19th century, and the purposes of use have evolved over the years. This point discusses the origin and brief history of the process and the evolution of the purposes of use.

### 2.2.1. ORIGINS

The basis of 3D printing is the layerwise creation of parts; two early roots can be identified: photosculpture and topography.

By 1860, François Willème invented photosculpture in order to replicate three-dimensionally an object (Willème, 1864). It was a setup with 24 cameras around an object, arranged at an angle of 15 degrees, taking photos of the object simultaneously. The different photos were used to reconstruct the object by carving each silhouette by an artisan, as shown in Figure 2.1.

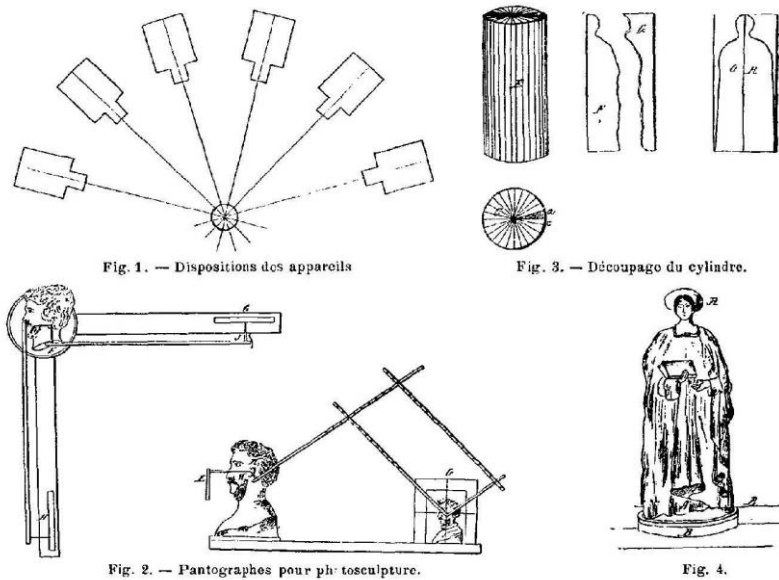


Figure 2.1. Illustration of the Photosculpture technique. Adapted from Willème (1864).

The successful process characteristic was the ability to reproduce in a systematic way the objects or the people that were in the setup. The invention was a big success due to the fast execution and reduction of the total cost of the sculpture. (Niewenglowski, 1897) The vogue of photosculpture had an



international impact, and some of the most famous persons at that time wanted a sculpture with the new “technology”. As an example, Figure 2.2 shows two of the captures of Francisco, Duke of Cádiz, King Consort of Spain in ca. 1865.



*Figure 2.2. Two captures for the photosculpture process ca. 1865.*

Baese (1904) improved this process using photosensitive gelatine that expands proportionally to exposure and graduated light. Some years after, Morioka (1935) described a process that combines photosculpture and topography. In this process, the projection of black and white bands of light (which nowadays is called structured light) creates contour lines of an object, obtaining the cross-sections.

On topography, Blanthier (1892) proposed a method to make a mould of layers from relief maps. The method was based on stacking wax sections of the terrain obtained from contour lines and then pressing a paper map between the positive and negative mould. This pressure created a three-dimensional surface of the terrain. Some inventors refined this process, and by 1972, Matsubara described a process using photopolymer resin. A selectively projected light is projected onto a photopolymer sheet, hardening the exposed area, and the unhardened area is dissolved away by a solvent (Matsubara, 1976).

Some years before Matsubara invention, Munz (1951) proposed a system that shares some characteristics with current AM technologies. He describes a

process where the cross-sections of an object are projected sequentially onto a photo emulsion, creating the object. The origin of the information comes from the scanning of an object, as described before by Morioka.

Ciraud (1973) proposed a different approach to building an object. He describes a method in which particles of a meltable material are spread or positioned, and a laser, electron, or plasma beam melts the particles. This process creates a bonding between the heated particles, and the object is created (Ciraud, 1973). As shown in Figure 2.3, he proposed different dispositions of the elements using the same method.

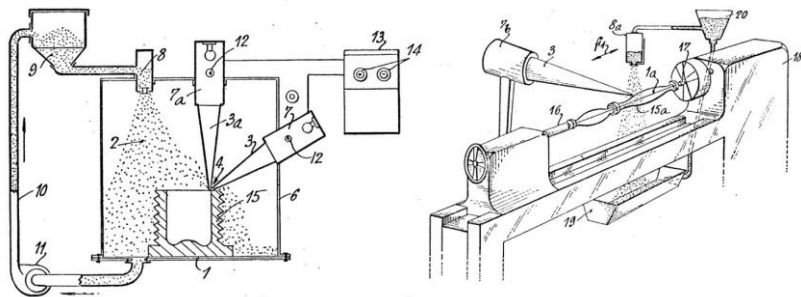


Figure 2.3. Two of the proposed configurations of the method described by Ciraud (1973)

Housholder (1979) described a process where the powder is deposited and bonded in a controlled way using heat. It is the earliest description of a powder laser sintering process in which layers could be solidified selectively. He built a functional prototype of the system, although the system required a mould to create the “voxels” (three-dimensional pixels ). Kodama (1981) developed a system that has been recognised as the first functional photopolymer rapid prototyping system. Although the previously described systems could produce some parts, the quality of results was deficient, and the efforts were more research-oriented than an actual viable fabrication process. As the processes of layer-based manufacturing began to become more defined, it became apparent that there were opportunities for it to be used industrially (Bourell, Beaman, et al., 2009).

In 1984 three different teams from Japan, France, and the USA filled a patent about the fabrication of an object by adding material layer by layer (Hull,

1984). The USA team, and Chuck Hull, his lead, managed to create and commercialise a functional machine. It was based on a photopolymer that is hardened selectively by the exposition to a laser. They coined the process as Stereolithography (SLA) and defined the most used file format in the industry, STL (STereoLithography). He started one of the most important companies in the sector nowadays, 3D Systems (Rock Hill, SC, USA).

Some other patents for different processes emerged in the following years, as Helisys with LOM ( Laminated Object Manufacture ), based on the adhesion of paper-based layers, or Cubital with SGC (Solid Ground Curing), which used photopolymer as SLA but instead of using a laser, it used an ultraviolet lamp and a mask to harden specific areas of the photopolymer bath. In 1986 DTM patented a process that bonded particles in a similar way as Ciraud (1973) described before, but depositing the powder layer by layer instead of spreading it (Deckard, 1986). This process was coined as Selective Laser Sintering (SLS), one of the most widespread AM methods nowadays.

In 1989 two crucial processes were patented. A method called three-dimensional printing<sup>2</sup> (3DP) was patented by MIT (Sachs et al., 1989). It was licensed to different companies, as ZCorp (Which was bought by 3D Systems too), which was the only process capable of producing parts in multiple colours for a long time. In the same year, Scott Crump patented the technology of Fused Deposition Modelling (FDM) (Crump, 1989) and founded the company Stratasys (Eden Prairie, MN, USA), one of the other most important companies in the industry.

During the 90s, some other companies were founded. In 1998, Objet (nowadays Stratasys) patented a process of ink-jetting photocurable resins, although it was not until 2007 when they introduced the first model (Bourell, Beaman, et al., 2009). This technology allows the deposition and hardening of different resins in a controlled way by using, in the first version of the machine,

---

<sup>2</sup> Note the difference between the name assigned to this process and the actual use of the word 3D Printing to a wide number of processes

1,536 nozzles. It is possible to manufacture objects with different materials inside the same volume (I. Gibson et al., 2015a).

It should be noted that some of the companies and patents described have disappeared, merged, or been bought by other companies (mainly by 3D Systems and Stratasys). A tiny sample of them has been mentioned, especially the metal-based systems, but these provided the grounds for the future developments of the technologies. A detailed chronicle can be found in (Wohlers, 2015).

The expiration of some patents in the late 2000s led to the emergence of new competitors and became the seed of a new market and industry sector called “desktop 3D printing”, which is the focus of this thesis. The ecosystem that led to the emergence of this new sector will be discussed in the later chapter.

In the following sections, the evolution of this process according to the two main uses of 3D printing will be described: Rapid prototyping and additive manufacturing.

### 2.2.2. RAPID PROTOTYPING

Rapid Prototyping (RP) term is used to the process of rapid creation of a part before final fabrication. The objective is to create a model or prototype quickly to evaluate different aspects of the product. A tangible visual representation of a design concept for all involved in the design process is a shared view. It is also used on management and software to test ideas during the development process and iterate them as fast as possible (Bäumer et al., 1996).

The prototyping task is an essential step in the design process, reducing the risks and cost of mistakes in production (Ulrich, 2003). The process of building and modifying a prototype can reveal design issues in ways that alternative representations often cannot. The fidelity of a prototype is often a trade-off between fidelity and the effort, time, and cost required to produce that prototype. However, it has been recognised that time spent on early stages of design on prototyping correlates with better design (Conejero Rodilla, 2009; M. C. Yang, 2005).

Visual Design Representations (VDRs), as prototypes, are essential elements in new product development. Pei et al. (2011) detected a lack of shared understanding of the different VDRs and defined a taxonomy to categorise them. Four main categories of VDRs can be identified: sketches, drawings, models and prototypes. Regarding the categories where RP is being used, models and prototypes, the authors divide the two categories into sub-groups depending on the user: a) an industrial designer, who focuses on the visual aesthetics and form, and b) an engineer, who aims to represent the technical aspects of a product with a VDR. Prototypes refer to VDRs that include working and functional components and are often built to full scale.

The VDRs system of classification helps distinguish the different purposes of using 3D printing as a Rapid Prototyping process. According to Pei et al., industrial design models encompass 3D sketch models, design development models, and appearance models. RP has barely been used in industrial design for the two first types in favour of manual model making. However, it is common to use RP design development models in architecture to understand the relationships between components, cavities, interfaces, structure and form. The third type, appearance models, is more common the use of RP in industrial design practice. As an example, in Figure 2.4 can be seen the application in shoe appearance models.



*Figure 2.4. Appearance model of a portable speaker. 3D printed with FFF. Workshop on Prototypes and Models subject. ETSID UPV.*

The second subgroup, Engineering Design Models, include the functional, concept of operation, production, assembly, and service concept models.

The prototypes category of VDRs system of classification include appearance, alpha, beta, and pre-production prototypes in industrial design; in engineering design, it encompasses experimental, system, final hardware, tooling, and off-tool prototypes. RP has been widely used in this category to facilitate the prototyping task (bin Maidin, 2011).

All the information supplied by the different VDRs was about what is known as the “3Fs” of Form, Fit, and Function. Initial 3D printing technologies could produce models used to convey the design appearance or shape (Form). Improved accuracy in the process enabled the possibility to build models and prototypes that allowed testing of the tolerance specifications of the design for assembly purposes (Fit). Improvements in material properties and processes made it possible to currently make models considered as “prototypes”, meaning that 3D printed parts can perform the actual function (Frank et al., 2003). In Figure 2.5, a fit evaluation model for customised glasses can be observed. It is the output of a study developed to find the suitability of the digital technologies for fit evaluation of a customised design (Rodrigo Corbaton et al., 2016).

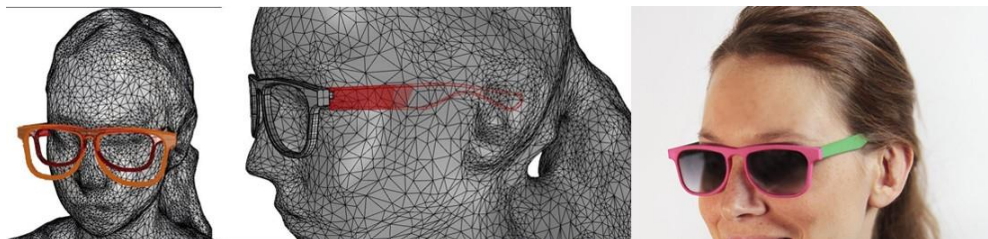


Figure 2.5. Fit evaluation model for customised glasses. (Rodrigo Corbaton et al., 2016)

Rapid prototyping was the generic term used to define the manufacturing technologies which enabled the fabrication of models and prototypes without manual work. The evolution of the technologies allowed the fabrication of functional tools directly in metals and ceramics. This new use of the technology was called Rapid Tooling (RT) (bin Maidin, 2011), with the idea behind RT of the fabrication of moulds directly using 3D printing. The use of this term has evolved to a particular application of the technology, as the term currently used is *additive manufacturing* (I. Campbell et al., 2012).

### 2.2.3. ADDITIVE MANUFACTURING

3D Printing technology for a long time was unable to manufacture end-use products. This limitation was due to lack of maturity of the process, scarcity of proper CAD software or poor and controlled material properties (Hopkinson et al., 2006). As these limitations have been overwhelmed, some of the processes have been developed to ensure that the output is suitable for end-use (I. Gibson et al., 2015b).

AM does not suffer from drawbacks of traditional manufacturing systems such as intermediation, stock flows, the divergence of functions or high costs for small production runs. AM provides a combination of benefits in flexibility, speed, complexity, and low cost for small quantities (Cozmei & Caloian, 2012).

Despite these advantages, for Campbell et al. (2012), the main limitations to AM are speed, accuracy, different resolutions depending on the axis, material properties and system cost. The developments in materials and processes combined with the reduction in system costs have helped open it up to a broader audience.

Bak (2003) studied the application of 3D printing and obtained a list of benefits of these technologies:

- Reductions or elimination of waste – The material volume used by these processes is almost the same as the final part, so there is no waste as chips on subtractive processes
- Elimination of inventory – As the designs are manufactured directly from raw material, there is no need to stock manufactured parts.
- Manufacturing Labour – The manufacture of near-net shapes helps eliminate manual tasks related to conventional manufacturing, such as assembly or machining.
- Improved quality control – The digitalisation of the design and manufacturing process reduces human error.

- **Setup of production** – As the main tasks of preparation and verification are done digitally, the machine production does not depend on the setup.

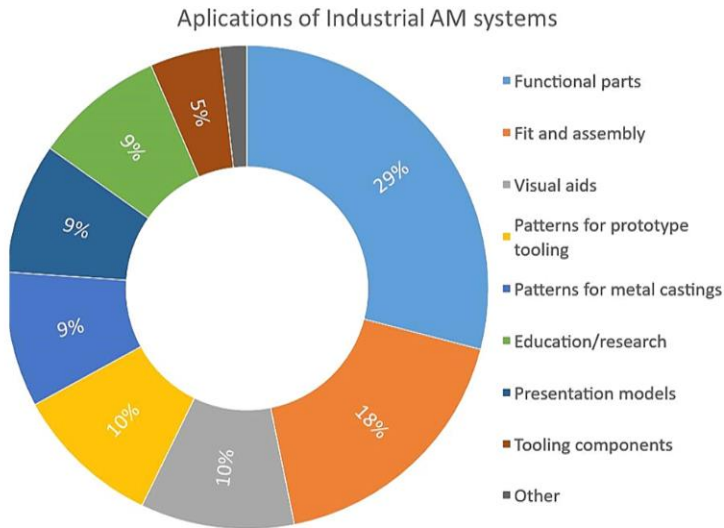


Figure 2.6. Areas where industrial AM is being used. Adapted from (Wohlers & Caffrey, 2015)

3D Printing allows the simplification of the part count. Having fewer parts means less to design, fabricate, assemble, debug, and maintain. In DFA methodology, the part count is often reduced by attributing additional functionality to existing parts (Boothroyd et al., 1998). Yang (2005) identified a positive association between a lower number of parts and design outcomes.

As shown in Figure 2.6, the application of AM for functional parts is the most common following by fit and assembly parts. This gives us information about how the AM systems output quality has evolved to a level where users trust the technology.



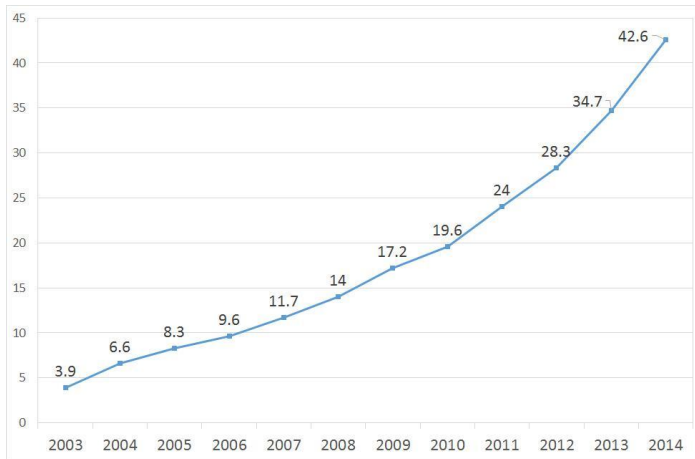


Figure 2.7. Percentage of direct-part AM production. Adapted from (Wohlers & Caffrey, 2015)

Wohlers & Caffrey (2015) report that most indicators suggest that we are headed toward a new manufacturing method and an industry worth tens of billions of dollars. In Figure 2.7 can be seen the AM for part production growth. It has increased from 3.9% to almost half of the total product and service revenues of 3D printing. Some economists theorised that 3D printing could be seen as the most promising element in an emerging revolution in manufacturing (Anderson, 2010; Hopkinson et al., 2006; Rifkin, 2011).

## 2.3. DESIGN POSSIBILITIES

The manufacturing processes evolved towards simplifying the manufacturing task since the invention of tools (Swift & Booker, 2013a). As described before, 3D printing was initially used to help in the design and development process. From a design point of view, the freedom in terms of geometry and materials is a game-changing characteristic when aiming to use it as the product method (Rosen et al., 2015).

In a comprehensive study of the implications on the design of these new technologies, Hague *et al.* (2003) indicate that this freedom changes the design process and introduces new possibilities in the designs of the parts, making conventional Design for Manufacturing (DFM) guidelines obsolete. It does not

mean that 3D printing could replace the conventional manufacturing processes in every situation but opens the door to new fields where 3D printing is more appropriate. Furthermore, they identified some key characteristics that boost the popularity of 3D printing nowadays, such as creating customised parts or the collaboration between the designer and the customer in the design process.

The main aspects of the 3D printing design potential can be categorised as follows:

- Geometrical freedom – which means that, as opposed to conventional manufacturing processes, the complexity of a geometry manufactured by 3D printing does not influence the manufacturing cost. Furthermore, it enables the manufacturing of complex parts previously impossible (I. Campbell et al., 2012). The geometrical freedom has opened the possibilities in areas such as:
  - Tooling elimination – The ability to fabricate complex parts without tooling is a key characteristic of 3D printing processes instead of conventional manufacturing. This characteristic reduces the lead-time and several aspects of the fabrication cost (Bak, 2003).
  - Design complexity – Related to the previous point, the foremost benefit of 3D printing is the capability to fabricate almost any complex geometry without incurring additional cost, as shown in Figure 2.8. A relationship between part complexity and cost is present in conventional manufacturing (Boothroyd et al., 1998). In contrast, additional tooling, increased operator expertise, or even fabrication time do not increase with the part complexity in 3D printing (Gao et al., 2015).

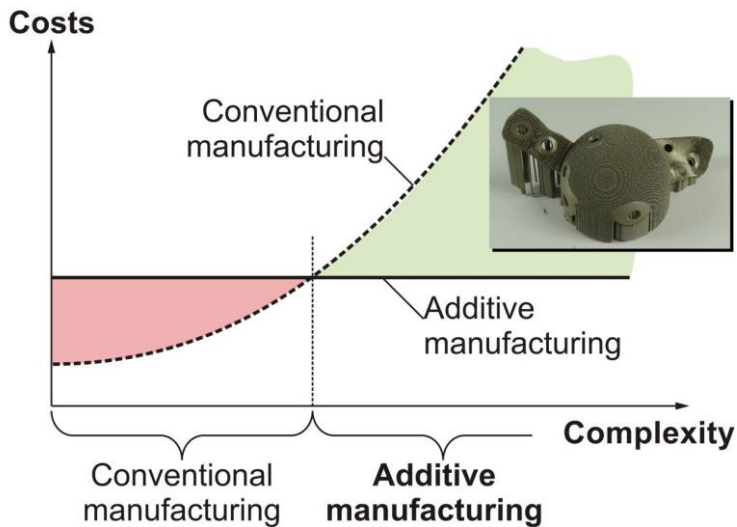


Figure 2.8. Part cost evolution with the increase of complexity. Comparison between conventional and additive manufacturing.

- Part consolidation – The geometrical freedom enables the fabrication of multiple discrete parts merged into a single part. This can improve the structural performance compared to the traditional multi-piece assembly (Liu, 2016). In modern manufacturing, reducing part count is one of the effective ways to reduce process time and cost. This method reduces the use of fasteners and avoids assembly difficulties such as the design of the joining methods (S. Yang et al., 2015). Becker et al. (2005) identified the benefits and principles of part consolidation in 3D printing. Atzeni et al. (2010) compared the cost of a consolidated SLS 3D printed part to a conventionally manufactured assembly and concluded that 3D printing is adequate for medium lot productions, even mass customisation products. However, the lack of how to achieve less part count and the dependence on designers' experience and understanding of functional requirements are the main drawbacks of the available consolidation methods (S. Yang et al., 2015). Furthermore, part geometry and build orientation

should be optimised to improve the structural performance of the consolidated 3D printed part (Liu, 2016).

- Part customisation – The fabrication of every part individually without tooling provides the additional benefit of producing each part with a different shape. It makes it economically feasible to produce products fitted to individual user requirements (bin Maidin, 2011). This benefit has excellent potential in parts that should be adapted to each client, such as medical applications (A. M. Paterson et al., 2014). According to the user needs, the customisation increases the comfort and adherence to the product (I. Gibson et al., 2015a). Furthermore, the consumer could be involved in the design process enabling the mass customisation of products (Sinclair, 2012). The involvement and commitment of the consumer in the design process for AM are getting increased attention in the literature (Ariadi, 2016; Conner et al., 2014).
- Multiple assemblies – The ability to access the inside of the parts enables the fabrication of assemblies in situ, also called non-assembly mechanisms (Cuellar et al., 2018; Lussenburg et al., 2021). Already assembled operational mechanisms can be fabricated by ensuring that clearances between parts are adequate. This can significantly reduce the number of parts that have to be assembled after the fabrication.
- Material complexity – The material can be fabricated differently at different points of the same part. Consequently, it provides different properties in different regions of the part. Furthermore, some 3D printing processes allow using different materials during the fabrication (Muller et al., 2014). This characteristic provides unique design opportunities and capabilities that are not possible using any other manufacturing processes. Given this capability, one of the challenges lies in creating software environments capable of enabling a user to efficiently model such complexity (Gao et al., 2015; Muller et al., 2014). These types of parts have been called functionally-graded materials or

heterogeneous materials and are receiving considerable attention in literature and industry (P. Huang et al., 2013; Loh et al., 2018).

It should be noted that some of the described benefits of 3D printing are due to the digitalisation of the design and manufacture process, also called “digital fabrication”. Digital fabrication reduces costs and supports a paperless design and construction process (Sass & Oxman, 2006). Furthermore, it provides several cost advantages, which are: waste reduction, physical inventory elimination, labour reduction, digital quality control, off-line part setup (Bak, 2003). These cost advantages are even more significant with 3D printing than with other digital fabrication processes such as Computer Numerical Control (CNC) or laser cutting. This is due to the possibility of automated process planning. The digital geometry can be sent directly to the machine, and the machine software can automatically calculate the toolpaths (I. Gibson et al., 2015a).

Over the past five years, 3D printing has received extensive media coverage and growing policy support. However, as Neil Gershenfeld, the head of MIT’s Centre for Bits and Atoms and Fab Lab network founder, argued speaking at the Royal Academy of Engineering’s Grand Challenges summit (Solon, 2013):

*«The coverage of 3D printing is a bit like the coverage of microwave ovens in the 50s. Microwaves are useful for some things, but they didn’t replace the rest of your kitchen... The kitchen is more than a microwave oven. The future is turning data into things, but it’s not additive or subtractive.»*

Harnessing the design possibilities of 3D printing systematically nowadays results from the designer’s experience and knowledge about AM design (Gao et al., 2015). New complex geometries and design solutions have been developed as 3D printing technologies have been used for new applications. However, few studies focus on classifying those design features to provide that knowledge for future product design. The series of studies by Maidin et al. offer probably the most comprehensive empirical analysis of this issue (bin Maidin, 2011; Maidin et al., 2012; Maidin & Campbell, 2010; Sever et al., 2009).

Maidin *et al.* recognised the lack of assistance during the creative phases. Their research aimed to develop a knowledge-based support tool for designers, with a database of AM design features used as a knowledge repository. They developed a taxonomy, or classification, of design features into subgroups based on their reasons of utilisation in order to make it accessible. The main reason to classify the features by their reasons of utilisation was the identification of the designers' necessity to understand the advantages and limitations of 3D printing and the reasons for its use prior to designing and producing parts. The design features are classified under four main reasons for 3D printing utilisation. These are:

- User fit requirement – This means the necessity to customise the part or product to accommodate user requirements by using the previously described benefit of customisation that provides the 3D printing processes. The design features under this requirement were grouped under sport, medical and consumer product
- Product functionality improvement – Under this type of requirement fall, the design features to improve part functionality using the capabilities of 3D printing. The functionality improvement features were sub-grouped in weight reduction, internal structure, increased surface friction and multiple product versions.
- Parts consolidation – The design features grouped under this category use the previously described 3d printing benefit of part consolidation, which allows the combination of different parts in a single geometry. The design features were classified from four approaches: Fasteners removal, instant assembly, multiple functions, and dual material features.
- Aesthetics or form – This category was defined for design features that could be added into a product design to improve product appearance using the capabilities of 3D printing. It included four sub-groups: visual features, surface features, embossed features and customised form features.

This previously described classification of 3D printing design possibilities provides an effective method to provide this information to newcomers (Kumke et al., 2016). It will be used as a layout in the following chapters.

Although these design possibilities are shared between almost every 3D printing process, the characteristics and limitations of those processes should be identified. As has been described before, there are a lot of different systems and technologies that comprise the 3D printing area. The different available processes will be described in the next point to differentiate the technology objective of this thesis.

## **2.4. OVERVIEW OF CURRENT TECHNOLOGIES**

The term 3D Printing is being used to refer to many different Additive Manufacturing processes. Those processes vary by their layer manufacturing method, and for each process, there are various technologies that differ depending on the material and machine technology used.

To classify the different processes, have been proposed different approaches. An initial approach was to classify the 3D Printing processes according to the technology, like using lasers, extrusion, inkjet, etc. (Kruth, 1998). Later a different approach was used, collecting processes together according to the type of raw material (I. Gibson et al., 2015a). This type of classification's main problem is that as entirely different processes get grouped together, and similar processes end up separated. Pham (1998) proposed a classification method based on the number of dimensions the layers are constructed, but many different processes fall into the same category, and it is difficult to compare them.

Stucker and Janaki Ram (2007) proposed a classification of processes that use a common type of machine architecture and similar materials transformation physics. Under this classification, all 3D Printing processes fall into one of seven categories. It allows the comparison of similarities, drawbacks, benefits, and processing characteristics between processes in the same group. ASTM and ISO embraced this approach to classify these technologies (ISO/ASTM, 2015). Table 2.1 shows the categories with some of the technologies currently available for each technology, the materials that can

be used, the power source, and some of the strengths and weaknesses of the processes.

*Table 2.1. Classification of AM processes and characteristics.*

	Technologies / Commercial terms	Materials	Power source	Benefits (+) Drawbacks (-)
Sheet lamination	– LOM, UAM	Paper Plastic film Metal sheet	Chemical reaction Thermal	+ Low process cost - Slow processing
Vat photopolymerisation	– SLA – DLP	Photopolymers	Laser beam Light	+ High building speed + Good part finishing - Over curing - High cost of supplies
Material Jetting	– Polyjet, MJP, Inkjet printing	Photopolymer Wax	Thermal UV light	+ Multi-material + High surface finish - Low-strength - High cost of supplies
Binder Jetting	– Color Jet Printing / CJP – Binder Jetting	Plaster PMMA Metal Sand	Chemical reaction	+ Full-colour + Wide material selection - Require infiltration - High porosity on finished parts
Powder bed fusion	– Laser-based in polymers / SLS – Laser-based in metal/ DMLS, SLM – Electron beam / EBM – Heat-based in polymers / SHS,MJF	Polymers Metals Ceramics Photopolymer ceramics	Laser beam IR projection Electron beam	+ High accuracy and details + Fully dense parts + High strength & stiffness + Support avoiding - Powder handling & recycling
Direct energy deposition	– LENS, DMD – 3D Laser Cladding – WAAM	Metals	Laser beam Electron beam	+ Fully dense parts + Microstructure control - Poor resolution and surface finish - Slow process
Material Extrusion	– FDM, FFF – Contour Crafting	Thermoplastics Ceramic slurries Pastes	Thermal Energy Chemical reaction	+Inexpensive equipment +Multi-material capability -Poor surface finish



The seven categories in which the different AM processes can be grouped are sheet lamination, vat photopolymerisation, binder jetting, powder bed fusion, material jetting, directed energy deposition and material extrusion.

- Sheet lamination processes are based on the addition of sheets in different ways. Under this category, there are two main processes: Laminated Object Manufacturing (LOM) and Ultrasonic Additive Manufacturing (UAM). The first uses sheets of paper and glue to add them together to build the object. In the latter are used sheets or ribbons of metal, which are bound together using ultrasonic welding. LOM fabricated parts have low internal tension, high surface finish details, and low process, machine and material cost (B. Mueller & Kochan, 1999). When the system finishes its fabrication, the non-required material from the laminated sheets should be removed. This tedious task has been an area of investigation and development (Chiu & Liao, 2003; Liao et al., 2003). Recent developments by the company Mcor Technologies have enabled the creation of colourful parts using low-cost printing (Mcor, n.d.).
- Vat photopolymerisation uses the hardening of photopolymers by the action of a light or laser to build the model. Under this category, the most used process is Stereolithography (SLA), which creates the model by curing liquid photopolymer in a vat. With this process, higher resolution models can be obtained than with other processes as the raw material is a liquid and the light that hardens the material can be controlled precisely. Because of its dependence on photopolymerisation, this technology is inherently limited to thermoset polymers, which could contain a mixture with, e.g. ceramics (Gao et al., 2015).
- Material jetting processes are based on the same principle as paper inkjet printers, which transfer ink droplets onto paper. The processes based on material jetting deposit droplets of photopolymer or wax onto the build surface or the previous layer and then are solidified by cooling or radiation (Le, 1998). The possibility to include hundreds or thousands

of nozzles enables the increase in printing speed or multiple materials. The multi-material capability of some of these processes, as of Stratasys' Polyjet or MultiJet Printing (MJP), enables the fabrication of high-resolution parts in 24-bit colour (Stratasys Ltd, n.d.). However, support structures for the overhanging features are needed. Support structures are built in a gel-like or wax material, removed by hand and water jetting (I. Gibson et al., 2015a).

- Binder jetting processes are based on the selective deposition of a liquid polymer onto a bed of powder to glue the powder particles together. This process was developed in the early 1990s and was called 3D Printing (3DP) originally. This technology could be used to process a wide variety of materials, such as metal, ceramic, polymers, or foundry sand (Sachs et al., 2003). Several companies have developed processes based on this technique, although the most well known are the ColorJet Printing (CJP) systems. These systems can deposit binder and colour, creating colourful models.

Furthermore, in binder jetting processes, the powder from previously deposited layers actuates as the support structure for overhanging features (I. Gibson et al., 2015a). These two fundamental characteristics make this technology appropriate for applications like architectural model creation, the reproduction of organic objects, or the creation of full-colour models for sales evaluation. The main drawback of this process is the need for infiltration in the post-processing to increase the part strength. Some companies as ExOne and Voxeljet have developed industrial machines capable of direct mould fabrication for the foundry industry (Wohlers & Caffrey, 2015).

- Powder bed fusion processes use a laser or electron beam to fuse selectively the powder that lays in a container. Usually, the powder is spread over the building platform or the previous layer, then the beam fuses the powder where it is required, and then it is spread to another layer of powder. The main materials used in this process are thermoplastics and metals. The processes that use this technique, as in

binder jetting processes, take advantage of the powder's capability to support the model above it, eliminating the need to design supports for overhanging geometries. This characteristic also allows the fabrication of various parts in the same build run, reducing the cost per part. However, in metal-based processes, sometimes are needed support structures to counteract the warping forces. Selective laser sintering (SLS), selective laser melting (SLM), direct metal laser sintering (DMLS) and Electron Beam Melting (EBM) are the most popular powder bed fusion techniques (I. Gibson et al., 2015a). The technologies Selective Heat Sintering (SHS) and Multi Jet Fusion (MJF) rely on IR radiation to fuse the powder and selective jetting of chemical agents to fuse the powder particles (HP, 2014). The machine and manufacturing cost of the SHS process is significantly reduced compared to the processes in the same category due to the avoiding of expensive power sources as laser or electron beams (Baumers et al., 2015). MJF, SHS and SLS use polymers as the raw material, while SLM, DMLS and EBM fabricate models using metal powder.

- Directed energy deposition processes create the objects by feeding powder or wire into the focal point of an energy beam to create a molten pool (Gao et al., 2015). The build-up of parts in these processes is made in a manner similar to the extrusion-based processes. The deposition head creates a track of solidified material, and adjacent material lines create the three-dimensional object. This approach enables the fabrication of parts onto the surface of already manufactured parts. For this reason, it is commonly used to repair or add additional material to existing parts (J. B. Jones et al., 2012; Wilson et al., 2014). Furthermore, these processes can fabricate parts of almost 100% density. Although it can be used with other materials, the main area of application of these processes is the AM of metallic components.
- Material extrusion processes are based on a tractor-feed system material pushing, which creates the pressure to extrude through a nozzle and the deposition of the extrusion in a controlled way. The extruded material is heated to a semisolid state to bond to the material that has already been



value creation and innovation to the company owner or the licensee of the patent, and consequently, the information sharing. The reduction of communication costs led to the emergence of new forms of information sharing (von Hippel, 2005). This opened the door to individuals and organisations sharing the workload of product development, also called open source development (Haefliger et al., 2008). By the early-2000s, the jurist and Harvard University professor Lawrence Lessig and colleagues proposed a new approach to protecting only a part of the rights with the *Creative Commons* licensing schema. These licenses allow creators to decide which rights they reserve and which rights they do not claim for the benefit of recipients or other creators (Lessig, 2005).

This open-source development model has been widely accepted and thriving within the software industry, with very popular projects like Linux, Apache and Firefox (von Krogh & von Hippel, 2006). The application of this model in the development of physical products, known as “Open Hardware”, has experienced increased attention in recent years (Viseur, 2012). The Open Hardware projects are where the authors make freely accessible the information needed to reproduce the physical product, such as components list, engineering drawings, mounting instructions or source code (Fernandez-Vicente, 2012). One of the most notable Open Hardware projects is the “Arduino” electronic prototyping board, launched in 2005, which provides an easy to use and low-cost platform to control physical objects (Mellis et al., 2007). This prototyping board and similar models enabled the control of complex mechanical systems by a broader range of users due to these two characteristics. Although in the beginning, these prototyping boards were used for simple projects, it was a matter of time that the innovators started to use them for controlling fabrication machines such as CNC, laser scanners, and 3D printers (Anderson, 2010).

The FDM technology was firstly commercialised in the early 90s, and in a decade, it became the most popular additive manufacturing and 3D printing process worldwide (Wohlers, 2016a). In 2006 two different research groups developed a 3D Printing system based on a material extrusion technique similar to FDM. At Cornell University, Dr Hod Lipson team developed the Fab@Home

project, and at Bath University, Dr Adrian Bowyer started the RepRap project (Malone & Lipson, 2007; Sells et al., 2010). These projects had three characteristics in common and were radically different from previous systems:

- Small enough to fit in an office environment
- Open-Source protection of design and user-editable
- Low-cost orientation

Both projects were based on an Open Hardware development model, but the RepRap project proposed an innovative approach, a machine that could build a copy of itself. In order to achieve this objective, they designed a machine with a large percentage of its mechanical components fabricated by the same technology. The extrusion method was based on the principles of the FDM technology, but it was coined as Fused Filament Fabrication (FFF) technology to avoid legal problems (Sells et al., 2010). A crucial characteristic was that RepRap was distributed under an open-source license, allowing the freedom to re-use the software for any purpose, including commercial (Sinclair, 2012).

In 2007 the RepRap project began to gain traction, coinciding with the expiration of some FDM foundation patents held by Stratasys, although some others expired in 2011 (Stratasys, 2010; Wohlers, 2016a). The disruptive yet successful element of the RepRap approach was to create a dedicated wiki with the instructions and digital files of the machine parts, with the support of an online forum. This situation created an ecosystem of individuals who built their own machines and manufactured parts for other people when they managed to have a functional machine (R. Jones et al., 2011). The self-replication characteristic of the RepRap project created exponential growth in the variations of machine designs and new solutions tests that were far beyond the FDM patent owner development (Gilloz, 2012).

Furthermore, the low-cost access to programmable controllers, lasers, inkjet printing and computer-aided design (CAD) software democratised the design process, allowing individuals to utilise, tinker with, and improvise these technologies (Gao et al., 2015). These early adopters of the technology were mainly part of the Do-It-Yourself (DIY) movement, also called “Makers” (Anderson, 2012), the design process and the manufacturing in this movement

are democratised, being carried out more closely to the end user who develops the product (Petrie, 2013).

Consequently, a vital element of this democratisation and the desktop 3D printing raise was the increasing availability of community workshops. The members share access to tools to produce physical goods in these places, such as Hackerspaces, Makerspaces and Fab Labs (van Holm, 2012). The term maker space refers to community workshops where members share tools and are formulated in contrast to hackerspaces, which were considered more focused on computers and electronics (G. Cavalcanti, 2013). These terms have evolved with the addition of other tools such as 3D printers, and currently, hackerspaces are also incorporating physical spaces for collaboration (Moilanen, 2012). In practice, the definitions of these names indicate various activities and suggest different degrees of community involvement (A. G. Smith et al., 2013).

In contrast to the decentralised development and proliferation of maker spaces and hackerspaces, Fab Labs originate directly from the Massachusetts Institute of Technology's Center for Bits and Atoms and the course "How to Make (Almost) Anything". The Fab Labs worldwide are connected in an online network and collaborate to develop Open Hardware projects (A. G. Smith et al., 2013). These workshops are equipped with a set of digital fabrication technologies, including 3D printers, and are open to anyone who wants to learn and fabricate his projects (Menichinelli, 2011). Although the first Fablab outside the MIT was established in 2002, after 2007 the network started to rise till near one thousand Fab Labs currently available around the world (*Labs / FabLabs*, n.d.).

Hackerspaces, Makerspaces and Fab Labs actuate as a local hub of digital fabrication learning and DIY culture spreading and provide the tools needed for new users of these technologies (Fernandez-Vicente et al., 2014). These hubs are physical spaces for the collaboration of "peer-production" communities. Some of the fundamental players of desktop 3D printing machines development, such as Reprap clones, Makerbot (New York, USA) and Ultimaker (Geldermalsen, Netherlands), started from peer-production communities (Moilanen, 2012).

In 2009 some individuals and companies such as Bits from Bytes (currently part of 3D Systems) and Makerbot started to sell do-it-yourself kits with all the components needed to assemble a machine (Pettis et al., 2012). The Makerbot founders “threw out the self-replication requirement” of Reprap and developed a consumer-friendly printer (Courtland, 2013). They included software for slicing STL files and sent the data to the machine in G-code, the standard in CNC machines, which helped the technology adoption by an increasing number of users (Gornet, 2015).

However, a crucial turning point was in 2010 and 2011 when these companies and new competitors, such as *Up!* machines by Delta Micro Factory Corp. (Beijing, China) or Ultimaker launched fully assembled desktop 3D printers. It helped in the widespread distribution of desktop 3D printing to new users without the previously needed electronics and programming knowledge (de Bruijn, 2010).

The launch of online 3D geometry repositories like Grabcad, Thingiverse, or project instructions like Instructables, enabled the sharing of 3D geometries between designers and non-specialised users. In addition, the release of easy-to-use free 3D modelling software like Sketchup provided the tools needed to create digital objects without the engineering knowledge needed in traditional CAD software (*About Instructables*, 2011; Baichtal, 2008; Fernandez-Vicente, 2012; Googler, 2012; G. T. Huang, 2011). Sinclair (2012) identified that the free availability of this type of software is a critical factor in the widespread consumer adoption of 3D printing.



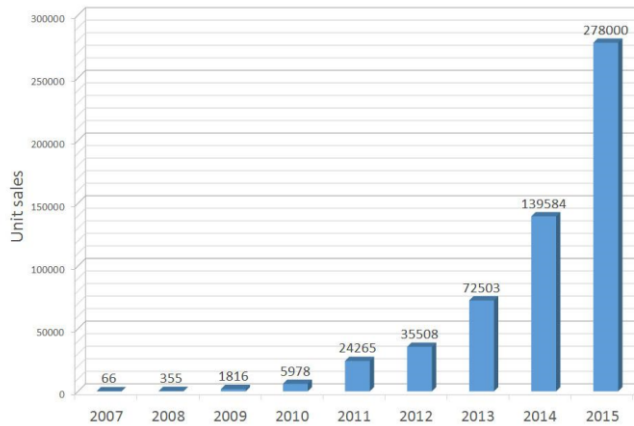


Figure 2.10. Evolution of desktop 3D printers estimated sales. Adapted from (Wohlers, 2016b)

The seed of an increasing community of users capable of fabricating their own goods, in a “*democratisation of manufacturing*” (Mota & Catarina, 2011) was enabled by various elements: More comprehensive offer of low-cost extrusion-based systems in a kit and assembled forms, the availability of 3D models and tools, mixed with the increasing amount of peer-production communities. Moilanen and Vadén (2013) used a survey to assess the 3D printing community patterns and practices and grouped the different stakeholders by their technology adoption: (1) Developers, concerned with the 3D printing development in terms of software or hardware; (2) Early adopters, which bought or assembled their machines in the first phases of technology and often contributed to the community by for example assembly instructions; and (3) Users, people who use 3D printing services. They obtained a model of the ecosystem and identified several elements such as usability, object quality, price and coordination of collaboration as bottlenecks for the third industrial revolution promised by some theorists.

Great attention of media since the presentation by Makerbot of a 3D printer at the Consumer Electronics Show (CES) in 2010, and the announcing of 3D printing as the leading technology of this “next industrial revolution” created a logarithmic growth of machine sales (Anderson, 2010; Markillie, 2012). As shown in Figure 2.10, it is estimated that 66 desktop 3D Printers were sold in 2007, but the actual number is unknown as many users assembled their 3D

Printers with parts printed by other users. These machine sales estimations increased exponentially to near 278,000 systems sold in 2015 (Wohlers, 2016b). This number is impressive compared with the only 12,850 industrial AM systems, priced at more than \$5,000, sold in 2014. Three market segments have emerged in the desktop 3D printing sector (Wohlers & Caffrey, 2015):

- *Good-enough* segment, with a machine price of about €500,
- *Mid-range*, with a price near €1700,
- and *Professional* segment, with a machine cost above €3000.

Nowadays, there are desktop systems based on different AM processes like SLA machines of Formlabs (Somerville, MA, USA). However, FFF technology is by far the main fabrication method (3D Hubs, 2016). This makes FFF the process where more focus is required.

This new industry sector requires tools to exploit the technical possibilities and learn the limitations. This requirement is due to its new type of users without specialised knowledge or dedicated training, as it occurs in industrial-grade AM machines (Gao et al., 2015). The FFF process characteristics will be described in the next chapter to understand the limitations and possibilities.

# Chapter 3

# Fused Filament Fabrication

## 3.1. INTRODUCTION

The FFF technology is based on the deposition of a semi-molten polymer in a controlled manner, as explained in the previous chapter. The polymer is deposited in continuous strands or tracks, usually referred to as beads.

This method of extruding thermoplastic material fed in filament reels offers an easy way to produce three-dimensional objects. As described in the previous chapter, the difference between FDM and FFF mainly relies on the brand registration by the machine manufacturer Stratasys (Eden Prairie, MN, USA). The term FFF is going to be used to refer to this method of manufacturing components.

The working principle of this process is more straightforward than other Additive Manufacturing processes (Canessa et al., 2013). This relative simplicity enables a reduction of the cost of the machines (Frank et al., 2003). In order to develop the knowledge about the behaviour and design guidelines for this process, it is required to identify the different elements involved.

This chapter aims to describe the different components and physics involved in a 3D printing system based in FFF to serve as the basis of the following chapters. Firstly, the different mechanical components that allow the FFF process will be described, and secondly, the process of FFF itself.

## **3.2. FFF 3D PRINTERS COMPONENTS**

The essential elements of a FFF machine will be described in this section to cover the wide range of FFF-based systems available: Extruder, build surface, and machine structure.

The basis of a FFF system is that the extruder deposits the filament, which is usually provided in filament reels, in a build surface in a controlled manner thanks to the machine structure.

### **3.2.1. EXTRUDER & MATERIALS**

Extrusion of viscous thermoplastic is a common industrial manufacturing process, used for a wide variety of applications and products, usually long and uniform profiles. Usually, the material is provided in pellets, and the extruder is a screw, which displaces the solid pellets through the extrusion die.

Some extrusion-based additive machines use pellets as feedstock for purposes such as increasing the range of materials (Spiller & Fleischer, 2018) or increasing the system's throughput by scaling it up (Moreno Nieto & Molina, 2020). However, in FFF, the most common form of feedstock is a filament between 1.75 and 3 mm in diameter, usually provided in spools.

The materials used in FFF systems depend on the machine capabilities and the purpose of the part, but the most common materials in desktop systems are polylactide (PLA) and Acrylonitrile Butadiene Styrene (ABS) (3D Hubs, 2017). A growing range of thermoplastic materials is available such as Nylon, HDPE, PPSF, PEEK, TPU, etc. However, one of the key requirements that determine the composition of the FFF materials is a low shrinkage coefficient (Wang et al., 2007).

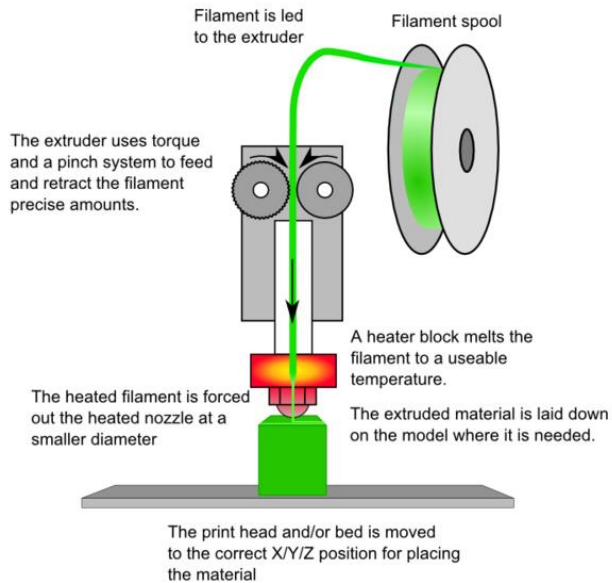


Figure 3.1, Extruder components in an FFF-based process. Source: Reprap.org

The extruder assembly comprises a pinch roller mechanism, which pushes the filament into the heater block, where the filament is heated, as shown in Figure 3.1. The fused filament is extruded through the heater block's end tip or nozzle, which usually has a smaller diameter than the feedstock filament (Bellini et al., 2004).

The filament viscosity is reduced in the heater block through the material heating above the Glass Transition Temperature ( $T_g$ ). This softening allows its deformation to a smaller diameter and improves the bonding with a previously deposited material. The feed rate and the temperature of the heater block determine the rate at which the material could flow through the nozzle, and consequently, the size of the printed bead (Roxas, 2008).

The reduction in diameter of the filament increases the torque required to extrude the material. The pinch roller mechanism provides the transfer of this torque from the motor to the filament. This mechanism has a toothed or grooved surface on one of the rollers, or drive gears, to increase friction. Some

examples can be seen in Figure 3.2. The pressure on the filament between the rollers needs to be enough to avoid slippage but not too much to avoid crushing the filament (Agarwala et al., 1996).



*Figure 3.2. 3D Printer Extruder Filament Drive Gears: a) Plain Insert; b) Raptor Filament Drive Gear; c) MK8 Drive Gear; d) MK7 Drive Gear. Source: Airtripper.com*

The configuration of these components varies from machine to machine. Some systems separate the extruding mechanism from the heater block, fixing the extruder to the machine structure and adding a liner tube between these, which reduces the weight of the moving head. Other large-scale systems include an additional filament pushing system to ease the filament feeding from the spool storage to the extruding head.

### 3.2.2. BUILD SURFACE

The creation of objects in an additive manner implies that the material is added on top of a surface, the build base or material previously deposited. Thermally-induced volume shrinkage of the deposited material happens in the cooling process after the deposition from the  $T_g$  to the chamber temperature. This shrinkage force can lead to warping, inner-layer delamination or distortion of the component (Wang et al., 2007).

Avoiding warping requires a relatively strong adhesion between the deposited filament and the build surface, as well as between the different layers. The polymer crystallisation affects crystalline polymers' thermal and mechanical properties, e.g. the specific heat, the coefficient of thermal conductivity, etc. (Costa et al., 2015). Consequently, the crystallinity of the specific polymer deposited affects the shrinkage and warpage of parts (Chang

& Tsauro, 1995). It determines the build surface selection and design depending as well on the material that is going to be deposited

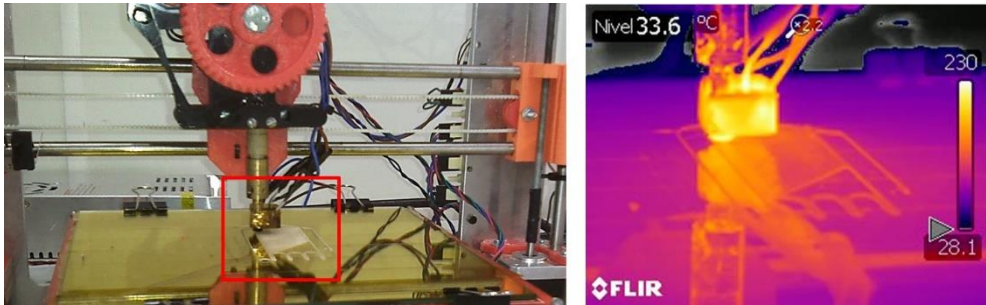


Figure 3.3. Thermal image capture to understand temperature behaviour in build adhesion.

One key element in FFF systems is that the components need to be removed easily from the build surface. Therefore, this adhesion needs to be strong enough during the fabrication, but at the same time should be easy to break to allow removing the component from the build surface afterwards.

There are two approaches to address this issue. One is reducing the thermal gradient between the build surface and the filament, which is achieved using a heated build surface, as shown in Figure 3.3. Some systems heat the building environment, currently under patent by Stratasys (Swanson et al., 2004), or enclose the build area to use the heat produced by the build plate. The other approach is to attach the deposited material mechanically to the build plate. Machine manufacturers have used different mechanical bonding methods:

- Use a perforated build surface, where the deposited material gets attached to the holes (Zortrax, n.d.).
- Use a rough surface; as disposable material such as tape (used widely in the DIY segment) or reusable build surface, e.g. powder-coated build surfaces (Kočí, 2019b).
- Addition of adhesives, such as lacquer or glue. E.g. Glue that the user should apply to the build surface in Ultimaker (Geldermalsen, NL) machines (Ultimaker, n.d.).

- Use a disposable build sheet made of a material that enhances bonding or is similar to the deposited material, e.g. build sheets for each material in Stratasys *Fortus* systems.

### 3.2.3. STRUCTURE

The structure of FFF printers design is a crucial defining element that mainly determines the speed of deposition and the overall machine size, an important factor in the desktop segment. Due to the usually lower cost of FFF printers, the design of the machine structure could determine the quality of the deposition.

The two main approaches are Cartesian and Delta, as can be seen in the figure below, the former being the main structure design currently in use. The Delta configuration provides a slight decrease in printing time compared with the cartesian. However, most vendors opt for the cartesian configuration as it allows a larger build volume area than the overall machine size (Bell, n.d.).

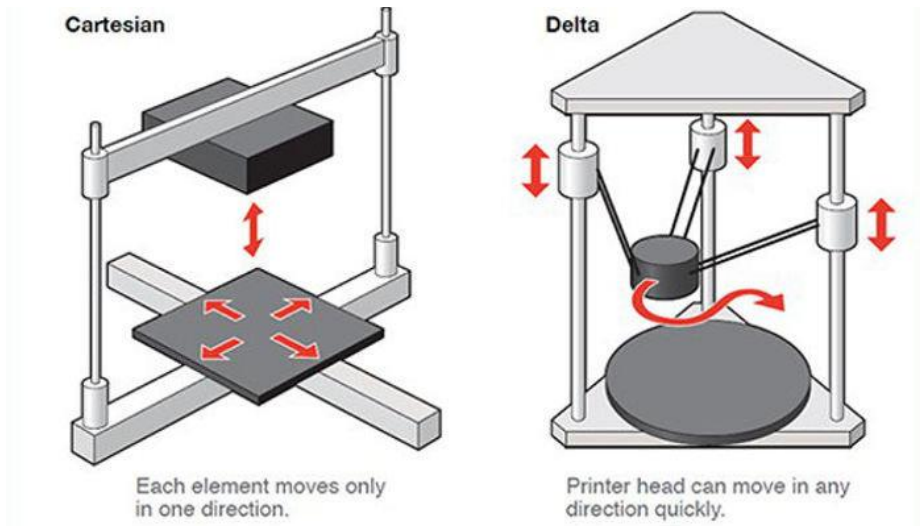


Figure 3.4. The difference between Cartesian and Delta 3D printers, both types of FFF 3D printers.  
Source: 3D natives.com

The configuration of the machine allows the relative displacement between the deposition head and the build surface. This deposition head usually comprises a single head with one or two extruders (Fernandez-Vicente, 2012).



However, some approaches use multiple heads moving independently, which reduce the weight of the deposition head and the risk of collision between the part and the non-working extruder (BCN3D, 2020; Wachsmuth, 2008). The use of two extruders allows depositing different materials through each extruder, enabling the deposition of the support structures with a soluble material (W. Priedeman & Brosch, 2004; Rosales et al., 2017).

The process of the deposition of fused filament is enabled by the components described before. This process is described in the next section.

### 3.3. FFF PROCESS

#### 3.3.1. PROCESS WORKFLOW

In order to understand the FFF process, it is necessary to describe the steps from the design to the final product. Usually, the digital design of the part is sliced in layers (Figure 3.5 B), which determines the accuracy of the physical reproduction of the design, as this produces a staircase-like effect in the surface of the components (Livesu et al., 2017). This effect results from the deviation from the nominal surface and is more pronounced as the surface is closer to the horizontal plane. Worth noting that some approaches are looking into the deposition of curved layers to reduce this effect (Guan et al., 2015).

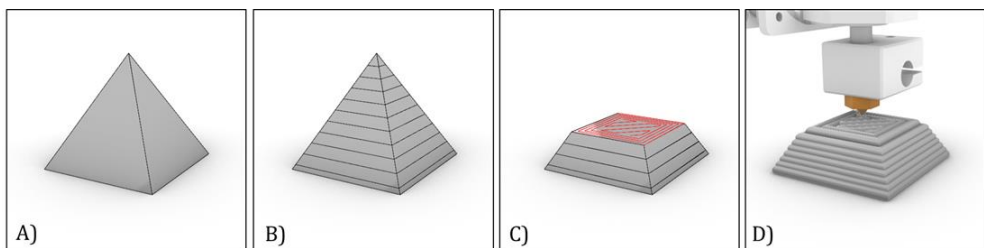


Figure 3.5. Design and build workflow of FFF printing. A) Geometry to be manufactured, B) slicing in layers, C) Toolpath generation for each layer, and D) deposition.

Then a toolpath to fill the area of each slice is needed as the FFF technology is based on the deposition of material by a discrete number of heads as described before (Figure 3.5 C). This toolpath information is then transferred

to the machine controller, following the instructions for building the component (Figure 3.5 D) (I. Gibson et al., 2015a).

Once the machine finishes, the part needs to be removed from the build surface and, if there are any, the supports should be removed. Then sometimes, a set of post-process operations are needed to finalise the product. These could be mechanical, such as sanding, or chemical finishing, such as coating (Chohan & Singh, 2017). These post-processing steps are covered in more detail in another chapter.

### 3.3.2. TOOLPATH

In extrusion-based additive processes, the toolpath to create a three-dimensional component is one of the critical design variables in parts production. It determines the mechanical and quality of the parts (B. Huang & Singamneni, 2012). The toolpaths structure usually comprises a contour or perimeter that helps have a uniform surface and an infill tailored depending on the part's functionality. As can be seen in Figure 3.6, the deposition could leave voids between beads. An infill with more space between beads can reduce build time when the required mechanical properties allow it. This mesostructure can be designed with different patterns to obtain customised anisotropic mechanical properties (Fernandez-Vicente et al., 2016). These anisotropic mechanical properties are due to the alignment of the polymer molecules along the direction of deposition (Es-Said et al., 2000). The deposition pattern significantly affects the part stresses and deflections (Nickel et al., 2001).

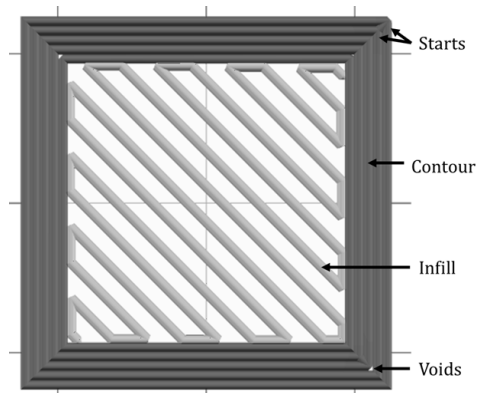


Figure 3.6. Toolpath areas in a FFF part.

The speed of deposition of the toolpath is not uniform and is determined by the capabilities of the filament feeding mechanism.

### 3.3.3. FEED MECHANISM

The diameter of the nozzle determines the extruded strands diameter and consequently the resolution, affecting printed geometry details minimum size and corners rounding radius. The extrusion of strands with a round nozzle and the molten polymer surface tension limit the capability of this type of machine to produce sharp corners (Bellini et al., 2004).

The diameter change inside the nozzle creates stress in the material, released when the polymer is extruded (Michaeli & Hopmann, 2016). This release creates a radial expansion of the melted polymer called die swelling, determining a minimum bead width of 1.2-1.5 times the nozzle diameter (Bellini et al., 2004). The addition of inelastic fillers such as carbon fibres or ceramic particles reduces the die swelling effect (Bellini, 2002; Shofner et al., 2003). Due to this effect, small-sized parts and circular shapes are sometimes oversized and have lesser dimensional accuracy, while shrinkage occurs in large-sized parts (Bakar et al., 2010).

### 3.3.4. DEPOSITION AND BONDING

The deposition of a uniformly sized bead is vital in order to be able to deposit several layers of material. Due to the die swelling effect, the nozzle needs to be

used as a flattening tool to improve the bonding with the build platform and the previously deposited beads (Turner et al., 2014).

The deposition of filaments next or above previous ones involves a cross-linking between them due to viscous sintering, also called the diffusion phenomenon. During this phenomenon, a connection zone between filaments called “neck” is created, which determines the quality of the bond (Costa et al., 2017) and consequently the mechanical properties of the parts produced (Abbott et al., 2018). The material temperature needs to be above the glass transition temperature,  $T_g$ , for this process to happen. The heat from the material being extruded increases the temperature of the bead already deposited above the  $T_g$ . As shown in Figure 3.7, viscous flow and molecular diffusion of polymer chains occur until they are randomised, and the surface tension plays a crucial role in this process (Bellehumeur et al., 2004; Sun et al., 2008). In a) the two beads are just in contact (usually there is an overlap between them to ease this process); b) Shows the neck formation and growth, with the start of the diffusion of the polymer chains; in c) there it is a diffusion, or randomisation, of the polymer chains between adjacent beads.

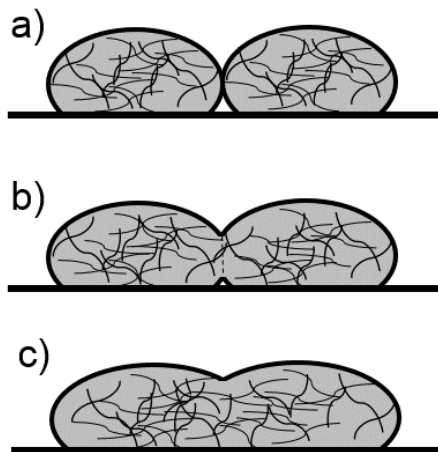


Figure 3.7. Polymer sintering in FFF: a) Contact, b)neck formation, c)diffusion.

The polymer solidifies in a short period involving a highly transient heat process when it is deposited. This quick change is because the build volume temperature is maintained at a much lower temperature than the material's

melting temperature. The bond quality depends on the envelope temperature and variations in convective conditions. Consequently, the diffusion phenomenon is more prominent in the bottom layers (Sun et al., 2008). The primary heat losing effects are conduction to the deposited material and convection to the building environment (Costa et al., 2015).

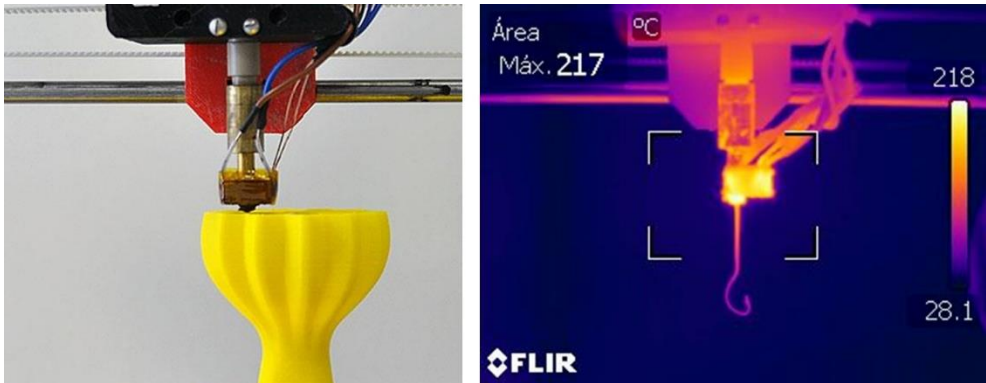


Figure 3.8. Thermal image capture to understand temperature transfer with the environment.

Due to this dependence on the bonding between filaments, the internal structure of FFF fabricated parts could be interpreted as a fibre reinforced composite (Bellini & Güçeri, 2003). However, the bonding formation is affected by the thermal history of the beads, and consequently by the order, or toolpath, followed to deposit each area of the part (B. Huang & Singamneni, 2015).

This influence determines especially the geometry of non-vertical walls. Due to the effect of gravity, the material requires to be deposited on top of other material or adhere to the material already deposited. This adhesion commonly occurs up to an approximate maximum of 45 degrees from the ground between the profiles of each layer (Hambali et al., 2012).

Although still in an experimentation stage, a potential method to improve the mechanical characteristics of FFF components seems to be the production under a nitrogen gas atmosphere. It seems to increase the tensile strength by 30% in ABS or PLA and improve the elongation at break. The improved mechanical properties seem to be due to improved layer adhesion and the

reduction of polymer surface degradation caused by oxidation process suppression (Lederle et al., 2016).

The most common methods to improve the bonding mechanism are fixing the material composition, developing the parameters for that material, and the control of the envelope temperature. These approaches are common in systems aiming at industrial applications and engineering-grade materials, such as Markforged (Watertown, MA, USA), Intamsys (Shanghai, China) or Stratasys systems.

### 3.3.5. PARAMETERS

The successful deposition of geometry depends on the proper selection of process parameters. The process parameters determine the failure rate and the quality of the deposition, influencing, for example, the dimensional precision. However, the FFF process comprises many factors that can affect the part quality and mechanical properties, as shown in Figure 3.9 and Figure 3.10.

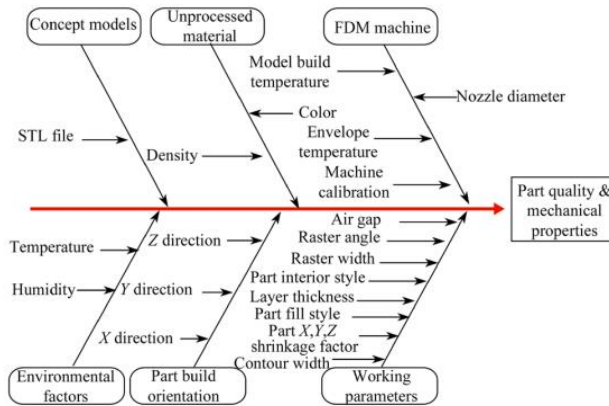


Figure 3.9. Influencing factors in part quality & mechanical properties in FFF (Mohamed et al., 2015).

The machine components can affect the reliability of the deposition, for example, with a drive gear not applying the correct torque to the filament. As described before, the polymer heating, the deposition next to another bead, and its cooling down are the main working principles of the FFF process. Consequently, the thermal characteristics of the material and the build volume

and heater block temperature are critical process parameters to allow the successful diffusion between beads. A large and growing body of literature has investigated the optimisation of these parameters (Alafaghani & Qattawi, 2018; Dey & Yodo, 2019).

The design parameters refer to the design of the geometry and the deposition toolpath. As a single head performs the deposition, it creates a structure of beads adhered between them. The design of this structure, such as the distance vertically (layer height) or horizontally (overlap or air gap), determines the aesthetic and especially the parts' mechanical properties. This topic will be addressed in detail in another chapter of this document.

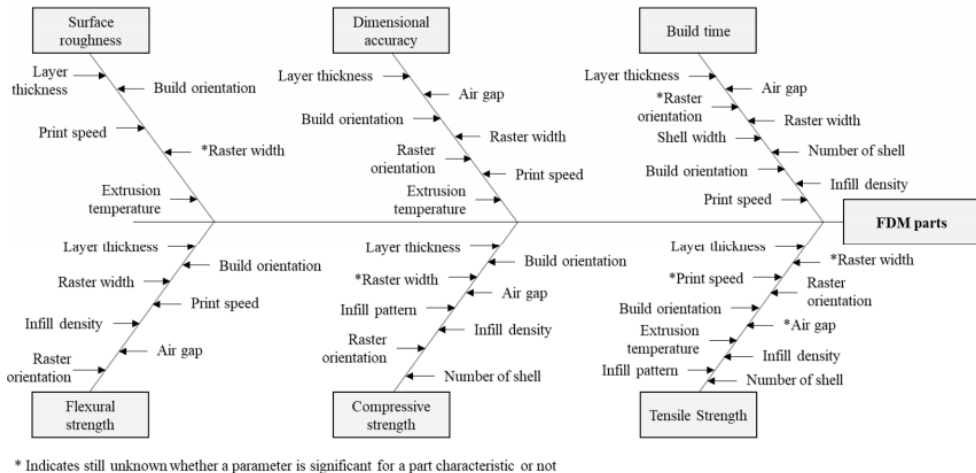


Figure 3.10. Fishbone diagram to illustrate the impacts of process parameters on part characteristics (Dey & Yodo, 2019).

As shown in Figure 3.10, the parameters can be classified by the type of part characteristic, such as surface roughness, dimensional accuracy, build time, or strength. The optimum value of the parameters is determined by the objective or functionally required by the part. For example, the parameter of height between layers determines the distance of a set of discrete steps in the z-direction, resulting in a staircase effect (Agarwala et al., 1996). Build time increases when slice thickness is decreased and increases the accuracy (Han et al., 2003; Turner & Gold, 2015). Therefore, the part characteristics, or purpose,

needs to be determined to identify the parameters that need to be modified and optimised.

### **3.4. SUMMARY**

This chapter has described the standard components that comprise the machines based on FFF and their influence in the process. The melting and deposition characteristics have been discussed, and the parameters involved in the process and their influence.

This chapter serves as the baseline and concept definition for other chapters in this document where the influence of the parameters in specific characteristics such as the geometry accuracy or the mechanical performance will be described in more depth.



# Chapter 4

# Design for Additive Manufacturing

## 4.1. INTRODUCTION

When designing innovative products or components, after a brief or set of requirements has been received, the designer needs to apply *divergent thinking* to create different concepts where the number is more important than their feasibility. These concepts need then to be refined, combined, and rejected, with a *convergent thinking* mindset, until one solution is developed, considering the manufacturing capabilities (Laurel, 2003).

The Design Council from the United Kingdom implemented these two types of mindset into a framework for innovation called *Double Diamond*, where divergent and convergent thinking are alternated. This framework includes four phases, which are: Discovery, Definition, Development, and Delivery, as can be seen in Figure 4.1. The first two focus on developing a valid problem statement. Then the Develop stage comprises the ideation of creative potential solutions to the problem. It is critical to support the designer at this stage to amplify the innovation (Camburn et al., 2017). In the last stage, Deliver, the designer transforms and synthesises the ideas into a final functional design outcome (Design Council, 2005).

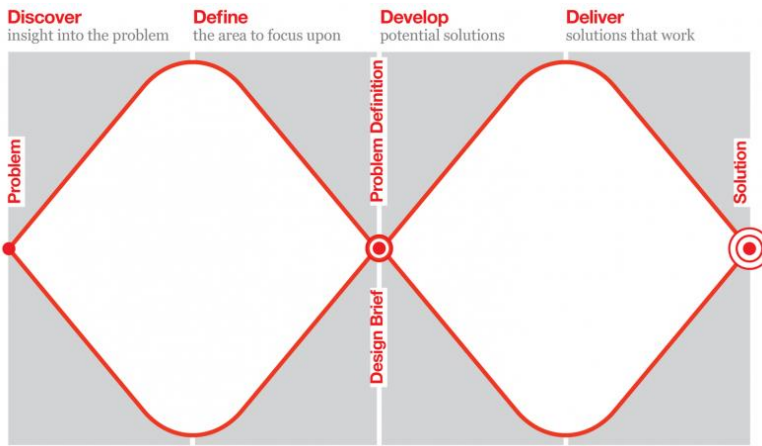


Figure 4.1. Double Diamond design framework.

3D Printing, or AM, allows the creation of complex design solutions and opens up new opportunities for improved products. Until recently, just prototypes and models could be produced due to the capabilities of the AM technologies. The technology users did not need to modify their approach to design because the components would end up being produced by traditional processes. Currently, end-use parts products and tools can be produced due to the maturing of the technology with improvement in material properties and accuracy (I. Campbell et al., 2012). Therefore, there is a need to help designers leverage the unique design opportunities and advantages of AM and obtain optimal results (Gerber, 2008; Perez, 2018).

Like any other manufacturing technology, each AM technology has its limitations that need to be considered. *Design for X* (DFX) refers to the methods for integrating different considerations into the design process, into the 'Deliver' phase. *Design for Manufacturing* (DFM) and *Design for Assembly* (DFA) are widely used DFX methods to optimise a product design with its production system. The aim is to reduce development time and cost and increase performance, quality, and profitability. These methods are commonly integrated under the term *Design for Manufacturing and Assembly* (DFMA) (Boothroyd et al., 1998).

The term DFM has been transferred to AM as *Design for Additive Manufacturing* (DfAM). DfAM is defined as

*Synthesis of shapes, sizes, geometric mesostructures, material compositions and microstructures to best utilise manufacturing process capabilities to achieve desired performance.* (Rosen, 2007)

DfAM is a set of methods and tools that help designers take into account the specificities of AM during the design stage and leverage the capabilities of the technology (Kumke et al., 2016; Laverne et al., 2015). It could be linked with the *Design With X* (DWX) approach, whose objective is “*to inspire designers and support them in creating products [because DWX focuses] on innovations so the product design solutions have always an innovative character*” (Langeveld, 2006). Therefore, while DFM is applied just in the ‘Deliver’ phase of the design process, the design of products for AM comprises the ‘Develop’ stage as well (*Design with AM*), as shown in Figure 4.2. At the Develop stage, the designers are working to produce design outputs that fulfil two essential criteria: originality and appropriateness (Howard et al., 2008).

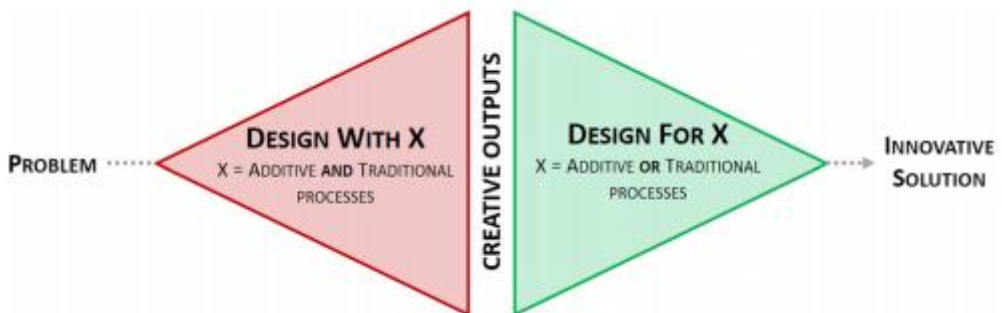


Figure 4.2. DWX and DFX in the innovation process. Adapted from Laverne et al. (2014)

This chapter aims to provide an overview of the models, strategies, procedures, methods and tools proposed in the literature to support the design of products produced by Additive Manufacturing. This review will help identify a promising approach for developing the design guide, the purpose of this thesis.

A large and growing body of literature has investigated the process of design products produced by AM for the AM processes. Some studies focus on the rules needed to get a successful outcome. However, these do not necessarily take into account or provide guidelines to leverage the AM-enabled design freedom. Some studies focusing on this aspect are covered in the next section. Laverne et al. (2015) distinguished these two approaches as 'restrictive' and 'opportunistic' methods. Some approaches combine both aspects or provide comprehensive DfAM methodologies. These are described in the last section.

## **4.2. USE OF AM POTENTIALS**

The creation of components sequentially layer by layer enables to make more complex geometries. The increase of complexity has a negligible impact on the cost of the parts, and the designers, therefore, require to be more creative to make full use of the capabilities and exploit the design opportunities that AM brings (Hague et al., 2003). Thompson et al. (2016) provide examples of these capabilities, or design freedoms classified by their scale: at the part level with macro-scale complexity (multicolour, internal geometries, topology optimisation, and mass customisation), at the material level with microscale complexity (multi-material composition, custom surfaces, and lattices), and at the product level (Part consolidation, embedded electronics, and direct production of assemblies).

Becker et al. (2005) studied the possibility of using 3D printing not only as a prototyping method but also to produce functional parts in small quantities. They introduced a series of design best practices to help design products with these technologies.

Most of the literature only discusses the benefits used in specific cases with specific requirements, which could be challenging to transfer to other product categories (Thompson et al., 2016). However, some studies provide methods to utilise a specific design opportunity by using general design methods. For example, Leary et al. (2014b) and Gaynor et al. (2014) describe the application of topology optimisation, a proven optimisation method to lightweight structures (Bendsoe & Sigmund, 2013), bringing as well the specific limitations

of AM. Another example is the use of the system of questions used in DFA and the TRIZ analysis to optimise designs by the consolidation of parts (Altshuller et al., 1998). Rodrigue and Rivette (2011) used this approach to develop a design methodology (Figure 4.3, left) that aims to reduce the number of joints between parts by using a flow chart in the embodiment phase of the design process. Boyard et al. (2013) developed a method of parts consolidation based on the principle of abstraction and parallelisation of DFA and DFM. In their approach, a structure graph composed of functional sets is developed (Figure 4.3, right), then for each functional set, a search in a database of existing solutions is performed and adapted to the specific geometry. Both flow charts and structure graphs are typical tools being used in conventional design methodologies.

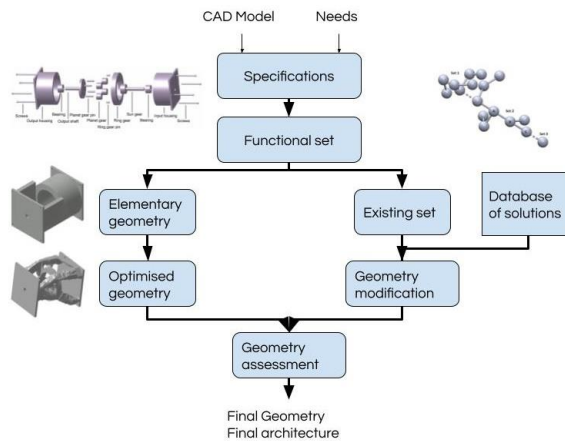


Figure 4.3. Part consolidation workflow methods, adapted from Rodrigue and Rivette (2011) and Boyard et al. (2013)

Some methodologies have been proposed for simultaneous use of more than one AM design potential. The approach by Burton (2005) used a questionnaire to identify the potentials that could be applied to the design. Bin Maidin et al. (2012) investigated further following this approach by developing a design feature database. They developed a taxonomy to classify the design opportunities and support the designer by providing examples of application for each design opportunity. Their taxonomy classifies 113 AM features into

four groups: user fit requirement, improve functionality, part consolidation and aesthetic. The provision of a database of examples was also used by Doubrovski et al. (2012), suggesting its implementation into a knowledge database that could be edited collaboratively, in a similar way as a wiki.

The extraction and codification of design knowledge to be communicated to designers is a further step from collecting and classifying examples to improve the quality of the designers' outcome. This design knowledge could be codified into design heuristics, guidelines or principles (Fu et al., 2015).

The approach of providing examples to elicit designers' creativity was further developed into design heuristics by Blösch-Paidosh and Shea (2017). After collecting AM components and analysing their key features, they compiled and combined context-dependent directives, design heuristics, which provide design direction to increase the chance of reaching a satisfactory solution. Blösch-Paidosh developed a set of cards to convey the relevant content to the designer, with text, schematic representation, and an application example, as shown in Figure 4.4. The use of images aids in comprehending the concepts and in the design by analogy (Perez, 2018).

They classified the 25 design heuristics into eight categories: Part Consolidation, Customisation, Convey information, Material, Material Distribution, Embed-Enclose, Lightweight, and Reconfiguration.

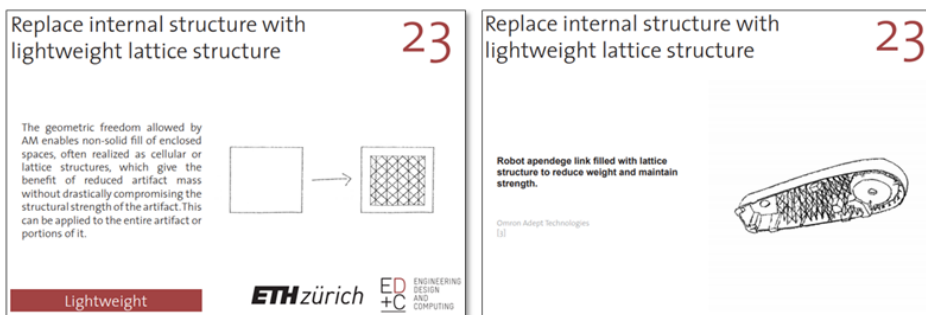


Figure 4.4. Example of the Design Heuristics for AM cards (Blösch-Paidosh & Shea, 2017).

The provision of these cards to novel designers seems to increase the novelty from an AM perspective and the range of the novel aspects (Blösch-

Paidosh et al., 2019). These seem to help integrate the four unique design complexity opportunities of AM, namely shape, material, hierarchical, and functional complexity (I. Gibson et al., 2010). Other studies have shown as well that the use of design heuristics seems to open up possibilities for engineers with limited experience in AM to clearly explore the new design space (Lindwall & Törlind, 2018). Furthermore, it seems that this type of inspiration is most helpful to designers who might have limited exposure or expertise to a specific technology or area (Perez et al., 2019).

Providing novice designers with examples and heuristics foster the creativity and the exploitation of the design opportunities provided by AM, as found by the previous studies. However, providing information to the designers just about the AM potentials seems to generate less feasible design concepts (Sinha et al., 2017). Therefore, it is necessary to provide as well information about the limitations of the technology or design rules. Some authors indicate that the AM processes design restrictions should be considered in the early stages to avoid many iterations of a design to get it suitable for production (Emmelmann et al., 2017). However, as Laverne et al. (2017) emphasise, to obtain better outcomes, it is helpful to provide the 'opportunistic' knowledge in the early design stages and the 'restrictive' knowledge later in the design process.

### **4.3. DESIGN RULES**

The need to provide information to the designers about manufacturing process capabilities and costs has been recognised for many years (Swift & Booker, 2013b). DFM as an integral methodology aims to simplify the manufacturing process, increase productivity and minimise cost while maintaining the product quality at a desirable level (Effa et al., 2015). It requires a fundamental understanding of (a) the technical capabilities and (b) variability in machine performance, dimensional accuracy and effects on the product quality (Kalpakjian & Schmid, 2013). This information transfer is done by providing a series of guidelines, principles and recommendations to modify component designs (Swift & Booker, 2013b).

The benefits of DFM can be summarised as (Asadollahi-Yazdi et al., 2016):

- Improving the quality of new products during the developing period, including design, technology, manufacturing or service.
- Cost reduction, including the cost of design, technology, manufacturing, delivery, technical support or discarding.
- Reduction in development time for new products, including design time, manufacturing preparing, and repeatedly calculation.
- Improving manufacturing by ensuring the quality and reliability.
- The manufacture participation in the upstream process.
- Improving the communication between the departments.

Swift & Booker (2013b) identified a number of DFM rules that could be applied widely for several processes, including AM, such as:

- Select materials to suit the process, as well as the lowest cost and availability
- Design parts without abort changes in section. Aim at uniform wall thickness, cross-sections and gradual changes.
- Put a price on every tolerance and surface finish (identify which tolerances are critical)
- Aim for minimum weight consistent with strength and stiffness requirements
- Aim to fulfil several functions with a single component

Their rules build on the earlier DFM principles and rules from Stoll (1986): Minimise the total number of parts, develop a modular design, use standard components, design parts to be multi-functional, and design parts for multi-use (Stoll, 1986).

These studies highlight how some of the principles of DFM are common between manufacturing processes. The main common element is the characteristic that DFM for any process aims to produce objects more efficiently and economically by setting a mindset in which manufacturing input is used at the earliest stages of design (Edwards, 2003). However, establishing quantitative relationships between the design and the physical component is



essential in order to be able to analyse and optimise a design for ease of manufacturing (Kalpakjian & Schmid, 2013).

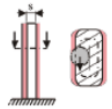
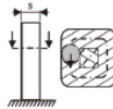


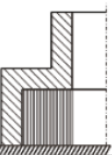
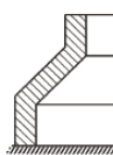
Element		Information	Examples		Techn.						
Group	Type	Attribute	Description	Not suitable for manufacturing	Suitable for manufacturing	LS	LM	FDM			
Basic Elements	Plates	Thickness	Plates should be so thick that each layer can be structured of a contour with inscribed raster to minimize dimensional deviations and to avoid defects.  LS: S > 1,0 mm LM: S > 0,6 mm FDM: S > 1,5 mm			X	X	X			
			Element transitions	Firmly bonded	Inner corners	Interior corners should be rounded to remove disperse support material more easily.			X	X	
			Aggregated structures	Overhangs	Length	The length of an overhang should be small enough to avoid solid support material. Otherwise overhangs should be designed with element orientations that don't require solid support material.				X	X

Figure 4.5. Standard elements and design rules. Adapted from Adam & Zimmer (2014)

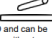



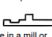



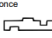
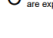


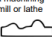
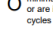


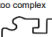
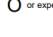





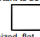
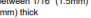


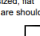



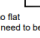
DFM applied to AM is one of the most well-researched areas of DfAM as most DfAM methods and principles fall into this category (Kumke et al., 2016). Most academic research on AM design rules comprises the compilation of design features catalogues for a specific technology. Most catalogues focus on Selective Laser Melting (SLM), Selective Laser Sintering (SLS), and Fused Deposition Modelling (FDM). For example, Thomas (2009) identified the quantitative limitations for geometric features in SLM and provided recommendations to obtain good results, such as the build orientation and surface roughness relationship. Seepersad et al. (2012) investigated the limiting feature sizes for different types of features (holes, cylinders, walls, and fonts) depending on their orientation to establish a designer's guide for dimensioning and tolerancing SLS parts. As can be seen in Figure 4.5, Adam & Zimmer (2014) developed a catalogue with *standard elements* (e.g. gap height, wall thickness), *element transitions* and *aggregated structures* (arrangements of

two or more *standard elements* and their transitions) for SLM, SLS, and FDM. Emmelmann *et al.* (2017) followed the same approach, using the VDI 2222 guideline as a template, but divided the catalogue sections into geometry form, part placement, and final machining.

Other approaches suggest a checklist of design features to help the designer systematically assess the detailed design of the parts (T. R. Kannan, 2017). Booth *et al.* (2017) developed the concept of a checklist into a single-page design assessment tool to filter out inefficient designs, as shown in Figure 4.6. After its application into their 3D Printing lab, where the users are usually novices, they observed an 81% reduction in designs not adapted to the process. These findings highlight the need to provide quick and easy to apply methods for novice designers.

**Design for Additive Manufacturing**

A quick method for reducing the number of printing and prototyping failures. by Joran Booth  
 Instructions: Mark one for each category for the part you plan to print. Check daggers and stars first, then scores

Mark One	Complexity	Mark One	Functionality	Mark One	Material Removal	Mark One	Unsupported Features	Sum Across Rows	Totals
<input type="radio"/>	The part is the same shape as common stock materials, or is completely 2D 	<input checked="" type="radio"/>	Mating surfaces are bearing surfaces, or are expected to endure for 1000+ of cycles 	<input type="radio"/>	The part is smaller than or the same size as the required support structure 	<input type="radio"/>	There are long, unsupported features 	x1 =	
<input checked="" type="radio"/>	The part is mostly 2D and can be made in a mill or lathe without repositioning it in the clamp 	<input checked="" type="radio"/>	Mating surfaces move significantly, experience large forces, or must endure 100-1000 cycles 	<input type="radio"/>	There are small gaps that will require support structures 	<input type="radio"/>	There are short, unsupported features 	x2 =	
<input type="radio"/>	The part can be made in a mill or lathe, but only after repositioning it in the clamp at least once 	<input type="radio"/>	Mating surfaces move somewhat, experience moderate forces, or are expected to last 10-100 cycles 	<input type="radio"/>	Internal cavities, channels, or holes do not have openings for removing materials 	<input type="radio"/>	Overhang features have a slopped support 	x3 =	
<input type="radio"/>	The part curvature is complex (splines or arcs) for a machining operation such as a mill or lathe 	<input type="radio"/>	Mating surfaces will move minimally, experience low forces, or are intended to endure 2-10 cycles 	<input type="radio"/>	Material can be easily removed from internal cavities, channels, or holes 	<input type="radio"/>	Overhang features have a minimum of 45deg support 	x4 =	
<input type="radio"/>	There are interior features or surface curvature is too complex to be machined 	<input type="radio"/>	Surfaces are purely non-functional or experience virtually no cycles 	<input type="radio"/>	There are no internal cavities, channels, or holes 	<input type="radio"/>	Part is oriented so there are no overhang features 	x5 =	
<input type="radio"/>	Some walls are less than 1/16" (1.5mm) thick 	<input type="radio"/>	Interior corners have no chamfer, fillet, or rib 	<input type="radio"/>	Hole or length dimensions are nominal 	<input type="radio"/>	The part has large, flat surfaces or has a form that is important to be exact 	x1 =	
<input type="radio"/>	Walls are between 1/16" (1.5mm) and 1/8" (3mm) thick 	<input type="radio"/>	Interior corners have chamfers, fillets, and/or ribs 	<input type="radio"/>	Hole or length tolerances are adjusted for shrinkage or fit 	<input type="radio"/>	The part has medium-sized, flat surfaces, or forms that are should be close to exact 	x3 =	
<input type="radio"/>	Walls are more than 1/8" (3mm) thick 	<input type="radio"/>	Interior corners have generous chamfers, fillets, and/or ribs 	<input type="radio"/>	Hole and length tolerances are considered or are not important 	<input type="radio"/>	The part has small or no flat surfaces, or forms that need to be exact 	x5 =	
<b>REID DESIGN LAB</b> RESEARCH IN ENGINEERING AND DESIGN				<b>Starred Ratings</b> + Consider a different manufacturing process + Consider redesign + Strongly consider a different manufacturing process		<b>Mark One</b> 8-15 Needs redesign 16-24 Consider redesign 25-32 Moderate likelihood of success 33-40 Higher likelihood of success		<b>Total Score</b> Overall Total	

Caution: The Design for Additive Manufacturing Worksheet by Joran W. Booth, 2015. This work is licensed under the Creative Commons Attribution-NonCommercial-ShareAlike 4.0 International License. To view a copy of this license, visit <http://creativecommons.org/licenses/by-nc-sa/4.0/>

Figure 4.6. Design for AM worksheet proposed by Booth *et al.* (2017)

In addition to academic research, the machine manufacturers and service bureaus have increasingly created design rules and best practice guidelines. In the case of FDM, Stratasys (2013) provides some information in the form of design guidelines and techniques to take advantage of FDM capabilities and

improve part quality and process efficiency. Through their service bureau, Stratasys Direct provides detailed design tips and recommendations for design features such as e.g. living hinges, pins, text, threads or wall thickness, and for finishing and secondary operations (Stratasys Direct, 2015).

3D Hubs, an online platform connecting several AM service providers, developed a knowledge base with various design guidelines for the processes offered. In the case of FDM, they provide “how-to” guidelines (e.g. how to design living hinges), design recommendations for various design features as well as general rules of thumb (Hudson, n.d.).

Due to the increased public attention to the FFF technology, some books have been published that provide design rules for this technology. Redwood et al. (2017), from 3D Hubs, collected the information of the knowledge base from their website in a book. They provided as well a summary of recommended design features dimensions for various technologies in a poster format, as can be seen in Figure 4.7. These values, however, are not based on test data or specify which boundary conditions were used. As Adam and Zimmer pointed out, numerical values are only valid for the respective boundary conditions (i.e. machine, material, parameter set and layer thickness) (Adam & Zimmer, 2014).

	Supported Walls	Unsupported Walls	Support & Overhangs	Embossed & Engrooved Details	Horizontal Bridges	Holes	Connecting /Moving Parts	Escape Holes	Minimum Features	Pin Diameter	Tolerance
	Holes that are connected to the rest of the part on at least two sides.	Unsupported walls are connected to the rest of the part on less than two sides.	The maximum angle a wall can be printed at without requiring support.	Features on the model that are added or removed below the model surface.	The span a technology can print without the need for support.	The minimum diameter a technology can successfully print a hole.	The recommended clearance between two moving or connecting parts.	The minimum diameter of escape holes to allow for the removal of build material.	The recommended minimum size of a feature to ensure it will not fail to print.	The minimum diameter a pin can be printed at.	The expected tolerance (dimensional accuracy) of a specific technology.
Fused Deposition Modeling	0.8 mm	0.8 mm	45°	0.6 mm wide & 2 mm high	10 mm	Ø2 mm	0.5 mm		2 mm	3 mm	±0.5% (lower limit ±0.5 mm)
Stereolithography			support	0.4 mm wide							±0.5%

Figure 4.7. Section of Design Rules for 3D Printing poster (Redwood et al., 2017)

Micallef (2015) provides an overview of different examples, free software to design FFF components, and guidelines and best practices for various design features. Other similar books provide a gathering of best practices for different features or situations (Smyth, 2015), or include information about other related technologies such as 3D scanning (Bernier et al., 2015).

## 4.4. COMBINED METHODS

The provision of the AM design potentials increases creativity, and the indication of AM design rules ensure manufacturability. However, the application of only one of these aspects could reduce the creation of optimal components. For this reason, some studies combine both design potentials and rules into their approaches.

Gerber (2008) identified the novel capabilities of AM and compared them to the capabilities of conventional manufacturing. He also created a classification of design recommendations on different design features for SLS (e.g. Corners, screw threads, ribbing or mounting bosses). However, the implementation of these is not discussed.

Ponche et al. (2012) and Vayre et al. (2012) propose similar DfAM methodologies that use the functional specification and process restrictions to define a part design, instead of using the 'original' geometry as starting point, to not limit the geometry by an initial idea of the part shapes. Ponche et al. developed further the design methodology to optimise the manufacturing process through process simulation by splitting it up into three steps (to balance functional requirements and process specifications): (1) part orientation, (2) functional optimisation, and (3) manufacturing paths optimisation (Ponche et al., 2014). Other studies combine the use of design rules with topology optimisation (Leary et al., 2014a), and a bionic catalogue (Emmelmann et al., 2011), or part consolidation (X. Fischer & Nadeau, 2011; S. Yang et al., 2015).

Klahn et al. (2014) proposed a method to identify the components of design for AM based on the criteria including integrated design, individualisation, lightweight design and efficiency. These components were analysed due to the different requirements to develop DFM in both technical and economic directions. A further case study identified the lack of guidelines for the overall design process (Leutenecker-Twelsiek et al., 2016).

The design knowledge could be codified into *design principles*, similar to the *design heuristics* previously described. Design principles are "*fundamental*

rules or laws, derived inductively from extensive experience and/or empirical evidence, which provide design process guidance to increase the chance of reaching a successful design solution” (Fu et al., 2015). Perez et al. (2015) extracted 23 design principles from the study of design evolution in a crowdsourced repository. These principles are constructed in a syntax to give an actionable recommendation to improve a specific design goal (*Improve x by doing y*). They classified them by the level of specificity into four categories: (1) design for manufacturing, (2) design for digital manufacturing, (3) design for AM, and (4) design for Fused Deposition Modelling.

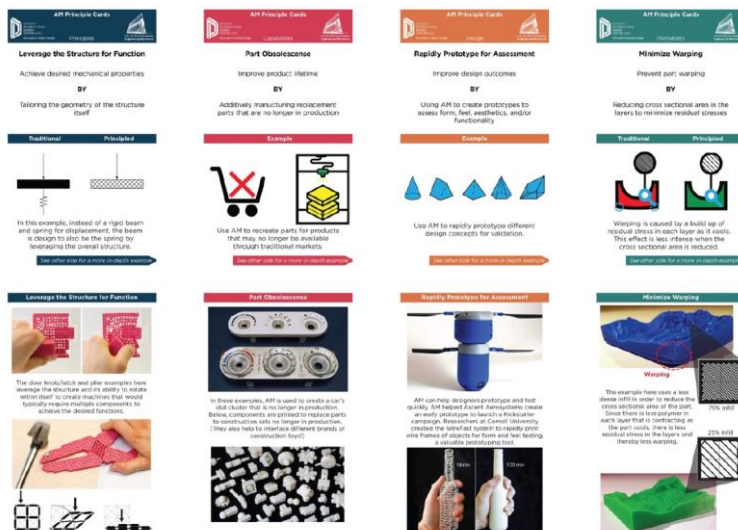


Figure 4.8. Examples of AM Principle Cards (Lauff et al., 2019)

They presented the principles to designers in card format, with a) the principle descriptions, b) a graphic illustrating the principle, and c) an example of application of the principle, as can be seen in Figure 4.8. These were categorised into product, business process, design process, and printing (in the cards ‘*principles, capabilities, design, and printability*’ respectively) (Lauff et al., 2019). It can be observed that some of the principles extracted are inherent to AM and do not directly support providing a better design outcome. However, the principles within the product category could support the use of the design

opportunities in the conceptual stage, and the ones in the printing category could be used in the detail stage.

## **4.5. SUMMARY**

This chapter has provided an overview of DfAM and the methods and tools proposed in the literature, from using the opportunities to the design rules. Several studies have highlighted the need to change the mindset from the Design *for* AM to the Design *with* AM. In different terms, but always with the idea that novel designers require support in divergent and convergent phases of the design process.

The following chapter will investigate the critical design features that need to be considered in DfAM.

# Chapter 5

## Design Features determination

### 5.1. INTRODUCTION

Understanding the geometrical and mechanical behaviour of the process is crucial for the successful design of functional components. The characteristics of each process determine the features that the designer needs to take into consideration (Boothroyd et al., 1998). The common practice to assess the capabilities of a process for each of those features is the development of benchmarking geometries, also called test parts or specimens. These geometries could be measured quantitatively or qualitatively. The quantitative dimensioning of features performed by a novel designer could be hindered by the lack of experience in Geometric Dimensioning & Tolerancing (GD&T) or adequate metrology tools. Therefore, the tools to support designers in understanding mechanical and geometrical behaviour should consider this limitation.

In AM, the test parts could be categorised into three different types according to their target functions: Geometric, mechanical, and process benchmark (Fahad & Hopkinson, 2012; Wong et al., 2002):

- Geometric benchmark – Used to evaluate the geometrical quality of the features generated by a specific set of Machine, Material and Parameters (MMP). These could measure tolerances, accuracy, repeatability and surface finish

- Mechanical benchmark – Used to compare the mechanical properties of features or geometries generated by a certain MMP. Properties such as tensile strength, compressive strength or creep.
- Process benchmark – Used to develop the optimum process parameters for features and geometries generated by specific process systems or individual machines. These are parameters such as temperature, layer thickness or speed.

The geometric and mechanical performances are essential elements to be understood by a designer. The scope of the process benchmark test parts focuses on developing process parameters instead of the design and therefore is outside the scope of this work.

This chapter will study the geometric benchmarking, while the next will investigate the mechanical performance benchmarking.

## **5.2. PRIOR WORK**

Much of the current literature to support designers in understanding AM geometric performance may be divided into three main classes: a) dimensional benchmarking and b) design rules.

Understanding the geometric capability of the processes is one of the key elements that helps designers produce successful outcomes (Seepersad et al., 2012). Various studies propose a Geometric Benchmark Test Artefact (GBTAs) to understand this capability (Fahad & Hopkinson, 2012; Johnson et al., 2014; Minetola et al., 2016; Moylan et al., 2012). This approach has even been taken by ISO and ASTM by developing a standard, ISO/ASTM 52902, to characterise AM systems' geometric accuracy, surface finish and minimum feature sizes. This standard provides a set ofGBTAs: Linear dimensioning, circular accuracy, minimum pin diameter, minimum hole size, thin walls, minimum slot width, and angled surface texture (ISO/ASTM, 2019). Some of these are illustrated in Figure 5.1.



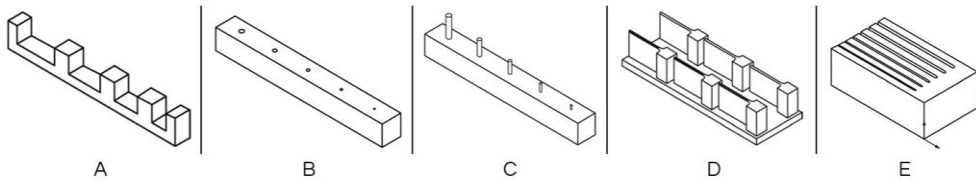


Figure 5.1. Illustration of some GBTAs from ISO/ASTM 52902. a) Linear dimensioning, b) resolution holes, c) resolution pins, d) resolution ribs, e) resolution slots.

In terms of design rules, the typical approach in the literature is to provide “best tips”, limitations, or considerations for a set of specific design features (Emmelmann et al., 2017; Stratasys Direct, 2015; Thomas, 2009). ISO and ASTM address this by the standard technical guideline ISO/ASTM 52910. As shown in Figure 5.2, this technical guideline classifies a broad range of design considerations into seven categories: Product, usage, business, geometric, material property, process, and communication.

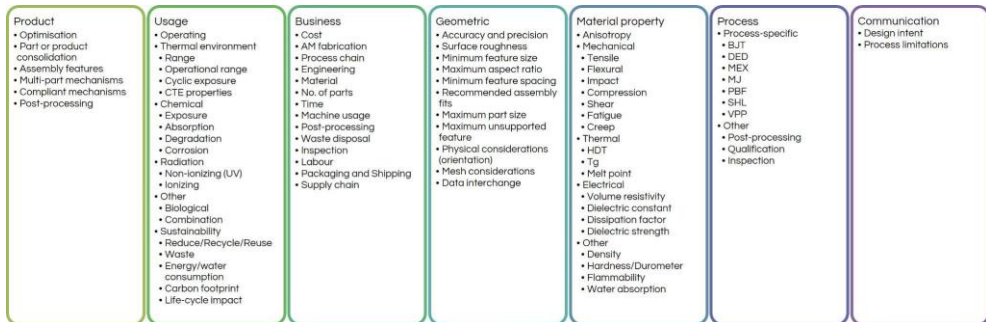


Figure 5.2. AM Design considerations identified in ISO/ASTM 52910.

This categorisation could be used to identify the requirements of a product to be produced by AM and define the scope of design guidelines. This technical guideline identifies design opportunities, limitations and considerations, providing general guidance but not specific design solutions or process/material-specific data.

### 5.3. FEATURES IDENTIFICATION

A set of design features could be extracted by analysing the literature regarding the design rules provided and the proposed GBTAs. Table 5.1 below illustrates

the breakdown of design features in the design guidance or benchmarking geometry found in some of the literature studies and online guidelines.

Table 5.1. Summary of design features found in the literature of design guidelines and benchmarking geometries.

	Adam (2014 & 2015)	Johnson (2014)	Minetola (2016)	Stratasys (2015)	Redwood (2017)	Micallef (2015)	Urbanic (2016)	ISO/ASTM 52902	ISO/ASTM 52910
Angled walls	x	x	x	x	x	x	x	x	x
Overhangs	x				x	x	x		x
Bridges	x				x	x			x
Details & text		x		x	x	x	x		x
Thin walls	x	x	x	x	x	x	x	x	
Columns and pins	x	x	x	x	x			x	x
Holes	x	x	x	x	x	x	x	x	
Gaps/slots	x		x		x		x	x	x
Hemisphere		x	x						
Threads				x					
Fillets				x		x			
Living hinges				x		x			
Clearance				x	x	x	x		x
Infill density & pattern					x	x			x

The table shows that the first eight features (up to gaps/slots) in the table and *clearance* are the most common in literature. The hemisphere is a common feature in dimensional metrology but not relevant for providing guidance. Threads and fillets are specific cases of detailed features. Living hinges behaviour is a particular case in assembly features. Infill density & pattern is a feature that seems to determine the mechanical behaviour (Afrose et al., 2016; Montero et al., 2001), and therefore will be covered in that section.

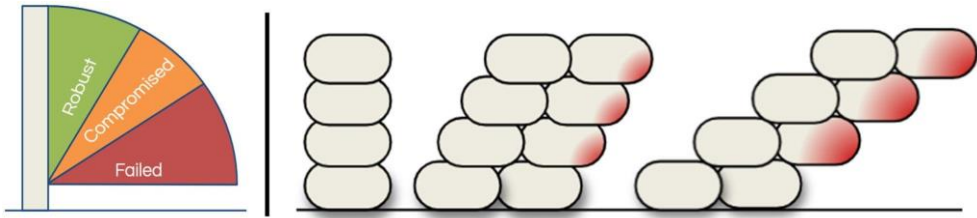


Figure 5.3. Distinct zones in angled walls (left) and an illustration of overhanging areas at the mesostructure level for various angles (right).

A set of design features are proposed to take further taking into consideration the literature and process characteristics:

- Angled walls – Downfacing surfaces without supporting structures underneath. As shown in Figure 5.3, the range of angles could be divided into Robust zone (without identifiable defects), Compromised zone (self-supporting but with identifiable defects) and Failed zone (complete delamination and not self-supporting).
- Overhangs – Cantilever surfaces without supporting structures
- Bridges – Downfacing surfaces parallel to the print platform with supporting material in the extremes of the surface.
- Details & text – Engraved or embossed features with dimensions near the resolution of the system.
- Columns and pins – Features with small area vs height or length. This feature is related to the maximum aspect ratio, as if surpassed, these could break, crumble or otherwise fail.
- Thin walls – Features with thickness near the resolution of the system. This feature is related as well to the maximum aspect ratio (ISO/ASTM, 2018).
- Holes – Negative features
- Gaps – minimum distance between adjacent features or parts to ensure that these do not fuse during manufacture.

- Clearance – Minimum space that shall be specified between mating features on parts that are assembled or to be assembled after production to avoid adhesion or allow movement in an assembly.

Each of the design features listed is a discretisation of typically occurring elements in more complex parts. The provision of design guidance into these discrete elements helps the designer understand the behaviour of the technology and eases the extrapolation into more complex geometry (Jee & Witherell, 2017).

As described in the previous chapters, some design guidelines provide tips for each feature and specific values or just rules of thumb. However, the behaviour depends on the specific set of MMP. Therefore, a representation of each feature needs to be manufactured for each MMP. This task is usually addressed designing and manufacturing a GBTA with various of these features integrated. The GBTA could be produced for each set of MMP. Then the system performance for each design feature could be captured. The main aim of manufacturingGBTAs is to evaluate and predict uncertainties and geometric capability of the process before printing the final part. These provide information about geometric capabilities such as dimensional accuracy, minimum feature size, repeatability or surface finish (Rupal et al., 2018).

In general, the GBTA design should not take long to produce, be easy to measure, have simple geometrical shapes, and require no post-processing such as support removal (Moylan et al., 2012). The integration of various design features in a single GBTA could create interference between features. Although this has been common practice in geometrical benchmarking literature (Cruz Sanchez et al., 2014; Fahad & Hopkinson, 2012; Minetola et al., 2016), modularity allows a single feature' behaviour evaluation and reduce the size of the GBTA. ISO/ASTM in the definition of standard GTBAs (ISO/ASTM, 2019) uses this approach currently.

A study, described in the following section, was developed to understand the behaviour of the technology with the first three design features listed before (angled walls, overhangs, and bridges).

## 5.4. OVERHANGS, BRIDGES AND ANGLES GBTAS STUDY

This section is an adaption to the thesis format from:

Fernandez-Vicente, M., Canyada, M., & Conejero, A. (2015). Identifying limitations for design for manufacturing with desktop FFF 3D printers. *International Journal of Rapid Manufacturing*, 5(1), 116-128.

### 5.4.1. INTRODUCTION

The industrial grade Additive Manufacturing (AM) technologies have enabled the fabrication of free form geometries for a long time (I. Gibson et al., 2010; Hague et al., 2003; Petrovic et al., 2011). However, an open-source project called RepRap, which permits the construction of a rapid prototyping machine for less than \$500 (R. Jones et al., 2011), has enabled the expansion of the users of this type of machines and the creation of an ecosystem of fast technological improving (Chulilla-Cano, 2011; de Bruijn, 2010).

RepRap machines have demonstrated their usefulness in conventional prototyping and engineering, and the production of spare parts and open-source functional designs (B. T. Wittbrodt et al., 2013). These machines have enabled to achieve an agile fabrication method to produce final parts directly, as some of the components of RepRap printers (Pearce, 2012).

Fused Filament Fabrication - FFF is the main extrusion-based technology of the RepRap project machines, and it is similar to the FDM technology. As in FDM, one substantial limiting factor of this technology is the need for structural supports in overhanging geometries. In these geometries, the building angle becomes more acute and the self-supporting ability of the filament is diminished (Leary et al., 2013). The supports take a longer time to print the model, adding costs. Once removed from the machine, parts may require an amount of additional cleaning up before they are ready for use (Comb et al., 1996). This, therefore, often requires time and careful, experienced manual manipulation. After this process, the surface of the object in contact with the supports becomes marked. Surface defects can be eliminated by a post-finishing treatment, which takes additional time and may affect the geometrical accuracy of the part (Galantucci et al., 2010).

Leary et al. (2013) developed a strategy for minimising the use of support material by comparing the geometric limits, and this generated a map of the feasible building orientations. Other studies addressed this problem by developing an optimal part-building orientation, also taking into account the surface roughness and the fabrication time (Byun & Lee, 2006). Armillotta et al. (2013) developed a tool focusing on improving surface finish by tool orientation but taking into account the staircase effect, the support marks and the loss of detail integrity. Some studies tackled this problem by topology optimisation (Gaynor et al., 2014; Leary et al., 2014b).

Some studies looked into these Additive Manufacturing design constraints in other technologies like Laser Melting or Laser Sintering techniques with commercial equipment (Adam & Zimmer, 2014; Ponche et al., 2014; Seepersad et al., 2012). In this aspect, although some industrial 3D printer manufacturers provide design guides, there is no information about FFF technology constraints.

The AM standard test parts could be categorised into three different types according to their target functions: Geometric, mechanical, and process benchmark (Fahad & Hopkinson, 2012). Due to the multiple process parameters and the wide range of software-machine-process configurations, the parts of this study should be classified as geometric benchmark parts.

For the geometrical test, Moylan et al. (2012) summarised some items to consider to establish 'rules' for a geometric benchmarking model. In this study, these rules were taken into account as the definition of simple geometrical shapes or the ease to measure.

Yang and Anam (2014) designed a standard test part in which various characteristics could be evaluated. Other studies tackled this task by using a single-feature test artefact built at multiple positions and orientations throughout the work volume (Cavallini et al., 2009). The present study follows this approach; 3 test pieces were designed to determine the maximum values of the three characteristic features where it is commonly necessary to build support structures. These are bridges, overhangs, and angles, as shown in Figure 5.4.

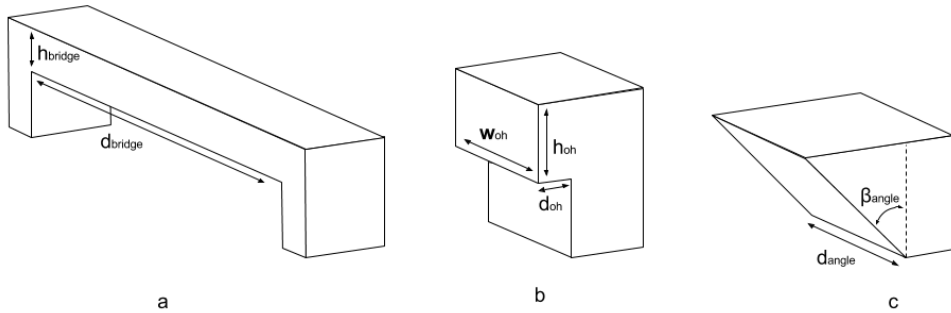


Figure 5.4. Characteristic geometries and variables studied for each a) Bridges b) Overhangs c) Angles

#### 5.4.2. MATERIALS AND METHODS

We printed test specimens with 3mm white ABS plastic in a room with a temperature between 23°C and a humidity level of 50-60% without specific control, to use the atmospheric conditions where this type of printers are used (Tymrak et al., 2014). The extruding temperature was 230°C, and the build surface temperature was 110°C.

The FFF 3D printer model chosen to build the specimens for this research was the “Prusa Iteration 3”, one of the most widely used at the time of this study of the RepRap project (Moilanen & Vadén, 2013). The extruding head, also called *hot end*, was the model J-head V5 (contributors, 2014), with a nozzle tip diameter of 0.5mm.

In the FFF desktop 3D printing ecosystem, there are many machine models and fabrication configurations. This study used the default configuration and parameters, to represent the broadest possible range of users. For the slicing process, the open-source software Slic3r was used (Ranellucci, 2013). With this software, a large number of parameters can be controlled, but for the reasons explained before, the predefined values of the parameters were used. The most characteristic manufacturing parameters were a layer height of 0.4 mm, three perimeters, three top and bottom solid layers, 20% infill density, and a rectilinear fill pattern.

Due to the different mesostructure of the features depending on the thickness (C. W. Ziemian et al., 2012), in the study of bridges and overhangs, four characteristic thickness values were defined, as can be seen in Figure 5.5: (a) Just one solid and rectilinear layer (0.4mm thickness), (b) two solid layers (0.8 mm thickness), (c) three solid layers (1.2 mm thickness) and (d) solid layers with an infill (5 mm thickness).

In order to decide the suitable range of the different values, a first batch of test specimens were examined through a visual inspection, taking into account the shape deformities and the surface quality. As to minimise the measuring error, five specimens of the different parameters studied were printed.

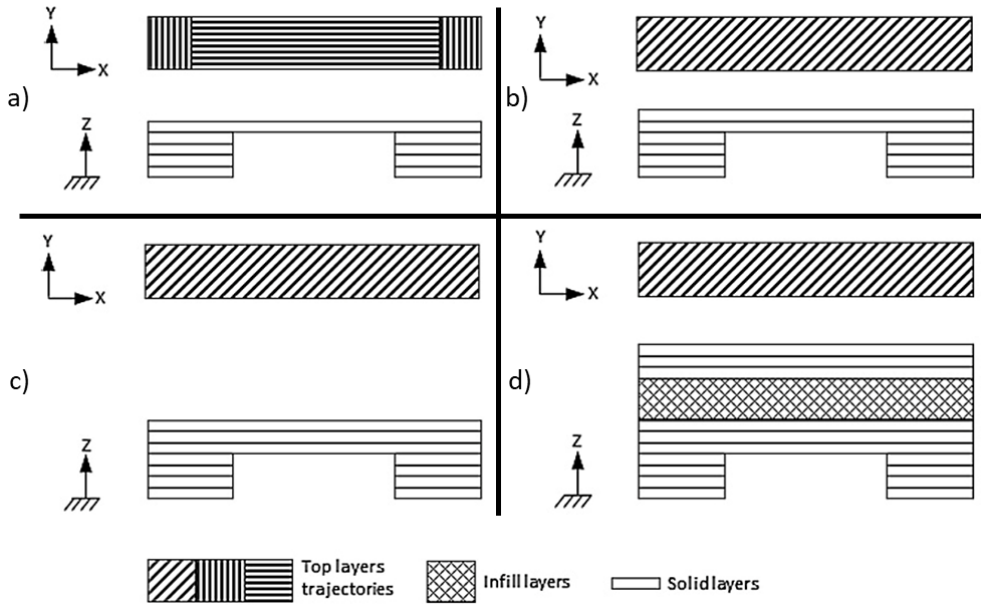


Figure 5.5. Top and side view of test specimens for the examination of different top-layer thickness possibilities; (a) 0.4 mm, (b) 0.8 m, (c) 1.2 mm, and (d) 5 mm.

## Overhangs

The sizes of the overhangs were chosen considering the limits defined by the study of Adam and Zimmer (2014) and the overhang mesostructure, as it changes with the thickness. The length of the overhang specimens,  $d_{oh}$ , was designed from 0.5 to 11.5 mm in steps between 0.1 and 0.5 mm. As explained



before, the thickness of the overhanging feature should be taken into account. Specimens with four different thicknesses  $h_{oh}$  were designed: 0.4, 0.8, 1.2, and 5 mm, as shown in Figure 5.5. The width of the specimens,  $w_{oh}$ , was 10mm, with a distance between the different specimens of 1 mm. 4 test pieces were designed, with the same range of measures (0.5/2.2/3.0/5.0/8.0), to allow the cooling of the previous layer as can be seen in Figure 5.6.

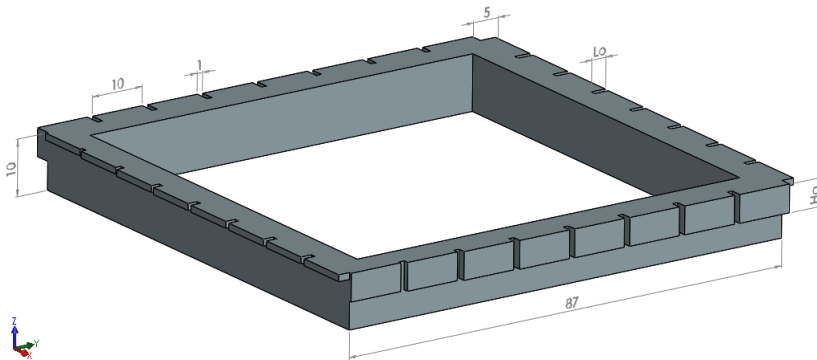


Figure 5.6. 0.5 to 2.2 Overhang test part.

## Angles

For the study of the angles, the three zones of interest described by Leary et al. (2013) were taken into account, starting the evaluation of angles  $\beta_{\text{angle}}$  in the *robust zone* (  $45^\circ$  ) to the boundary of the *compromised zone* (  $60^\circ$  ) in steps of 5 degrees.

Considering the heat transfer between layers (Graybill, 2010), the width of the angle  $d_{\text{angle}}$  was modified between 5 to 60 mm to allow the cooling of the previous layer and study the influence of this parameter in the surface finish. As shown in Figure 5.7, testing parts with different  $d_{\text{angle}}$  and the same  $\beta_{\text{angle}}$  angle were designed.

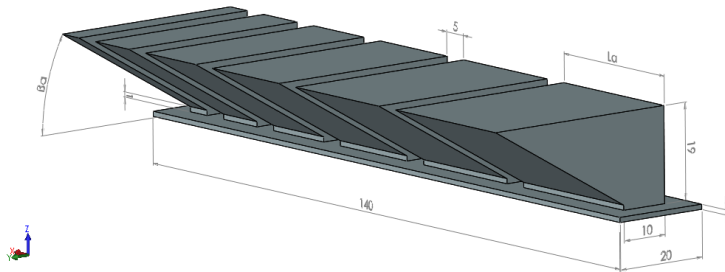


Figure 5.7. Angles test part.

## Bridges

The last features studied were bridges. These are surfaces perpendicular to the build direction, as overhangs, but with supporting pillars or walls on more than one side. The bridging distance,  $d_{\text{bridge}}$ , is the gap that can be fabricated without compromising manufacturability (Leary et al., 2014a). The length of the bridges  $d_{\text{bridge}}$  was 15/20/25/30/35/40/45/50/55 mm.

The bridges mesostructure and the geometry of the top layer, as explained before, are critical factors that were studied, with four different thicknesses  $h_{\text{bridge}}$ : 0.4, 0.8, 1.2, and 5 mm, as shown in Figure 5.5. The bridges were designed with a distance from the build base of 15 mm to avoid the heated build base influence in the results, as shown in Figure 5.8.

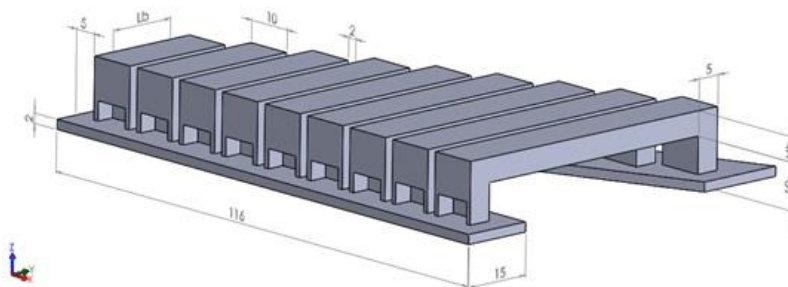


Figure 5.8. 5mm thickness bridges test part.

### 5.4.3. RESULTS AND DISCUSSION

#### Overhangs

The deviation values were obtained by comparison of expected and obtained length  $d_{oh}$  of the overhang geometry. In Figure 5.9, this comparison is represented as variation in mm. The horizontal axis represents the nominal length of the overhang  $d_{oh}$ , and the vertical axis the deviation. More difference from the horizontal zero line represents more deviation from the nominal.

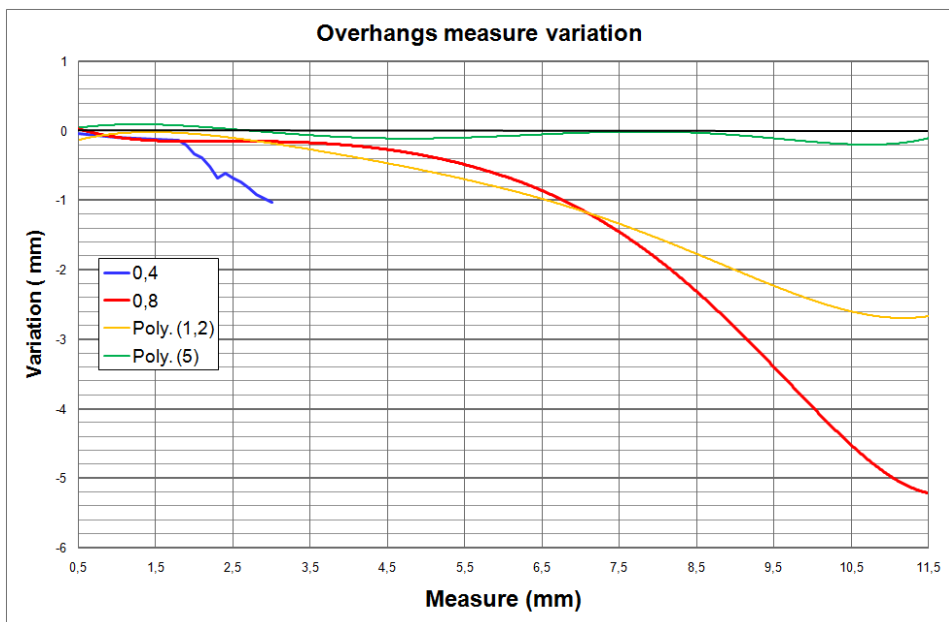
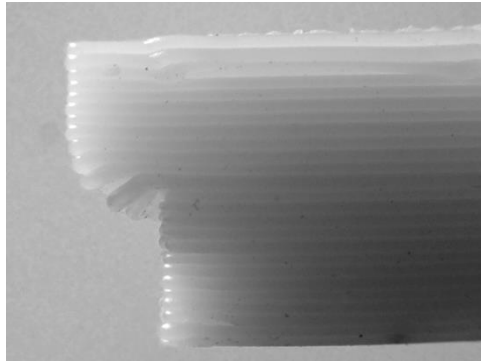


Figure 5.9. Overhangs chart results.

For the one layer feature, 0.4 mm, the first set of values, the deviation grows as the  $d_{oh}$  increases. At a nominal 3 mm length, it deviates -1mm, so the obtained overhang length  $d_{oh}$  was 2 mm. This situation is similar in features with more than one layer, but the deformation starts at a larger nominal value. Between 0 to 3.5 mm, the deformation does not surpass 10% of the nominal value. This result can be due to the overhang first layer solidification, which actuates as a support structure for the following layers. As the thickness  $h_{oh}$  of the overhang increases, this situation becomes more visible. Even width 5 mm of  $d_{oh}$  the deformation is nearly zero, in some cases positive, due to the irregular width of

the different layers. In Figure 5.10, it can be observed that the first layer of the overhang is significantly deformed, but the deformation is reduced in the following layers. It can also be observed that the overhang external profile is not regular, which increases the error in the measures.



*Figure 5.10. Detail of the 3x5mm overhang.*

As shown in Figure 5.11a, which represents the top surface of the 1.2mm specimen, the deformation not only occurs on the length of the overhang, but also affects the definition of the feature on the XY plane. Compared with Figure 5.11b, which has a different mesostructure, the improvement in the definition of the feature can be observed. In Figure 5.11c, the simulation of the same feature of Figure 5.11b is represented. The three external perimeters are visible, and the raster filling of the central area. Therefore, the deposition trajectory, where the perimeter is first deposited, also significantly influences the geometry. The external perimeter filament cannot be bonded to near filaments and falls down.

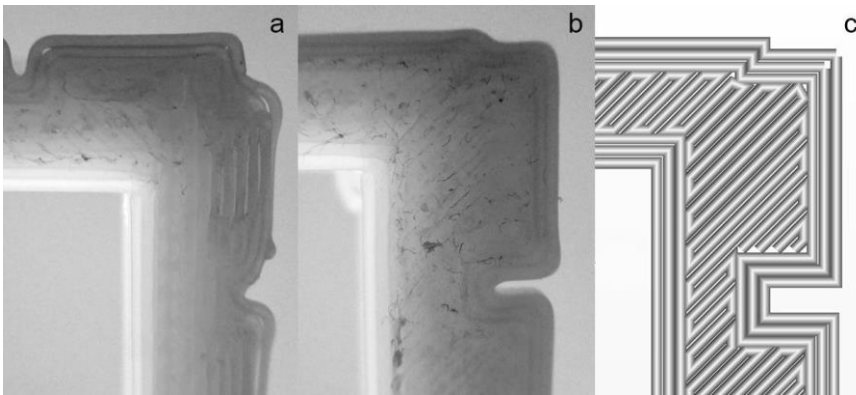


Figure 5.11. Overhangs detail pictures and simulation. a) 1.2 mm thickness. b) 5mm thickness. c) 5mm simulation.

## Angles

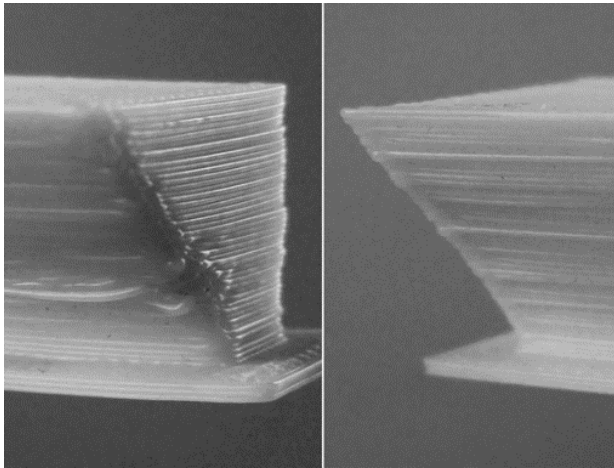
The evaluation of the results for the angles feature was developed by visual inspection of the specimens. Table 5.2 shows the results obtained. The cells with light and dark background represent the good or poor surface finish, respectively.

Table 5.2. Angles deformation results.

Angle/Width	5	10	15	20	25	30	35	40	45	50	55	60
45°												
50°												
55°												
60°												

The angle features with a small width  $d_{\text{angle}}$ , below 30 mm, had a bad finishing in general, in angles inside the *robust zone* as well. It was observed that the shrinking in the specimens of  $d_{\text{angle}}$  length below 30mm deforms the geometry up, and consequently the correct deposition of the successive layers. This result can be due to the lack of time for the lower layer cooling.

For 50 ° angles, the minimum length has to be 35mm to get a good result. An increase can be observed in the minimum length from 50 to 55 degrees, which determines the secure  $\beta_{\text{angle}}$  in general cases. In Figure 5.12, the difference between 30mm and 35mm length in 55° angle specimens can be observed. It reveals the influence of the geometry in the performance of angle construction.



*Figure 5.12. Finish comparison between 55° angle specimens.  $d_{\text{angle}}$  length: 30 mm on the left, 35 on the right.*

As Leary et al. (2013) described, the specimens with  $\beta_{\text{angle}}$  of 60 degrees had a poor surface finish in all  $d_{\text{angle}}$  lengths.

### Bridges

Figure 5.13 shows the observed deformation as  $d_{\text{bridge}}$  length changes and compares the results between the different  $h_{\text{bridge}}$  thicknesses. It can be observed that deformation grows as the distance becomes longer.

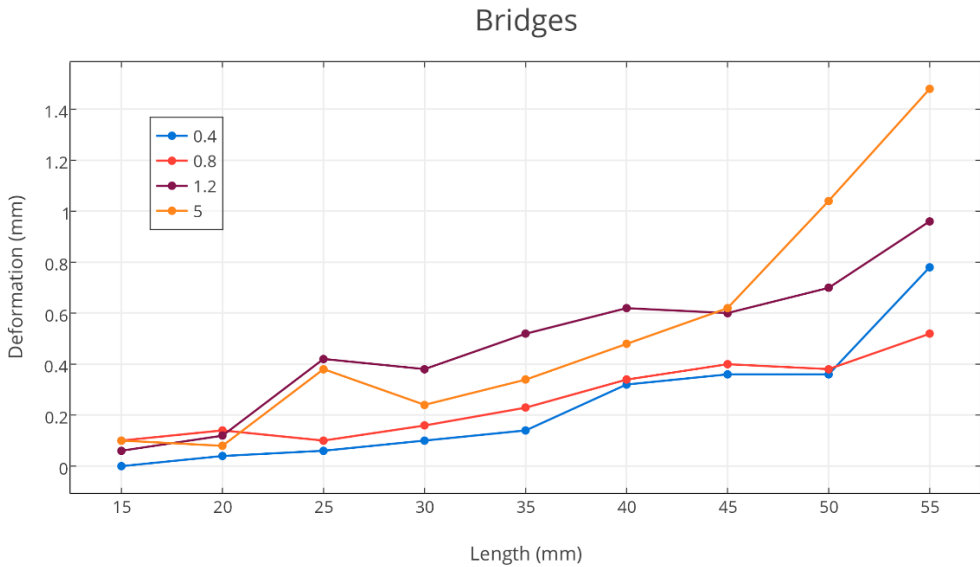


Figure 5.13. Bridges diagram results.

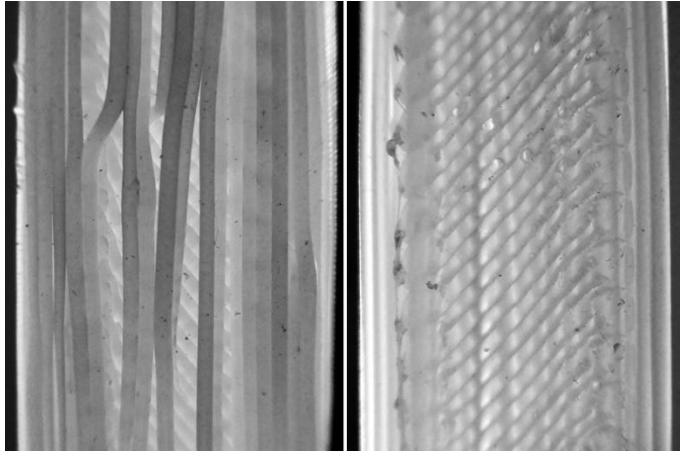
The evaluation of the different features showed a linear increase of their deformation, with a maximum value observed of almost 1mm. For 0.8  $h_{\text{bridge}}$  thickness, the average deformation was below 0.6 mm, showing the best average result of the different thicknesses.



Figure 5.14. Bridge feature measuring 5mm in thickness and 50mm in bridge length.

A more significant deformation can be observed as the thickness increases. This result can be due to the increase in the weight of the bridge. The more material is added – more layers –, the bigger the deformation becomes. However, as shown in Figure 5.14, only the bottom layers were affected by the deformation. The first layers were deposited on the air, but those served as

support for the following layers, resulting in a good surface finish of the top layers, as shown in Figure 5.15.



*Figure 5.15. Comparison between the bottom layer (left) and the top layer (right) of the 1.2mm thickness bridge test.*

#### 5.4.4. CONCLUSION

The 3D printing technology allows creating more complex geometries than with other manufacturing processes. However, some geometric limitations should be identified for every type of technology.

The RepRap project has enabled the development of a new industry called “desktop 3D printing”, but due to its newness, there is a lack of design rules for this type of technology. This research aims to establish a first step in defining the geometric limitations of the FFF technology. This technology differs from commercial FDM technology mainly in the lack of control of the environmental conditions, and the wide range of machine configurations, as the extrusion tip diameter.

This study was focused on three characteristic geometric features: overhangs, angles, and bridges. Thus, their maximum values were studied in order to obtain the correct geometry.

For overhang geometries, an influence in the printing result of the feature mesostructure and trajectory has been observed, as the lower layers serve as



supports for the following layers. In general, the maximum length of an overhang feature with all the layers correctly fabricated is 2 mm.

The study of angle features shows a relation between inclination and length, as observed from the results: As the angle increases, more length will be needed to have a good surface finish. It means that the time between layers determines the ability to self-support. 45° can be determined as a rule to design these features, but the size of the feature to be fabricated should be considered.

For bridge features, the maximum length value recommended is 45 mm. However, as in overhang geometries, the thickness of the feature has an important role in the correct fabrication of the upper layers. The bottom layers act as support for the following layers.

The developed design guidelines for the three features can be used as rules only with the boundary conditions of this study. This limitation is due to the fact that an expert user can change printing parameters to improve the results, or the environmental conditions can change between different prints. However, the results obtained serve as a first approximation of the process behaviour.

The desktop 3D printing technology is a promising technology that is opening rapid manufacturing to a wide range of users. Though it is still under development, the standards being defined in this area will help obtain the expected results of a print.

---

## **5.5. BENCHMARKING GEOMETRIES PROPOSAL**

The study described in the previous section helps to identify the characteristics that affect those features, as well as to improve the design of the GBTAs. For example, the study reveals an influence of the overhang mesostructure in the performance. Therefore, the new design of this GBTA included versions with three different lengths, as shown in Figure 5.16.

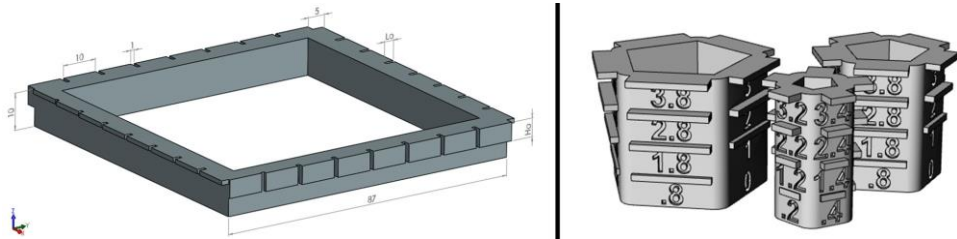
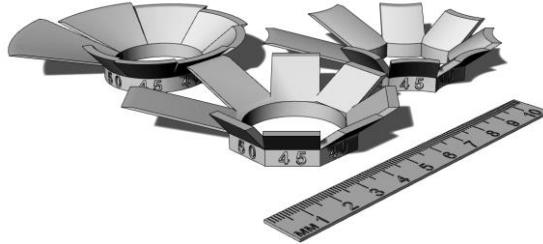


Figure 5.16. Overhang benchmark from the study (left) and new version (right).

The proposedGBTAs for each feature are depicted in Table 5.3, described according to the structure of ISO/ASTM 52902. The study, the literature described earlier, and theGBTAs proposed in online repositories (mifervi, 2021) served as a baseline for the definition of these. EachGBTAs has one or more Key Feature Parameters (KFP), which are the variables that the designer needs to obtain a successful outcome for each MMP set.

Table 5.3. Geometrical test components.<sup>3</sup>

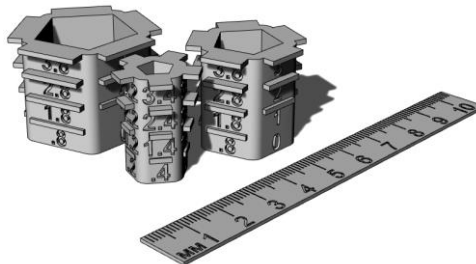
### Angled walls

**KFP:** Extreme angle values for robust, compromised, and failed zones.

**Geometry:** 3mm thick x 8mm high angled walls  $15^\circ \Rightarrow 50^\circ$  from the horizontal in steps of 5 degrees. These are arranged radially to randomise the effects of an uncontrolled build environment. Text engraved. Three versions are provided to represent straight, concave and convex surfaces, as the behaviour is expected to be different depending on the wall's curvature.

**Measurement:** Minimum angle without identifiable defects (Robust), self-supporting but with identifiable defects (Compromised), and complete delamination and not self-supporting (Failed).

**Considerations:** Support structures should not be used with these artefacts. Potential angle failure should be considered when positioning the artefact to avoid adversely affecting the print process of the remaining artefacts.



### Overhangs

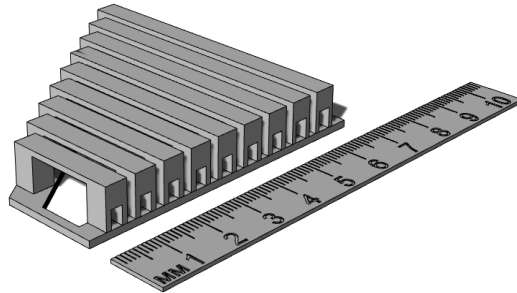
**KFP:** Maximum self-supporting length.

**Geometry:** Overhang length from 0 to 3 mm. These are arranged radially to randomise the effects of an uncontrolled build environment. Three versions are provided, with a different overhang width to reduce bias due to this characteristic.

**Measurement:** Average maximum overhang without beads sagged.

**Considerations:** Support structures should not be used with these artefacts.

<sup>3</sup> Note: ruler just for scale



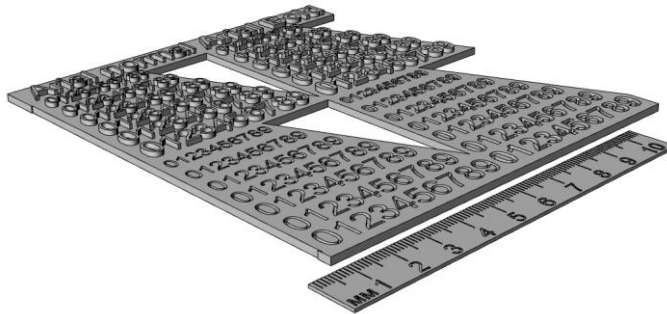
### Bridges

**KFP:** Maximum self-supporting length.

**Geometry:** Bridging distance from 15 to 55mm. This GBTA is updated from the study reducing the width of the bridges. All the bridges are at the same height to keep a uniform layer time for all distances.

**Measurement:** Maximum length with an acceptable sagging.

**Considerations:** Infill angle of the further layers after the first one could modify the result.



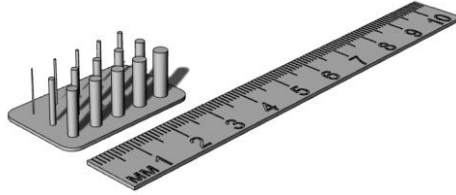
### Details and Text

**KFP:** Minimum character width and height.

**Geometry:** Embossed and engraved text in Arial font from 4 to 7mm height in two widths (regular and bold) to allow identification of missing details in various characters.

**Measurement:** Minimum text size and weight with all characters distinguishable.

**Considerations:** The clarity of text could be affected by the orientation and the usage of other fonts.



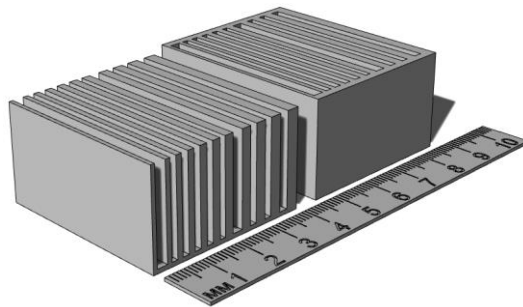
### Columns and pins

**KFP:** Minimum diameter.

**Geometry:** 10 mm height columns of 0.2 to 3 mm diameter. 1 mm thick base to reduce the time required for manufacturing.

**Measurement:** Thinnest pin successfully manufactured.

**Considerations:** The reduced time required to print this GBTA could affect the result. Therefore producing it together with other geometries is recommended.



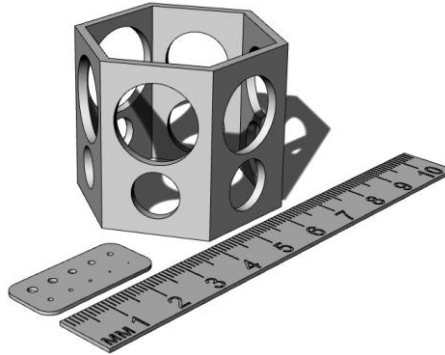
### Thin Walls

**KFP:** Minimum wall thickness. Supported yes/no.

**Geometry:** 45x25mm walls of 0.2 to 3mm thickness. One version with walls on the sides to evaluate the behaviour in situations where the thin wall is just a section.

**Measurement:** Thinnest wall without distortion

**Considerations:** These could be produced at different angles to understand the behaviour.



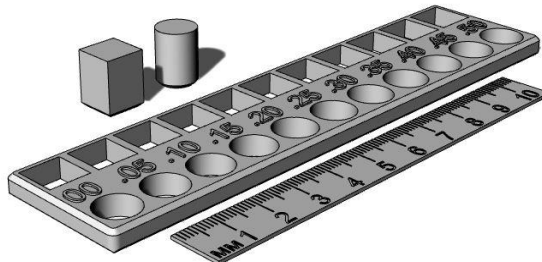
### Holes

**KFP:** Minimum (vertical) & maximum (horizontal) diameter.

**Geometry:** Vertical: 0.2 to 2mm diameter holes. Horizontal: 9 to 18mm diameter holes, arranged in various orientations to avoid the influence of this element.

**Measurement:** Vertical: minimum opened hole. Horizontal: Maximum hole with no sagging filaments in the top area of the hole.

**Considerations:** The horizontal holes GBTA could be affected by the layer printing time. It is recommended to produce it with other components.



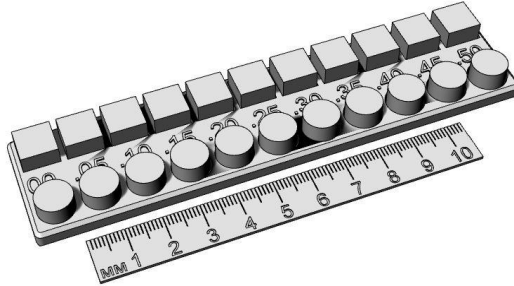
### Clearance and interference fit

**KFP:** Clearance and interference fit dimensions in horizontal and vertical holes.

**Geometry:** 10 mm square and round pegs and holes with 0 to 0.5mm clearance to identify the fit difference between square and round assembly features.

**Measurement:** Test the assembly of both square and round pegs in the holes, finding the clearance that provides an interference and clearance fit in vertical holes, and then repeat with the horizontal holes.

**Considerations:** The main body should be printed in horizontal and vertical orientations.



**Gaps**

**KFP:** Minimum gap avoiding adhesion.

**Geometry:** 10 mm square and round pegs in place and holes with 0 to 0.5mm gaps to identify the difference between square and round profiles of multipart assemblies.

**Measurement:** Identify the peg that can be extracted from the smallest hole.

**Considerations:** The bead size calibration is critical for this feature.

## 5.6. RESULTS

The time required to produce theGBTAs ranges between 1:49 hrs (gaps) to 1:20 min (vertical holes) when using the default parameters with a nozzle of 0.5mm and layer thickness of 0.3mm. Although the range to produce eachGBTA is large, it can be seen in Figure 5.17 that most of theGBTAs are under approximately 30 minutes.

The chart shows the material required for eachGBTA to evaluate the influence of speed process parameters. As can be seen, most of the test artefacts use less than 10g of material, just 1% of the standard material spool (1 kg).

## Analysis to support design for additive manufacturing with desktop 3D printing

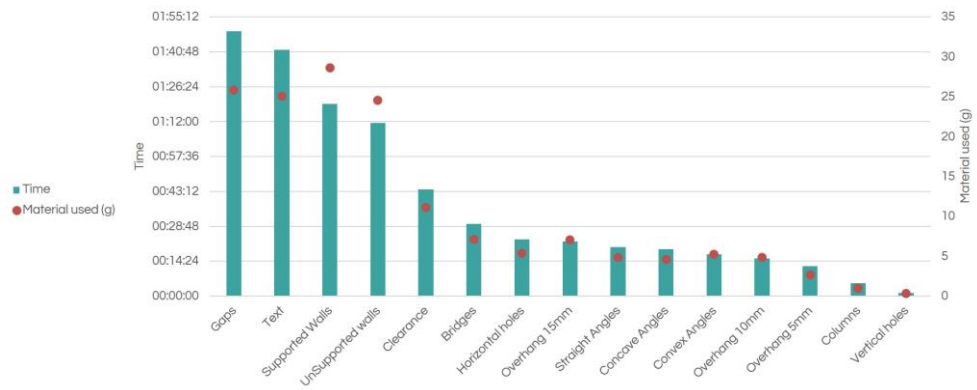


Figure 5.17. Chart of estimated printing times for each GBTA.

TheseGBTAs were produced with various materials and parameters to validate their variability with various MMPs. Figure 5.18 shows the outcome of the narrower overhangs GBTA produced in brown ABS and grey PLA with the same machine and parameters (apart from extrusion temperature). A significant difference in the result can be observed, making it easier to identify the successful value.



Figure 5.18. 5mm wide overhang GBTA produced in ABS (left) and PLA (right).

As shown in Figure 5.19, the results change in theGBTAs with the same material (PLA) but with a different variation; in this case, the surface curvature. The concave surface at  $25^\circ$  has already lost its profile, while with convex curvature still maintains its profile and surface quality. Therefore, the designer can decide which angle would be more suitable for the type of surfaces of the object being designed.





Figure 5.19. Angled walls GBTA. Concave (left), straight (centre) and convex (right) surface.

The outcome of the manufacturing of the other GBTAs showed similar results as the ones depicted. The minimum or maximum values for each feature can clearly be observed without the need for dimensioning tools, and the variation of the machine configuration, material, or parameter set change the results. Taken together, the results suggest that the proposed GBTA geometries are suitable to support the provision of guidance on design features.

## 5.7. SUMMARY

This chapter has identified the key common features that determine the geometrical behaviour of FFF components. A set of geometric benchmarking test artefacts have been proposed to fill the current gap of suitable artefacts for users of FFF.

Although there is already a standard that provides this kind of GBTAs, most of the geometries lack applicability for FFF. Therefore, the geometries described in this chapter will be proposed to the designers to understand the critical dimensions of key features.

While this chapter looks at the key geometrical features, the next chapter studies the mechanical behaviour, emphasising especially in the design-defined characteristics of the components.



# Chapter 6

## Mechanical properties

### 6.1. INTRODUCTION

FFF has been mainly used in, for example, art, education, demonstrations or visual aids. The wider adoption of this technology for functional parts is still slowed down by limitations such as the surface finish quality (Boschetto et al., 2016a) and the reduced knowledge about their mechanical behaviour (Cuan-Urquizo et al., 2015).

In contrast to the previously describedGBTAs, the mechanical benchmarking test artefact designs for plastics are widely available and standardised. E.g. ISO 178 (2019) for determination of flexural properties, ASTM D638 (2014) / ISO 527 (2019) for tensile properties or ISO 179 (2020) for impact properties. These standard specimens, however, are designed assuming a fully solid volume. In FFF, the components are not fully solid, as described before, generating issues such as stress concentrations, gaps, or overloading of the external perimeter in tensile specimens (Ahn et al., 2002; Torrado & Roberson, 2016).

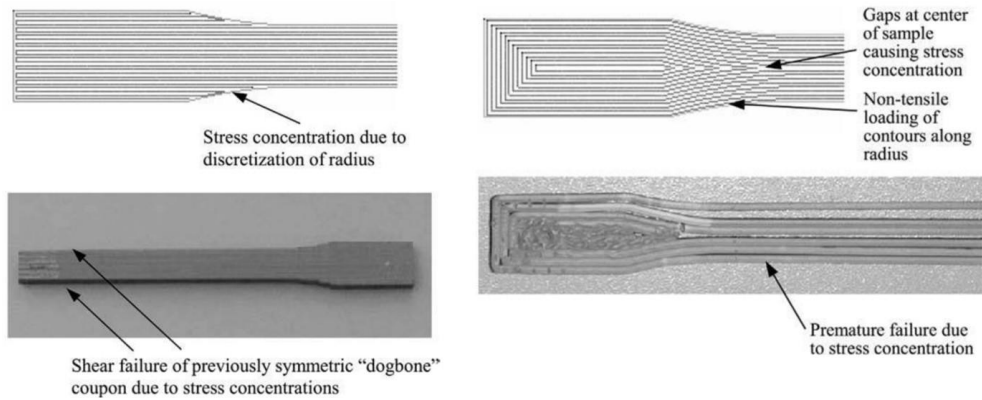


Figure 6.1. Issues with standard plastic tensile specimens. Adapted from Ahn et al. (2002)

These issues have been overcome in literature by modifying the geometry from the standard, for example, by modifying the fillet radius, as shown in Figure 6.1, or by using the specimen design from the composites standards, such as ASTM D3039 (Ahn et al., 2002; Rankouhi et al., 2016).

This lack of specific standards for testing the mechanical properties of FFF components creates divergent conclusions of manufacturing parameters and test results. E.g., there are reports of ABS's tensile properties between 11 and 40 MPa (Tymrak et al., 2014). This difference could be due to the inherently anisotropic nature of FFF components or to the large number of influential parameters and factors in the FFF process, as shown in Figure 6.2.

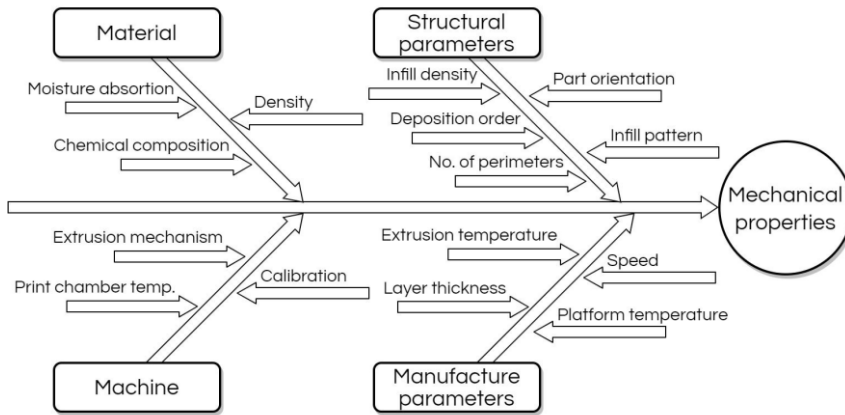


Figure 6.2. Reported parameters and factors influencing the mechanical properties in FFF.

Since the early days of development of the FFF process, understanding the mechanical properties and the influence of the parameters has been the objective of many studies (Cuan-Urquizo et al., 2015). An early analysis and discussion on the subject was presented by Fodran et al. (1996), in which preliminarily, they studied the independent variation of various parameters to identify each parameter effect on the tensile strength. They mechanically tested the ABS specimens after impregnating some of the samples with various bonding agents. The post-processing influenced the failure mode, while the non impregnated parts showed that the mechanical properties change by modifying any one parameter. Other studies reveal that the manufacturing parameters such as platform temperature, printing speed, or extrude temperature seem to have less influence on the mechanical properties than structural parameters such as part orientation, infill density, and infill orientation (Afrose et al., 2016; Montero et al., 2001). This variation in influence highlights the importance of understanding the structure-property relationship in parts manufactured with this technology.

Two studies were defined looking into two of the designer-controlled structural parameters to develop this understanding about this structure-property relationship:

- To identify if the structural parameters infill density and pattern affect the bending behaviour and how it affects, included in the section after next.
- To understand the influence of the structural parameters infill density and pattern on the tensile behaviour, which was published and is described below.

In both cases, the material ABS was selected as the focus of study due to its resistance to temperature, good mechanical properties, and easiness of post-processing (e.g. sanding, machining or chemical finishing) as opposed to the other primary material used in FFF, PLA(Hunt et al., 2015). This last characteristic is critical for the development of prototypes or components with low surface roughness requirements.

## **6.2. EFFECT OF INFILL PARAMETERS ON TENSILE BEHAVIOUR**

This section is an adaption to the thesis format from:

Fernandez-Vicente, M., Calle, W., Ferrandiz, S., & Conejero, A. (2016). Effect of infill parameters on tensile mechanical behavior in desktop 3D printing. *3D printing and additive manufacturing*, 3(3), 183-192.

### **6.2.1. INTRODUCTION**

Additive Manufacturing, also called Rapid prototyping, since its origins in the '80s, has been a useful tool for the process of design and development of products and often represents a considerable saving in time in this process (Chua & Leong, 2003). For the addition of material, there are different Additive Manufacturing techniques, based mainly on three types of construction: solidification of a liquid, sintering or fusion of powder, and deposition of material. Several different systems have been patented with each of these techniques, such as SLA, SLS, or FDM (I. Gibson et al., 2015a).

The expiration of those patents, firstly of FDM technology and later SLA and SLS, is leading to a growth in interest in developing and improving these technologies. The seed of this interest is the RepRap project, which aims to

create a self-replicating manufacturing machine. A 3D printing machine that uses a manufacturing technique similar to FDM technology was designed, but to avoid legal problems, it was named Fused Filament Fabrication (FFF) technology (R. Jones et al., 2011). One characteristic of this new approach was to build the machines small enough to be desktop 3D printers, opening the door to a new industry currently called “desktop 3D printing”. The disruptive yet successful elements of this approach were to share on the internet the design and building instructions for the construction of a similar machine by anyone and the inclusion in the design of a large percentage of the pieces built by the same machine. This new approach means that a single machine can fabricate pieces for the building of other machines, creating exponential growth in the number of users, new designs, and developments that have never been done by the patent owner (de Bruijn, 2010). Many desktop 3D printing companies have emerged from this project and have experimented a significant growth in the number of sold systems. The average estimated unit sales growth over the past four years (2011-2014) was 135.2%. The estimation of desktop 3D printers sold is 72,500 in 2013 to near 140,000 in 2014 (Wohlers & Caffrey, 2015).

### 6.2.2. LITERATURE REVIEW

The process of 3D printing with FFF technology consists of pushing a thermoplastic filament using an extruder element into a fusion chamber, known as a hotend. The fused material is pushed through the tip of the hotend, and it is deposited in a controlled way, generally at an inferior distance than the diameter of the tip hole. The process from the digital design to the deposition needs to transform the 3D geometry using movement commands, known as Gcode, which are interpreted by the machine control electronics, which then executes the commands.

#### Process characterisation

Many variables may affect the characteristics of the object manufactured (Rankouhi et al., 2016). These characteristics have been studied mainly by three aspects: surface quality, dimensional accuracy, and mechanical behaviour. On surface quality, Boschetto et al. (2013) developed a mathematical model of the surface profile in order to determine the best object orientation. The

mechanical and dimensional characteristics have been the objective of studies since the early years of FDM technology. By 1996 Fodran et al. studied the tensile behaviour and dimensional integrity with different flow rates and bonding agents (Fodran et al., 1996).

One of the characteristics that has received a great deal of attention in the literature is mechanical behaviour. Rodriguez et al. developed a series of studies in order to study the mechanical behaviour of ABS fused deposition. Firstly, they characterised the mesostructure of the materials (Rodriguez et al., 2000). Secondly, they studied a single RAW filament's tensile strength and tested unidirectional FDM specimens (Rodríguez et al., 2001). Additionally, they measured the polymer chain orientation, as the raster orientation causes alignment of polymer molecules along the direction of deposition (Es-Said et al., 2000). Finally, they developed an analytical model for unidirectional FDM ABS, using laminate theory, and concluded that voids form show a remarkable influence in mechanical properties. Furthermore, they observed that the change in the infill angle changes the fracture from ductile to brittle. This is due to the dependence on the bonding between filaments (Gurralla & Regalla, 2014; Rodríguez et al., 2003).

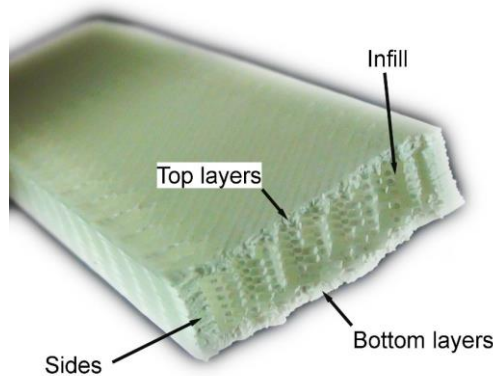
The internal structure of an FDM part is not significantly different from that of a fibre reinforced composite, as it can be interpreted as a composite structure with vertically stacked layers of polymer fibres and air (Bellini & Güçeri, 2003; Sood et al., 2010). In FDM, a solid filament is extruded in a semi-molten state and solidified in the chamber at a temperature below  $T_g$  of the material. The temperature changes from  $T_m$  to  $T_g$  in around 0.55 seconds (Rodriguez et al., 2000). Consequently, volumetric shrinkage occurs, developing weak fibre bonding and high porosity of the structure (Es-Said et al., 2000).

The bond quality between filaments depends on envelope temperature and variations in the convective conditions (Sun et al., 2008) as it is needed a molecular diffusion and cross-linking between the polymer deposition (Es-Said et al., 2000). As a single head generally does material deposition, the deposition pattern significantly affects the part stresses and deflections (Nickel et al.,



2001). The accumulation of residual stresses can bring about warp, inner-layer delaminating or cracking (Wang et al., 2007; Y. Zhang & Chou, 2008).

In the FDM or FFF parts structure, three distinct zones can be distinguished, and these can be seen in Figure 6.3. The first deposited zones are several solid layers that form the lower area of the outside of the piece. Next, the main body of the piece is built, in which a set of perimeter filaments are deposited. The interior is built using an infill of a density and a mesostructure that can be controlled. Finally, the upper layers are deposited, which are usually solid, to close the piece's exterior.



*Figure 6.3 Section of the printed specimens. Characteristic areas*

The complexity of such structure determines an anisotropic behaviour. The variables that influence this characteristic can be classified in material properties, build specifications, part positioning and orientation, and environment (Montero et al., 2001).

Ahn et al. (2002) studied this anisotropic behaviour taking into account variables from the different classifications, analysing the tensile and compressive strength. It was obtained that air gap and raster orientation have more influence than other variables. Ziemian et al. (2012) developed a similar study. They evaluated the effect of raster orientation in the direction of the strain. Tests for tensile, compression, flexural, impact and fatigue were developed, and the results were then compared with the properties of injected

sample pieces. From this study, information was obtained on the optimal factor levels for improving strength.

Some studies have developed models for the prediction of mechanical behaviour. Bellini et al. (2003) presented a methodology to determine the stiffness matrix, interpreting the structure as orthotropic, and compared the results with experimental tests. Croccolo et al. (2013) determined variations in tensile strength by studying the effect of “contouring”, which is modifying the number of contours, and developed an analytical model. They then compared the results with the experimental data. Gurrala & Regalla (2014) developed a mathematical model for tensile strength by predicting the bonding surface between fibres. Their results show that the temperature is not enough to cross-link the fibres fully.

Regarding the study of different infill structures, Baich & Manogharan (2015) analysed the correlation between cost and time based on infill pattern and desired mechanical properties using a production-grade FDM system. They concluded that solid infill has greater strength performance than double-dense infill at the same production cost. This study also highlights the need for additional analysis of ‘custom’ infill patterns with respect to mechanical loading.

### Mechanical behaviour in FFF technology

Although FFF technology is similar to FDM, there are a series of factors that open new areas to study. However, due to the novel development of FFF technology, there have been very few studies on this technology.

One of those factors is the uncontrolled environment parameters, as Tymrak et al. (2014) based their study. Furthermore, in their study, different machines with different slicing and control software were used as well as different extrusion temperatures and materials. While in FDM, the air gap can be controlled, in FFF can be controlled the infill, but the real value varies among printers. In their study, the specimens were printed with 100% infill, but the uncontrolled air gap derived in a wide dispersion of the results. Higher

mechanical properties than similar studies on FDM were obtained, although the raw filament mechanical characteristics were not determined.

Lanzotti et al. (2015) studied the influence of layer thickness, infill orientations and the number of shell perimeters but obtained only the PLA mechanical characteristics. Rankouhi et al. (2016) analysed the same parameters using ABS, layer thickness and orientation, and performed a fractography to determine the failure modes. They observed that smaller layer thickness increases the strength and that a large air gap causes inter-layer fusion bonds to fail.

Akande et al. (2015) studied the significance of layer thickness, fill density, and deposition speed on the mechanical properties. Furthermore, they developed a low-cost test jig and compared it with a conventional testing machine, obtaining a valid method for quality testing. Qureshi et al. (2015) synthesised the parameters analysed in research before and selected a list of 13 controllable factors, which may affect the mechanical behaviour. The mean UTS obtained was similar to earlier research. They used Taguchi's method of Design of Experiments to obtain the optimised parameter values.

Lanzotti et al. (2015) made an analysis of effects on the dimensional accuracy when changing three of the deposition variables (layer thickness, deposition speed, and flow rate) and found a recommended combination of these. Afrose et al. (2016) studied the static strength and fatigue behaviour of PLA material with different orientations. They obtained a 60% tensile stress of that of injection moulded PLA material.

Nonetheless, until now, there has been no study that evaluates the different patterns that can be selected in the infill or the influence of their density on mechanical strength. These parameters can be controlled in this Open Source technology but could not be controlled in FDM technology. For this reason, this study aims to evaluate the influence in this technology of two parameters, the pattern and the density of the infill, emulating the printing conditions of an inexperienced user. With these two objectives in mind, the raw material mechanical characteristics were obtained and were compared with the three most common pattern types and three infill densities.

### 6.2.3. MATERIALS AND METHODS

A series of specimens were produced using an open-source desktop 3D printing machine in order to emulate the fabrication conditions of an inexperienced user of this type of technology. Due to the existence of a very large range of options of mechanical and electronic configurations and software chains, listed below are the more relevant details of the configuration of the equipment used for this study.

The structure of the 3D printer was the model RepRap Prusa i3, one of the more widespread models nowadays (3D Hubs, 2016). The tip for the fabrication had a diameter of 0.5 mm. The control electronics of the machine was the Arduino Mega board, the RAMPS v1.4 adaptation board, and motor drivers A4988. The firmware loaded in the board was Marlin version 1.0.

Regarding the software and printing configurations, the toolpath calculation was made with the open-source software Slic3r version 1.0 (Ranellucci, 2013). With this software, a range of parameters can be controlled, and modifications to these could lead to the improvement in the results. However, a particular set of parameters could not be transferred to other geometries. Moreover, one of the study’s objectives would be lost: to emulate the printing conditions of an inexperienced user. Therefore, the predefined configurations of the software were used. The values of the most characteristic parameters are listed in Table 6.1. The specimens were printed without a raft, a previous grid to improve adherence, as bed heating and adhesion were good enough to avoid it.

*Table 6.1 Values of the most characteristics fixed parameters*

<i>Parameter</i>	<i>Value</i>	<i>Units</i>
Bed temperature	110	°C
Nozzle temperature	230	°C
Layer thickness	0.3	Mm
Perimeters	3	
Solid top layers	3	
Solid bottom layers	3	
Infill pattern top/bottom	Rectilinear	
Infill angle	45	°C
Extrusion width first layer	200	%

In this study, the infill of the intermediate zone was modified. The parameters evaluated in this study were the infill density and pattern. For the infill, three levels were evaluated: 20%, 50%, and 100%. The first level is predefined by the software; the last one was selected to obtain information about the behaviour with full infill; the intermediate level, 50%, was chosen to evaluate how it is the evolution of mechanical behaviour between the other two levels. For the infill pattern, due to the software's capabilities, it is possible to use eight types of patterns. However, only the three most widely used were selected: Line, Rectilinear, and Honeycomb. Line pattern generates a random infill pattern with linear connections between the walls. A Rectilinear pattern creates a rectangular mesh, predefined at 45° from the machine axis. The honeycomb pattern produces a structure of hexagonal cells similar to a honeycomb (Hodgson et al., 2014). A measurement of the printed density was carried out to detect possible causes of mechanical behaviour. The methodology used for measurements was image analysis. The images were captured with the aid of an Olympus CH2 microscope (Olympus Optical Co., Ltd., Tokyo, Japan) and were analysed using ImageJ software (National Institutes of Health, Bethesda, Maryland), as can be seen in Figure 6.4. The values measured presented an average deviation of less than 6% from the virtual density.

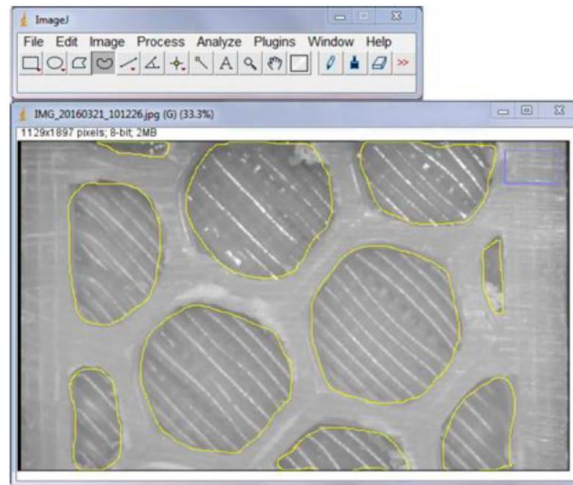


Figure 6.4 Density analysis on ImageJ software.

For evaluation of the dispersion, and according to the standard, five test pieces were produced with each combination of printing parameters considered as variables. Figure 6.5 shows screenshots of the different patterns: a) Rectilinear, b) Honeycomb, c) Line, and a representation of the infill density with the rectilinear pattern with values of d) 20%, e) 50% f) 100%.

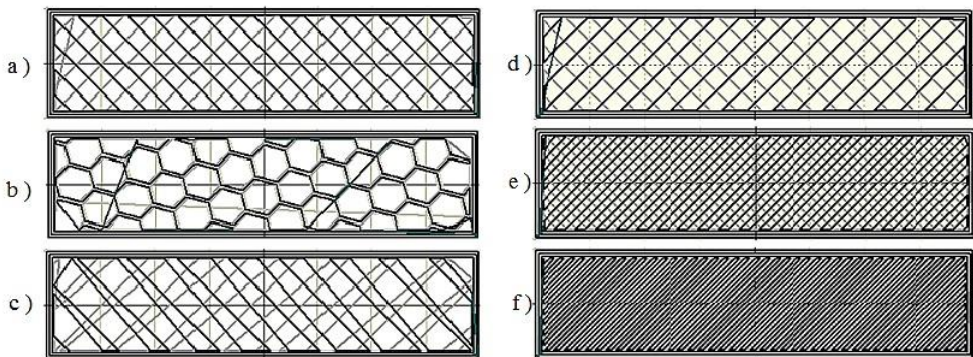


Figure 6.5 Infill patterns (a) rectilinear, (b) honeycomb, (c) line, and densities (d) 20%, (e) 50%, and (f) 100% used as variables.

The material used to manufacture the test pieces was a 3mm diameter filament of acrylonitrile-butadiene-styrene (ABS Nature, Torwell Technologies Co. Shenzhen, China). Although the manufacturer provides information about

the material, in order to obtain the reference values for the behaviour and strength of the material, injection moulded sample pieces were tested. The same ABS filaments used for printing the test pieces were cut into pellets in a plastic shredder, and another series of injection-moulded test pieces were tested in accordance with ISO 527. The values obtained from the test were an ultimate strength of 36.56 MPa and an elasticity modulus of 1826 MPa.

The same standard was used as a reference for the tensile test and the design of the pieces. However, in order to avoid the stress concentration at the transition zones of the specimens' head, as tested by Croccolo et al. (2013), and to leave enough space for the infill geometry, the pieces were designed without a bigger clamp connection, as can be seen in Figure 6.6. Some previous studies tested an adapted specimen geometry from the standard ASTM D3039 to avoid the same problem (Ahn et al., 2002; Rankouhi et al., 2016; Rodríguez et al., 2001). In this study, a preliminary experiment was carried out in order to analyse the suitability of this geometry, and the results were admissible.

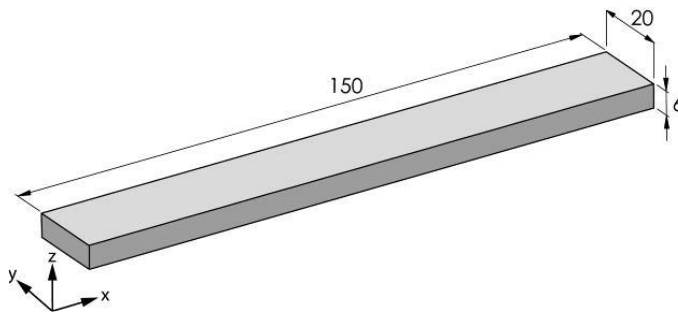


Figure 6.6 Test specimen with the main dimensions in mm and print orientation

All specimens were fabricated in the horizontal plane, where the orientation of the fibres and their bonding is better than in other planes (C. W. Ziemian et al., 2012). One factor that determined this situation was the infill pattern, as until now, it cannot be oriented in different planes and remains in the X-Y plane. Only one orientation of specimens was used, along X-axis as shown in Figure 6.6, in order to obtain results dependent upon the fibre-to-fibre fusion, and consequently the internal mesostructure (C. W. Ziemian et al., 2012). Therefore, the specimens were formed with a total of 20 layers.

The tensile strength tests were performed in an Instron model 5967 double-column universal test machine with a load capacity of 30 kN. Prior to the tests, a software calibration of the load cell was done. The tests were carried out according to the ISO 527, with a preload of 20 N and a 2 mm/min test speed.

#### 6.2.4. RESULTS AND DISCUSSION

The results obtained from the test show differences between the different pairs of parameters of infill density and pattern, also called mesostructures, of the specimens.

As can be seen in Table 6.2, a higher level of density resulted in a lower amount of voids in the infill, and subsequently, higher tensile strength. This situation is similar for the three types of infill patterns, especially in the rectilinear pattern, where at 20% density, the tensile strength is the lowest, but at 100%, the value is the highest of all of the results, 36.4 Mpa. An additional column with average specimen weight has been added to evaluate its influence.

*Table 6.2 Average tensile characteristics of the different mesostructures for ABS FFF 3D printed specimens*

Infill pattern	Infill density	Tensile strength (MPa)	Tensile strain (%)	Elastic modulus (MPa)	Weight (g)
Line	20	16.00	4.76	499	11.06
Line	50	20.06	4.86	640	13.98
Line	100	35.68	5.30	784	17.54
Rectilinear	20	15.62	5.30	408	10.64
Rectilinear	50	19.58	4.62	659	13.98
Rectilinear	100	36.40	5.36	834	19
Honeycomb	20	16.52	4.44	568	11.22
Honeycomb	50	21.78	4.38	745	14.76
Honeycomb	100	36.10	5.42	802	18.88
Raw ABS	-	36.56	5.44	1826	-

Observing the change in the stiffness in the specimens with the elastic modulus, this value increases as the density increases. To evaluate these changes, Figure 6.7 shows the comparison between the change in the tensile strength, whose values are from the left Y-axis, and the change in the Young modulus, using the right Y-axis as a reference for the values.



An increase in the tensile strength of the three patterns can be observed, with a very similar evolution in the values. The value increases from 20% to 50%, but the change is more significant between 50% and 100%. This situation is different in the case of the elastic modulus, as from 20% to 50%, there is an increase, but it is smaller than that from 50% to 100%.

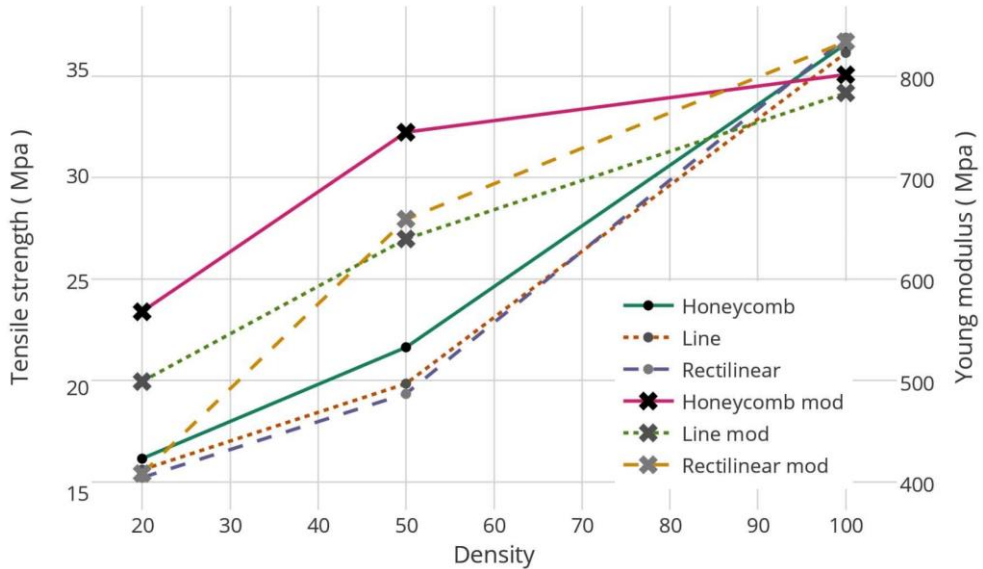
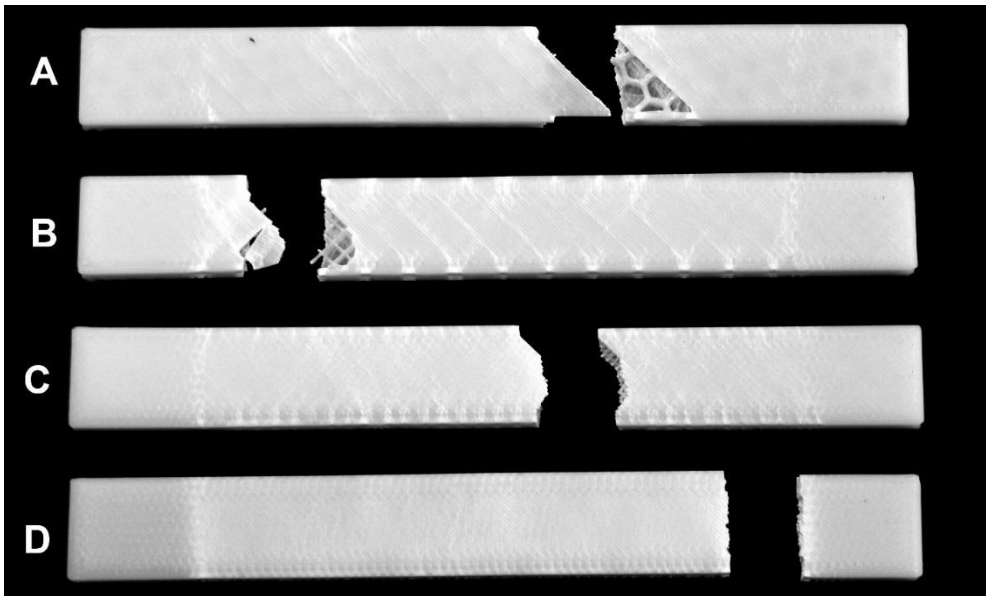


Figure 6.7 Tensile strength and Young modulus evolution with density change

This difference may be due to the ability of the infill fibres to deform and absorb the stress prior to a break in the bonds between the different fibres. This capability increases as the density also increases. When that density starts to create bonds between the different pattern sections, the tensile strength improves. However, the increase in the ability to deform is reduced.

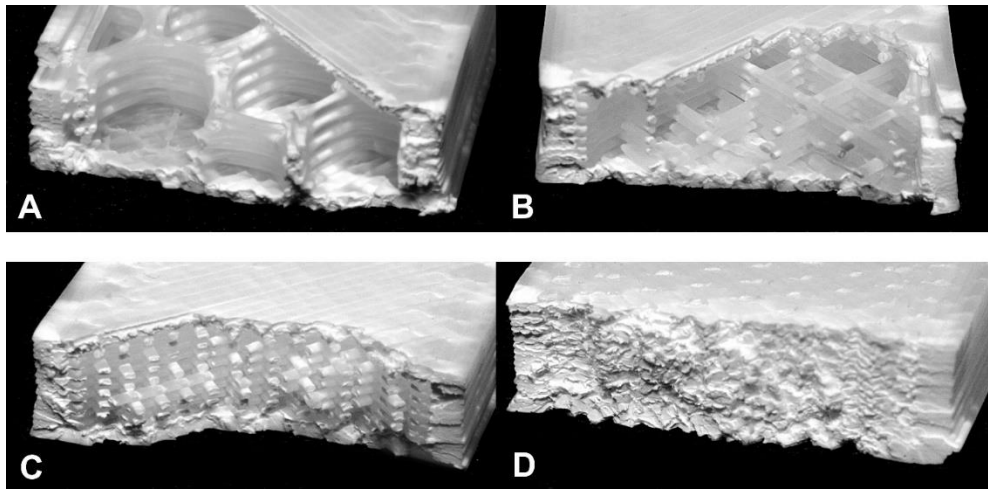


*Figure 6.8 Examples of tested specimens. A: Honeycomb 20%. B: Rectilinear 20%. C: Rectilinear 50%. D: Rectilinear 100%*

In Figure 6.8 and Figure 6.9, four representative examples of tested specimens can be seen to illustrate the failure mode. The fracture in other specimens with different parameters is similar. The sample specimens A and B show two different infill patterns with the lowest density. In Figure 6.8 are visible the different stress distributions in each of the infill densities. It is evident comparing B, C and D specimens, where the distance between the whitening areas reveals the pattern size.

Looking closely into fracture zones in Figure 6.9, a failure that occurred across the layers can be observed, in intralayer and interlayer bonds. It can be seen from specimens C and D a decrease in the inter-layer bond failure, although it is still present. These results are in agreement with those obtained by previous studies (Gurralla & Regalla, 2014; Rankouhi et al., 2016). Comparing specimens A and B, it can be observed how the failure follows the weaker zones in the pattern, where there is less material. The upper layer failed along the 45° line. This reveals repeated failures of individual filaments by shearing and tension as observed in earlier studies (Ahn et al., 2002; Riddick et al., 2016).

Interestingly, it can be seen that the bonding zones between different layers are different in each pattern. In the honeycomb pattern, each layer lays down on a similar previous layer. In the rectilinear pattern, the bonding zone between each layer corresponds only to the points where the filament crosses the previous layer filaments. This characteristic can be a possible explanation of why the honeycomb pattern shows a higher elastic modulus. However, the variation of weight and stress distribution between patterns could be the reasons too. These results, therefore, need to be interpreted with caution.



*Figure 6.9 Fracture detail of example tested specimens*

To evaluate the deviation of the tests, the following figures show the results in a box plot. Figure 6.10 shows the results in the tensile strength grouped according to infill density, and Figure 6.11 shows the Young modulus with the same configuration as the previous figure.

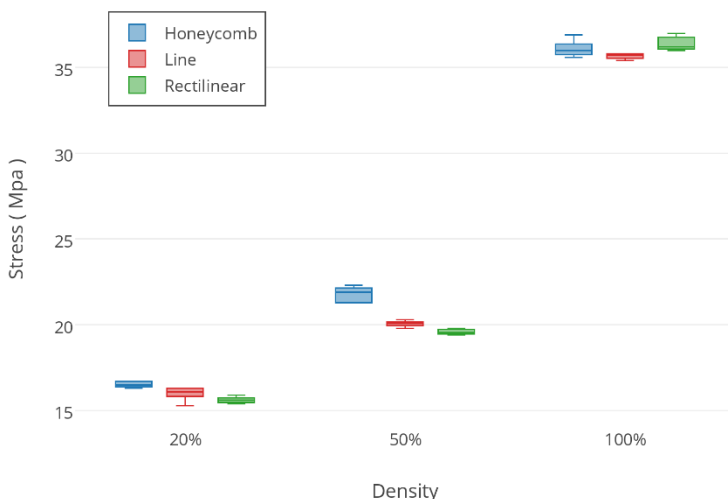


Figure 6.10 Tensile strength box plot

Less than 2Mpa difference can be observed between each pattern. The Honeycomb pattern generally shows the higher values of the three patterns. However, this can be due to a higher density, as can be observed in Table 6.2. An exception is in the 100% infill density, where the rectilinear pattern is higher. This may be due to an inability of the software to generate a full infill with the other two patterns. These relationships may partly be explained by the slight weight variation and, consequently, the density between patterns of the same virtual density, as shown in Table 6.2.

On the other hand, in Figure 6.11, the dispersion of the measures of the Young modulus is higher than in the tensile strength evaluation. The comparison between the different patterns shows an improvement in the dispersion for the 50% infill density. However, the stiffness increases between 20% and 50%, the dispersion of the values is higher as the density increases. The reason may be explained due to the lack of control in the environment temperature. As discussed before, the bonding between the different fibres is crucial to the mechanical characteristics in this process. Therefore, the thermal conditions of the environment clearly affect the bonding conditions of the different samples (Roxas, 2008).

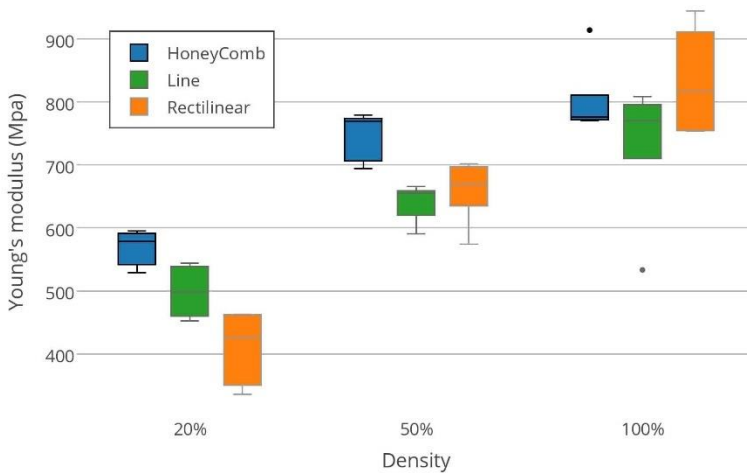


Figure 6.11 Elastic modulus box plot

Taking into consideration the dispersion of the data in Figure 6.11, it is necessary to evaluate the evolution and dispersion of the stress during the test. Figure 6.12 shows a graph of the strain-stress relation. In addition to the usual representation of the average value of the different mesostructures, the standard deviation of the different samples in each step of the data capturing is also shown. This deviation is expressed as a shadow in the same colour as the average value of the mesostructure. The upper limit of the shadow is the average value plus the standard deviation, and the lower limit corresponds to the average value minus the standard deviation.

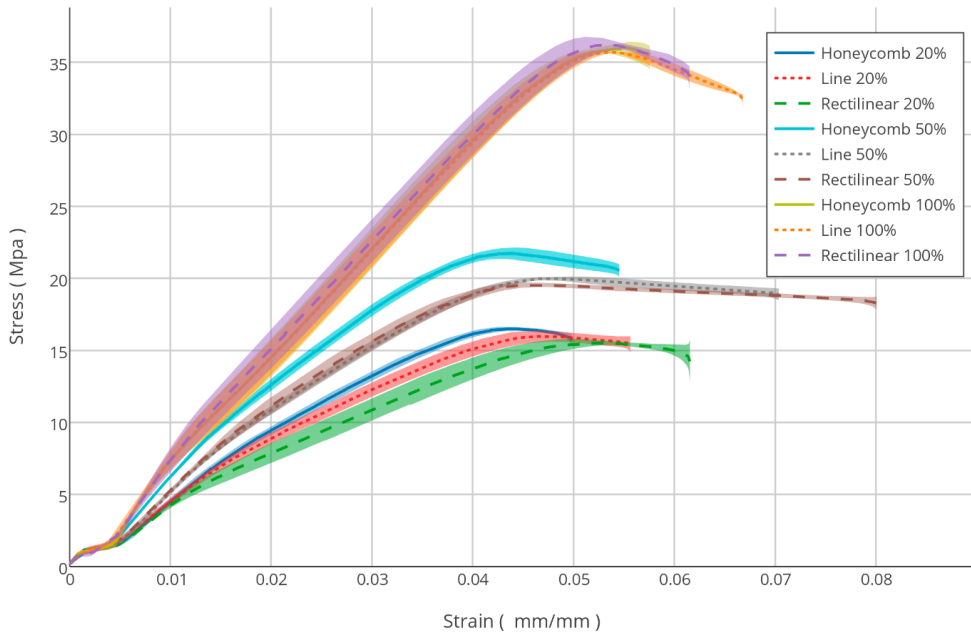


Figure 6.12 Strain-Stress diagram of the different mesostructures

As seen in Figure 6.12, the behaviour of the different mesostructures corresponds to the normal behaviour of the RAW ABS material, with a similar elastoplastic transition and a ductile break. In general, the deviations in the measurements are smaller than 5% of the value, with the exception of the rectilinear in 100% of infill, which is between 5% and 10% of deviation.

A stiffer behaviour of the honeycomb than the other two patterns was observed, resulting in better tensile strength. As commented before, this situation changes in the 100% infill density, possibly due to the software algorithm.

A squared-x model to describe the relationship between the tensile strength with the density modification was as follows:

Equation 6.1

$$\sigma_p = 15.2364 + 0.002083 \cdot x^2$$

Where

- $\sigma_p$  is the predicted tensile strength and

- $x$  is the infill density.

This model was evaluated with a lack-of-fit test. An ANOVA analysis was then carried out, as can be seen in Table 6.3.

*Table 6.3 Analysis of Variance with Lack-of-Fit of the squared- $x$  model*

<i>Source</i>	<i>Sum of Squares</i>	<i>Df</i>	<i>Mean Square</i>	<i>F-Ratio</i>	<i>p</i>
Model	3315.34	1	3315.34	6898.89	0
Residual	20.6642	43	0.480562		
Lack-of-Fit	0.021498	1	0.021498	0.04	0.8353
Pure Error	20.6427	42	0.491492		
Total (Corr.)	3336.01	44			

The test was performed by comparing the variability of the current model residuals to the variability between observations at replicate values of the independent variable  $X$ . Since the  $p$ -value for lack-of-fit in the ANOVA table is greater or equal to 0.05, the model appears to be adequate for the observed data at the 95.0% confidence level.

### 6.2.5. CONCLUSIONS

In this research, the significant effects of infill density and pattern on mechanical properties of the desktop FFF 3D printing process have been experimentally studied. Practical findings in the 3D printing process showed that:

- The combination of Rectilinear pattern in a 100% infill shows the highest tensile strength, with a value of 36.4Mpa, a difference of less than 1% from that of Raw ABS material.
- Under the same density, the Honeycomb pattern shows a better tensile strength, although the difference between the different patterns is less than 5%. This discrepancy could be attributed to small variations of the amount of plastic deposited for each pattern.
- The deposition trajectories and consequently the inter-layer bonding zones are very different between Honeycomb and Rectilinear patterns.

This could be a reason to explain the elastic modulus difference. However, more research on this topic needs to be undertaken before this association is more clearly understood.

- The change in the infill density determines mainly the tensile strength, and the stiffness, especially between 20% and 50%.
- The mechanical behaviour between the different mesostructures is similar, and the dispersion between the samples is below 10%.
- The relationship between infill density and tensile strength can be fitted in a squared-x model.

Further studies are needed to understand the crystallinity volume fraction of the samples as previous studies developed on PLA, as it was observed a strong relationship between this characteristic and the tensile strength (B. Wittbrodt & Pearce, 2015).

The scarcity of studies in the literature about the influence of mesostructure, as well as other factors such as environment, reveal a need for further research into the mechanical behaviour of the 3D printed pieces.

---

### **6.3. STUDY: DETERMINATION OF INFILL DENSITY AND PATTERN INFLUENCE IN THE BENDING BEHAVIOUR**

The structure of FFF components can be understood at multiple scales: (1) the microstructure, the scale of the polymer chains alignment in the filament beads, (2) the mesostructure, the scale of the distribution of the beads, and (3) the macrostructure, which comprises the design of the component. As shown in Figure 6.13 (left), the microstructure of the beads changes during the extrusion. Figure 6.13 (right) shows the common mesostructure of FFF components, which comprises: a) a set of solid boundary areas, called top layers, bottom layers, and perimeters or contours, and b) an infill structure or pattern. The



perimeters and top/bottom layers become indistinguishable in curved components and form a 'shell' around the infill pattern.

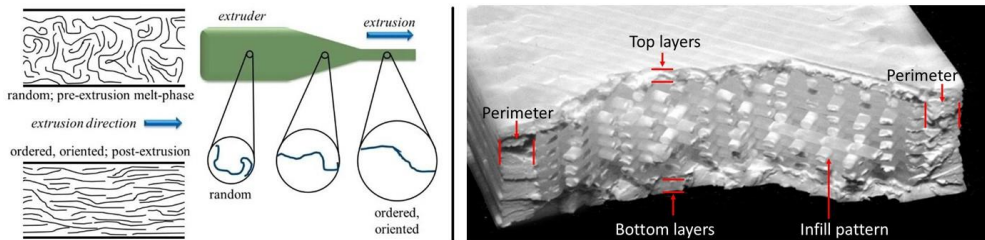
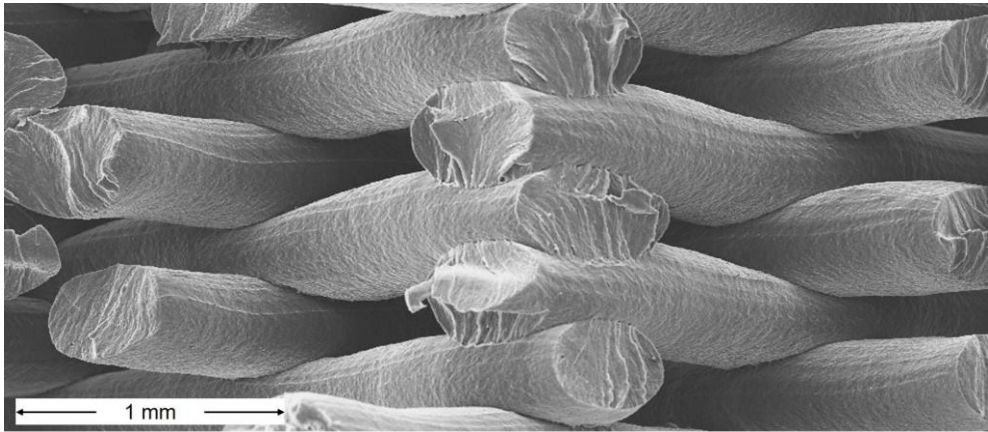


Figure 6.13. Microstructure (left), adapted from (Azo materials, 2018), and mesostructure in FFF (right).

Although the material properties are one of the key contributors to the mechanical behaviour, the quality of the polymer molecular diffusion between beads and alignment of these seem to be the main determinants of the part's behaviour (Abbott et al., 2018). The mesostructure design determines how and when the beads contact each other, changing, for example, the fracture behaviour from ductile to brittle (Rodríguez et al., 2003).

Some studies compare this structure to that of fibre-reinforced composites (Bellini & Güçeri, 2003; Sood et al., 2010), as the deposition with the beads aligned to the loading is stronger than across (Rodríguez et al., 2003). The extrusion of filament creates an alignment of the polymer chains in the direction along the beads (Es-Said et al., 2000), making this direction stronger than the perpendicular, mainly determined by bonding and molecular diffusion between beads (Tymrak et al., 2014). Similarly, the load capacity in the direction across layers is determined by the bonding quality between beads of different layers. Usually, the interlayer bonding (between layers) is weaker than the intralayer bonding (between beads of the same layer) (Abbott et al., 2018).

As shown in Figure 6.14, the bead is deformed to enhance the polymer diffusion with beads in the same layer or below. The bead in the already deposited layer needs to be just above the  $T_g$  in a semisolid state to be capable of not deforming when the new layer is deposited (Abbott et al., 2018).



*Figure 6.14. Beads mesostructure in a flexural test specimen SEM micrograph of the fracture surface.*

Due to the limitation of the process to deposit material by (usually) a single head, the time required to produce components increases exponentially with the increase of size in the case of producing fully solid parts. In FFF, there is no need to remove the non-solidified material from inside the components, as would be the powder liquid in other AM processes. Therefore, it is common practice to reduce the amount of material in the infill structure by increasing the space between beads. This space, also called gap, allows utilising a different structure or pattern design depending on the component function, as shown in Figure 6.15.

The mesostructure leads to a non-uniform distribution of the strain energy (Rezayat et al., 2015). Therefore, it is an element that the designer needs to consider when designing components for FFF.



*Figure 6.15. Examples of various patterns that could be used to reduce the density of FFF components.*

There is a growing body of literature studying the mechanical characterisation of FFF. This characterisation can be found on mechanical fracture (Hart & Wetzel, 2017), tensile and compression tests (Sood et al., 2012; Tanikella et al., 2017; S. Ziemian et al., 2015), bending and torsion (Hong et al., 2019; Wu et al., 2018), impact (Roberson et al., 2015; Tsouknidas et al., 2016), or fatigue (Afrose et al., 2016; J. Lee & Huang, 2013; S. Ziemian et al., 2015). Among the structural parameters studied, the most common is the orientation of the specimens or the infill beads. It should be noted that in FDM systems, the software generates by default a meander pattern, which rotates 90 degrees every layer. However, the software tools for toolpath preparation for the other systems commonly allow a more extensive range of infill patterns, as illustrated in Figure 6.15. This study aims to examine the relationship between three infill patterns and densities and the bending behaviour.

### 6.3.1. MATERIALS AND METHODS

The material used for this study was nature colour ABS provided by Torwell (Torwell Technologies Co. Shenzhen, China), provided in the form of a filament of 3mm in diameter. The technical datasheet of the material indicated a flexural strength of 70.5 MPa and a flexural modulus of 1990 MPa. However, injection-moulded sample pieces were tested to obtain the reference values for the behaviour and strength of the material. Some of the filament was cut into pellets

in a plastic shredder, and a series of test pieces were injection moulded under the standard ISO 178. The obtained properties were a flexural strength of 70.62 MPa and modulus of 2,064 MPa.

The specimen dimensions indicated in this standard were adapted for the FFF specimens to allow more area for the infill structure. Figure 6.16 shows the dimensions of the specimens and the orientation of manufacturing. The pattern is for illustration purposes only, as the specimens included solid top and bottom layers.

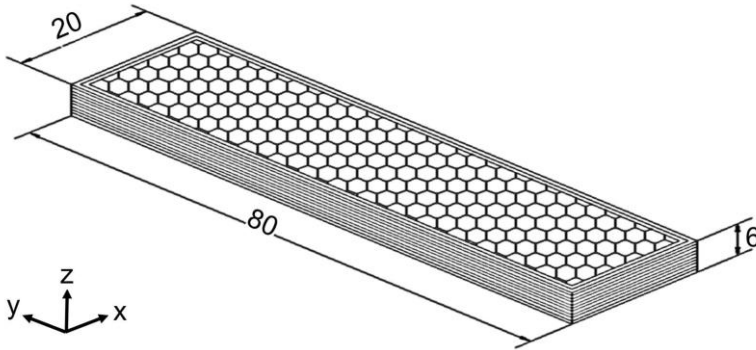


Figure 6.16, Dimensions, in mm, and orientation of the test specimens. Infill pattern for illustration purposes only.

A desktop-grade open-source FFF machine with a nozzle of 0.5mm in diameter was used for this study. The design of this machine, Reprap Prusa i3, is currently one of the most widespread machine configurations (Wohlers, 2016a).

The Marlin (RepRap, n.d.) open-source firmware and Slic3r (Ranellucci, n.d.) toolpath generation software were used respectively to command and control the 3D printer and to generate the toolpath files for the fabrication of the specimens.

The most significant parameters that were kept fixed during the study are shown in Table 6.4. The predefined software values were used in the case of the parameters not mentioned in the table.

*Table 6.4. Values of some of the fixed parameters.*

Parameter	Value
Layer thickness	0.3 mm
Perimeters	3
Solid top & bottom layers	3
Infill pattern top & bottom layers	Rectilinear
Infill angle	45°
Extrusion width first layer	200%
Bed temperature	110°C
Extrusion temperature	230°C

The effect of infill density and pattern were studied by varying these parameters according to the experimental setup summarised in Table 6.5<sup>4</sup>. Five specimens of each design were produced to identify any dispersion between specimens with the same designed geometry.

*Table 6.5. Specimen designation and parameters setup.*

Designation	Infill pattern	Infill density
H20	Honeycomb	20%
H50	Honeycomb	50%
H100	Honeycomb	100%
L20	Line	20%
L50	Line	50%
L100	Line	100%
R20	Rectilinear	20%
R50	Rectilinear	50%
R100	Rectilinear	100%

<sup>4</sup> Note: The density is the value specified in the software, not the measured density of the specimen

The flexural strength tests were performed in an Instron model 5967 double-column universal test machine with a load capacity of 30 kN. The three-point flexural tests were carried out according to the ISO 178 standard, as shown in Figure 6.17. A crosshead speed of 2 mm/min was used, with a separation between supports of 64 mm, and a preload of 20 N. The order of testing of the samples was randomised to avoid influences in the testing setup.



*Figure 6.17. Testing experimental setup.*

The specimens were sectioned and gold sputtered to add a conductive coating for SEM microscopy once the mechanical tests were carried out. As shown in Figure 6.18, just a small section of the specimens was used. It can be observed that the fracture zones are not in a single plane. The fracture zones were analysed using a JEOL JSM 5410 scanning electron microscope.

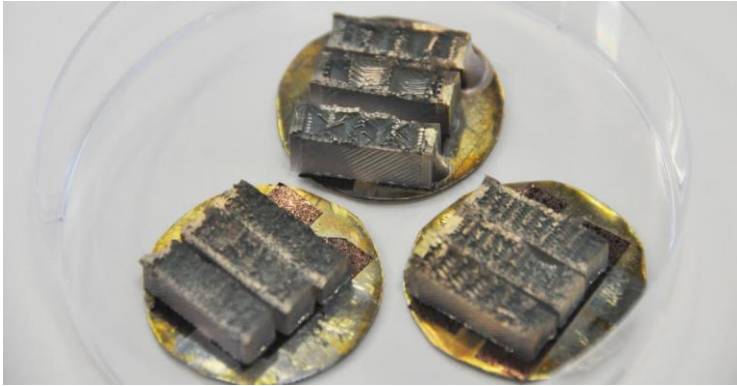


Figure 6.18. Specimens prepared for SEM microscopy. 100% (left), 20% (top), and 50% (right) infill density.

The data was plotted, and an analysis of variance (ANOVA) was performed to evaluate the influence in the tensile strength and confirm the visual evaluation of the data and graphs.

### 6.3.2. RESULTS AND DISCUSSION

Figure 6.19 shows two examples of the load vs displacement graphs from the testing of two sets of specimens. As can be observed, there is a low dispersion between results, which indicates a controlled manufacturing and a low impact from the uncontrolled environmental conditions. The results of the other sets were similar.

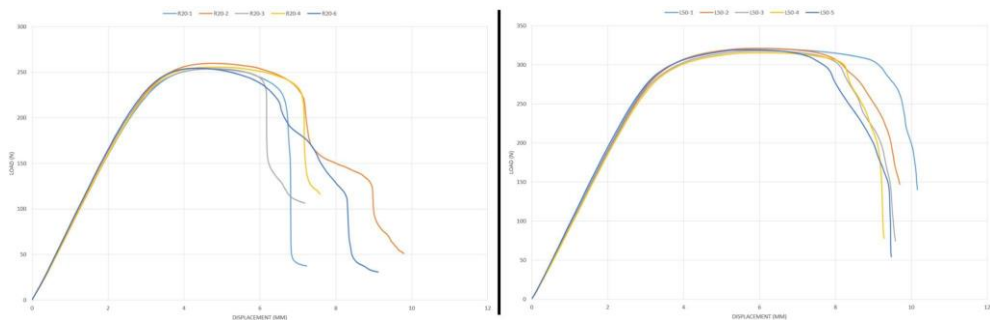


Figure 6.19. Load vs displacement graph of the specimens with 20% rectilinear pattern (left) and 50% linear pattern (right).

As can be observed, the behaviour of the specimens is very similar in the elastic zone and starts diverging in the plastic area. The fracture behaviour seems to differ between samples and between patterns as well. The fracture behaviour is ductile, unlike the brittle behaviour when the main loading direction is parallel to the layers (Hart & Wetzel, 2017).

The load and displacement values were used to calculate the flexural strain and stress of each series of specimens using the equations 6.1 & 6.2.

Equation 6.2

$$\sigma_f = \frac{3FL}{2bh^2}$$

Equation 6.3

$$\varepsilon_f = \frac{6sh}{L^2}$$

Where  $\sigma_f$  is the flexural stress,  $\varepsilon_f$  the flexural strain,  $F$  the load,  $L$  the separation between supports,  $b$  the width of the specimens,  $s$  the deflection, and  $h$  the thickness.

The flexural modulus was calculated by finding the flexural strain of the two points of  $\varepsilon_{f1} = 0.0005$  and  $\varepsilon_{f2} = 0.0025$ , and using the equation 6.3

Equation 6.4

$$E_f = \frac{\sigma_{f2} - \sigma_{f1}}{\varepsilon_{f2} - \varepsilon_{f1}}$$

Where  $\sigma_{f2}$  is the flexural stress in  $\varepsilon_{f2}$  and  $\sigma_{f1}$  is the flexural stress in  $\varepsilon_{f1}$ .



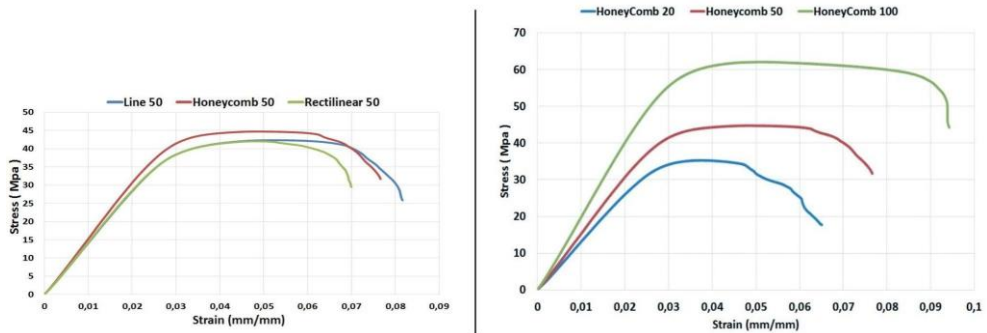


Figure 6.20. Average strain-stress graphs, comparing patterns and infill densities. Left – different infill patterns at 50% density. Right – comparison between infill densities with the honeycomb pattern.

The comparison of the average strain-stress graphs between patterns shows a similar behaviour during the testing and an apparent increase in stiffness and strength between the infill densities, as shown in Figure 6.20.

Looking into the dispersion, Figure 6.21 shows the flexural strength and modulus of the specimens. The specimens prepared by injection moulding seem to show the highest flexural strength (70.62 MPa) and modulus (2064 MPa). This could be because injection moulding involves applying pressure to compact the material in the mould cavity, while in FFF, the beads are just deposited next to each other (Dawoud et al., 2016).

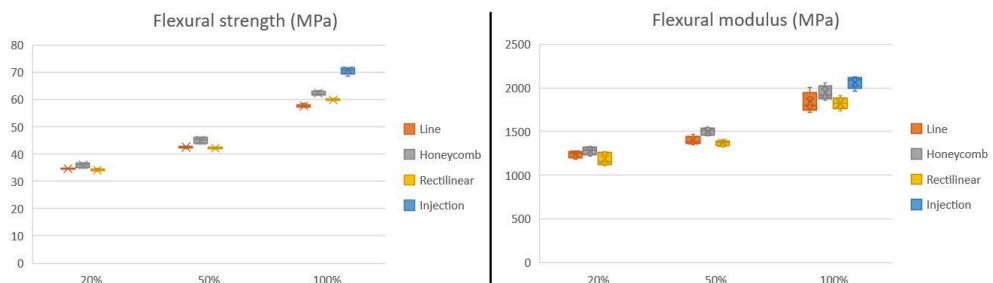


Figure 6.21. Flexural strength (left) and modulus (right) of FFF and injection moulded specimens.

The configuration of variables that gave the greatest flexural strength was the Honeycomb pattern and a density of 100%, with an average maximum resistance of 62.34 MPa. The lowest value obtained came from the Line pattern with a density of 20%, with a flexural strength of 34.08 MPa.

The average flexural modulus increased as the infill density was increased, going from 1186 MPa with a density of 20% to 1946 MPa with a density of 100%. The deformation under maximum load did not show significant variations, around 5%, between the different infill densities of 50% and 100%.

The honeycomb pattern shows a slightly higher strength and stiffness than the other patterns. This difference could be due to the capability of stress distribution and high stiffness of the honeycomb pattern, used by nature in several structures with stiffness requirements (L. J. Gibson et al., 2010).

However, a possible explanation for this result might be an increase in the amount of material deposited and, therefore, in the components' actual density, as shown in Figure 6.22.

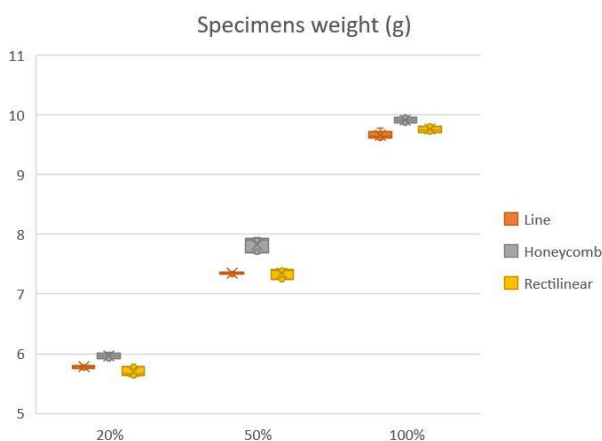


Figure 6.22. Comparison of specimens weight.

An analysis of variance (ANOVA) was performed to confirm the visual evaluation of the data and graphs, taking the flexural strength as the dependent variable and the density and pattern as principal effects.

Table 6.6. Results of the ANOVA of the flexural strength.

Source	Sum of Squares	df	Mean Square	F	Sig.
Principal Effects					

A:Infill density	4898.96	2	2449.48	6199.48	0.0001
B:Infill pattern	69.8973	2	34.9487	88.45	0.0001
<b>Interactions</b>					
AB	19.1067	4	4.77667	12.09	0.0001
Waste	14.224	36	0.395111		
Total (Corrected)	5002.19	44			

Table 6.6 shows the results of the ANOVA, showing an evident influence of the infill density (as expected) in the flexural strength at a 95% confidence level. The pattern and the combination of both have less influence than the infill density by itself.

The manufacturing time could be a reason as well for the designer to utilise one pattern or density instead of another. Figure 6.23 shows the average manufacturing time of the specimens in the study.

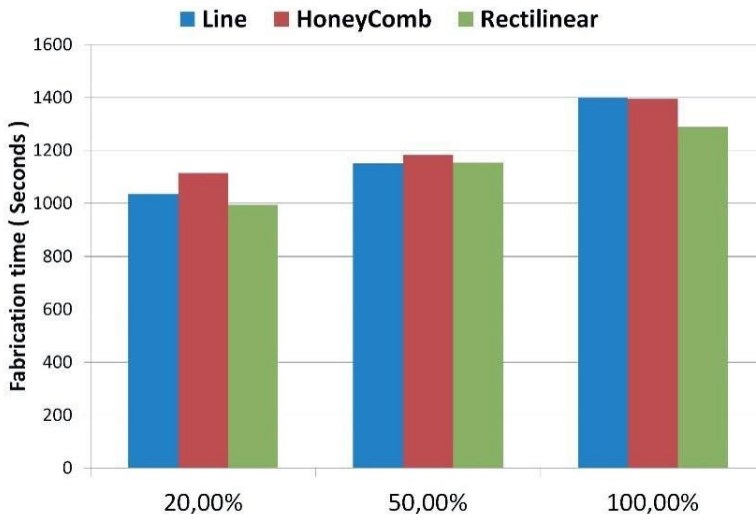
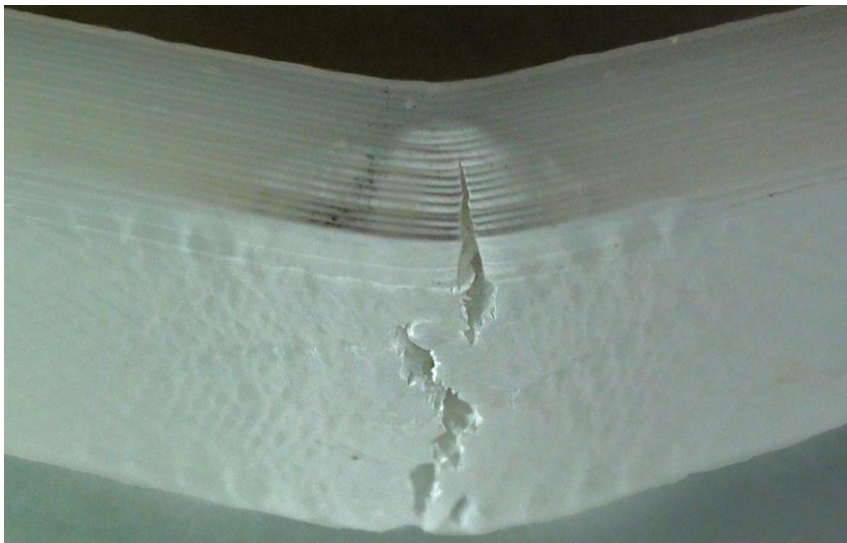


Figure 6.23. Comparative graph of production times.

As shown in the figure, there is a slight increase in manufacturing time between 50% and 100%, while the strength shown in previous figures increases in a more significant proportion. This difference could be due to the mesostructure of the specimens, as the solid boundary areas make up to 40% of the total sample volume.

A macro photograph of the fracture zone in one of the samples can be seen in Figure 6.24. As expected in a beam under bending load, the tensile stress in the bottom layer initiates the fracture. Whitening can be observed in the area under higher strain, closer to the fracture, and building up across the crack propagation path. This whitening is caused by shear yielding (due to the alignment of polymer chains) and cavitation by the rubber particles (due to the breakage of the van der Waals bonds with the matrix, leading to microvoids), commonly observed in ABS failure (Ramaswamy & Lesser, 2002).



*Figure 6.24. Specimen macro photography during fracture.*

A SEM examination of the fracture surface morphologies was performed to help understand the characteristics of the fracture behaviours. Figure 6.25 shows the comparison of the fracture surface of the 100% specimens with different patterns. The voids between the beads can be seen in the form of

macroporosity and visible top ‘arches’ of the beads. In the line pattern micrograph, the beads can even be seen delaminated between layers and within the same layer. This situation could explain the lower strength of this pattern.

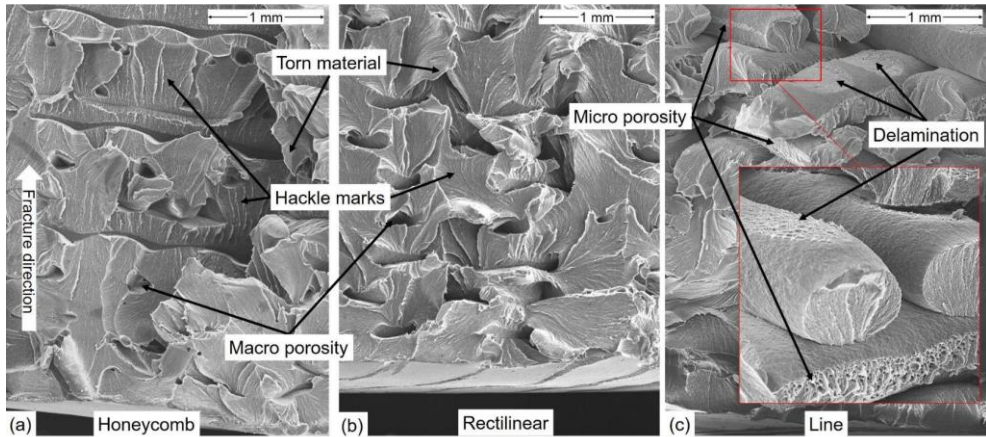


Figure 6.25. SEM micrograph of the fracture surface of 100% infill specimens with (a) Honeycomb, (b) Rectilinear, and (c) Line patterns.

The torn material’s distortion, stretching, and shearing reveal a ductile fracture for all patterns, as expected from the shear yielding observed in the macro photography (Hayes et al., 2015). However, the microporosity or fibrillation observed in the interfaces between delaminated filaments reveals a brittle fracture on those interfaces.

Linear markings, or hackles, can reveal high crack velocity regions due to localised plastic deformation on the fracture surface. These are also visible in the SEM micrographs of the patterns with a lower density, as shown in Figure 6.25. In this figure, the solid bottom area could be clearly distinguished from the infill section. In the honeycomb figure (right), a localised fibrillation micro shearing on the bead surface of topmost of the bottom layers can be seen, suggesting a poor adhesion between the beads of the same layer and a brittle fracture. The reduction in density creates mesostructures that reduce the contact surfaces between beads and, therefore, the effective cross-sectional area to which load is applied, contributing to knockdown in strength.

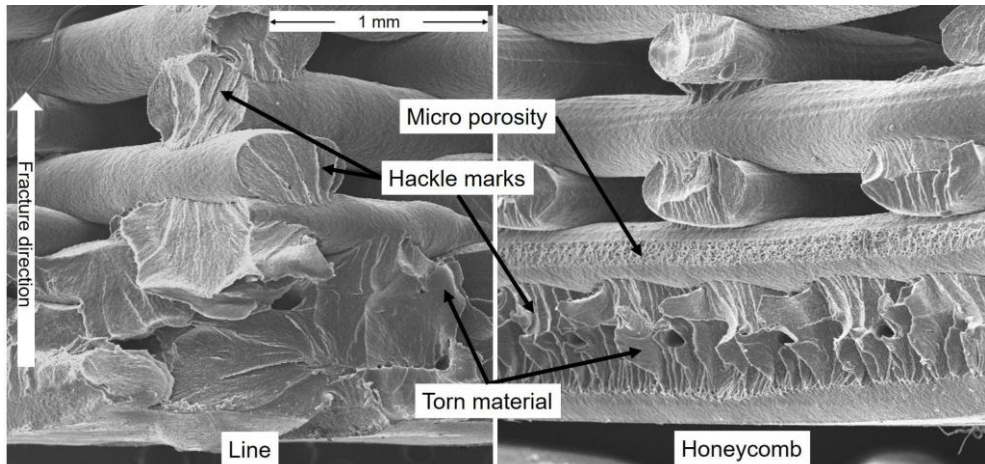


Figure 6.26. 50% density SEM micrograph of the line (left) and honeycomb (right) specimens.

Although the figure above shows no bead delamination, it is not clear to assess the quality of the adhesion of the layers. Figure 6.27 below shows the fracture surface of two specimens in areas with discrete high density. It can be seen that the continuous hackle areas between layers, suggesting a good interlayer adhesion.

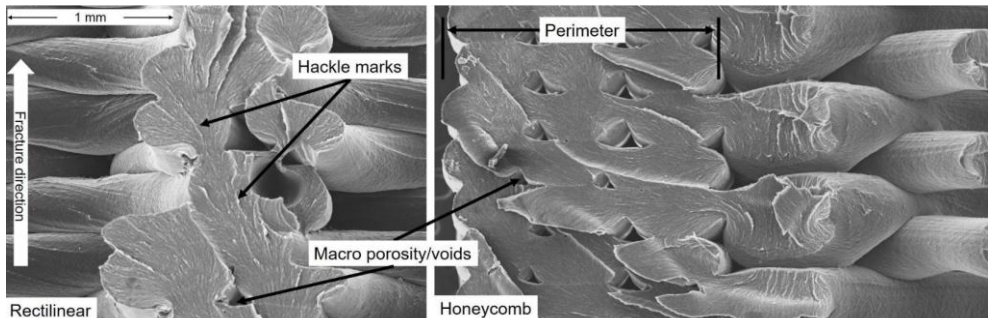


Figure 6.27. SEM micrograph of 50% dense specimens in the infill area of the rectilinear pattern (left) and perimeter area in the honeycomb pattern (right).

The separation (or not) of beads between layers in the different densities of the line pattern is due primarily to the low inter-laminar bond strength that results from incomplete polymer melt diffusion as the hot polymer is deposited onto the cooler, solidified polymer part (Hart & Wetzal, 2017). The 100%

density pattern takes longer to be produced, and therefore the previous layer is cooler than in the 50% specimen.

### 6.3.3. CONCLUSIONS

The maximum flexural strength values achieved in this experiment were similar to 3D printing processes using commercial ABS thermoplastics extrusion (Crocco et al., 2013). The strength of the 100% dense patterns showed a flexural strength of 88% from the injection moulded samples.

A density of 100% in a Honeycomb pattern provided an average flexural strength of 62.34 MPa, the maximum value obtained in the study. However, this increases drastically the time and material required, and the pattern virtually disappears. Between a density of 20% and 50%, the difference in printing time is negligible compared with the improvement of flexural strength. Therefore, it is recommended to reduce the density from 100% to 50%. The influence of infill density on flexural strength is greater than the influence of infill pattern.

The fracture analysis shows that, in 100% infill specimens of the honeycomb and rectilinear patterns, the individual filaments are squeezed together resulting in a structure similar to that of injection moulded parts, in line with the literature (Dawoud et al., 2016). This effect also occurs in the line pattern, but some areas show the same behaviour as less dense patterns, with fibrillation and failure similar to that of composites (Bellini & Güçeri, 2003; Sood et al., 2010). The time required for the deposition seems to influence the failure behaviour; therefore, reducing the density to reduce the layer time should be considered.

The orientation, time, density, and pattern of the infill should be considered to control the bending behaviour of FFF components. This could be done by (1) understanding the behaviour of parts through prototyping with various parameters or (2) predicting the behaviour with physics models (Cuan-Urquizo et al., 2015) or CAE software tools developed for this purpose (e-Xstream engineering, n.d.).

---



## 6.4. MECHANICAL PROPERTIES STUDIES. CONCLUSIONS

Considering these two studies, the infill pattern influences the mechanical behaviour of ABS components slightly, while the density is the most significant contributor. The results obtained show that the influence of the different patterns causes a slight variation of up to 4.7 MPa in maximum tensile strength, although the behaviour is similar. Under tensile loading, the rectilinear pattern with a 100% density shows the highest strength with 36.4 MPa, while it was the honeycomb pattern under bending loads with 62.34 MPa in 100% density as well. Compared with the raw material properties obtained from the testing injection moulded specimens, the strength difference seems lower in tensile, 1%, than in bending loading, 12%.

These results should be taken with caution as the continuous material and technology development and the large number of factors that influence the mechanical behaviour make it very difficult to provide “definitive” information in this regard. In particular, the perimeter walls, or shell, thickness could determine the mechanical behaviour in great measure, as these are fully solid areas (with some voids as observed above). The wall thickness could be increased to obtain better mechanical properties (Ćwikła et al., 2017).

Other parameters that greatly determine mechanical behaviour are the orientation and the layer thickness. Various studies document the influence of the orientation in the strength of FFF components, indicating that the components are weaker and show more brittle fracture when the stress is perpendicular to the layers (Afrose et al., 2016; Es-Said et al., 2000; Popescu et al., 2018). The change in layer thickness modifies the bead contact area between layers, modifying the size of the voids shown in the SEM above (Rankouhi et al., 2016), and therefore influences the strength, with observations of 8% in ABS to 11% in PLA (Rodríguez-Panes et al., 2018).

The large number of materials available makes it challenging to provide information about each material. Furthermore, the raw material that each manufacturer provides varies in its composition and consequently in its behaviour (Tanikella et al., 2017). However, it seems that the infill density, and



therefore the weight of the component is a crucial mechanical strength determinant for various materials.

Therefore, the geometric benchmarking of FFF components is recommended to be performed by using a representative section of the geometry of the component and applying the loads expected to that section. Alternatively, off-the-shelf software tools could be used to predict the behaviour of the components (e-Xstream engineering, n.d.).

## **6.5. SUMMARY**

This chapter has identified the geometry parameters that determine the mechanical behaviour of FFF components. The design-defined parameters that modify the mechanical behaviour have been identified, and the lack of a suitable standard to test these properties. Without access to calibrated mechanical testing equipment, the designers need to rely on the emergent software tools or on testing sections of the design.

A linear correlation was obtained between the tensile strength and infill density in ABS. This approach could be developed in further work to help the designer make an educated guess of the mechanical behaviour of FFF components when the manufacturer provides the material properties.

The lack of standard definition of materials, processes and testing methods reduce the capability to provide fixed guidance on the mechanical behaviour. The author is actively participating in the ISO & ASTM standardisation efforts to provide a uniform definition of process, material and design guidelines, to help designers leverage this technology.

As identified, the properties and performance of the FFF part are affected by the extruded filament shape, the beads interaction, and strongly by the deposition trajectory. For this reason, the determination of the build strategy, such as part orientation, number of parts printed at the same time or the infill density will be included in the designers' support tool as important characteristics to pay attention to in an early stage of the design process.

The geometric and mechanical features described in this and the previous chapters are oriented mainly to help the designer understand the FFF process capabilities and part properties. However, the parts usually require a series of processing steps after the printing finalises to match the surface or the properties required. The next chapter will cover these steps.

# Chapter 7

# Post-processing of FFF parts

## 7.1. INTRODUCTION

Post-processing is the set of steps taken after completing an Additive Manufacturing (AM) build cycle to achieve the desired properties in the final product (ISO/ASTM, 2015). These are crucial to address the main issues that arise from AM-produced (and FFF-produced) components, such as porosity, anisotropy, roughness or dimensional accuracy.

FFF allows control of a wide range of parameters to partially enhance the produced component's quality to address some of these issues. Even if process parameters can be optimised, some issues still affect the printed components. In these cases, post-processing is crucial since it may be the only way to enhance the component further.

Post-processing could be the way to obtain specific characteristics such as higher thermal resistance, conductive or metallised surfaces, better mechanical properties, or transparent components. These techniques have been highlighted as the potential enabler to broaden the AM application range (I. Campbell et al., 2018).



*Figure 7.1. Post-processing steps of a functional FFF component.*

As shown in Figure 7.1, the post-processing of FFF components usually comprises phases determined by the material, shape, and component purpose. Each phase could be performed with various post-process techniques that have different design considerations. For example, sanding internal surfaces would be very challenging without large enough access openings.

The component purpose determines the phases and techniques required for the post-processing of a component. A component aimed to be part of the structure would need post-processing steps to improve its dimensional tolerances and roughness of mating surfaces, while a user-facing standalone product would require post-processing techniques aimed to enhance the aesthetic appeal of the surface.

Defining the end-to-end manufacturing process early in the design process is crucial to design, considering the limitations and characteristics of the post-processing techniques. Sometimes the steps from the moment the component comes out of the machine to the final product influence the design more than the process parameters themselves (J.-Y. Lee et al., 2020). E.g. The component shown in Figure 7.2 needs features to fix it to the CNC machine and alignment features.

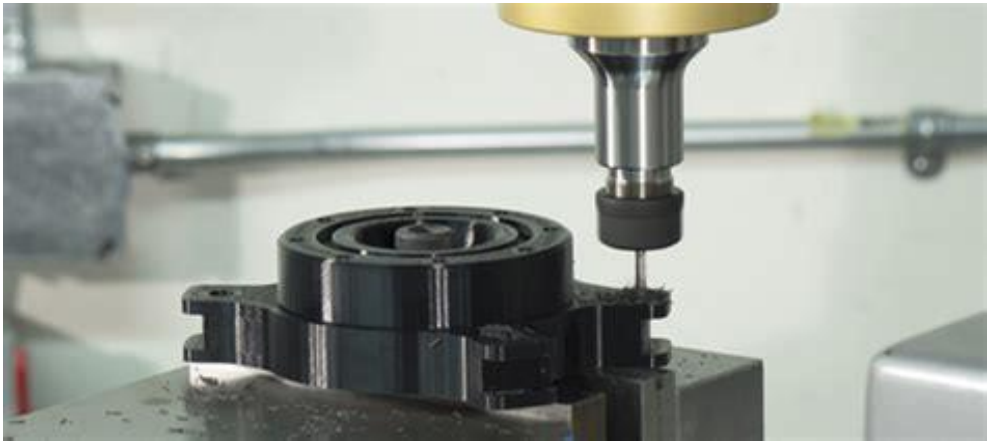


Figure 7.2. Machining of the mounting areas of an FFF component. Source: [stratasysdirect.com](http://stratasysdirect.com)

We documented and described some of the techniques in this section in a book oriented to support industrial designers in developing physical prototypes. We provided an overview of the materials and methods to produce aesthetical prototypes, including the 3D printing technologies and surface finishing techniques (Conejero et al., 2019).

This chapter aims to categorise and discuss the existing post-processing techniques adopted to improve the components produced by FFF, analysing their potential and limitations.

The structure of this chapter follows the phases of post-processing of FFF components, which usually comprise: (1) support removal, (2) Surface modification, (3) Coating and (4) assembly.

## 7.2. SUPPORT REMOVAL

The FFF process requires adding material (in addition to the primary body material) that functions as scaffolding for overhanging surfaces usually below 45°. These surfaces can be tubular sections, cavities, slender geometries, or cantilevers, which would be challenging to manufacture successfully without this material (Fernandez-Vicente et al., 2015). This scaffolding, commonly referred to as *support structure* or just *supports*, performs two main functions:

- Stabilises the part during manufacturing – as many systems rely on the print platform movement for one of the axes. The stabilisation is required because the filament is squeezed with the previous when deposited, creating downwards and sideways forces.
- Counteracts the Gravity force – which could overcome the bonding between beads in overhanging features, as described in a previous chapter.

The design of the support structure is usually automatically generated by the print preparation software. Most of the software tools allow modification of the support structure characteristics and deposition parameters. These structures could be created in the CAD software by the designer automatically (Schmidt & Umetani, 2014; Vanek et al., 2014) or added manually, as shown in Figure 7.3. The latter allows defining the areas where it would be challenging to remove the supports or supporting cantilever features at their extremities. This last approach helps avoid the generation of supports in the rest of the overhanging surface (Dumas et al., 2014).

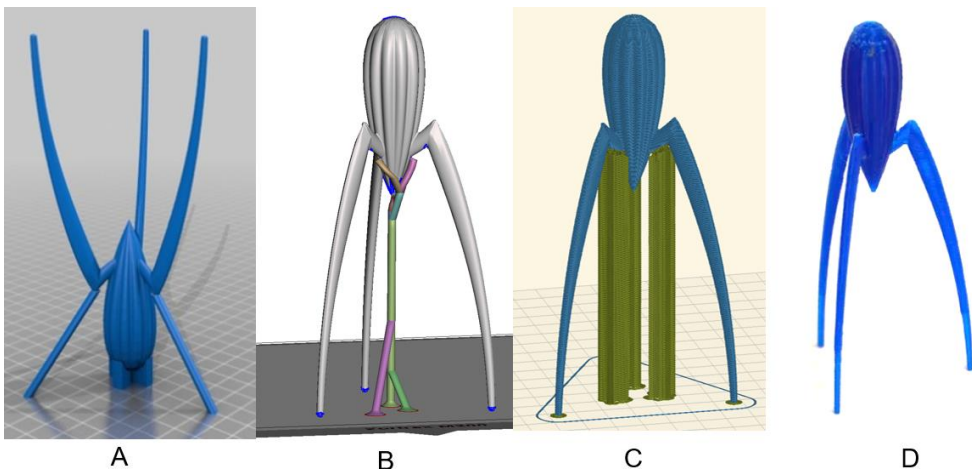


Figure 7.3. Different methods of supports structure generation: a) Manually in CAD, b) automatically generated in CAD, c) automatically generated by the print preparation software and B) the printed component after support removal.

These structures' purpose is to withstand relatively low forces and be removed just after finishing the print. Therefore, these are usually built of thin

walls with minimal contact area, creating a weak bond with the main component. The supports thin walls architecture aim is to be dissolved or broken easily. The minimal contact area purpose is to the removal facilitation without part damage (Chalasanani et al., 1995).

The support structure could be produced using the same or a different material than the component. The system capabilities or the material determine this decision. The support structure material needs to be produced with a material capable of withstanding the deposition conditions of the primary component material. The main aim of using a different material for the support structures is to remove it by chemical reaction.

The chemical composition of the support material needs to be different enough to be dissolved in the solvent while the primary materials stay unaffected. The polymer polyvinyl alcohol (PVA) is water-soluble and compatible with the common FFF build materials (ABS, PLA, Nylon and HDPE) (Duran et al., 2015). However, this material absorbs moisture from the environment, so it needs storage in a controlled environment. PLA could be used and the support structure for ABS components and removed with sodium hydroxide (caustic soda) in an ultrasonic bath (Kuo et al., 2012). However, this process involves handling hazardous material and specialised equipment. The author tested this method, finding that the PLA material does not get wholly dissolved, requiring manual intervention.

For high-temperature materials such as polyetherimide (PEI) (>350 °C in the extrusion and >180 °C in the building environment), it could be a challenge to use a material with enough chemical characteristics to be able to be removed by these methods. Polyphenylsulfone (PPSF) is commonly used as support material for PEI, or commercially known as ULTEM™, and is usually manually extracted (Stratasys, 2017b). Chueca de Bruijn et al. (2020) identified PPSF as a potential soluble support material for engineering-grade PEI material and developed a solvent-removal methodology.



*Figure 7.4. Process of manual support removal.*

Support structures need to be manually removed when the same material, or another without the possibility to be dissolved, are used to produce these. The optimisation of support structures parameters is even more critical in this case than with dissolvable supports. These will need to be broken by applying pressure, usually with nose pliers, and mechanically separated from the part, as shown in Figure 7.4.

In this method of support removal, the supports need to be accessible. Therefore, enclosed cavities need to be designed to be self-supporting or include openings.

The removal of supports sometimes leaves marks in the component (Karasik et al., 2019) or support material still attached to the component, as shown in Figure 7.4. Depending on the component's purpose, this requires an additional step of surface modification. The methods for this phase will be described in the next section.

### **7.3. SURFACE MODIFICATION**

One of the main challenges when producing any product is to determine the required surface quality. It is crucial to ensure proper operation of mechanisms or assembly and affects its final appearance. It is essential to understand its function and then select the proper process and parameters.

Literature usually refers to surface quality as the roughness parameters, such as the arithmetic mean roughness (Ra), Root mean square deviation (Rq) or maximum height of the profile (Rt), among others.



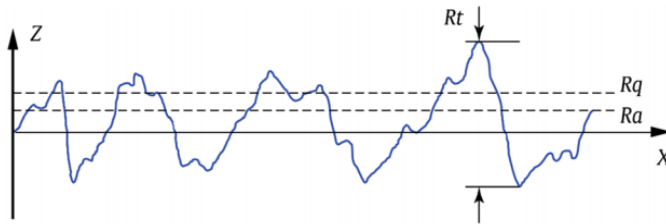


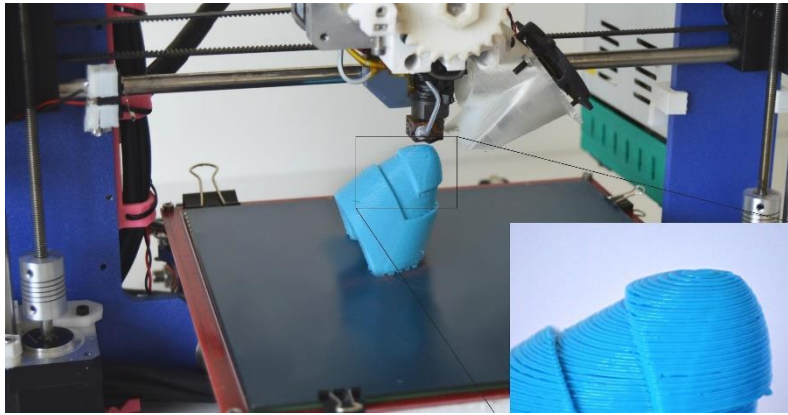
Figure 7.5. Surface roughness parameters  $R_a$ ,  $R_q$  and  $R_t$  (Castro-Casado, 2021)<sup>5</sup>

Although roughness can be measured and expressed quantitatively through these elements, the surface quality usually is expressed and assessed with qualitative attributes such as “shiny”, “good”, or “matt”. Therefore, it is paramount to understand the purpose of the product and the customer preferences to downselect the right type and amount of surface finishing required.

The surface quality of FFF components after support removal sometimes does not meet the requirements of the functionality. As described in a previous chapter, the discrete deposition of a filament layer by layer has the consequence that the surfaces of the components show the paths of the nozzle. These paths create terraces on the surface, also called the *staircase* effect, as shown in Figure 7.6, leading to relatively high average roughness values (Livesu et al., 2017).

The scale of this staircase gets determined mainly by the size of the nozzle and the layer thickness (Nancharaiah et al., 2010). The designer could minimise this effect could by optimising the layer thickness. Using thin layers reduces the surface roughness but requires more time to produce the component than using thicker layers (Mwema & Akinlabi, 2020). Various software tools allow a layer thickness adaptation driven by the surfaces’ steepness in a component section (Sabourin et al., 1996). Other alternative strategies of slicing have shown potential to improve the quality of the components (B. Huang & Singamneni, 2012).

<sup>5</sup> Reprinted with permission of Springer Nature Customer Service Center GmbH



*Figure 7.6. Staircase effect in a component printed with FFF.*

An area of active research is the development of methods to decide the suitable surface modification technique. Gordon et al. (2016) identified the benefits and complexities of each post-processing technology for metal AM and proposed using a decision tree with a series of yes/no questions.

There are two main post-processing or surface engineering approaches to counteract the staircase effect: removing material from the component surface until removing the *tips* of the beads or filling the gaps between beads. The former, surface modification, is covered in this section, and coating is covered in the next. The material is added to the surface in coating processes, and the underlying material or substrate is not detectable on the surface. In the surface modification, the surface properties are changed, but the substrate material is still present (Mattox, 2010). As shown in Figure 7.7, the surface angle determines the quantity required of material removal, or addition, to achieve a smooth surface. This dependency is a challenging characteristic for some post-processing methods that affect all the surfaces uniformly: too much surface modification in some areas might mean not enough for other areas.

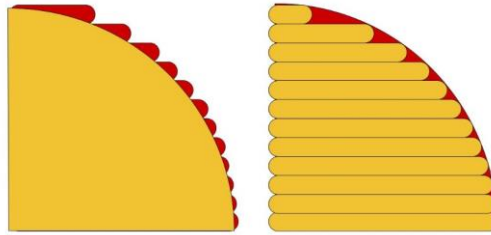


Figure 7.7. Approaches to remove the staircase effect to form a curved surface. Surface modification (left) and coating (right).

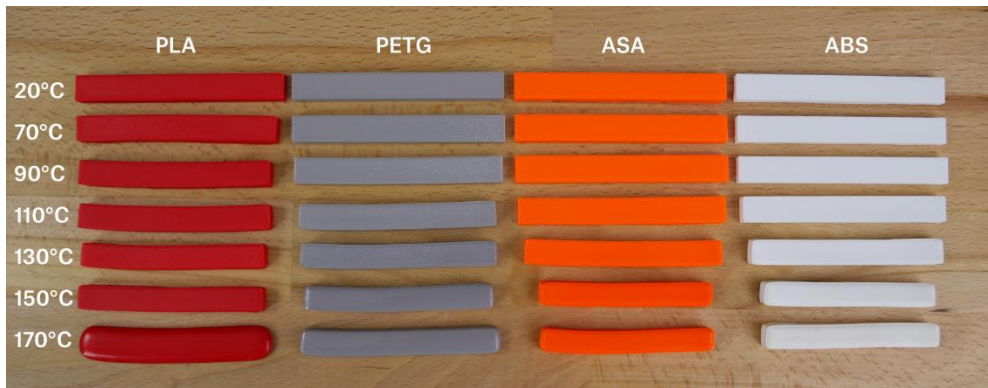
The methods developed to modify the surface in FFF components can be categorised into heat, chemical and mechanical (Wickramasinghe et al., 2020). These methods' effects on the surface quality improvement and the mechanical characteristics are described below. Some of these methods improve the bonding between layers, and therefore the strength of the components.

### 7.3.1. HEAT

A method to modify the surface of FFF components is to use thermal annealing or heat treatment to improve the surface quality and strength of the components. Thermal annealing seems to increase the toughness of the adhesion between layers. This effect has been observed in ABS (S. Singh & Singh, 2016) and PLA (Hong et al., 2019). In ABS, when the annealing temperature reaches the glass transition temperature, the molecular surface tension minimises, and the material flows on the surface. This flow fills the gaps, removes the typical layer marks on the surface, and improves the bonding between layers and, consequently, mechanical properties. It seems that annealing temperature is a crucial parameter that impacts the mechanical properties.

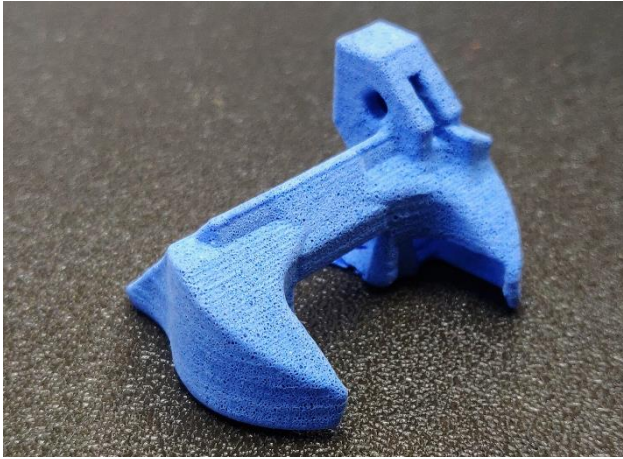
In contrast, the duration seems not to affect these (S. Singh et al., 2019). However, in PLA, a high temperature and long exposure seem to increase the bond between layers, increasing the strength and reducing the ductility. A lower temperature with a longer exposure time seems to be a reasonable approach to both preserve ductility and improve strength (Torres et al., 2015).

Some non-academic experiments tried to identify the effects of this method on the mechanical and surface. Kočí (2019a) found pronounced dimensional changes in four common FFF materials after 30 minutes of exposing them to a range of temperatures, as shown in Figure 7.8. Applying the method to complex shapes revealed that it seems unusable for components with complex shapes and precise dimensions.



*Figure 7.8. Dimensional change of PLA, PETG, ASA and ABS after thermal annealing. Source: Prusarinters.org*

Another technique is to embed the components in salt. The variation of dimensional tolerances seems to be lower than without surrounding media. However, it seems that grain size determines the texture of the final components (Hermann, 2020), as can be seen in Figure 7.9.



*Figure 7.9. Surface finish in a PETG FFF component after thermal annealing embedded in salt.  
Source: cnckitchen.com*

This type of post-process is needed, for example, when using filaments loaded with metal. The polymer acts as a binder between the metal particles. The heat treatment removes the polymer and sinters the metal parts together (Tosto et al., 2021).

This method seems promising due to the easy access to low-cost ovens. However, this implies ancillary equipment and consequent costs of energy for the heat treatment.

### 7.3.2. CHEMICAL SOLUTIONS

When using chemicals to modify the surface of FFF components, the polymer gets exposed to a solvent that makes the surface become viscous and reflow temporarily. In this state, the beads surface tension that determines their oval profile gets diminished or broken. This tension becomes shared between all the layers, smoothing in this process the staircase effect (Anthamatten et al., 2004).

As shown in Figure 7.10, there are mainly two approaches to expose the components: through vapour and immersion. In the former, the component is placed in an enclosed environment, where the container could be heated, accelerating the solvent evaporation. Then it is taken out to allow the solvent on the component surface to evaporate (W. R. Jr. Priedeman & Smith, 2003). By

immersion, the treatment is more aggressive and requires less processing time, but the exposure control is more complicated than the vapour method. There is a risk of the solvent penetrating the component structure, making it unusable.

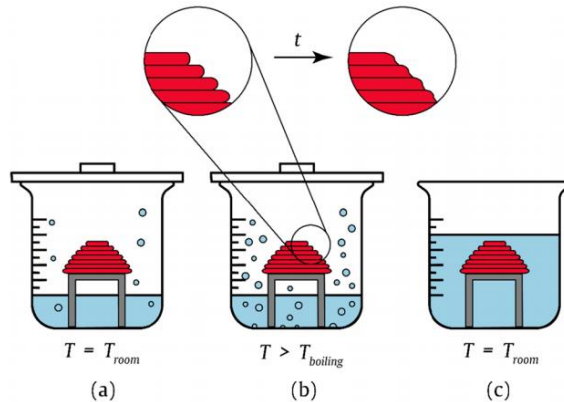


Figure 7.10. Methods of chemical post-processing by (a) natural evaporation, (b) forced evaporation and (c) immersion (Castro-Casado, 2021).<sup>6</sup>

Much of the current literature on this topic pays particular attention to the treatment of ABS with acetone (Colpani et al., 2019; Garg et al., 2017; Khan & Mishra, 2020). This situation could be due to the availability of ABS as material for FDM for a period longer than other materials. Nonetheless, some authors have explored the exposure of PLA to acetone as well (Havenga et al., 2018; Jin et al., 2017).

In treating ABS components with acetone, the gaps between layers and voids on the surface are filled with dissolved polymer becoming smoother when drying. However, this modifies the mechanical properties of the components in a negative way (Garg et al., 2017).

### Acetone dipping experiment

This study set out to investigate the usefulness of the immersion method for FFF ABS components. As shown in Figure 7.11, two types of samples were exposed to acetone to understand this technique's effects on the wall thickness

---

<sup>6</sup> Reprinted with permission of Springer Nature Customer Service Centre GmbH

and the geometric tolerances (cylindricity, planarity and dimensional accuracy).

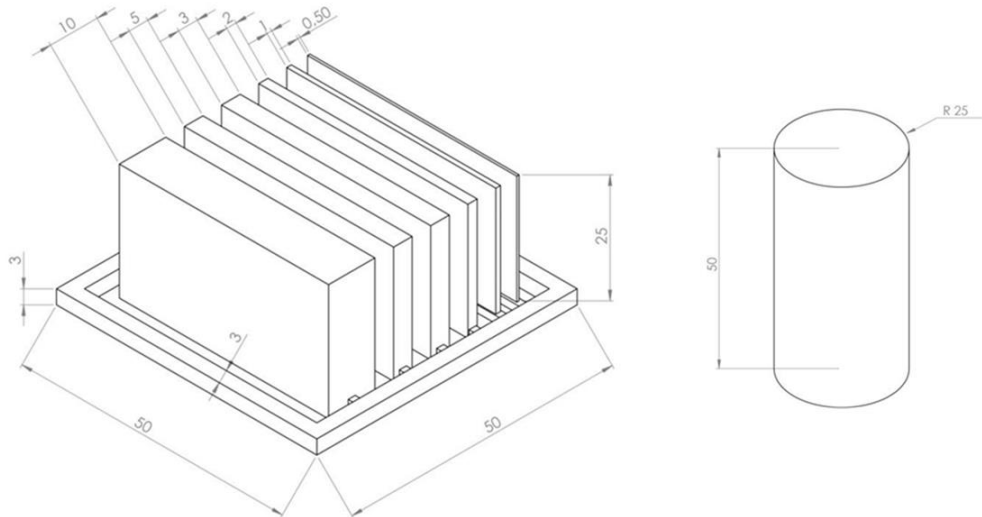


Figure 7.11. ABS Specimens that were used in the experiment of acetone dipping. Wall thickness (left) and cylindricity and tolerances (right).

Using the work of Galantucci et al. (2009) as reference for the testing values, the influence of the immersion time and acetone concentration was evaluated, including an ANOVA analysis of the influence of each parameter. Table 7.1 shows the levels of each parameter. A set of five samples were produced for each combination of levels.

Table 7.1. Acetone dipping experiment parameters and values

Parameter	Range of values
Immersion time (seconds)	300, 700
Water/Acetone concentration (%)	10/90, 25/75, 50/50

The specimens' roughness, cylindricity, planarity and dimensions were measured to understand the effect of the parameters on these characteristics. Figure 7.12 shows the setup of these measurements. The dimensional measurement was performed manually using a calliper.

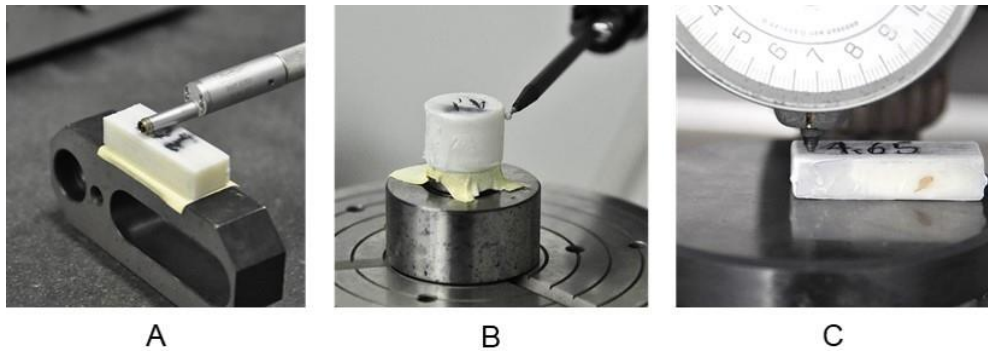


Figure 7.12. Measurement setup for a) roughness, b) cylindricity, and c) planarity.

The results showed that the 10/90 acetone concentration with the longest exposure time successfully improved the surface roughness, but the process damaged some of the thinner samples. As shown in Figure 7.13, the concentration of acetone seems to have more influence than the exposure time, although this result needs to be interpreted with caution due to the number of levels of exposure time.

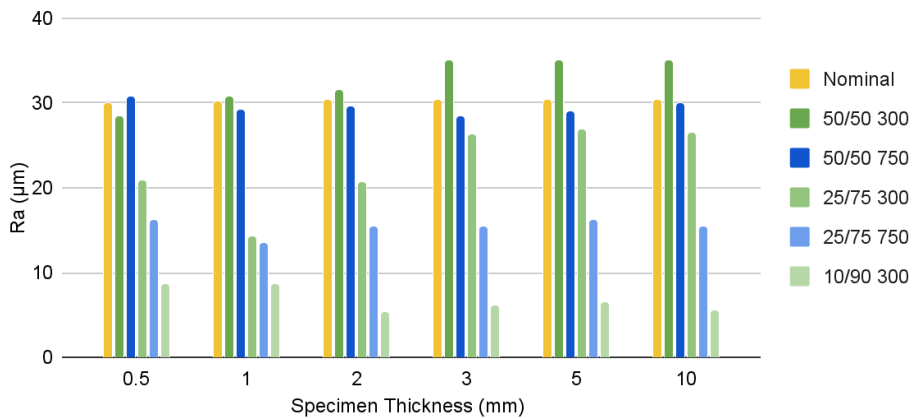


Figure 7.13. Roughness results of the acetone dipping experiment.

The cylindricity and planarity analysis revealed a general specimens' deformation, with a 35% cylindricity loss and up to 254% of planarity distortion.



This experiment shows that the overall roughness is reduced, but the solvent deforms the geometry. Therefore, the immersion of ABS components in acetone solution might not be a suitable method for improving the surface finish.

More details of the experiment can be found in Sanabria Aguirre (2016).

### Chemical Solutions. Summary

Other studies show an increase in weight due to chemical absorption and a volume reduction due to shrinkage. Mechanical tests also show lower tensile strength, higher ductility and greater flexural strength (Galantucci et al., 2010; Garg et al., 2017; Jayanth et al., 2018).

As shown in Figure 7.14, other solvents are far more suitable for chemical treatments in the case of PLA, demonstrating particular effectiveness compounds such as chloroform and tetrahydrofuran (Panda et al., 2020; Valerga et al., 2019). Unlike ABS, PLA is not soluble in acetone, resulting in minimal improvement when used as a solvent.

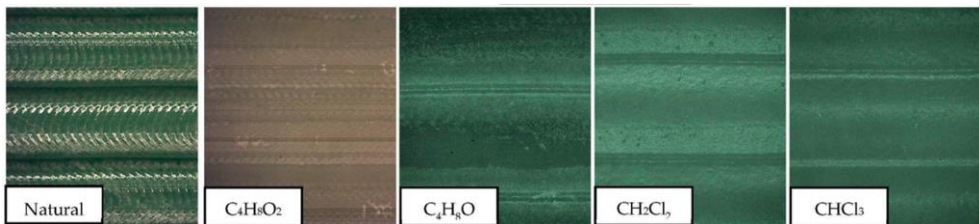


Figure 7.14. Effect of immersion in solvents on the surface of FFF PLA (Valerga et al., 2019).

Due to the uniform actuation of the chemicals in all the surfaces of the components, these methods are usually not suitable for components with assembly features with tight tolerances such as lap joints or predominantly made of thin walls. The effect on these features is more pronounced than in the external surfaces making these unusable.

Chemical treatments are relatively straightforward and inexpensive methods for achieving an extremely low surface roughness on FFF-manufactured parts, close to injection moulding. Integrating different post-

processing technologies and chemical treatments can also be very promising and allow a wide range of surface finishes.

### 7.3.3. MECHANICAL

The mechanical techniques aim is to cut or compress the peaks of the surface profiles. The most commonly used mechanical methods for enhancing the surface quality of FDM prints are machining, sanding, polishing, abrasion and barrel finishing (Chohan & Singh, 2017).

#### Sanding & polishing

Manual sanding or polishing is potentially the most conventional method to improve surface finishing and enhance edge definition. It comprises the usage of sandpaper or sometimes even files, for example, to remove the support marks. Sanding is one of the more common methods in the prototyping practice (Conejero et al., 2019). Usually, sanding is performed with a set of tools or papers with a graded value of roughness. The sanding steps usually go from more aggressive tools, such as files, to gradually less aggressive. It is common to start with coarse sanding paper of a lower grade, progress using medium grade, and then fine grades. The function of the surfaces determines the number of steps and the highest grade used.

The sanding paper could be attached to a sanding block that could help reduce or increase the stiffness of the tool and, therefore, the amount of material removed. E.g. Some sanding paper is available being bonded to a sponge, reducing the amount of material in each back-and-forth movement and therefore helping obtain a uniform surface.



*Figure 7.15. Sanding tools, including a sanding paper attached to a customised curved wooden baking tool for sanding curved areas.*

The development of sanding blocks with tailored profiles, like the one shown in Figure 7.15, could help to sand challenging to reach areas and remove material uniformly in curved geometries.

If the function requires it, the final steps of sanding include the operation of polishing. This operation could start with high-grade wet-sanding paper and then move to soft tools with polishing paste. It should be noted that usually, this step occurs after the application of putty to fill any gaps or imperfections.

Usually, this technique is applied manually. The application using lamellar abrasive paper in abrasive milling controlled by a CNC machine has been tested by some studies achieving surface finish improvement close to 90% (Lavecchia et al., 2018). However, this technique is limited to specific geometries and requires various iterations of parameter development to achieve the desired quality.

One of the main challenges of sanding and other manual mechanical methods is that consistency and precision rely on the operator's ability. Therefore, this technique is easy to apply, inexpensive, and very common in the post-processing of FFF components.

### Shot blasting

Shot blasting comprises the erosion of the surface by impacting it with an abrasive medium, usually sand or other softer media, such as garnet grit, as can be seen in Figure 7.16. This method is applied manually and is very sensitive to the process parameters and application technique depending on the media used (Bastian, 2013).

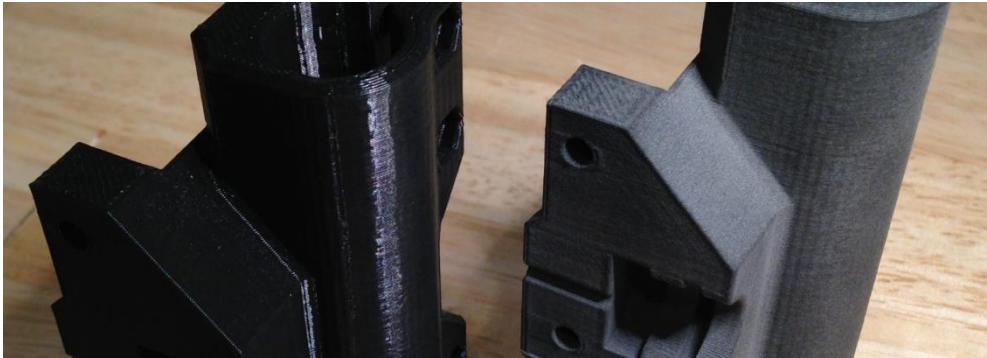


Figure 7.16. Effect of shot blasting on the surface of a PLA component (Bastian, 2013).

Shot blasting can be applied as the single method for surface finishing, although it requires more aggressive application, increasing the risk of abrasive penetration by breaking interlayer bonds (Castro-Casado, 2021). Sodium bicarbonate or glass beads could be used to reduce the roughness of as-printed components, with the former being more suitable due to its lower hardness (Gajdoš et al., 2015).

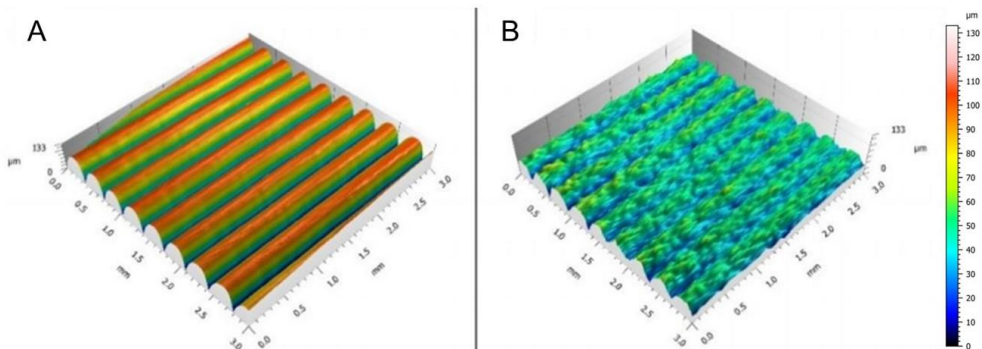


Figure 7.17. 3D Reconstructed 3D surface topography of ABS as-printed (a), and after alumina grit blasting (b) (Xu et al., 2018).

A recommended method is to use a surface chemical treatment and then blast the surface to remove the glossiness (Zinniel, 2009). However, if instead a material-addition pre-treatment method is used, such as sealer or spray putty, the blasting removes these materials and the roughness increases (Gajdoš et al., 2015).

### Machining

CNC machining for the surface is a technique that provides a controlled surface finishing with a repeatable outcome instead of some of the previously described methods.

The capability to define the toolpaths that the milling cut will follow allows tailoring the toolpaths to the component's purpose. For example, a pattern or a detail could be engraved in a FFF component area instead of finishing all the component surfaces, as shown in Figure 7.18.



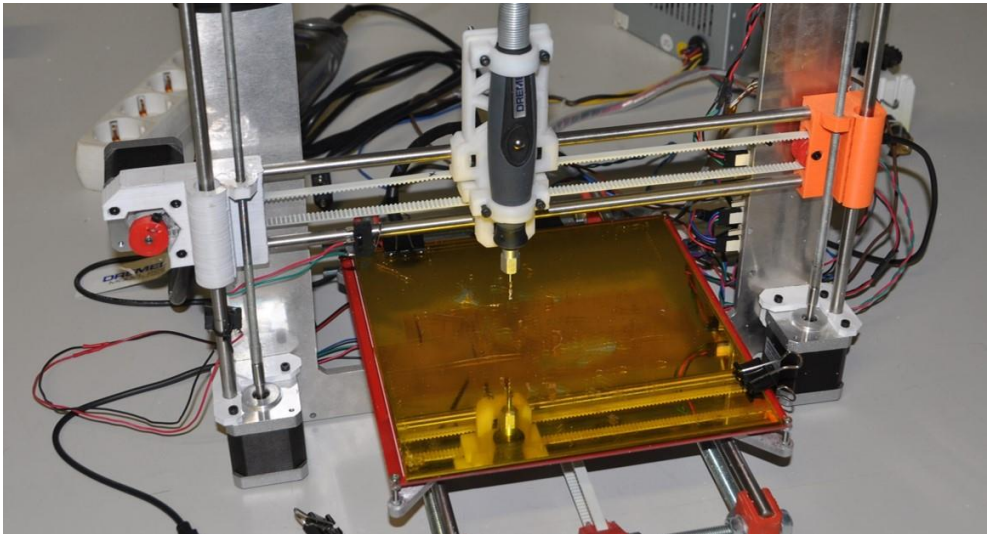
*Figure 7.18. Engraved product logo with CNC in a finished FFF prototype of a portable Bluetooth speaker. Academic project from the Workshop on Prototypes and Models subject. ETSID UPV (Conejero Rodilla, 2018).*

The achievable feature size of machining cutters can be smaller than with the FFF system, rendering this approach suitable for detailed features.

### **FFF machining experiment**

The lack of literature on this topic and the potential to provide a repeatable surface finishing method sparked the definition of an experiment to evaluate the feasibility of this process.

A rotary tool was fixed in a preliminary test to the head of a FFF machine to test a hybrid approach, as shown in Figure 7.19. However, the structure stiffness and component adhesion to the print surface were too low for the loads involved in the machining.



*Figure 7.19. The rotary tool attached to the FFF machine.*

This issue highlighted the need to change the processing plan. The use of machining for surface finishing requires developing a processing plan to identify potential issues and requirements (Hur et al., 2002). Considering the individual characteristics of each of the phases helps in obtaining a successful result.

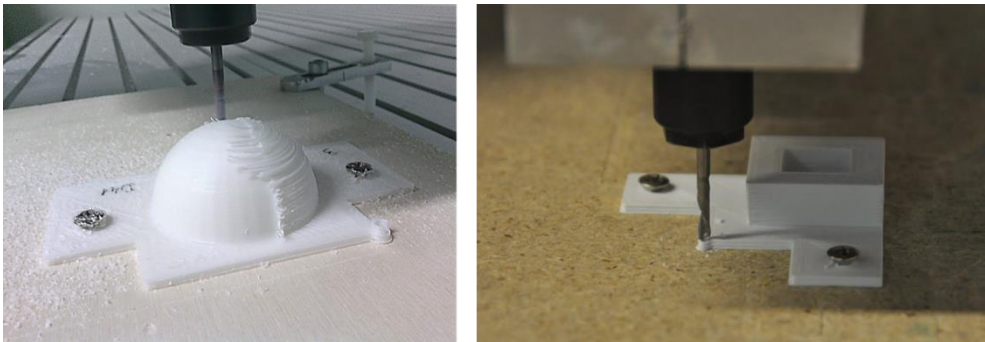
The processing plan was modified by opting to use a woodworking CNC machine available in the lab. This modification meant that the components needed to be removed from the FFF build surface and fixed to the CNC machine platform.



The components need to be fixed to the CNC machine platform to counteract the loads produced by the milling. The bonding of the components to the build platform during FFF is strong enough for the deposition, but we found that this was not enough for machining. Therefore, a fixturing feature needs to be added to the geometry.

Every CNC system requires the definition of a coordinate system and its origin that allows a machine to move to a specific location in space. A datum feature needs to be added if the component is machined in a different location than the printing.

Two testing specimens were designed and manufactured by FFF to understand the behaviour in curved and planar surfaces, as can be seen in Figure 7.20. A thin wall was added to fix the component to the platform, and a cylinder was included to allow the definition of the origin of the coordinate system (Figure 7.20, right)



*Figure 7.20. Machining in the curved surface specimen (left) and datuming in the planar surfaces specimen (right).*

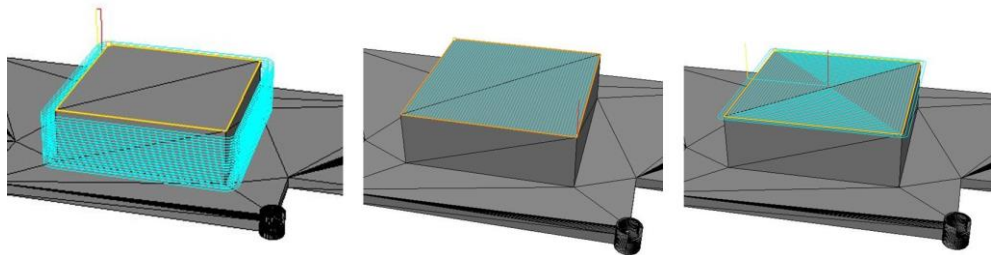
As described earlier, the purpose of mechanical post-processing is to remove the cusps in the ridged surface of FFF components. Therefore, an offset needs to be applied to the CAD geometry to account for this material removal, as shown in the curved sample in the figure. Two thicknesses of the offset were tested for both types of samples: 0,5 and 1 mm. These matched with one and two beads thick for that system and material.

For this experiment, the material used was ABS, one of the most common for FFF. The machining of polymers usually provides lower dimensional stability due to their higher coefficient of thermal expansion (around 20 times of metals), lower stiffness and young's modulus (Patel, 2008). During the machining, the main issues that could occur are:

- A component cracking or delamination due to weak bonding strength between beads.
- Overheating of the component due to the low heat conductivity of the material. The overheating could make the swarf fuse together around the milling tool.

A high feed rate (spindle speed of 6000-12000 rpm and cutting speed of 3000 mm/min), pressurised air blown in the area, and a two-flute milling tool for polymer were used to avoid these potential issues.

A contouring and two types of facing toolpaths were used for the planar surfaces specimens, as shown in Figure 7.21. The side and top walls roughness was measured, and the results were averaged.



*Figure 7.21. Operations applied to the planar specimens: contouring (left), parallel facing (centre) and concentric facing (right).*

The hemispherical specimen purpose was to identify the suitable approach to generate toolpaths for FFF. Three types of toolpaths were tested, as can be seen in Figure 7.22: Parallel (parallel to one of machine axis), spiral (following a spiral as seen from the top) and radial (all the paths with a common point in the centre of the component)



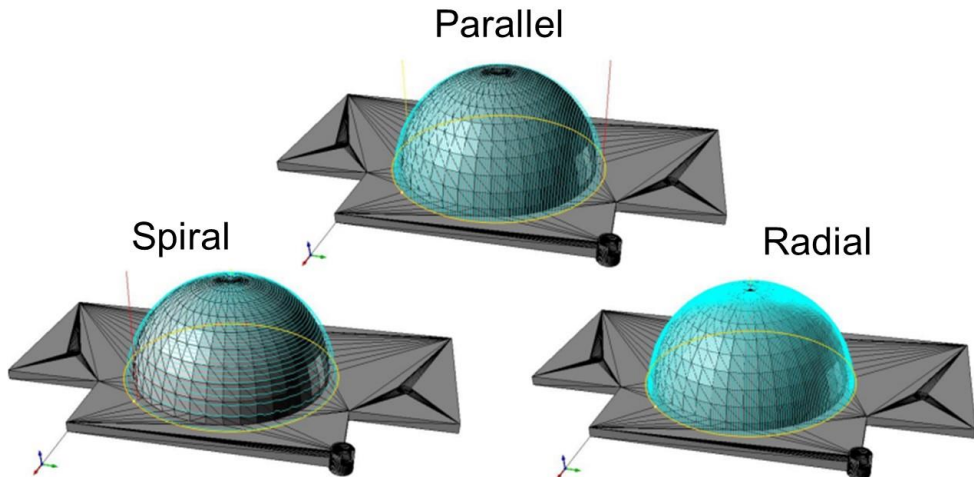


Figure 7.22. Types of toolpaths used in the hemispherical specimens.

The rugosity of the planar samples before and after the machining was evaluated. The results of the rugosity in the planar samples after the machining show an improvement in the roughness.

Table 7.2. Roughness ( $R_a$ ) comparison before and after machining.

	As-printed ( $\mu\text{m}$ )	Iso scale	After machining ( $\mu\text{m}$ )	Iso scale
Top face	11.54	N10	4.26	N8
Side face	24.58	N11	1.99	N7

A defect can be observed in the surface finish of the hemispherical specimens. Some perimeter beads separate during machining, appearing as threads on the specimen surface, as shown in Figure 7.23.



Figure 7.23. Comparison of hemisphere specimens during machining.

The change in toolpath trajectories seems to influence the quality of the finish. The spiral toolpath shows less separation of the outer filaments during machining. This effect is probably due to the absence of shear forces perpendicular to the filaments. Another possible explanation for this is the existence of some compression loads on the filaments.

There was no observed change in behaviour between the two thicknesses of the offset in either hemisphere of planar surfaces specimens.

This experiment highlighted some of the already described elements that need to be considered when using machining. It also revealed the need to account for the load applied to the surface beads to avoid separating the filaments.

More details of the experiment can be found in Martinez Abellan (2016).

### **Machining. Summary**

The use of machining as a post-processing technique provides some advantages:

- Dimensional accuracy, increasing the range of applications where FFF could be used. E.g. mechanical assemblies, mould tooling or prosthetics.
- Low material waste, as just a small area of the component is machined
- Cost reduction for the production of series
- Potential integration of the end-to-end process in a single machine

This last point has been one of the main approaches in additive manufacturing, not just in FFF but also in other AM processes (Merklein et al., 2016). It allows the retrofit of CNC machines, adding the capability of generating components, which is beneficial from the procurement point of view. Its application to large-scale polymer material extrusion AM (FFF using pellets instead of filament) seems to provide significant advantages (Moreno Nieto & Molina, 2020). An example is the fast production of large composite mould tools, as shown in Figure 7.24.



*Figure 7.24. Composite mould tool being machined, produced by large-format additive material extrusion. Courtesy of The Manufacturing Technology Centre (UK).*

However, one of the main challenges of using machining as a post-processing method is the limitation to access intricate features (Kulkarni & Dutta, 1998). To counteract this challenge, the modularisation of the geometry seems to be a potential solution. This approach helps in potential future modifications of the geometry due to wear and tear or design changes (Townsend & Urbanic, 2011). Advanced configuration and increased processing time are required for complex geometries, highlighting the need to balance speed and quality (Pandey et al., 2003).

Another challenge is the difference in surface quality depending on the slope of the surfaces. Shallower surfaces show more increased staircase effect (Ahn et al., 2008). A potential approach to overcome this is to consider a variable cutting depth to avoid inner defects. The surface morphology changes with its slope, and therefore the machining parameters need to be variable for components characterised by surfaces with different slopes (Boschetto et al., 2016b).

In summary, machining as a method for mechanical surface modification seems a promising technique as it provides a controlled way to remove material, increasing its suitability for series finishing. However, the limited access to some features and the increase of complexity in the process planning

could hinder its applicability for the individual production of individual FFF components.

### Rotary/vibratory tumbling

Mass finishing processes rely on the rubbing of the soft polymer components against harder abrasive media. The movement of media and components could be performed through various techniques, with vibration and rotation of the enclosure being the main ones for AM polymer components (Boschetto & Bottini, 2015).



*Figure 7.25. Effect of tumbling smoothing (left) and polishing (right) media in a FFF component (Schneider, 2019)*

The material, geometry and purpose of the components determine the selection of the method, the abrasive media, and parameters. Rotary tumbling is usually more gentle than vibratory finishing, making it more suitable for components with fine details (Boschetto & Bottini, 2015). Aiming at smoothing or polishing, the typical two operations, defines the usage of harder, such as ceramic, or softer media, such as corn starch. The abrasive media is available in many different sizes and forms. As shown in Figure 7.25, selecting the right one

determines the capability to access recessed areas and processing speed (Wellborn, 1995).

These processes are relatively slow, in the range of hours, but this allows tailoring this time to the application. This characteristic and the wide range of abrasive media available allow finding the parameters to the specific application (R. Singh & Singh, 2015). However, the random movement of the components and the media in the enclosure produces different results between components. The variable staircase effect in FFF components, as shown in Figure 7.7, generates inconsistent surface finish and between surfaces of the same component (Bottini et al., 2014). E.g., the effect on a vertical wall is more pronounced than on a horizontal one after the same processing time.

Some of the benefits of these processes are (Boschetto & Bottini, 2015):

- Almost every material can be processed, as compared to chemical treatments, media of different hardness is easy to be obtained.
- The components do not need to be fixed.
- The equipment is not expensive, and no specialised operators are required. Even some designs of DIY rotary tumbling machines are available.

However, there are some challenges for complex and intricate geometries. The process could distort the part geometry and dimensional instability due to the rounding of sharp edges and corners by the abrasive action of media (Chohan & Singh, 2017). Besides, Gaps, holes, recessed surfaces within grooves or cavities are usually areas where these processes are less effective, as the abrasive media cannot access these. This effectiveness depends on the abrasive media size and could cause media entrapment, which may further reduce effectiveness (M. Fischer & Schöppner, 2013).

Therefore, these processes seem effective and suitable for round products or with rounded edges, also considering the lack of uniform finish between surfaces.

### 7.3.4. SURFACE MODIFICATION. SUMMARY

A summary of the distinctive advantages and limitations of the surface modification processes described earlier can be seen in Table 7.3.

*Table 7.3. Advantages and limitations of the main surface modification techniques for FFF.*

Technique	Advantages	Limitations
Thermal annealing	Improves mechanical properties & roughness	Energy-demanding
Chemical bath	Fast and low cost, complex and internal features can be treated	Small features can be eroded, low process control, challenging to control tolerances, dimensional deviations, limited materials
Vapour smoothing	Minor dimensional deviations, short processing time	Hazardous, non-uniform finishing, limited materials
Sanding and polishing	Inexpensive	Low repeatability
Shot blasting	Wide range of blasting media	Line of sight needed, sensitive to the media and technique
Machining	Repeatability and automation	Complex surfaces can be inaccessible, long processing time.

Sometimes the surface modification of a component still does not match the requirements of the product, or additional functionality is required. In these cases, additional steps are needed to add material or features for assembly. On other occasions, the surface modification happens after another material has been added to the surface of the printed part. The following section describes the post-processing methods where the purpose is not to remove material from the component's surface but to add instead.

## 7.4. COATING

Depending on the purpose of the component, a material addition phase is added to the post-processing. This material addition, or coating, aims to improve the surface finish towards the product requirements or improve its functionality.

Coatings can be applied by dipping the component into a tank containing the coating product (K. M. Lee et al., 2019; Zhu et al., 2015) or by manual spraying or brushing (Leite et al., 2018; Vicente et al., 2019). Process parameters, such as immersion time in dip coating, play a significant role in the coating thickness and surface profile. However, the prominent influencers are the coating material properties, such as viscosity and surface tension (Tamburrino et al., 2021).

Coatings in FFF are commonly used to provide: additional functionality, sealing, smoother surfaces or colour.

#### 7.4.1. ADDITIONAL FUNCTIONALITY. METALLISING

FFF components' functionality can be added or improved by adding a thin metallic conductive layer on the surface, as shown in Figure 7.26. This addition can improve the thermal resistance or conductivity and the structural integrity and durability (Olivera et al., 2016). The metal layer creates a sandwich effect in thin walls, with the metal coating as the faces and the polymer as the core. The dense metal layer also prevents outgassing, preventing water and liquid plastic residues from escaping (Dietz, 2019). Static charging of the surface can also be avoided through the metal layer. Metallisation has shown potential for antennas (Ghassemiparvin & Ghalichechian, 2020), electroforming patterns (Monzon et al., 2010), or electroluminescent devices (Brubaker et al., 2019), among others.

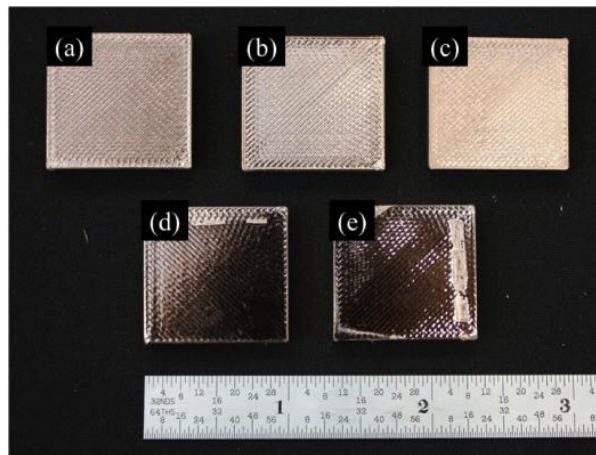


Figure 7.26. Samples metallised by PVD after various surface modification treatments: (a) control, (b) atmospheric plasma (etched with an atmospheric hand-held plasma etcher), (c) 2000 grit sandpaper, (d) acetone vapour treatment, and (e) acetone dip treatment (White et al., 2018).

Apart from painting, there are mainly two methods used in polymer components: Plating, which could be electroplating or electroless plating, and physical vapour deposition (PVD)

In plating, the polymer surface needs to be conditioned by etching in an acidic bath to clean the surface and then with the addition of a conductive layer by spray or brush (Dixit et al., 2017). Then in electroplating, the functional metallic layer is deposited by immersing the part in an ionised solution where the electrical current induces the metallic ions to migrate from the anode to the component (Akhouri et al., 2020). In Electroless plating, a chemical reduction of metal ions in an aqueous solution deposits the thin metallic layer (Equbal & Sood, 2014). Usually, the materials used in plating are nickel, due to its low cost, aesthetics and hardness, and copper, for its visual appearance (Olivera et al., 2016).

Plating in FFF components enhances surface smoothness and light reflectance (Khan et al., 2018) due to the addition of the layer of material, which as its thickness increases, seems that surface roughness decreases (S. Kannan & Senthilkumaran, 2014). This thickness needs to be accounted for by the designer, being usually between 0.1 and 0.2mm.



Plating enhances the corrosion resistance, hardness, tensile strength and impact of components (Arun et al., 2018). However, due to intrinsic porosity, the parts can also absorb significant fluid volume when submerged.



*Figure 7.27. Prototype with a metallised component using vacuum PVD. Note that the deposition lines are still visible due to not enough surface preparation. Academic project from the Workshop on Prototypes and Models subject. ETSID UPV.*

This method provides advantages when durability and thermal resistance are needed, although the arrangements for setting up the process make it suitable for small series. This method increases the hardness and mechanical strength, but the dimensions of the components change as well due to the addition of a layer, which sometimes could provide a non-uniform surface finish (Chohan & Singh, 2017).

The other method to metallise components, PVD, is a set of techniques that rely on the condensation under vacuum, or low pressure gaseous (or plasma) environment, of a vaporised form of the metal on the component's surface. The vaporisation could occur by heating the source, as in vacuum deposition, by bombarding the source with ions or plasma, such as in sputter deposition, or by a high current electric arc erosion in the source, used in arc deposition (Mattox, 2010).



*Figure 7.28. FFF gear metallised by PVD. Courtesy of Fraunhofer IST.*

As shown in Figure 7.28, It can achieve a consistently thin coating in the range of nanometers, resulting in an auspicious process such as for the biomedical field (Martin et al., 2017) or for creating functional chips (Keough et al., 2021). The advantages of this method are (a) the low environmental impact thanks to the elimination of dangerous chemicals used in other conventional metallisation techniques, (b) its possible use on almost any type of inorganic material, (c) the capability of covering corners uniformly, and (d) has no issues of liquid uptake (White et al., 2018). In contrast, the high costs due to requiring complex machines operated by skilled people and low coating rates could be a disadvantage (Romani et al., 2021).

#### 7.4.2. SEALING

The minor errors and voids between filaments in FFF make it challenging to produce watertight components for applications under pressure or exposed to liquids. The presence of roughness on a surface enhances its natural hydrophilic or hydrophobic behaviour (Jordá-Vilaplana et al., 2014). FFF surfaces are intermediate surfaces between hydrophilic and hydrophobic, depending on the layer thickness (Vicente et al., 2019). The diffusion of water molecules in the microvoids between polymeric chains, which in FFF are generated by higher extrusion temperatures, is another important mechanism for water absorption (Espert et al., 2004).

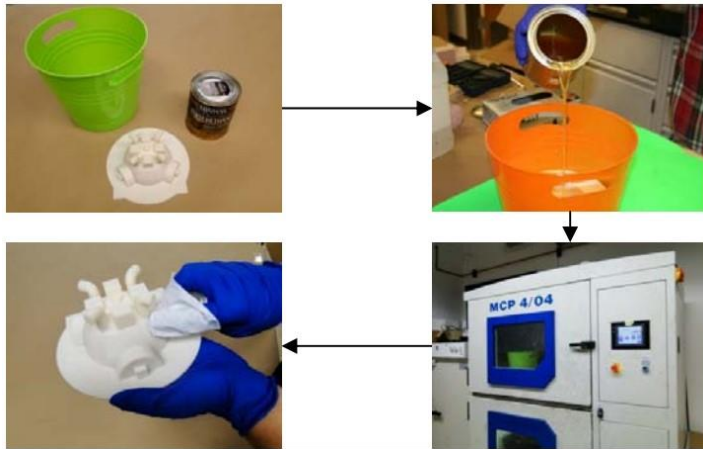


Figure 7.29. Vacuum infiltration procedure (Mireles et al., 2011).

Various methods could be applied to seal components, as can be seen in Figures Figure 7.29 and Figure 7.30. The previously described vapour smoothing is capable of sealing the gaps and improving the water tightness of the components. Another in-process method is to increase the thickness of the perimeter walls (Stratasys, 2017a).

From the coating perspective, the primary methods to apply sealant materials are brushing, spraying, or vacuum infiltration (Stratasys, 2014). Mireles et al. (2011) tested the sealing of ABS components by brushing and then infiltration with a wide range of readily available consumer and industrial sealants. They found that the dimensional change is minimal with some sealants and the outcome depends on the user. Using acrylic and polyurethane varnish seems effective in stopping the water absorption in FFF PLA. With polyurethane, the water absorption can be reduced by 38%, while the tensile strength and ductility increase by 24% (Vicente et al., 2019).



*Figure 7.30. Brush application of epoxy resin to seal and smoothen the surface (BJB Enterprises, n.d.).*

### 7.4.3. SMOOTHER SURFACES

One of the main effects of adding a coating layer on a FFF component is creating a continuous layer filling the spaces between beads, as shown in Figure 7.31. This continuous layer could help reduce the inherent roughness of the FFF component (Kuo & Su, 2013).

Furthermore, the filling of gaps in the surface can help distribute the load and prevent crack propagation. This distribution could increase the mechanical properties, such as in the study by Leite et al. (2018), where the application of acrylic varnish on FFF ABS components resulted in a >30% increase of yield strength.

The surface tension of the material being used to coat the surface and the thickness of the coating are the main parameters that determine the effectiveness of the roughness reduction.

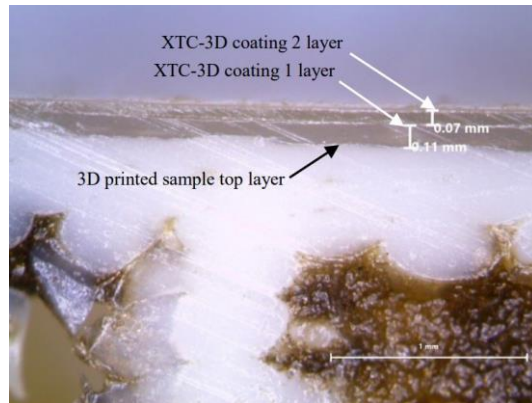


Figure 7.31. Cross-section of a sample with two layers of coating (Haidiezul et al., 2018).

As shown in Figure 7.31, coating with a self-levelling material, epoxy resin XTC-3D from Smooth-On, USA, reduces the staircase effect. Although the addition of more than one layer improves the surface, it should be taken into account that dimensional accuracy will be affected (Haidiezul et al., 2018).

This loss of dimensional accuracy is an additional effect of some of the methods described before in plating and sealing. However, if the coating layer is thin enough in plating, it can make the defects on the surface more evident (3DDC, n.d.).

The coating layer to smooth the surface can be applied:

- by spraying, for less viscous materials,
- by brush, for materials such as the epoxy described earlier, as can be seen in Figure 7.30,
- Alternatively, with spreading tools, for very viscous materials or semisolids, such as polyester, epoxy, or nitrocellulose putty, as can be seen in Figure 7.32.



*Figure 7.32. Application of nitrocellulose putty to fill gaps in a FFF component. Workshop on Prototypes and Models subject. ETSID UPV.*

The coating of FFF components can have a functional purpose, such as assembly with other components. However, for human interaction applications, the coating plays an aesthetical role since surface finishing strongly influences the performance of a specific product and its perception and the emotional response of customers and final users (X. Chen et al., 2009). However, little is known about how important it is to remove the ridges from the surface. A study was developed to evaluate the perception of various surface methods, which is described in the next chapter.

The smoothing of FFF surfaces could be performed by several iterations between the removal and addition of material. This iterative process is a prevalent situation in the case of aesthetic components.

When the purpose of the object is aesthetical, the post-processing of an FFF component usually comprises the addition of a coating layer with colour.

#### 7.4.4. COLOUR

The widespread adoption of FFF by nonprofessional enthusiasts has encouraged many material manufacturers to produce filaments without the functional purpose as the primary objective. E.g. the production of materials of a broader range of colours or even with colour-changing properties. However,

the pigments added to the materials modify their mechanical properties (Pandzic et al., 2019).

Colour coating of parts, or painting, could be performed through brushing and spraying, with the latter being the most common. The coating function could be aesthetical or functional, e.g. increasing the conductivity, as described in the plating section. The aesthetic coating is a common technique in FFF in design studios and service bureaus due to the widespread use of 3D printing to create prototypes and models (I. Campbell et al., 2018).

Usually, the painting of FFF components requires a set of steps to remove any imperfections in the surface and prepare it for a successful adhesion of the paint.

#### 7.4.5. COATING. SUMMARY

As seen, the coating of FFF components could be performed to achieve different objectives, and often it is part of an iterative set of operations between material removal and coating.

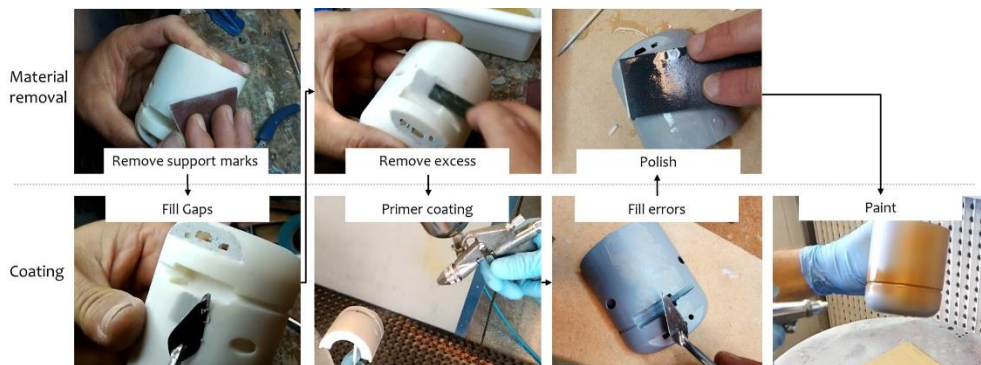


Figure 7.33. Coating and material removal steps for an aesthetic evaluation prototype. The component was printed with the curved surface of the cylinder facing downwards.

Coating operations are applied to fill the gaps where the staircase effect is more pronounced or where flat surfaces are needed, as shown in Figure 7.33. A primer coating, sometimes matte acrylic primer, is applied to the surface to identify marks or errors that need repairing by sanding or coating. Then a final fine sanding or polishing is applied to the surface according to the desired

surface roughness (Conejero et al., 2019). As shown in Figure 7.18, sometimes the manufacturing witness marks are left intentionally, or even the FFF staircase is left as a surface pattern.

Many times one of the functions of the component is being part of an assembly with higher-level functions. E.g. an electronics enclosure. This function supposes that some operations will need to be performed and considered in a component's design and post-processing steps. For example, the chemical treatments strongly affect thin structures, which assembly features are usually part of, and therefore are not suitable when components need to be assembled.

The following section describes the different methods for assembling FFF components and the considerations from the design perspective.

## **7.5. ASSEMBLY**

The assembly considerations are reduced with Additive Manufacturing due to the capability to produce complex geometries capable of performing various functions simultaneously (S. Yang et al., 2015). Nevertheless, the need for joining these parts with ones fabricated by other technologies remains.

Most dimensional and tolerance specifications in the requirements of components have an origin in the assembly of those components with others. The consideration of the assembly characteristics and manufacturing from the design perspective is an area for active research in general manufacturing, as described earlier in this document, like Design for Manufacturing and Assembly (DfMA)(Boothroyd et al., 1998).

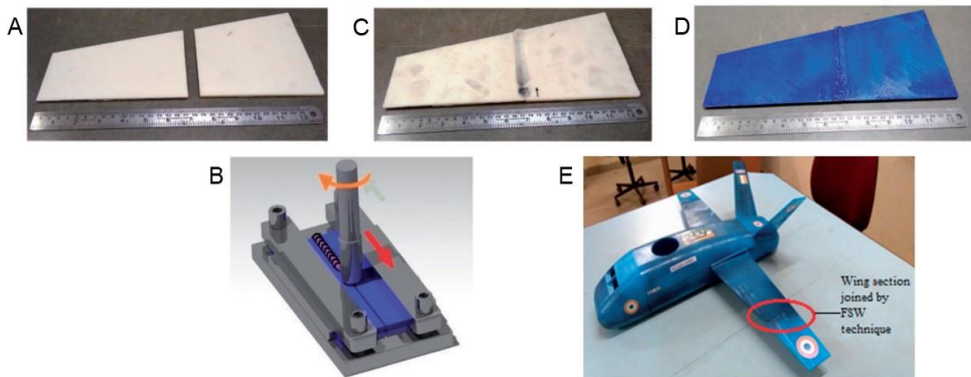
The range of post-processing methods for assembly involving polymer materials is extensive. This section describes the most common methods used with FFF components, such as adhesive bonding and welding, drilling, threading, and hardware embedding.



### 7.5.1. ADHESIVE JOINING & WELDING

The orientation of FFF components determines the mechanical strength, surface quality and overhanging areas needing supporting structures, as described in previous chapters. Sometimes, the components are too large for the machine's build volume, ideal orientation, or storage and transportation. For any of the reasons described before, the components need to be separated for manufacturing and assembled in post-processing (Tiwary et al., 2021). Manufacturing smaller parts and later joining them helps align each small component into the most appropriate direction for increased strength and reducing the usage of support structures.

One of the methods to bond parts together is by welding. Friction stir welding could be used by spinning a filament along the weld seam, as shown in Figure 7.34. The advantages of this process are the ease of automation and the ability to weld almost any thermoplastic (Tiwary et al., 2020). Some of the limitations are that thermoplastics are thermal insulators, so the melting occurs just in a shallow area, and the difficulty to join dissimilar materials (R. Kumar et al., 2019).



*Figure 7.34.* Application of friction stir welding on a UAV. a) parts to be welded; b) welding movement schematic; c) welded parts; wing after spray painting; d) wing after assembly. Adapted from Tiwary et al. (2020).

The bonding surfaces need to be prepared by sanding, blasting or grinding to enhance the adhesion to components produced by FFF (Bürenhaus et al., 2019). This preparation breaks the beads' smooth surface, helping develop the

intermolecular forces between the adhesive and the components (Kah et al., 2014). The surface morphology modification in the overlap regions, e.g. creation of sawtooth patterns improves the load capacity and stiffness of the joints (D. K. K. Cavalcanti et al., 2019). This modification increases the effective bonding area and modifies the crack propagation direction (García-Guzmán et al., 2018).

Cyanoacrylate and Epoxy adhesives are standard glues used in various studies for joining FFF components (Arenas et al., 2012; Yap et al., 2020). Cyanoacrylate possesses significantly higher adhesive strength than epoxy for ASA and Nylon 12 (with carbon fibre loading) (García-Guzmán et al., 2018). For ABS, polyurethane and acrylic adhesives were found to be the most suitable (Arenas et al., 2012). A summary of the suitability in terms of strength and application is presented in Table 7.4.

Another method of bonding ABS or HIPS components together is the (1) application of acetone to the surface of both components, which dissolves the surface, and (2) assembly before it evaporates. This method has been used as well by diluting ABS in acetone to create a *slurry* and then applying this mixture to the joining surfaces (Havenga et al., 2014). However, this method comprises altering the assembling surfaces of the components and therefore has the risk of not obtaining a proper alignment of the components.

*Table 7.4. Suitability of adhesives with different types of FFF materials according to literature. Source: (Espalin et al., 2009; Kovan et al., 2017; Lipina, Krys, et al., 2014; Suder et al., 2020)*

	ABS	PLA	ASA	PA+CF	PPSF	PEI	PETG	PC
Cyanoacrylate	***	***	***	***		**	***	***
Polyurethane	***					*		
Epoxy	*	**	*	*	*	***		
Acrylic	***					*		
Solvent	**							

Adhesive joining provides some advantages compared to other joining methods: (1) there are no stress concentration regions in the bonded parts, (2) can be used to join dissimilar materials, and (3) generates a uniform distribution of load along the bonding line.

Some drawbacks of using adhesives to join components are the need to prepare the surfaces, adhesive filling unwanted areas, the potential elastic mismatch while joining dissimilar material components, and the incapability to disassemble the components after joining (Tiwary et al., 2021).

### 7.5.2. DRILLING

The joining of components with hardware such as screws or bolts requires the creation of holes. These holes could be printed, but when close tolerances are needed, the quality of FFF is too low.

The use of patterns to reduce the density is a common characteristic of FFF components, as was described in previous chapters. The pattern of FFF components external wall is usually composed of parallel beads. Therefore, after directly drilling an FFF component, adding fasteners creates a stress concentration area where the loads cannot be transferred.

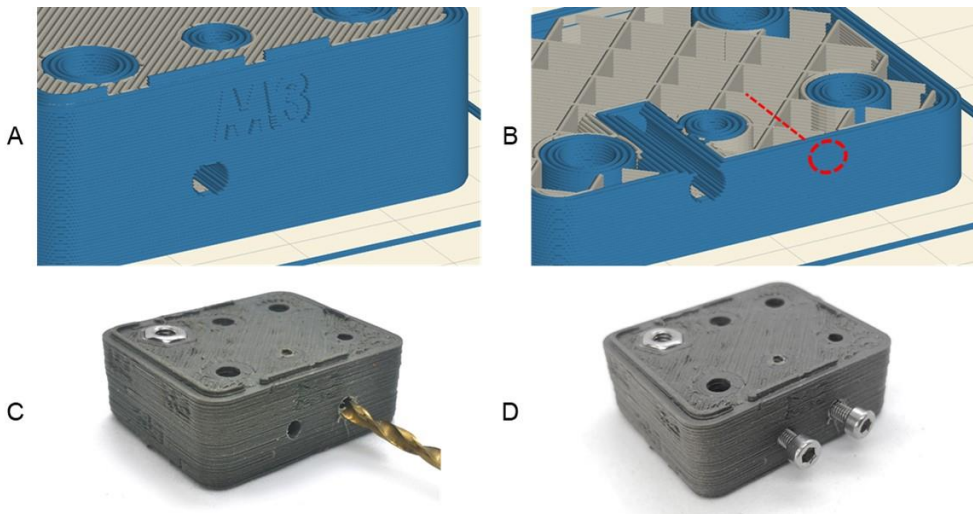


Figure 7.35. Drilling a hole in a FFF component. A) layers of the component; B) cross-section with the infill visible and the planned drill in red; C) Drilling ; D) Misalignment of the bolt.

As shown in Figure 7.35, when the holes are added to the design of the component, full size or pilot holes, the print preparation software understands this area as external perimeters. Therefore, fully dense material is created around the holes and following the profile of the hole. Furthermore, it happens

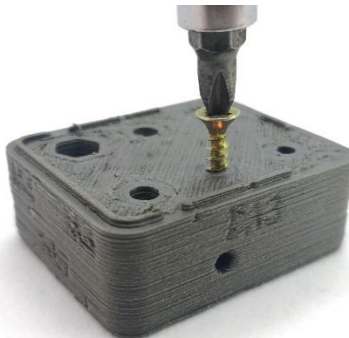
not just on the external faces of the component but across the thickness as well (Lipina, Marek, et al., 2014). In conjunction, these actions increase the fasteners' successful load transfer to the FFF component (Clark, 2019). Therefore, this is the usual practice for adding hardware fasteners such as bolts: drilling the holes to achieve the desired tolerances and strength.

The drilling parameters such as feed rate, spindle speed and cutting speed, and the tool parameters affect hole's accuracy and quality (Raju et al., 2011). When finding the suitable parameters, the main challenge is avoiding cracks and fatigue due to the poor adhesion between layers. In the same way, as it was explained in machining, a slow feed rate with high spindle speed could create melting of the material

Dezaki et al. (2021) found that a moderate feed rate of 1100 mm/min and spindle speed in the range of 800-100 rpm produce the best surface quality for 20 mm holes in PLA.

### 7.5.3. THREADING

Threads are a particular case of joining feature with tight tolerances where the joining hardware engages with the component being assembled. The relatively low accuracy and resolution, need of supports and adhesion between beads limit the capability to manufacture threads without post-processing. However, considering these, threads could be designed and produced by the FFF process.



*Figure 7.36. Self-tapping screw being inserted in a testing part.*

Threading or tapping of a FFF component comprises cutting the thread profile across layers or perimeters. As with other polymer components, a hole with a smaller diameter than the tapping tool diameter. This hole could be printed or drilled, considering the characteristics described earlier.

Another method that relies on the same mechanical approach is the usage of self-tapping screws, as can be seen in Figure 7.36. Three phases could be identified in the joining using a self-tapping screw (Cumbicus et al., 2021): (1) Thread forming, (2) thread increase due to the advance of the screw, and (3) the union tightening between components. An additional (undesired) fourth phase would be the failure of the join. These are illustrated in Figure 7.37.

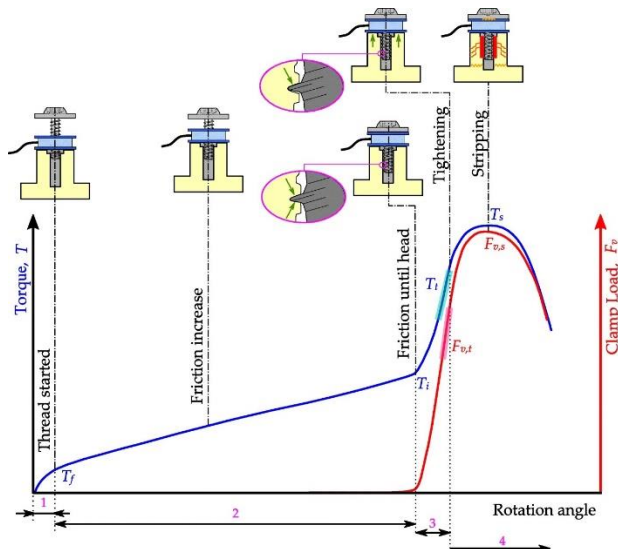


Figure 7.37. Torque and clamp load curves in the forming process using self-tapping screws (Cumbicus et al., 2021).<sup>7</sup>

In the first phase, the screw (or tap in the case of threading) deforms the polymeric material by displacing it radially, generating the forming torque. As the screw progresses in the second phase, the friction torque increases until the components contact. In FFF, this friction could be higher than the bonding strength between filaments hindering the thread profile creation. In the third

<sup>7</sup> Reprinted with permission of Springer Nature Customer Service Centre GmbH

phase, a sudden increase in torque occurs while the clamp load is created. This load results in compression between the screw head and the surface of the thread. If the maximum torque is surpassed, the union fails in a fourth phase. As described in the previous section, in FFF, if the hole has not been printed, the thread would be generated just in the perimeters, increasing the risk of thread failure.

This type of assembly method provides a quick way to assemble components with bolts. However, the disassembly and re-assembly with self-tapping bolts risk creating another thread crossing the original, reducing the join loading capability. Although the usage of taps to thread the FFF component reduces this risk, the relatively weak filament bonding strength reduces the strength of the join. The stiffness difference between the metal bolt and the polymer component could wear the thread in the polymer, increasingly reducing the load capacity of the join (A. Kumar et al., 2021).

#### 7.5.4. HARDWARE EMBEDDING

The inclusion of hardware in plastic parts for assembly is a common practice in the conventional manufacturing of polymer components. Metallic inserts are embedded by moulding around them or inserted in place afterwards (Heaney, 2018). These allow adding threads to polymer components and improve the part's mechanical characteristics. Therefore, the component strength and durability are increased. This method is commonly used in FFF to join components to create assemblies, although the two methods used are: adding the hardware during the build and in a post-processing operation (Stratasys, 2015b).

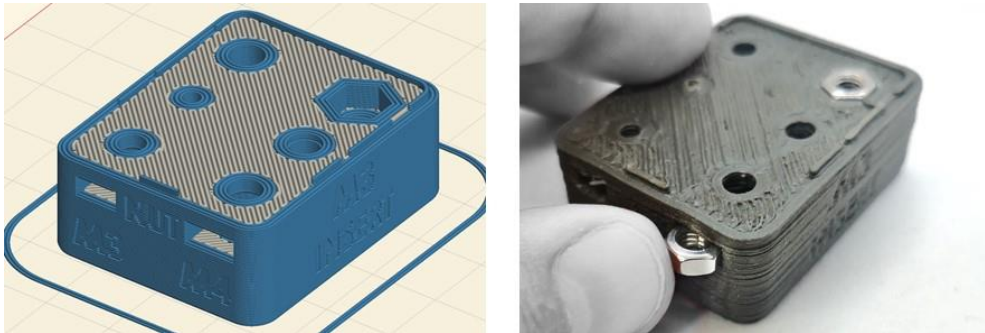


Figure 7.38. Screen capture of the print preparation software (left); hardware embedding by press fit in a cavity on the top and side surfaces (right).

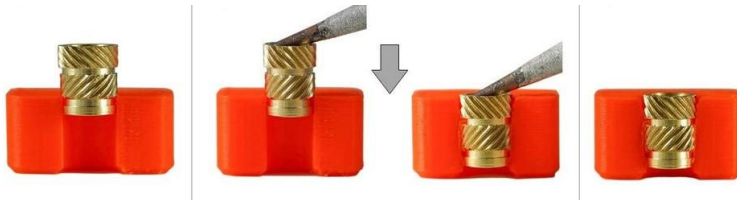
The insertion of hardware during the build requires pausing the process at a specific step, placing the hardware in position, and resuming the build. This technique provides the added value that the hardware is fully enclosed by the FFF component and, therefore, a good load transfer for pullout strength (Ahlers et al., 2021). This method requires taking into consideration (1) potential collisions of the deposition nozzle and the hardware, as well as (2) the fixing of the hardware in place, which could be by tight tolerances or by use of an adhesive, and (3) the supporting of the overhanging surfaces above the hardware and their adhesion to it (Stratasys, 2015a).

As a post-processing operation, hardware inserts could be added mainly by three methods: adhesive joining, heat setting, and press fit.

- **Adhesive joining** – comprises the application of glue to fix the hardware in place. Usually, the adhesive applied does not play an essential role in the load capacity but helps keep it in place (Lipina & Krysz, 2016). Therefore, surface preparation is usually not needed. The cavity for the insert determines the load transfer. Attention should be taken to avoid the transfer of glue into the threads if a threaded insert is being joined.
- **Heat setting** – is a method where the metal insert is heated to embed hardware by softening the polymer. A soldering iron or heat staking press heated to a temperature around 170% of the glass transition temperature ( $T_g$ ) of the polymer material is placed on the insert, and then pressure is applied to embed the insert in the cavity (Stratasys,

2015b). The polymer conforms to the insert geometry without stress building during insertion, increasing its loading capacity.

- Press-fit – requires an interference fit between the FFF component and the hardware. The hole sometimes needs to be drilled to ensure adequate tolerances. The retention mechanism of this method relies on the stresses created when inserting or expanding the hardware. However, the ridged surface of FFF components helps in increasing the retention of press-fit inserts.



*Figure 7.39. Steps of inserting a heat-setting insert. Alignment (left), heating and inserting (centre), and cooling down (right) (Giller, 2021).*

The inserting of hardware into FFF components could enhance their functionality. For example, reinforcing threads, reducing wear with bushes or bearings, increasing component alignment through location pins, or improving load transfer with metal sleeves.

This technique requires no surface preparation compared to the joining of components by adhesives (Bhudolia et al., 2020) and does not show the thermal degradation that could occur in welding. When the hardware being inserted are threaded inserts, these are not as affected by wear as when directly threading the components.

Some drawbacks are the components weight increase and the stresses development around the fastened hole (Garcia & Prabhakar, 2017). The fasteners' insertion could sometimes be cumbersome and damage the surrounding areas of the component as well (Tiwary et al., 2021).



## **7.6. SUMMARY**

This chapter has described the characteristics of the main post-processing methods relevant to FFF components. As described in the introduction, the selection, order, and iterations of the post-process methods are determined by the material, application, and availability.

The next chapter will describe a study performed during the development of this research to evaluate the impact of some of the post-processing methods on the user's perception.



# Chapter 8

## Perception of components due to surface quality

This chapter is an adaption to the thesis format from:

Fernandez-Vicente, M., & Conejero, A. (2016). Suitability study of desktop 3d printing for concept design projects in engineering education. *INTED2016 Proceedings*, 4485-4491.

### 8.1. ABSTRACT

Rapid Prototyping technologies have demonstrated the capacity to help and improve the product concept design and development process. However, the cost of these technologies has been excessive to be integrated into design engineering educational programmes. This limitation has been reduced due to the existence of a new low-cost 3D printer market, opening the possibility to integrate the prototyping culture into educational laboratories, thus the materialisation and physical evaluation of design ideas

However, in the field of product design, functional and aesthetic aspects have to be taken into account. In this sense, low-cost technologies do not yet offer professional quality; thus, the evaluation of design concepts could be affected. Therefore, the main objective of this study presented is to evaluate the suitability of desktop 3D printing technologies for design concept evaluation, as well as the two most common post-processing techniques through a group of 22 students of the Degree of Product Design Engineering

The results show a positive assessment of the technology, but the need for a post-processing of the parts is recognised. This factor highlights the necessity to improve this aspect in low-cost 3D printer systems.

## 8.2. INTRODUCTION

The product design process can be differentiated in conceptual design and detail design. Testing in the first phase usually requires models, simulations, and physical prototypes to optimise the design (Irwin et al., 2014).

Prototypes allow designers to evaluate different aspects of the product before being manufactured. Different types of prototypes are used in many different ways to address different types of questions. In the manufacturing context, a prototype proves a process or procedure. In the marketing context, the prototype is a vehicle through which the marketer simulates customer response or finalises design requirements (Ulrich, 2003).

In this sense, the development of Rapid Prototyping (RP) technologies in the early 1990s has demonstrated the capacity to help and improve the product concept design and development process. While research studying the effect of RP in the design process for practising engineers and industrial designers has been completed (Evans, 2002; Hallgrímsson, 2011), literature regarding the effectiveness of RP in teaching and learning the design process is lacking (Ulrich, 2003).

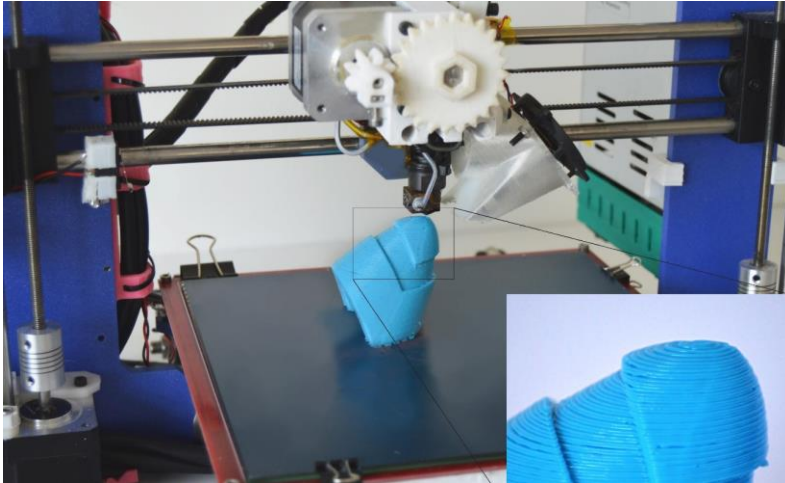
RP has been understood as subtracting material from a stock or adding material. The first requires cutting, shaving, turning, or machining using a CNC machine. The last, called Additive Manufacturing (AM) or 3D printing, builds models by adding material, creating objects near the final shape. Making near-final shape prototypes avoids much of the work of the construction process. Both methods are based on Computer-Aided Design and therefore allow the precise control of object geometry (I. Gibson et al., 2010).

There are different 3D printing techniques that use different materials. These techniques can be classified by the solid construction process: Sintering or fusion of powder, solidifying a liquid, and material deposition. Different

technologies have been trademarked for each of these techniques, such as SLS, SLA, or FDM. The protection of knowledge has enabled the 3D printers manufacturers to invest in the technologies development.

However, the high cost of this type of equipment has been, in the majority of cases, unaffordable in an educational design context. In this sense, the Open Source development models have opened the door to a way of using this technology that has been both accepted within the software industry, particularly in the case of Firefox and Apache servers, among others. In the hardware area, the introduction is taking place a little more slowly, but examples such as the electronics prototyping platform Arduino serve as an inspiration for other projects in so-called “Open Hardware” (Viseur, 2012). In 3D printing technologies, the RepRap project, initiated by Professor Adrian Bowyer by 2005, aims to create a self-replicating manufacturing machine. It was developed a 3D printer based on the patented FDM technology, but to avoid potential legal issues, it was coined as Fused Filament Fabrication (FFF) technology (R. Jones et al., 2011).

The disruptive yet successful element of Bowyer’s approach was: a) to share on the Internet the design and building instructions for the construction of a similar machine by anyone, and b) the inclusion in the design of a large percentage of the pieces built by the same machine (de Bruijn, 2010). The cost of these systems is about €500, and some studies have calculated a simple payback time in 4 months (B. T. Wittbrodt et al., 2013). This was the seed of a new industry called “desktop 3D printing”, which in the past few years has experienced exponential growth. As an example, in 2014 were sold about 140k systems, the double of the precedent year (Wohlens & Caffrey, 2015). In this sense, low-cost 3D printers, all using FFF technology, emerged in the last years due to the expiration of the key patents. This has led to a manufacturers proliferation, resulting in a dramatic reduction of the machine and materials cost (Cazon et al., 2014), which makes it imperative to consider for any educational purpose. In fact, it has been used in a wide range of educational environments (Gonzalez-Gomez et al., 2012; Irwin et al., 2014; Kentzer et al., 2011).



*Figure 8.1. FFF printing and stair-stepping effect.*

However, due to the deposition technique, the external surface of 3D printed objects generally shows a stair-stepping appearance, as shown in Figure 8.1. In particular, low-cost 3D printing technologies show a staircase-like surface that mainly appears along the inclined surface of the part and becomes worse as the inclination of the part increases. This means that layer thickness has a significant effect on surface roughness. In this respect, it is often desirable for an RP model to have minimised surface roughness, particularly in areas of aesthetic importance, so the overall design concept could not be compromised. Especially in the case of physical appearance, models, which are an essential part of industrial design, practice (Evans & Ian Campbell, 2003).

Nevertheless, It is also possible to improve the surface roughness of RP models through post-processing surface treatments. However, once again, this is time-consuming and often leads to a degradation of the geometrical definition of the model. Such treatments should be therefore minimised (R. I. Campbell et al., 2002).

Consequently, the main objective of this study presented is to evaluate the suitability of desktop 3D printing technologies for design concept evaluation and the two most common post-processing techniques through a group of 23

students of the Degree of Product Design Engineering of the Universitat Politècnica de València.

### **8.3. MATERIALS AND METHODS**

The Product Design Engineering programme of the Universitat Politècnica de València includes in the 3<sup>rd</sup> year a subject called “Taller de Modelos y Prototipos” (Models and Prototypes Workshop). The main objective of this subject is to teach the students about the different techniques and tools available to build models and prototypes.

The project’s main goal was to make an appearance model of a design concept of a bottle of water. For this purpose, it was planned to create the main body in two thermoformed transparent plastic sheets by making in a first step a positive wood mould by CNC milling. On the other hand and being the main purpose of this study, was the manufacture of the bottle cap in ABS material by using a low-cost 3D printing process.

This technique allows the direct fabrication of the final form. However, as previously said, there is a big sign of material deposition. As part of students formation, the different finishing techniques were explained, such as sanding, polishing, or painting. The objects fabricated by FFF present a surface characteristic that is similar to those obtained by rough machining. For this reason, it was applied the conventional finishing technique of plastics as can be seen in Figure 8.2. This technique consists in sanding the surface with water-based sandpaper, filling the gaps and scratches with mastic, and painting the surface.



*Figure 8.2. Students sanding 3D printed bottle caps and thermofforming process.*

Due to their low melting temperature and crystallinity, some polymers used in prototype construction are very difficult to sand, like PLA. This material has a wide adoption by desktop 3D printing users due to its low shrinkage rate and ability to print large parts without part deformation. Furthermore, as the object geometry is sometimes difficult to sand, such as cavities or undercuts, other techniques need to be explored.

One of the bottle cap designs was selected, printed three times, and the different post-treatments were applied to the same design to evaluate the different post-treatment techniques. This method was used to eliminate the variable of user opinion about the design.

Some studies examined acetone chemical treatment for ABS polymer by dipping the parts in an acetone solution with water (Galantucci et al., 2009) or by vapour treatment (Garg et al., 2015). This chemical product melts the surface and reduces its roughness of the surface. A preliminary test was developed with the dipping technique, but the presence of voids in the surface led to the acetone infiltration and, consequently, the deformation of the parts. For chemical treatment, was used cold vapour following the work of Garg et al. (2015). One of the parts was put inside a container, which had the walls lined with tissue paper soaked in acetone. As liquid acetone is vaporised at room temperature, it fills the container with vapour. After 40 minutes, the part was extracted and left in a ventilated room to get dry.



As acetone does not affect PLA polymer, the suitability application of a novel epoxy resin, XTC-3D (Smooth-On, Macungie, USA), was also examined. Another part was treated following the vendor instructions. This material is a two-component resin that should be applied with a brush to the surface and left to dry.



*Figure 8.3. From left to right: Original 3D printed part, acetone treated, XTC-3D treated and final appearance model with traditional post-processing techniques.*

A questionnaire was designed to evaluate these two finishing techniques, and the students were asked to score between 1 and 5, using a Likert scale (Likert, 1932), their opinion using the three parts that can be seen in Figure 8.3.

Firstly was asked their opinion about the negative effect of the staircase effect for the aesthetic evaluation of the part. This was questioned to scale the following results and analyse the importance for the design students of this issue.

Secondly, it was asked the relevance of this characteristic compared with other characteristics of 3D printing, such as printing speed, material capabilities, etc. This second question was selected to reaffirm the first one and determine if other characteristics should be analysed in future studies.

After these first two questions, a set of specific questions were asked for each one of three different parts: part without finishing, part with acetone vapour treatment and part with XTC-3D surface treatment. In the first one of

these questions, students were asked to score the surface finish to capture their first impression. In the second question, they were asked to evaluate the finish quality for concept validation, as the visual appearance could be decisive in the case of design projects. The last question asked was to determine if they considered necessary a surface post-processing with traditional techniques. This question captures the optimistic or pessimistic opinion of the design students regarding the finishing technique.

## 8.4. RESULTS

Twenty-three students answered the questionnaire, and their responses were captured and plotted in different graphs that can be seen here.

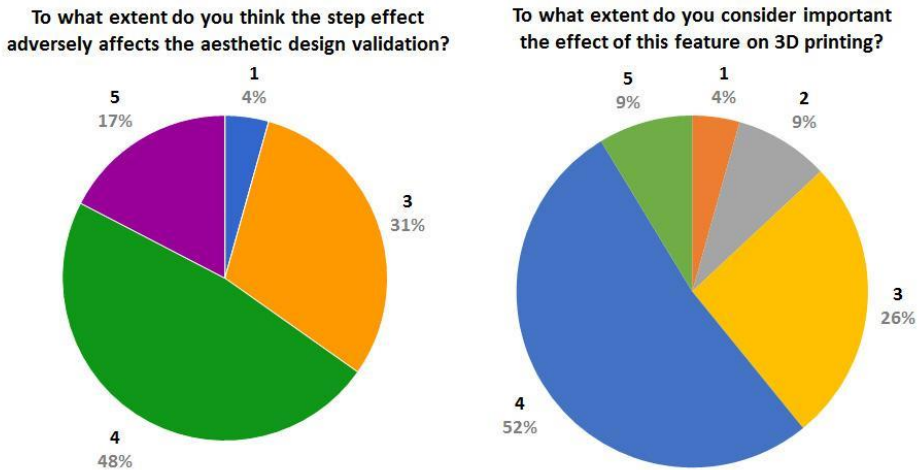
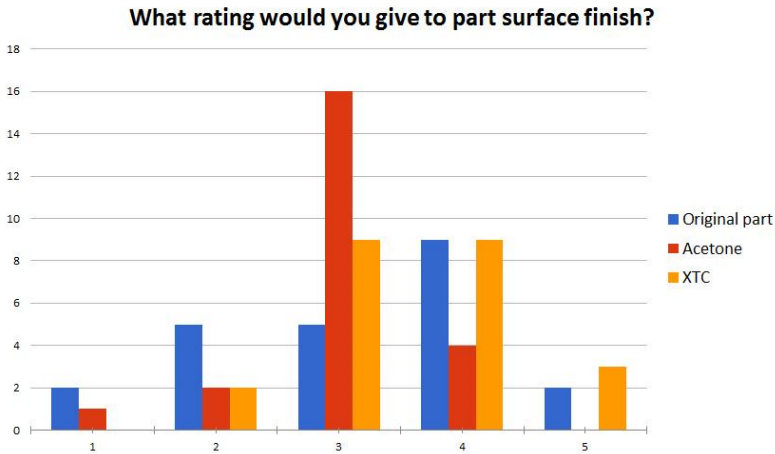


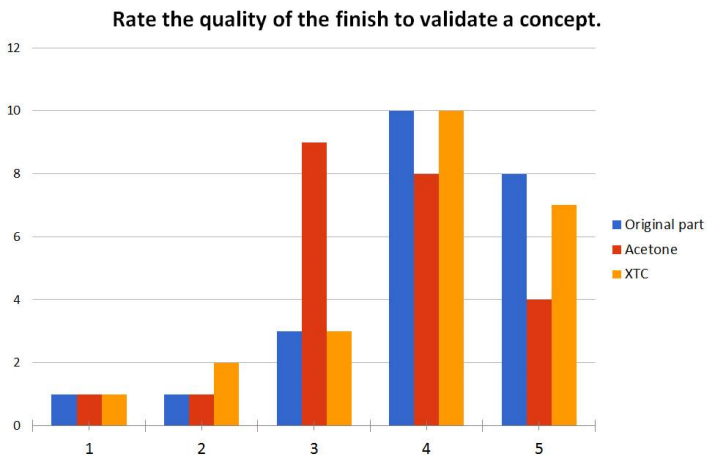
Figure 8.4. General initial questions answer distribution.

From the answers to the first general question, it can be extracted that the majority of students think that the staircase effect is an element to improve from the 3D printed objects. The answers to the second general question are very similar to the first one, as 61% of students think that this effect is important and 65% in the first one think that the stair casing affects adversely.



*Figure 8.5. First specific question.*

In the first question of the specific set, which was repeated with the different post-treatments, the students generally gave a neutral score. As shown in Figure 8.5, the scores are similar, and especially in acetone treatment, the score is neutral. This reveals that the different post-treatments do not seem to affect their perception.



*Figure 8.6. Second specific question.*

The second question evaluated with different finishing techniques yields a result similar to the first question. As can be seen in Figure 8.6, the score is

similar to the different finishing techniques. Even with acetone treatment, the score is lower than for the original part.

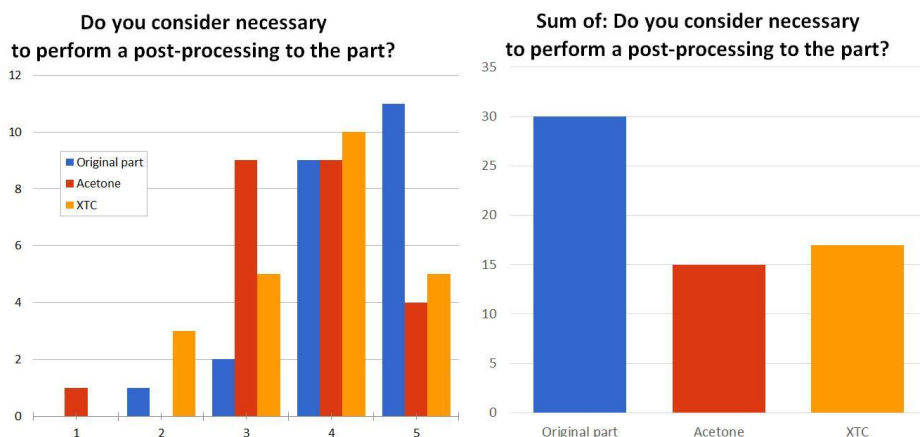


Figure 8.7. Third specific question answers.

In Figure 8.7, it can be observed that the answers to the last question are repeated for every finishing technique. It can be seen higher values in the original part. In the case of acetone, the treatment seems to be a neutral general consideration. However, as the graph on the right reveals, the students consider that the performance of a post-processing treatment to the part is important. In order to obtain these results, it was summed the values of every answer ( -2 points for 1, -1 point for 2, 0 points for 3, +1 points for 4 and +2 points for 5). It can be observed that the original part doubles the score value of the two finishing techniques. This reveals a decrease in the perception of a necessity in post-processing the part in those cases.

## 8.5. CONCLUSIONS

The decrease in the cost of 3D printing systems has enabled their use in higher engineering educational programmes. However, due to the novelty of this technology, it is necessary to analyse the different problems related. The study analysed the suitability of this technology and two of the different existing finishing techniques for product design. It has been highlighted the importance of the surface quality in design models for aesthetic and concept validation.

The results show that the design students consider suitable to use the FFF technology for this task, but it is necessary to improve the surface finish. Regarding the finishing techniques (acetone and XTC-3D), it seems that these are potential solutions to increase visual perception. However, the results indicate that it is still necessary to manually post-process the parts to obtain a good result.

As future work, it is proposed to analyse other finishing techniques to improve the surface finish to avoid traditional post-processing methods.



# Chapter 9

## Case study. Thumb orthosis

This chapter is an adaptation to the thesis format from:

Fernandez-Vicente, M., Chust, A. E., & Conejero, A. (2017). Low cost digital fabrication approach for thumb orthoses. *Rapid Prototyping Journal*.

### 9.1. ABSTRACT

**Purpose** - This paper aims to describe a novel design workflow for the digital fabrication of custom-made orthoses (CMIO). It is intended to provide a more straightforward process for clinical practitioners and orthotic technicians alike. It further functions to reduce the dependency of the operators' abilities and skills.

**Originality** - Although some research has been developed on the digital fabrication of CMIO, few studies have investigated the use of desktop 3D printing in any systematic way. This study provides a first step in exploring a new design workflow using low-cost digital fabrication tools combined with non-manual finishing.

**Social implications** - The feasibility of the process increases the impact of the study, as the great accessibility to this type of 3D printers makes the digital fabrication method easier to be adopted by operators.

**Methodology** – The technical assessment covers low-cost 3D scanning, free CAD software, and desktop 3D Printing and acetone vapour finishing. A cost comparison was carried out between the proposed workflow and the traditional CMIO manufacturing method to analyse its viability.

**Findings** – The results show that the proposed workflow is a technically feasible and cost-effective solution to improve the traditional design and manufacturing process of custom-made static TMC orthoses. Further studies are needed to become a clinically feasible approach and estimate the efficacy of the method for the recovery process in patients.

## **9.2. INTRODUCTION**

Orthoses are often classified as either static or dynamic. Static orthoses have no movable parts and are designed to support or limit joint activity. The principal objective of thumb TMC orthoses is to decrease inflammation by providing rest and immobilisation, to decrease pain, and to prevent subluxation and deformity by the stability of the thumb (W. Zhang et al., 2007). Thumb immobilisation orthoses can be prescribed for various conditions, including rheumatoid arthritis, osteoarthritis, de Quervain tenosynovitis, and carpal tunnel syndrome (Barron et al., 2000; Coldham, 2006; Heath, 2010; Mardani-Kivi et al., 2014).

Currently, the manufacturing process of immobilisation orthoses is typically manual (Austin, 2003; Coppard & Lohman, 2008). A significant number of thumb orthotics designs are available but mainly based on two types of designs: the short type that is based in the palm and immobilises the thumb only, and the long type that includes the wrist. When considering the manufacturing process, two types of orthoses can be observed: custom-made and off-the-shelf, both in different types of material.

Custom-made static immobilisation orthoses (CMIO) commonly are manufactured by orthotic specialists out of thermoplastic sheets. There are mainly two approaches. The first approach uses low-temperature thermoplastic (LTT) that is adapted directly on the skin. If desired, the orthopaedic cast thermoplastic material can be heated before or after placing it



on the patient's extremity (Green, 1984). The second approach, Mould Casting Splinting (MCS), entails the creation of a mould from the patient's hand with alginate. It is then filled with plaster to make a hand model. When it rigidifies, the model is used to adapt pre-heated thermoplastic sheets to the surface. For this step, a vacuuming system can be utilised to increase the adaptation precision and rigidity (Lusardi et al., 2013). The last steps entail the cut of extra material and finishing (Palousek et al., 2014). Then it is fitted with fasteners to ensure a secure fit for the patient and provide partial immobilisation of the radial wrist in the case of de Quervain tenosynovitis (Coldham, 2006; Mardani-Kivi et al., 2014), as can be seen in Figure 9.1. This type of orthoses should optimally support the thumb TMC joint while leaving other joints of the thumb and hand completely free to maintain thumb and hand function (Weiss et al., 2004).



*Figure 9.1. Long thumb CMIO made by MCS process.*

The LTT conventional process, widely used among professionals, is unpleasant for the patient. Moreover, it often involves an iterative process if the product initially has a poor fit to the patient's anatomy (A. M. Paterson et al., 2015). By contrast, the MCS process allows better fitting and rigidity of the orthosis. This process is depicted in Figure 9.2 and can take up to 2 hours of fabrication time per part for an experienced practitioner. However, the orthosis

finishing for this approach is more time consuming as it usually includes personalised designs or perforations. This results in a procedure with high material waste, and excessive time and effort, both for the specialists and the patients (Chandra et al., 2005).

Furthermore, the fact that this work is manual makes it utterly dependent upon the skills and abilities of the specialist (Cottalorda et al., 2005). It may also result in an inadequate or poorly fitting orthosis. This causes friction, directional misalignment, excessive pressure in some areas and pressure ulcers, amongst other problems (Coppard & Lohman, 2008). In addition, the limited skin ventilation of CMIO generates problems such as excessive perspiration, bacteria growth, and difficulty keeping it clean (Coppard & Lohman, 2008).

Consequently, several factors may adversely affect the patient's satisfaction, such as inconvenience and discomfort, along with dissatisfaction with aesthetics. This often results in less willingness to wear orthoses and follow the prescribed treatment. Aesthetics of orthoses may have implications on implementing the duration and suggested guidelines treatment (Veehof et al., 2008).

### 9.2.1. ANATOMICAL DATA ACQUISITION

3D scanning is becoming more prominent within medicine. Paterson et al. (2010) concluded that laser scanning appears to be the most suitable to meet all needs in terms of accuracy, resolution, patient safety, cost, speed, and efficiency. However, they identified that one significant problem is the inability to capture wanted internal structures and intricate surfaces due to line-of-sight limitations. Various sources suggest using reverse engineering software capable of post-processing to produce a 'watertight' model by repairing and resculpturing void data (Gonzalez-Jorge et al., 2013; Surendran et al., 2009). Another solution is the use of sensors based on infrared structured light projection and computer vision techniques, such as the 3D Systems SENSE (3D Systems, Rock Hill, SC, USA), the Microsoft Kinect™ sensor (Microsoft Corporation, Redmond, WA, USA) or Asus Xtion™ (ASUSTeK COMPUTER INC., Taipei, Taiwan) (Gonzalez-Jorge et al., 2013). These sensors can scan the whole

field of view at a maximum of 30 frames per second. This means that it allows performing the scanning process at a very fast speed, reducing issues such as the noise and distortion due to the involuntary movement of the patient (A. M. J. Paterson et al., 2010).

### 9.2.2. ADDITIVE MANUFACTURING OF ORTHOSES

To date, some studies tested the efficacy of Additive Manufacturing, or 3D Printing, for upper extremity immobilisation orthoses. The principal objective of using 3D printing for manufacturing orthoses is to achieve higher levels of compliance amongst patients. Kelly et al. (2015) summarised the reasons for non-adherence to wearing a wrist orthosis and identified various examples of how AM has been implemented to produce CMIO.

In this regard, Laser Sintering (LS) is an extended technique to 3D print orthoses, the benefits of which include the relative freedom of design compared to other AM processes due to the capacity of the powder to support any overhanging geometry and the fabrication of part batches in the same print. Cortex (Eville, 2013) was one of the first orthoses to appear in the general media. The Hash Cast project (Studio Fathom, 2014), which creates the orthosis structure with the characters of messages sent by the patient's friends, and Splint+ (Carmichael, 2013) varied the density to increase the orthosis rigidity in fracture location. Paterson et al. (2015) also investigated the use of this AM process and compared it with other AM processes, such as Stereolithography (SLA), to improve fit, functionality and aesthetics.

SLA is one of the processes with better surface quality. The upper and side areas of the parts have a good finish. However, the lower areas and those that have been in contact with the support structure show imperfections. This is due to support removal. It can cause damage and discomfort in patients, requiring post-processing and later work to completely remove those supports (A. M. Paterson et al., 2015).

Another promising approach is material jetting, as proposed in the project Connex Carpal Skin (Oxman, 2011). In this project, an orthosis that integrates flexible rubber-like materials with rigid materials for custom motion in specific

directions was created. Paterson et al. (A. M. Paterson et al., 2012b) proposed multi-material jetting for wrist immobilisation orthoses to integrate different functions in the same part. They developed a range of orthosis prototypes using different processes and multiple materials and found that the heterogeneous orthosis was the most versatile and open to new possibilities.

On the other hand, Fused Filament Fabrication (FFF), also referred to as Fused Deposition Modelling (FDM), is one of the most widespread methods to fabricate 3D printed orthoses due to the rise of desktop 3D printing (de Bruijn, 2010). This type of 3D printers has demonstrated its usefulness for concept generation in the first phases of design (Rodrigo Corbaton et al., 2016). Moreover, in the literature, there can be found fully functional applications in fields such as tissue engineering (Drescher et al., 2014; He et al., 2015), biomedical devices (Melgoza et al., 2012), scientific equipment (Pearce, 2012), education (Canessa et al., 2013; Fernández-Vicente & Conejero, 2016; Irwin et al., 2014), eyeglasses (Gwamuri et al., 2014), or electronic sensors (Leigh et al., 2012), to name a few.

The use of this type of system for orthoses manufacture results in a dramatic reduction of the cost (Cazon et al., 2014). Palousek et al. (2014) tested the use of FDM for the production of wrist orthoses and confirmed its technical viability. To date, although several projects and designs have tested the use of this technology in CMIO manufacture, no controlled studies of its application in actual patients have been reported. ActivArmor is a product line of 3D printed orthoses used on bone healing as a substitute for traditional casts (ActivArmor, 2014). Only as pilot prototypes, can be found examples as HealX, an orthosis composed of two parts glued to the patient (Kelly et al., 2015); Open Bionics, a dual-material flexible orthosis (Open Bionics, 2015); Novacast, which generates the orthosis shape without the need of a 3D Scan of the patient's limb (Mediprint, 2016); or Osteoid, which uses a low-intensity pulsed ultrasound bone stimulator system to reduce healing time of fractures (Karasahin, 2013) while Exovite integrates an electro stimulator system to accomplish the same objective (Sher, 2015). Other designs by Bush (Royeen, 2015), WASP (2015), Zdravprint (Zdravprint, n.d.) or piuLab (2014) use the 3D printer to create a flat

pattern that, after heating it is adapted to the user, in a similar way as the traditional process.

### 9.2.3. POST-TREATMENT OF FFF PARTS

The FFF process has a higher surface roughness compared to other additive processes such as SLA. Consequently, it was not recommended for applications that require products with a reduced surface roughness (A. M. Paterson et al., 2015).

Tumbling and abrasive hand sanding are standard finishing techniques but have some drawbacks, such as the impossibility of reaching the interior of small holes. Another possibility is chemical post-treatment, as it does not require excessive human intervention. Havenga et al. (2014) compared different part finishing techniques on ABS FFF parts to improve their appearance, performance, and quality. They suggested that stain and acetone vapour finishing methods provide an adequate finish.

ABS is a copolymer with a low reticulation degree, including nitrile functionality having weak interaction with polar solvents such as acetone, ester and chloride solvents. This produces significant improvements in mechanical strength and surface quality (Percoco et al., 2012). In Galantucci et al. (2009), the authors presented a chemical treatment of ABS printed parts based on a bath of dimethyl ketone (acetone) for enhancing the surface finish. The chemical bath partly dissolved the surface layers that subsequently became joined. This reduces the roughness and increases the flexural strength of the treated ABS parts (Galantucci et al., 2010).

### 9.2.4. OPEN LATTICE STRUCTURES IN ORTHOSES DESIGN

The use of AM in the fabrication of orthoses enables the easy incorporation of lattice structures into the orthoses design (A. Paterson, 2013). This includes using open lattice structures, such as voronoi patterns that provide lightweight comfort, maintaining its rigidity to immobilise the articulation (L. J. Gibson & Ashby, 1999). The open lattice structure in orthoses design also preserves a dry orthosis interior by increasing ventilation and reducing the moisture trapped between skin and orthosis (Paterson, 2013). Moreover, in natural Voronoi

patterns, cell sizes vary across the surface, such as the ones in cork or leaf structures (L. J. Gibson et al., 2010). Its similarity to natural structures increases its aesthetic appeal (Clifford, 2011).

### **9.3. AIMS AND OBJECTIVES**

Although some research has been carried out on digital orthosis design and manufacturing methods, few studies have investigated the use of desktop 3D printing in any systematic way. This study aims to contribute to this growing area of research by exploring a new design workflow using low-cost design and manufacturing tools combined with non-manual finishing. It will be applied for static long thumb immobilisation orthoses in particular, used to treat de Quervain tendinitis (Coldham, 2006).

Regarding the surface design, the inclusion of a Voronoi pattern aims to create a comfortable and aesthetically pleasing orthosis for the user without sacrificing any of its functionality. A cost comparison was carried out between the proposed workflow and the traditional CMIO manufacturing method to analyse its viability.

### **9.4. METHOD**

The proposed workflow, as can be seen in Figure 9.2, may be divided into six main steps: (1) 3D Scan data acquisition; (2) CAD process; (3) 3D Printing; (4) Supports removing; (5) Chemical post-processing; and (6) Fastening. Each stage is described and discussed in the following sections. The person who performs the tasks will be referred to as 'operator', as this could be performed by clinical practitioners or orthotics technicians in actual practice.

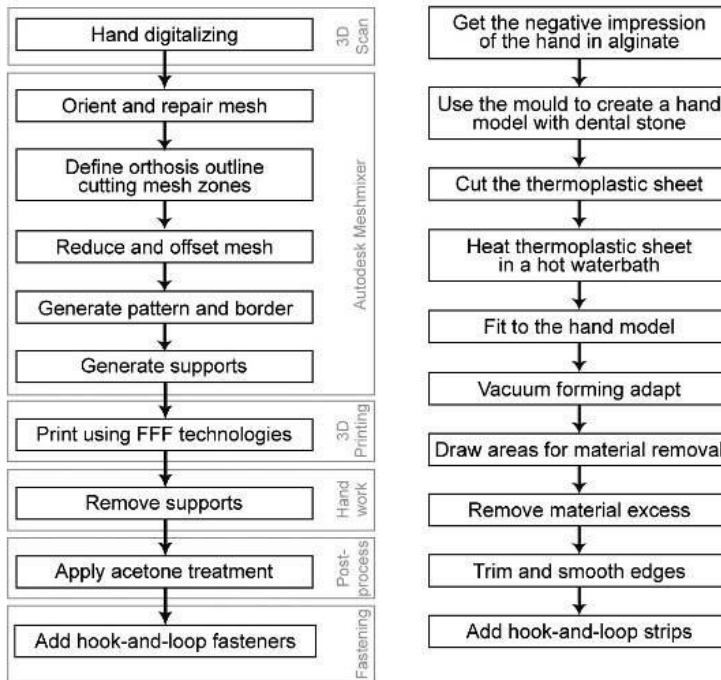


Figure 9.2. Comparison between CMIO fabrication workflows. Left: Proposed workflow. Right: MCS traditional method.

#### 9.4.1. 3D SCAN DATA ACQUISITION

In order to deliver a precise CMIO, it is necessary to acquire and convert the limb geometry into a digital file. 3D scanning from a healthy volunteer was performed with a 3D Systems SENSE hand-held 3D scanner (3D Systems, Rock Hill, SC, USA). It is specially designed for ease of use and to capture a 3D body surface with a spatial accuracy of 1mm and a depth resolution of 0.9mm (3D Systems, 2016). This sensor is based on infrared structured light projection, as explained before. With a cost of around €430, the investment required for its acquisition is significantly lower than other 3D scanners, usually above €30,000.

The fingers, hand, and wrist position during digitisation should be identical to the position inside the orthosis. Therefore, the hand was scanned in the picking position with contact between the thumb and the index finger without

jigging the limb. This position allows palmar pinch without movement, stabilising the thumb in slight adduction (Chaisson et al., 1997).

The 3D scanning was performed by moving the scanner around the hand and following the indications of the scanning software. The time required for the scan was close to 40 seconds, obtaining an accurately enough geometry for the following steps. However, a method of limb immobilisation would be necessary in the case of patients who suffer from medical conditions, such as Parkinson's disease (A. M. J. Paterson et al., 2010).

It is important to remark that even though holes in the scanned mesh can be repaired, the time invested in the design process increases noticeably. This may result in a lower quality product, as the area covered will not be identical to the hand surface. Therefore, holes are something to avoid. 15 minutes were required approximately for the whole process of setting up, scanning, and file exportation.

#### 9.4.2. CAD PROCESS

The design stage of the method was developed entirely using Autodesk Meshmixer free software (Autodesk Inc., San Rafael, CA, USA), as it is oriented to amateur users. Furthermore, features to support the creation of custom-fit prosthetics and orthotics devices have been included in a recent software update (Meshmixer, 2016). These characteristics will allow operators with minimal training to follow the sequence of steps.



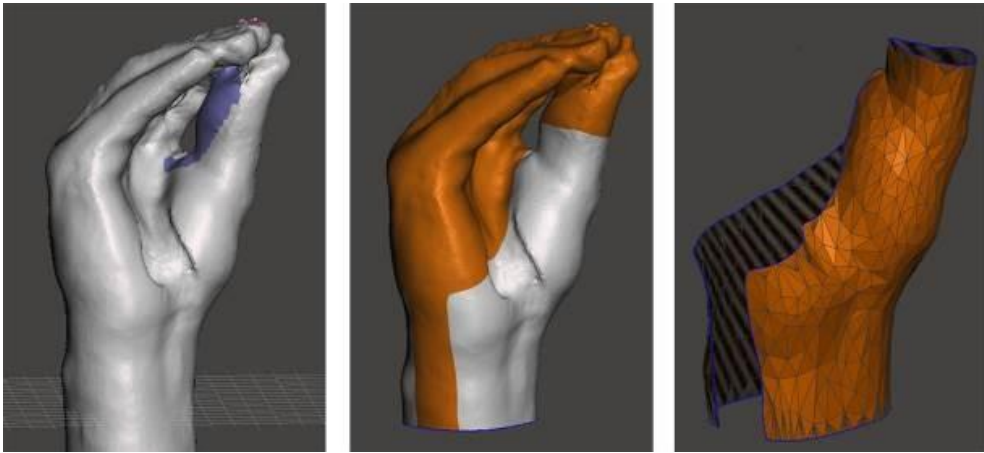


Figure 9.3. From left to right: Mesh filling/zones to cut / final shape with the reduced mesh.

The scan was imported into Meshmixer, where firstly, the arm was oriented vertically, and the holes were filled with the *Smooth Fill* mode of the *Inspector* tool. Then, the mesh was cut following the orthosis outline to obtain the shape according to clinical indications, in this case, for long thumb CMIO (Austin, 2003). For this step, the outline zones were selected using the *Brush select* tool, then the selection was smoothed using the *Smooth Boundary* tool, and finally, the selected triangles were deleted using the *Discard* tool. It should be noted that a narrow section in the wrist zone was also cut to allow the donning and doffing of the orthosis. Some screenshots of these steps can be seen in Figure 9.3.

Once the orthosis shape was obtained, a reduction of the mesh density by the *Reduce* tool was necessary as it defines the final pattern design. This reduction was determined by allowing a maximum deviation of 0.1mm from the original mesh but preserving the boundaries. A 1mm offset of the mesh was made to compensate for the thickness of the final structure.

The open lattice structure was generated using the *Dual Edges* option of the *Make Pattern* tool; this generates a Voronoi structure by connecting the centres of each triangle (Schmidt and Singh, 2010). Various thicknesses of the structure were printed and tested manually to find a suitable value between stiffness and printing time. The selected thickness of the structure was 2 mm.

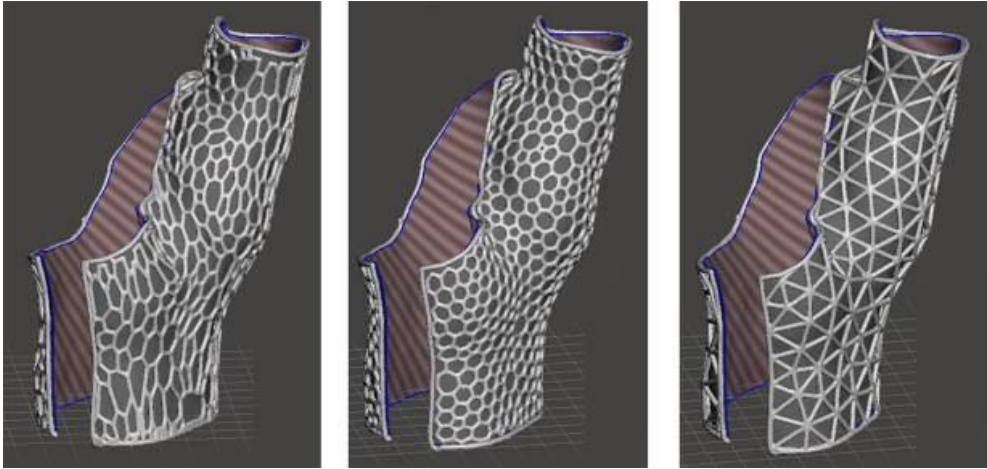
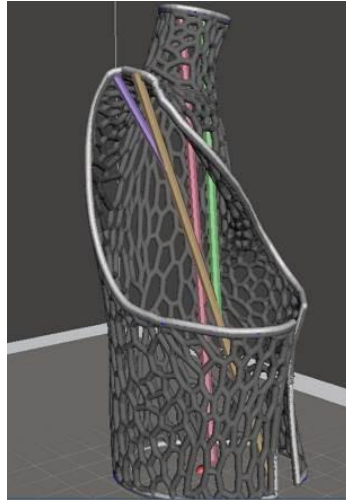


Figure 9.4. Different structures. From left to right: non-uniform Voronoi, regular cell, mesh edges pattern.

This operation was repeated using the *Face Group Borders* option of the same tool to create the borders. This creates a rounded edge that provides rigidity to the orthosis and a smooth contact for the skin. It also avoids forearm pinching in the same way as traditional orthoses (A. M. Paterson et al., 2012a). Increasing the cell size regularity could generate a different structure design to attain a more isotropic mechanical behaviour (C. Chen et al., 1999; L. J. Gibson & Ashby, 1999). A different design could be obtained too by selecting the *Edges* option in the *Make Pattern* tool, as shown in Figure 9.4. However, it was decided to select the non-uniform Voronoi structure design due to the reasons explained above.

In Figure 9.5 can be seen that *branching tree* supports were generated with the software mentioned above, Autodesk Meshmixer (Schmidt & Umetani, 2014). As the walls of some cells from the final pattern surpass the  $45^\circ$  angle, the software automatically added supports inside the cells. However, the findings from previous studies about maximum bridge length were taken into account, and those supports were removed digitally (Fernandez-Vicente et al., 2015). Then the geometry, orthosis and supports, was exported to the printing software.



*Figure 9.5. Final geometry ready for fabrication. Structure, border, and supports in different colours for better visualisation.*

#### 9.4.3. 3D PRINTING

The open-source software package Slic3r (Ranellucci, 2013) was used to convert the CAD model into 3D printer G-code. The predefined configuration was used as there are a large number of parameters that can be modified. The main slicing parameters used were: 0.2mm layer height, three perimeters, and 100% infill density. This last parameter, infill density, was not crucial as the perimeters filled all of the orthosis structure due to its thin thickness. 3 mm black ABS copolymer thermoplastic filament was used due to its capability to be post-treated by acetone, as explained before.

The FFF 3D Printing system chosen was a RepRap-based low-cost 3D Printer model, BCN3D+ (BCN3D Technologies, Castelldefels, Spain). The printing temperatures used were 230°C for the extruder and 110°C for the printing bed. It took six hours to fabricate the part.

#### 9.4.4. SUPPORT REMOVING

After removing the part from the build plate, it was necessary to remove the supports manually using long nose pliers (Figure 9.6). The contact surfaces between the part and the supports were filled to reduce its roughness. Due to

the optimised supports design, this manual process took only 10 minutes to complete.



*Figure 9.6. Manual removal of supports process.*

#### 9.4.5. SURFACE TREATMENT

In this study, acetone was chosen due to its low cost, very low toxicity and, added to this, very high diffusion. Currently, dipping in acetone, acetone hot vapours or cold vapours could be used for treatment. However, it was observed in preliminary tests that immersion in a bath of lukewarm acetone resulted in infiltration and liquid entrapment in the interior of the part. This was due to the small voids that the 3d Printing process leaves between filaments. On the other hand, it becomes difficult to control the chemical reaction using hot vapours because of the high speed of the treatment, as it leads to uneven smoothness (Garg et al., 2015). Therefore, the printed model was enclosed in an environment with a high concentration of acetone vapour at ambient temperature (22°C), following the method described by Garg et al. (2015).



Figure 9.7. Illustration and images of the two steps of the acetone treatment.

A 100x150 mm cylindrical container with one open side was used to create the enclosed environment. The container was lined with tissue paper, and it was impregnated with 99.6% pure liquid acetone (MPL SRL, 2016). The container was then placed upside down above the part on a planar surface, as shown in Figure 9.7. Therefore, this setup creates an airtight environment where liquid acetone gets vaporised and fills the container due to its volatility at ambient temperature.

Different exposure times were tested, obtaining enough layer melting in a one-hour exposure period without any unwanted part deformation, but with edges and sharp corners rounded off, as observed by Garg et al. (2015).

After exposure, the container was removed to allow the acetone evaporation from the part surface for two hours prior to the final fastening step.

#### 9.4.6. FASTENING

The hook-and-loop fastening method was selected to provide a way to don and doff the orthosis easily. Two circles were added to the orthosis on each side of the opened section of the structure. Then a short hook-and-loop strap was adhered to the circles to finalise the process, as can be seen in Figure 9.8. It should be noted that a longer strap could be used to encircle the wrist in order to increase the fastening strength.



*Figure 9.8. Hook-and-loop fastening.*

### 9.5. COST ANALYSIS

An initial cost analysis was performed in order to confirm the economic viability of the new method proposal. This analysis was based on a real scenario that would take place in a company. All the materials and equipment needed were taken into account, based on the cost calculation method reported by Jumani (2013).

Table 9.1. Cost calculations using the proposed workflow.

Number of parts/build	$N_p$	3 parts
Build time/batch	$T$	21 hours
Production rate per hour	$R = N_p/T$	0.1428 parts
Working days/year	$W_d$	220 days
Operation hours/year	$H_y = (W_d \times T)$	4620 hours
<b>Production volume per year</b>	<b><math>P_v = R \times H_y</math></b>	<b>660 parts</b>
Machine equipment cost	$E$	€1000
Depreciation cost/year	$D = E/5$	€200
Maintenance cost/year	$M = E \times 0.10$	€100
<b>Machine cost per year</b>	<b><math>M_c = D + M</math></b>	<b>€300</b>
Material cost per kg	$M_{cm}$	€30 <sup>1</sup>
Model material cost/part	$M_m = 0.120 \text{ kg} \times M_{cm}$	€4
Support material cost/part	$M_s = 0.030 \text{ kg} \times M_{cm}$	€1
Fastening/part	$M_f$	€1 <sup>2</sup>
<b>Material cost per year</b>	<b><math>Mat = (M_f + M_m + M_s) \times P_v</math></b>	<b>€3630</b>
3D printer energy consumption	$E_{3d}$	0.27 Kw/h <sup>3</sup>
Energy cost	$E_c$	0.184 €/Kwh <sup>4</sup>
Energy cost/hour	$E_{ph} = E_{3d} \times E_c$	€ 0.0497
<b>Production overheads per year</b>	<b><math>Ovr = E_{ph} \times H_y</math></b>	<b>€230</b>
Hardware ( Computer + 3D Scanner )	$H_c = €700 + €435$	€1135 <sup>1</sup>
Software purchase	$S_{ft}$	€0
Tools and ancillary	$T_a$	€100
Hardware depreciation	$H_d = H_c / 5 \text{ years}$	€227
<b>Software and Hardware cost per year</b>	<b><math>Spy = T_a + H_d</math></b>	<b>€327</b>
3D scanning	$S_t$	15 minutes
Design time per part	$D_{tp}$	20 minutes
Post-processing time/part	$M_{tp}$	15 minutes
Operator total hours	$O_{th} = S_t + D_{tp} + M_{tp}$	50 minutes
Operator cost/hour	$O_{ch}$	€11
Operator cost/part	$O_{cp} = O_{ch} \times O_{th}$	€9.17
<b>Labour cost per year</b>	<b><math>Lbr = O_{cp} \times P_v</math></b>	<b>€6050</b>
Total cost per year	$T_c = M_c + Mat + Ovr + Spy + Lbr$	€10536
<b>COST PER PART</b>	<b><math>T_{cpp} = T_c / P_v</math></b>	<b>€15.96</b>

<sup>1</sup> Cost quotation from 3D Printing Services S.L.U., Spain, 2015<sup>2</sup> Cost quotation from EMO – especialidades médico ortopédicas, SL, Spain, 2015<sup>3</sup> Wittbrodt, 2013<sup>4</sup> Minetur Spain, 2016

The cost breakdown and total cost of the new proposed approach are shown in Table 9.1. It is calculated for a single printer and operator. The printing

volume of the machine, a BCN3D+, can accommodate a maximum of three parts. The software calculated a build time of 21 hours per batch. Due to the characteristics of the process, it was assumed that the 3D printer could keep printing beyond the operator's working hours. Considering the values of Jumani (2013), the machine was assumed to work for 220 days per year, one run per day. This gives a total of 660 parts per year.

Machine cost was calculated using the depreciation cost of the machine per year and a 10% maintenance cost. The depreciation time for the machine was assumed to be five years. Material cost was calculated by weighing the material consumed in the orthosis part and the support structure. The weight of total material consumed was then multiplied by the associated cost per gram of the material. The material consumed for the orthosis fabrication was 120 grams and 30 grams for the support structure.

The energy cost of the fabrication was calculated using the average 3D printer consumption values from Wittbrodt (2013) and the estimated cost of energy for Spain (Minetur Spain, 2016). This gives an estimated €6930 per year for production overheads. A uniform cost of €327 per year was included as hardware and software expenses.

Regarding the labour cost, it was calculated by the time required of the operator per part. For one 3D printed part was estimated 15 minutes for limb scanning, 20 minutes of design and 3D printer set up, and 15 minutes for post-processing of the part. These times could be reduced with the increase of operator experience, but it was decided to study the cost in the worst case.

It should be noted that this is a very time-dependent selection of processes and materials; access and affordability of equipment and materials are rapidly changing, so it is anticipated that these costs will reduce with time.

A thorough cost-benefit analysis against current splinting practices was then required, considering the cost analysis performed for the new approach. In Table 9.2, the analysis done for the proposed workflow was repeated for the MCS process, as illustrated in Figure 9.2, guided by an orthotic and prosthetic specialist.



Table 9.2. Cost calculations using traditional MCS fabrication process.

Number of parts/build	$N_p$	1 part
Build time/part	$T$	2 hours
Production rate per hour	$R = N_p/T$	0.5 parts
Working hours/day	$W_h$	8 hours
Working days/year	$W_d$	220 days
Working hours/year	$W_y = (W_d \times W_h)$	1760 hours
<b>Production volume per year</b>	<b><math>P_v = R \times W_y</math></b>	<b>880 parts</b>
Vacuum forming machine	$E$	€ 1500 <sup>1</sup>
Depreciation cost/year	$D = E/5$	€300
Maintenance cost/year	$M = E \times 0.10$	€150
<b>Machine cost per year</b>	<b><math>M_c = D + M</math></b>	<b>€450</b>
Mould material cost/part (alginate, plaster)	$M_{cm}$	€2 <sup>1</sup>
Orthosis material cost/part (Thermoplastic sheets, "hook- and-loop" fastener)	$M_{cs}$	€3.92 <sup>1</sup>
<b>Material cost per year</b>	<b><math>M_{at} = (M_{cm} + M_{cs}) \times P_v</math></b>	<b>€ 5210</b>
Vacuum/heating consumption	$V_{cs}$	4 Kw/h
Vacuum time/part	$V_t$	30 minutes
Energy cost	$E_c$	0.184 €/Kwh <sup>2</sup>
Energy cost/part	$E_{cs} = V_{cs} \times V_t \times E_c$	€0.368
<b>Production overheads per year</b>	<b><math>O_{vr}</math></b>	<b>€324</b>
Operator cost/hour	$O_{ch}$	€ 11
Operator cost/part	$O_{cp} = O_{ch} \times T$	€ 22
<b>Labour cost per year</b>	<b><math>L_{br} = O_{cp} \times P_v</math></b>	<b>€ 19,360</b>
Total cost per year	$T_c = M_c + M_{at} + O_{vr} + L_{br}$	€ 25343
<b>COST PER PART</b>	<b><math>T_{cpp} = T_c / P_v</math></b>	<b>€ 28.8</b>

<sup>1</sup> Cost quotation from EMO – especialidades médico ortopédicas, SL, Spain, 2015<sup>2</sup> Minetur Spain, 2016

## 9.6. RESULTS AND DISCUSSION

A significant reduction of manual steps can be observed comparing the proposed digital fabrication workflow and the traditional MCS process in Figure 9.2. This improvement reduces the dependency on the operator skills and abilities. In the digital fabrication method, the clinical practitioner only needs to scan the patient's hand, while the rest of the process needs to be performed by an orthotics technician (Strömshed, 2016). However, all of the processes in this workflow can also be used in small clinics by the practitioner itself.

The results concerning the 3D scanning process show that low-cost sensors could be accurate enough for this process, which enables a broader range of practitioners to embrace the digital fabrication method.

In regards to the design process, Autodesk Meshmixer has demonstrated its efficiency as all the design steps could be performed on the same free software platform. Furthermore, the open lattice structures of the free software provided lightweight aesthetic constructions and the possibility to be printed with only a few supports.



*Figure 9.9. Orthosis surface before (left) and after (right) acetone post-treatment.*

In terms of the post-treatment process, an increase in the part ductility was observed for up to two hours after treatment. After the drying time, it was observed that the acetone post-treatment provided a surface with no visible layers and an enhancement of the part rigidity. The result was a shiny and smooth surface, as can be observed in Figure 9.9.

For the fastening, a standard solution was selected that simplifies this step. However, it has been observed that this feature could be included in the 3D printed part to reduce the manual fastening work.

The cost analysis of the traditional MCS process shows an estimation of €15.95 for each part under the proposed workflow and €28.8 for the traditional MCS process. This result suggests an approximated 55.4% cost reduction between the proposed workflow of the digital fabrication method and the traditional MCS process.

## 9.7. CONCLUSIONS AND FURTHER RESEARCH

Several conclusions can be drawn from this study and must be highlighted. Despite its exploratory nature, this study offers some insight into the potential benefits of a digital design and manufacture process identified previously for other types of orthoses (Eggbeer et al., 2012; Palousek et al., 2014; A. M. Paterson et al., 2015; Strömshed, 2016). This study has presented a novel workflow using the digital fabrication methodology that validates an efficient and effective low-cost approach using low-cost 3D scanning, free CAD software and desktop FFF 3D Printing. The use of FFF technology was the key to reducing the costs of a 3D printed orthosis. The accessibility of this type of machines makes the digital fabrication method easier to be adopted by operators.



*Figure 9.10. Final orthosis fitted to the user.*

Under the digital fabrication method, the operator needs to perform completely different tasks than the traditional method. These new tasks give

rise to the need for specific 3D Printing education, as identified by Campbell et al. (2012). In the MCS process, the result has a significant dependency on the operator ability. A great reduction of this dependency can be observed when using the workflow proposed. Further development of the fastening method could improve the process.

This feasibility study did not capture the intent of the clinical practitioner design. The integration of this information in the workflow should be evaluated in further studies. Furthermore, it would be interesting to assess the new capabilities and education required to help the clinicians and operators to embrace these technologies and methods.

The cost analysis results reveal a great reduction in cost per part and labour costs compared with current practices, more than 50%, and corroborates the ideas of Paterson et al. (2012a). As they pointed out: *'The materials costs incurred in current practice are minimal, and by far the greater proportion of the cost is attributed to the time and salary costs for the professionals involved'*. It opens the door to the scalability of the process, in which the clinical practitioner could scan the patient's limb, design the orthosis, and send the order to a queue for manufacture, using services such as Voodoo manufacturing (Voodoo Manufacturing, n.d.).

These data must be interpreted with caution because the costs have been calculated with quotations from Spain, and these would change significantly if the method is applied in other countries.

However, for this study to become a clinically feasible approach, a material suitability analysis must be performed, and a perception and usability study on actual patients should be conducted. Although that is not within the focus of this investigation, further investigation and experimentation into the mechanical behaviour and FEA is strongly recommended to address issues regarding structural integrity as evaluated in previous studies (Palousek et al., 2014). More research using controlled trials is required to determine the efficacy of the method for the recovery process.

# Chapter 10

## Development of a DfAM toolkit

### 10.1. INTRODUCTION

The design of functional components produced by AM requires a breadth of knowledge obtained through experience or information gathering. The rise of 3D printing, especially desktop systems, has opened the doors of the technology to users without the knowledge required for a successful outcome.

As described in the Design for AM chapter, the design knowledge transfer in AM has been the subject of several studies. Most of the studies focused on the restrictions and limitations of the process and gathered the information, e.g. in feature catalogues (Kumke et al., 2016). In the non-academic field, there has been recently an increase in the availability of design guidelines and tips for users of the FFF technology. This increase is due as well to the accessibility and availability of these systems. However, both feature catalogues and design guidelines only provide support in the design process's 'deliver' stage (Design Council UK, 2019)

Novel designers also require support in the 'develop' stage with information about the opportunities that AM can provide (Laverne et al., 2015). Some authors have referred to this difference as the distinction between Design *for* AM and Design *with* AM (DwAM) (Perez et al., 2019). Therefore, to support designers in the whole DwAM process, methods to leverage the AM capabilities and limitations need to be included.

## Challenges

As described in the FFF technology chapter, these systems are composed of several different components that influence the quality of the result. Only a few manufacturers produce machines for that technology and all the machine components in industrial AM systems. These machines are calibrated and run by trained operators, and process engineers review the designs.

The desktop 3D printing sector comprises a large number of manufacturers of whole systems and machine components. This large number is due to the rise of media interest described in the 3D Printing chapter and the knowledge sharing community created around these systems, which originates in the RepRap project's open-source approach (Sells et al., 2010). The use of low-cost printing raw material in the form of filament provided by several manufacturers enabled this rise as well. These characteristics represent a challenge because of three reasons:

- Not a single set of design guidelines could be applied. There are many machine manufacturers, and customisation of the machine by the user is a common practice. There are, therefore, many elements of 'noise' that could modify the outcome, see Figure 10.1.
- The user changes the printing material often, and not a single supplier is used. This change means that the design rules need to be adapted to a new material more often than with industrial machines.
- The designer and the operator usually are the same person and is commonly not a dedicated professional.
- There is a growing knowledge being developed in shared repositories but no information on how to leverage it.

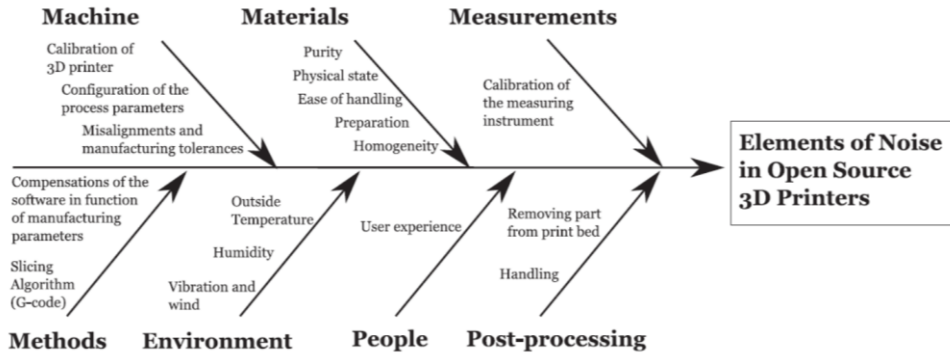


Figure 10.1. Cause-and-effect diagram of the factors that could affect the outcome of desktop 3D printers. Source: (Sanchez et al., 2014)

A multiple format toolkit to support the designers (and users) in the whole Design with AM process is described in the following sections (and is available in Appendix). It considers the challenges described before with a proposed new approach.

## 10.2. TOOLKIT STRUCTURE

The structure of the proposed toolkit comprises a set of tools aimed to be used in different stages of its application. The process of application of the toolkit is illustrated in Figure 10.2.

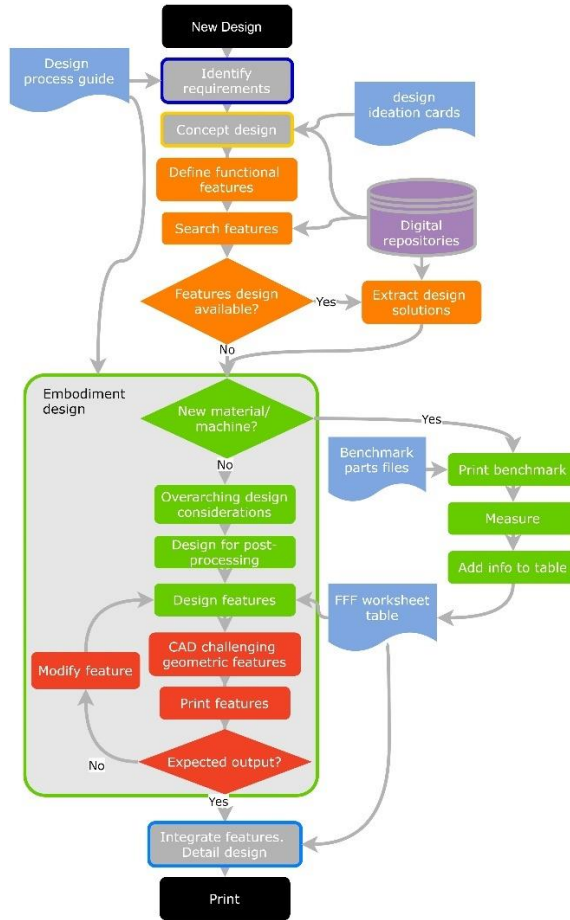


Figure 10.2. The design process for the application of the proposed toolkit

The typical design engineering steps are depicted with a grey background, while the novel steps of the method proposed are painted with similar colours. The elements of the toolkit are depicted in blue, and external information in purple.



The design process guide is the primary document used across the toolkit and interlinks the other tools. It includes an introduction to the proposed design process with an illustration of the tools that comprise the toolkit, as shown in Figure 10.3. This introduction allows the designer to identify when to use the different tools provided within the toolkit.



Figure 10.3. Initial slides of the design toolkit indicating the design process and tools available

### 10.3. IDENTIFY REQUIREMENTS

The freedom enabled by AM requires a structured approach to identify the functional requirements of the object (Ponche et al., 2012). In product design, this phase is called Product Design Specification (Morris, 2016). This activity covers a wide range of requirements, from the costs to the recyclability of the product. The requirements capture has been simplified into six categories as this toolkit is aimed at the novel users of the technology. It is therefore proposed to the designer to identify:

- **Function/functions of the object** – Sometimes a product or component is composed of a set of parts to perform a single function or various functions. One of the key characteristics of these technologies is the capability to produce monolithic components replacing a set of parts in an assembly (S. Yang et al., 2015).
- **Objectives of using AM** – Establishing the reasons to use AM against other processes allows the designer to identify which innovative features provide more benefits in the ideation stage (e.g. lightweight).

- Functional Surfaces (FS) characteristics – This determines the volume of the object and the design space, and the tolerances and finishing requirements. Identifying these surfaces allows the designer to focus on the "important" features of the object and the best way to resolve the connection between those surfaces.
- Dimensional and geometrical specification – The FS determines these. Having a separate specification allows identifying a mismatch between the machine characteristics and the object requirements.
- Mechanical, usage & aesthetical requirements – These determine the material needed, the object design, as well as surface finishing requirements. E.g. requirements for aesthetic evaluation prototypes (Fernández-Vicente & Conejero, 2016) or harsh environments (Ko et al., 2017). These include:
  - Usage requirements such as thermal environment (e.g. range of temperatures or thermal expansion requirements), chemical (e.g. liquid absorption, UV degradation, or reactive compounds exposure), or biological exposure (e.g. food contact).
  - Mechanical requirements, including steady, impact, or fatigue loads in tension, bending, shear, or compression.
  - Material requirements such as dielectric strength, density, hardness, or flammability.
- Non-design volumes – These are the volumes outside the boundaries, which must not contain material due to assembly with other components or other requirements such as see-through features. This information and the FS define the boundaries of the design space, where the designer has the freedom to create the objects.

## 10.4. CONCEPT DESIGN. IDEATION CARDS

As described previously, novel (and not so novel) designers in AM require support to innovate and exploit the potential in the ideation stage. While some studies have looked at providing this information to designers in software tools

(Laverne et al., 2017), databases (Maidin et al., 2012), or guidelines (Burton, 2005), the codification of the knowledge into physical cards seems to be the most appropriate format to deliver this information. Previous studies have shown that this format increases the novelty and quality of ideas (Blösch-Paidosh et al., 2019; Perez et al., 2019; Yilmaz et al., 2012). The information included in these cards needs to be easy to understand and elicit creativity. The presentation of just examples could avoid the designer extrapolating the design principle (DP) or benefit being presented (Perez et al., 2019). Therefore, it is needed to compile these DPs and associate the examples with them.

The two common methods to compile or derive DPs are a) analysis of existing designs and b) literature review. The compilation of the DPs was performed following a methodology, shown in Figure 10.4. This methodology is similar to the described by previous studies for extracting DfAM heuristics (Blösch-Paidosh et al., 2019) and DPs (Perez et al., 2019; Valjak & Bojčetić, 2019).



Figure 10.4. Design principles compilation method.

The design principles can be classified in terms of the benefit provided into four categories: Optimisation, Improve functionality, production flexibility and use complexity. The design principles that have been identified are:

- Optimisation
  - Incorporate standard interfaces to reduce costs and satisfy product requirements
  - Hollow out parts to reduce weight and cost
  - Optimise the geometry using computational design to take advantage of the geometric freedom
  - Replace solid volumes with cellular structures to reduce cost, weight and improve the structure

- Improve functionality
  - Embed off-the-shelf functional components to reduce interfaces, improve assembly and integrate additional functions
  - Adjust the wall thickness and design to control the flexibility and reduce assembly components
  - Consolidate components to incorporate multiple functions
- Use complexity
  - Design and print assemblies together to achieve complex systems
  - Customise the surface texture to improve the functionality or aesthetics
  - Add engraved or embossed text or data details to the surface to convey information with geometry
  - Structure the design to achieve the desired material properties (metamaterials)
- Production flexibility
  - Design modular elements to improve product flexibility
  - Reuse component geometry to minimise design effort and time
  - Customise the geometry to suit the needs of each user

These design principles of heuristics aim to avoid detail or connection to a specific material or feature to help at the conceptual level. As it can be observed, the statement in each principle contains a recommendation and the reasoning of why this advice is provided. This approach provides a structure for further increasing the number of these principles by the growing development of design solutions.

These principles are provided in the toolkit as a set of 14 AM design ideation cards (available in the Appendix). As shown in Figure 10.5, the main elements of the cards are:

1. The category of the design principle
2. A text description of the benefit/design principle
3. Example of application (and reference)



Figure 10.5. Some examples of the ideation cards.

The inclusion of text and a visual representation helps in increasing the interest and comprehension of the concept (Sadoski et al., 1993). The objective of providing these cards is to help the designer be more creative and leverage the capabilities of the technology. For this purpose, the designer is encouraged to print the card set and use it as design inspiration in the conceptual stage. The design tool provides guidance on how to use these cards, as can be seen in Figure 10.6.

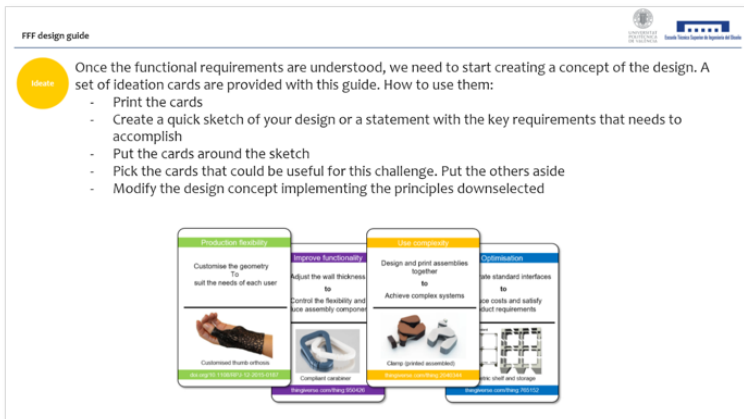


Figure 10.6. The guidance that is provided in the design tool to utilise the cards.

## 10.5. EXTRACT DESIGN SOLUTIONS

As discussed in the *3D Printing* chapter, the rise of desktop 3D printing has democratised the access to the technology. The democratisation of manufacturing, where the Internet provided wider access to information and multiple platforms to share knowledge, might share the innovations observable in music or film economies (Rifkin, 2011). As Von Hippel (2005) stated:

*«User-centred innovation processes offer great advantages over the manufacturer-centric innovation development systems that have been the mainstay of commerce for hundreds of years. Users that innovate can develop exactly what they want, rather than relying on manufacturers to act as their (often very imperfect) agents. Moreover, individual users do not have to develop everything they need on their own: they can benefit from innovations developed and freely shared by others.»*

This democratisation could potentially lead to economic innovations of millions of people inventing technology rather than merely consuming it (Lipson & Kurman, 2010). The difficulty lies in parts' globally distributed peer production identifying the *grassroots innovation* (Troxler, 2010).

Design innovation on industrial-grade AM processes was usually obtained only by interviewing designers from companies, mediatic art projects or demonstration parts from machine manufacturers (bin Maidin, 2011; Thompson et al., 2016). This limitation could be due to two main reasons: (1) The industrial-grade AM parts usually are part of confidential projects reducing the availability of these examples, and (2) the cost and number of these machines. However, this situation is different in desktop FFF 3D printing, as hobby users and professional designers share their novel designs in open repositories of 3D designs (Pearce et al., 2010). This characteristic and the relatively low cost of the machines have increased the popularity of these systems. A growing number of companies are embracing desktop FFF 3D printing as a prototyping or manufacturing method, and therefore do not share their proprietary designs (Moilanen et al., 2015).

An average of 30% of 3D printed parts designs from one-time, beginners, and medium users are downloaded from the Internet (Bosqué, 2015). The number of such repositories focused on 3D printing has increased in the last few years (Rayna et al., 2014). In terms of designs available, the largest repository of this kind is the website thingiverse.com (Moilanen et al., 2015). Makerbot launched it in 2008 to answer the question “Why do I need a Reprap machine?” (Z. Smith, 2008). By 2015 this website stored more than 1.5 million designs, while the following repository provided about 20k designs (Oehlberg et al., 2015). For this reason, the data from this website can be interpreted as the leading showcase of open designs for FFF.

One of the most recent examples that shows how the availability of design repositories provides a more efficient and responsive innovation is the design and mass production of COVID-19 personal protective equipment (PPE). The rapid global spread disrupted the delivery capability of PPE by the supply chains (T. Mueller et al., 2020). The release of functional designs of PPE equipment by FFF companies and makers helped overcome shortages in many areas. Its impact was so crucial in the early stages of the pandemic that the central health bodies released guidance (UK’s MHRA, n.d.) and even set up repositories of designs of 3D printed PPE (U.S. NIH & FDA, n.d.). One of the quickly widespread components, and produced in the tens of thousands, was the face shield design by Josef Prusa (Prusa Research, 2020).



*Figure 10.7. Face shield design (left), in use (centre), the stacked version for production (right).*

The design’s open license helped accelerate the design iterations, with versions derived from the original design for utilising different AM technologies, or improving the production capability, as seen in the right image of Figure 10.7.

As Maidin et al. (2012) predicted, new design features emerge as AM becomes widely used. Furthermore, Campbell et al. (2012) identified that due to the extensive design freedom enabled by AM, the new features would come from the designers' creativity, as the identification of process capabilities evolves as the users find them.

One of the critical design paradigm shifts that Thingiverse enabled is the encouragement to reuse design features to create other designs. Using the similitude to software development where code reusing is a common practice and several platforms are focused on this, Thingiverse allows the designer to indicate which other designs in the platform were used as sources and shows which designs were derived from a *source* design (Papadimitriou et al., 2015).

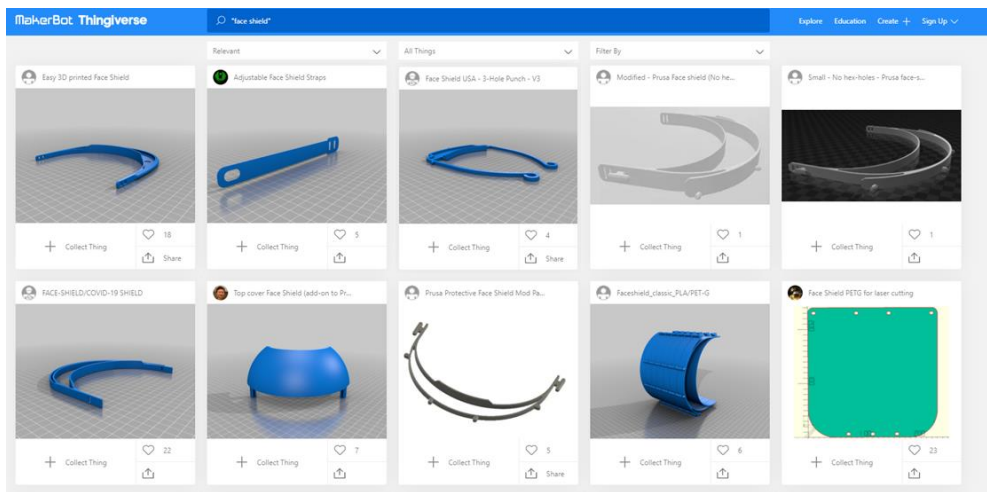


Figure 10.8. Some of face shield designs from thingiverse.com website.

The reuse of features helps novel designers to find proven geometrical solutions. This characteristic could help improve the outcome of the design. Therefore, a method to leverage this resource is included in the toolkit. This phase of the design process comprises four steps: Definition of functional features, searching solutions to functional features and extraction of design solutions.



- Definition of functional features – The designer is asked to identify the product’s functional features being designed. *Functional features* refers to geometry areas that could be challenging or that perform a specific function. These could be aesthetical features such as patterns, assembly features such as hinges, functional surfaces such as gears, or even general product functions such as holding a phone. The term functional surface refers to the outer boundary of an object that isolates that object from the surrounding environment (Lonardo et al., 2002).

This step helps the designer stop and think about what he wants to achieve with the designed product. As described earlier in this document, some researchers propose this approach to allow the designer to leverage the geometrical complexity enabled by Additive Manufacturing (Kumke et al., 2016; Ponche et al., 2012).

- Search features – The designer is encouraged to use the repositories of designs. It is proposed to focus on potential terms associated with the functional surfaces identified in the previous step or products containing those features. E.g. search for *hinge*, *compliant* or *casing* if the intention is to find a solution for a box with a living hinge.
- Extract design solutions – If the functional features are found in the repositories, the designer is provided with guidance to use those features. The recommended approach is to focus on the functional features identified previously. These features could be dimensioned and designed from scratch or reused directly by separating them from the rest of the downloaded design geometry, such as a gear surface.

Although there is documented design fixation, examples are also shown that the provision of examples, such as in the ideation cards and extraction of design solution, can improve novelty and potentially quality as they allow designers to focus on detailed aspects of a design that impact these two metrics (Sio et al., 2015).

## 10.6. EMBODIMENT DESIGN

At the embodiment and detail design stages, designers require a series of guidelines, principles and recommendations to improve the manufacturing quality, as described in the Design for Additive Manufacturing chapter. These have been usually provided in the form of design rules and best practice guidelines. The best practice guidelines contain general information that could be applied for different systems, as they are related to the technology’s inherent limitations.

On the other hand, design rules provide detailed information about specific features, such as minimum dimensions, and allow the user to validate the design. Design rules usually consist of a list of design features with recommended dimensions, depending on the boundary conditions (i.e. machine, material, parameter set or layer thickness) (Adam & Zimmer, 2014).

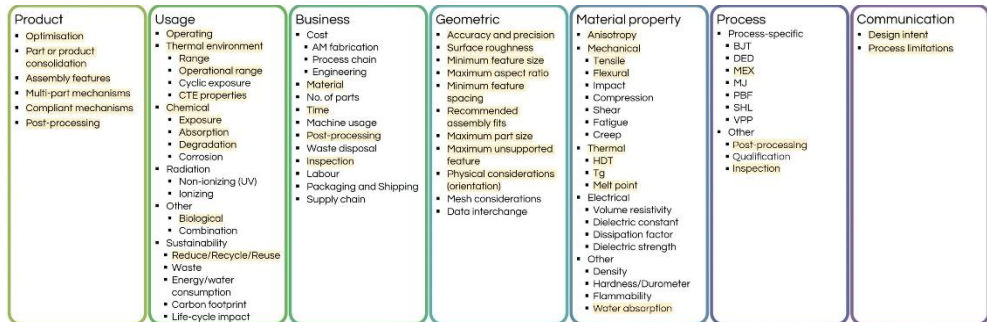


Figure 10.9. AM Design considerations identified in ISO/ASTM 52910. Highlighted elements are included in this section.

The standard guideline for AM in ISO/ASTM 52910 identifies a broad range of aspects that need to be considered when designing components for AM, as shown in Figure 10.9. This section covers most of the elements in the standard (highlighted in yellow in the figure) to provide comprehensive guidance in design considerations.

The information provided here is based on the studies and research described in previous chapters. A set of printable benchmarking geometries is provided with the toolkit to help the designer find the optimal values for each

design feature. This embodiment design stage helps clarify, confirm or optimise the many details required to produce a final design (Grauberger et al., 2019).

Design for FFF worksheet

Machine	Nozzle	Material	Parameter set	R: Robust zone C: Compromised zone	L: Overhang length	L: Bridge length	EW/H: Emboss Detail width/height DW/H: width/height	EH: Emboss Test Height DH: Engraved height	Ø: Min diameter / h: Min. height	S: Supported wall width U: Unsupported width	V: Vertical Min. plane, H: Horizontal Max. diam. Min.
Prusa i3	0.4 V6	PLA 11/20	Set1120	R:45/C:30	L:0.6 mm	L:25 mm	EW/H:1.3 mm DW/H:0.5/1 mm	EH: 5.5 mm DH: 5 mm	Ø:2/h:4 mm	S: 2 mm U: 3 mm	V:0.5/H:3/R:6 12
BCN1D	0.4	ABS yellow	Set08942	R:45/C:30	L:0.6 mm	L:30 mm	EW/H:1.3/2.2 mm DW/H:0.6/1 mm	EH: 5.5 mm DH: 5.5 mm	Ø:2/h:3 mm	S: 2.3 mm U: 3.4 mm	V:0.5/H:3/R:6 12
Zortrax M200	0.3	PLA grey	Set	R:45/C:30	L:0.3 mm	L:25 mm	EW/H:1.5/2.5 mm DW/H:0.3/0.7 mm	EH: 4.5 mm DH: 4.5 mm	Ø:1.6/h:4 mm	S: 1.8 mm U: 2.7 mm	V:0.5/H:3/R:6 12

Figure 10.10. Design for FFF worksheet table provided in the toolkit.

The best practices are provided in the design process guide, while the design features specific values are formatted in a printable table, a 'Design for FFF worksheet' as shown in Figure 10.10 ( and available in the Appendix), to provide general and detailed information. The designer obtains the values of the table following the steps:

1. Is a new material or machine going to be used?  
This question allows the user to determine if there is a need to develop a new set of values for each geometric feature.
2. (if yes to the above) Print benchmark geometries. As the parameters modify the results, a recommendation is given to the designer to fix these parameters.
3. Measure the dimensions recommended in the guide
4. Add information to the table. Indications are given to create a new line in the table specifying the Machine, Material and Parameters (MMP) used. Then for each feature measured, add the information in the correct cell.

This method allows the designer to capture a large number of data and come back to it quickly.

### 10.6.1. MAIN DESIGN CONSIDERATIONS

This section of the toolkit consists of a guideline that provides advice on a number of design considerations. This first part provides guidance on overarching principles, while the second focuses on specific design features.

#### Heat management

The designer needs to ponder the mechanics of heating & cooling when considering manufacturing a concept design using FFF technology, as described in the FFF chapter earlier in this thesis. These are the cause of various guidelines described later and affect several characteristics of the parts.

- The material must be heated up to be able to extrude and fuse it with the previously deposited material or adhere to the build surface.
- The stiffness is reduced. Therefore, the effect of Gravity is more prominent when the material is above the glass transition temperature.
- The material shrinks when it cools down to the build chamber or build surface temperature in the lower layers.
- The deposition trajectories determine the fusion quality between beads as these determine the temperature of the previously deposited material when the new bead is deposited. These determine the form and area of the fusion zones between beads.

#### Volume

As the expected users of the toolkit are not experienced users, it is necessary to mention the importance of the impact of part size vs time & heat management. Scaling a part by  $x$  would mean multiplying by  $x^3$  the time & material required. This scaling also affects the time required to deposit a layer, and consequently, on the structural strength & possibly on the surface finish.

#### Orientation

The component orientation influences many of the properties and features of the parts. It is recommended to define the part orientation in an early stage of the detail design. The orientation impacts mainly four aspects: a) Surface

accuracy, b) Bottom surface area, c) Overhanging surfaces d) Mechanical properties. The reasoning for the inclusion of these aspects & the key points described in the toolkit are described below.

- a) Surface accuracy – As described in a previous chapter, the standard layer-wise deposition method in FFF creates a staircase effect in the surface of the components, as shown in Figure 10.11. This effect results from the deviation from the nominal surface and is more pronounced as the surface is closer to the horizontal plane. The designer needs to understand that the part's orientation determines the angle against the horizontal plane for each surface, and therefore the accuracy of those surfaces.

It is indicated as well in this section that the designer should think about which material and post-processing methods would be used if the staircase effect needs to be removed.

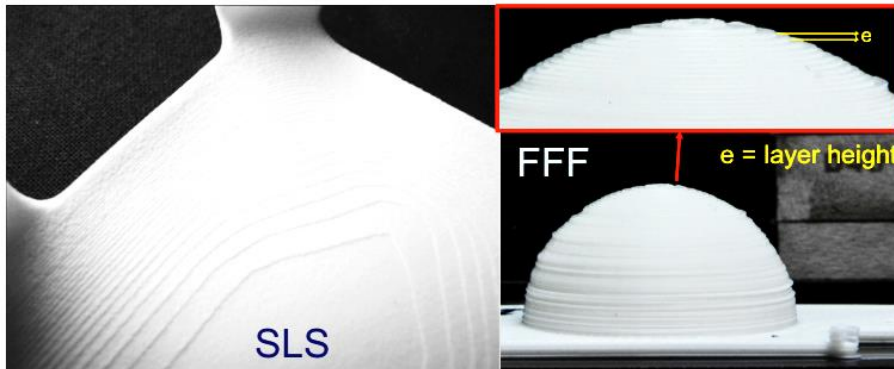


Figure 10.11. Staircase effect in 3D printed components. In SLS technology (left) and FFF (right).

- b) Bottom Surface area – It is essential to highlight the significance of the contact area with the build surface to avoid detachment during the printing and consequent distortion or failure. This effect was described in the Fused Filament Fabrication chapter.
- c) Overhanging surfaces – The filament gets stacked layer by layer. The filament in each new layer in an overhang area bonds by a reduced area to the material from the previous layer and (depending on the deposition

parameters) the internal material of the same layer. This characteristic implies that an area of the filament is overhanging and can sag or break the bonds and fall if the gravity is higher than the bonding strength and surface tension. These types of surfaces determine the requirement of support. Therefore, this section introduces (a) the concept of supports, and (b) the situations where these are required. Although most print preparation software generates support structures, it is essential to make the designer aware that those could be generated in areas where cannot be removed. Designing self-supporting geometries and supports that could be cut away is a good practice in many cases.

- d) Mechanical properties – As described in previous chapters, the mechanical properties of the extrusion-based parts depend on the design of the structure of beads and the bonding between them. This structure is different depending on the orientation

### Tolerances & Accuracy

Independently to the provision of the optimal deposition parameters for a material by the machine manufacturer or not, the tolerances are a consequence of various factors and need to be considered. The heat & cooling cycle could affect the accuracy of the parts and the orientation of the features that require specific tolerances. Although this is mentioned in other areas of this guide, it is important to make the designer aware that this must be considered.

The origin of the *bumped* surface of FFF parts, which determines the tolerances, is described as well in this section:

- As described in a previous chapter, the surface tension and the nozzle cross-section create the extrusion of a cylindrical bead.
- To increase the surface area of cross-linking polymer chains, the gap between the nozzle and the bed or previous layer is smaller than the nozzle diameter.

- This *squeezing* creates an oval bead profile, whose width control by the hardware and software is critical to determining the tolerance and dimensional accuracy, as shown in Figure 10.12.



*Figure 10.12. Example of an irregular profile of the deposited strands, reducing the ability to determine dimensional tolerance.*

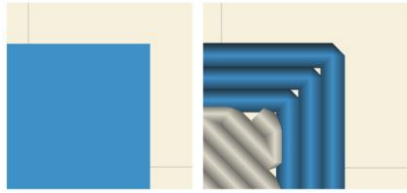
### Distortion

The consequence of the expansion and contraction of the polymer is the creation of stresses inside of the part. Although this phenomenon is explained earlier in the heat and base sections, the designer needs to understand how this could create cracks and how to avoid it. Another effect worth mentioning is the over-extrusion in the first layers, which distorts the part as well.

### Resolution

This principle determines the features that can be produced and therefore is vital for the designer to consider it when designing components. The user can determine the resolution by changing the deposition parameters, so the consequences of changing these need to be understood.

The oval profile of the deposition determines the roundness of the sharp corners in FFF components, as can be observed in Figure 10.13.



*Figure 10.13. CAD (left) and simulation (right) of a corner. The corners are rounded due to the roundness of the deposited bead.*

## Density

One of the main characteristics of FFF compared with the other Additive Manufacturing processes is the capability to create fully enclosed hollow volumes. This capability enables the manufacture of non-fully solid components, as shown in Figure 10.14, compromising the mechanical properties. The investigation about the effect of the infill density and most common infill patterns in the tensile mechanical properties was described in a previous chapter. This principle is essential to be understood by the designer as it helps reduce the weight and manufacturing time efficiently.



*Figure 10.14. Examples of various patterns that could be used to reduce the density of FFF components.*

## Optimisation

This section refers to the consideration of general, non-exclusive to FFF, tips that help obtain a better outcome. The tips provided are:



- Add material just where it is needed – Although this element is discussed in various areas of the design guide, it is essential to highlight the importance of changing the mindset. Parts with large areas of solid volume are more prone to distortion, and the layer time increases, and therefore the strength is reduced (Bhavsar et al., 2020).
- Add ribs to strengthen thin walls or create bridges – This is a common practice in design for injection moulding, which is also applicable for FFF. The creation of ribs helps reduce the wall thickness and keep strength at the same time (Kinnear et al., 2016).
- Fillets – Sharp corners are inherent stress concentrators. Therefore, a recommendation is provided to create fillets to reduce stress concentrations. This method is also advised for thin walls or small features, as it reduces the risk of breakage (Rosato et al., 2000).
- Section parts (part decomposition) – Parts could be cut into sections and built separately in an orientation that brings one or various benefits. These could be: To build parts too big for the machine size (Luo et al., 2012), avoid the need of supports (and therefore decrease print & post-processing time as shown in Figure 10.15)(Demir et al., 2018), create interchangeable features, produce a more robust part (Zhou et al., 2013), or preserve fragile features that could be damaged in post-processing (Stratasys Direct, 2015). When decomposing a part into an assembly, the designer needs to consider the orientation of each section and the assembly method between sections (Oh et al., 2018).

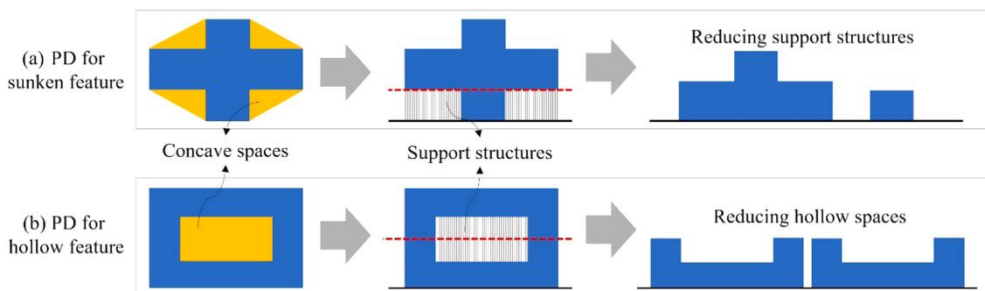


Figure 10.15. Part decomposition to avoid supports in sunken (a) and hollow (b) features (Oh et al., 2021).

## Post-processing

Additive Manufacturing of functional components comprises not just the 3D printing itself but the production of the final component. This technology's relatively low dimensional accuracy often requires post-processing operations to assemble or obtain a final product (Msallem et al., 2020).

Some of the dimensional inaccuracies, mechanical properties and surface quality could be partially addressed by following the earlier guidance, but some issues still affect the components. Furthermore, as described in a previous chapter, some post-processing methods could provide additional functionality to the component. Therefore, the designer needs to include those post-processing steps as part of the considerations. This consideration is highlighted on various occasions in the design guide, but this section focuses on this topic to help the designer consider any missed requirements.

The guidance supplied for post-processing is structured in (a) planning, (b) support removal, (c) surface modification and (d) coating.

### Planning

The guidance provided in this section advises the designer to (1) define the end-to-end manufacturing process of the components, (2) identify the requirements for each step and (3) consider those requirements in the detailed design.

To define the components' end-to-end manufacturing process, the best practice is to use the specifications defined at the beginning of the design (described here in the 'identify requirements' section) and analyse how the as-printed FFF component would fail to match those. The designer is advised to utilise the various tools available for this purpose, such as the Design Failure Mode and Effect Analysis (or Design FMEA) method, where the potential issues that could arise are identified, and the ways to address those are defined (Zagidullin et al., 2021). This first step helps identify pre-processing to improve the surface and component characteristics, such as selecting process parameters (e.g. build orientation, layer thickness, material, etc.) or design considerations (such as wall thickness, part consolidation, infill density, etc.).



An example of a functional prototype product post-processing steps and a custom-made orthosis case study are provided to illustrate this process mapping. The former can be seen in Figure 10.17, and the latter is described in this document.

The information about each step requirements identification is provided to the designer by introducing the techniques described in the post-processing chapter. The design considerations for assembly operations are described in their section later in the guide.

### Support removal

Support removal is usually the first step of post-processing a component. The concept of the supports and their avoidance methods was introduced in the orientation section of the FFF guide. In this section, the guidance provided focuses on how these supports get generated, how they impact the surface finish, and especially how to improve the design to remove them.

One of the best approaches of support removal is the avoidance of supports altogether. Therefore, other methods to avoid the need for supports, apart from component orientation, are introduced in this section. E.g. a supporting column or wall can be designed at the extreme of a cantilever, creating a bridge and avoiding the need for more support structures.

The designer is made aware that the supports should ideally be produced with a different material to allow their removal chemically. If this is not possible, then the way to mechanically remove it needs to be planned. This planning is essential for cavities, as it might be difficult to access those areas with the standard tools for support removal, such as pliers, files, chisels and knives.

### Surface modification

This section provides guidance on material removal and surface topology modification by various methods. As the designer was made aware earlier that post-processing is a set of steps where the order and number of iterations vary,

the techniques described here need to be understood as a part of a more extensive process.

- Heat – Simple geometries are more suitable due to the inherent warping as an effect of the heat treatment. The designer should account for the potential dimensional distortion of the component and its suitability depending on the material. This post-process method affects the mechanical properties of the components as well (S. Singh et al., 2019). If a compaction material is used during the heat treatment, such as salt, the texture of the component gets determined by the salt particles size (Hermann, 2020).
- Chemical treatment – The different chemical treatment types are shown, highlighting the findings from the experiments and literature described in previous chapters. For E.g. The immersion of ABS in acetone is an effective method, but there is a risk of solvent penetration. This section indicates the suitability of this technique for specific materials as well. Furthermore, examples are provided of the type of geometries that could benefit from this process, such as non-detailed complex geometries and those that could provide worse results, e.g., with small features.
- Sanding – This is usually an unavoidable step if same-material supports are generated, so the designer is advised again to find design solutions to avoid supports. Planning which surfaces need to be sanded helps identify if a customised sanding block must be produced, as shown in Figure 10.18. Advice is provided to consider the lack of consistency of this technique and the difficulty of applying it to small and thin features without damaging them.

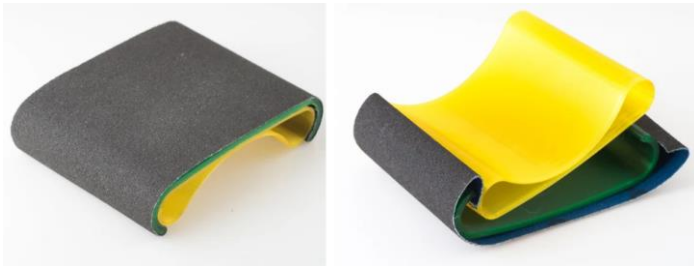


Figure 10.18. Customised 3D printed sanding block. Source: (Hsiao, 2018)

- **Shot blasting** – The design considerations for shot blasting are mainly the need for line-of-sight and this technique’s suitability with other methods. E.g. It could be helpful to remove the glossiness of components treated chemically, but its application after coating could remove the coating. The designer is advised to select soft media such as sodium bicarbonate to reduce the risk of damage to the components.
- **Machining** – The areas to be machined need to be fully solid and thickened if a design uses machining as a post-processing method. Therefore, the designer is advised to thicken those areas (also called adding stock material) at least half a bead width. Another consideration is planning how the machining operations (e.g. profiling, engraving or contouring) will be performed and in which order. This planning helps in identifying the potential need for fixturing features and account for tool access limitations. Another best practice provided to the designer is defining the toolpaths avoiding crossing beads where possible, to avoid delamination. The advice provided is to use this technique for small engraved details, high-tolerance features, or continuous surfaces in small series of components production. These could leverage the capabilities of this technique more than other types of geometries. This technique suitability is reduced when (1) a single copy of a geometry is needed, and (2) all the component surfaces need to be post-processed without a high-tolerance requirement.
- **Tumbling** – The characteristics to be taken into account for this technique are that it can modify mainly the convex surfaces and remove the same amount of material. Therefore, the surfaces with a more

pronounced staircase effect are less smooth than the other surfaces. Areas with cavities or sharp concave corners are at risk of not being affected by this technique. Therefore, the advice provided is to consider this technique for non-complex geometries with rounded edges, with the potential need for additional post-processing to finalise some areas.

### Coating

FFF components could be coated by various methods, such as brushing, dipping, or spraying. The availability of the tools to apply each method would determine which one the designer selects. The advised first step of post-processing was to plan the operations. Therefore, this section is structured by the objective of the coating. This method of classification helps the designer to select the more suitable option for each purpose.

- For smoothing – An overview of the methods described in a previous chapter for filling the ridges of the staircase effect is provided. The advice provided is to consider the potential iteration between these techniques and the material removal ones when selecting the methods. It is not uncommon to use a technique for smoothing and then another to modify the properties, such as strength or colour. Therefore, the designer needs to consider the compatibility between the coating materials and the FFF component. Some materials such as polyester, epoxy or nitrocellulose can be applied through different methods (spreading, brushing, or painting) depending on the selected product. The smoothing results and the application requirements are different. Therefore, it is advised to evaluate the material properties and the method of application as well.
- For metalising – The advice provided is to use these techniques when higher conductivity, abrasion, hardness, strength, temperature transfer, or EV resistance are needed and simulate metal finish for aesthetic purposes. The metallisation processes tend to highlight the inconsistencies in the surface underneath, so for aesthetic purposes, the recommendation is to prepare the surfaces beforehand. While plating thickness needs to be accounted for during the geometry design, the thickness of the metal layer in physical vapour deposition is negligible.

However, the cost of these processes could be higher than other coating techniques, so it is advised to consider this.

- For sealing – Some of the techniques described earlier, such as epoxy coating or chemical treatments, can close the gaps between beads and increase the water tightness. The designer is advised to adapt the process parameters, such as layer thickness or the number of perimeters, as this enhances the component’s surface sealing capabilities.
- For colouring – This purpose is sometimes achieved directly by producing the components with materials of different colours. As with the metallisation techniques, the addition of coating for colouring does not fill the gaps or surface errors. Therefore, previous surface preparation is recommended. The considerations for applying colour are the same as for polymer components produced by other methods, so the designer is referred to other sources for guidance on this matter, such as Conejero et al. (2019).

### 10.6.2. DESIGN FEATURES

This section provides best practices for each design feature that requires special attention in the FFF process. While the dimensional benchmarking literature mainly investigates the influence of some factors, the design rules in literature usually provide agnostic guidance or just a set of values. So far, very little attention has been paid to connecting these aspects to support designers in the variable geometric capability depending on the Material, Machine, and Parameter (MMP) set. Understanding the behaviour of each feature for the specific MMP could help the designers achieve an outcome right the first time.

The specific values for each design feature are characteristic of each MMP set. A benchmarking specimen is proposed for each feature to obtain the working values. This section of the guide describes each feature, the main MMP affecting their manufacturing, and guidance about reading the results from the benchmarking specimens to fill the *Design for FFF worksheet* table.



## Angled walls

**Characteristics** – The bonding strength between filaments in overhanging angled walls depends on the material properties, deposition parameters, and angle of the angled wall. Therefore, this is a design feature the designer needs to define specific values for each MMP set. The study described in a previous chapter revealed an influence of the time of deposition as well. This influence is due to the time required for cooling down between features. Therefore, the designer needs to consider this as well, especially in components with small cross-sectional areas.

**Benchmark** – For this feature, the objective is to obtain the extreme values for three areas: Robust zone (without identifiable defects), Compromised zone (self-supporting but with identifiable defects) and Failed zone (complete delamination and not self-supporting). The challenge with the design of this benchmark is to avoid generating a *bridge*, which would invalidate the applicability for more complex geometries and represent flat and curved surfaces. For these reasons, as shown in Figure 10.19, three versions of the benchmark geometry are provided: straight face, convex face, and concave face. The designer can print just one or all versions to get a realistic value for this feature.

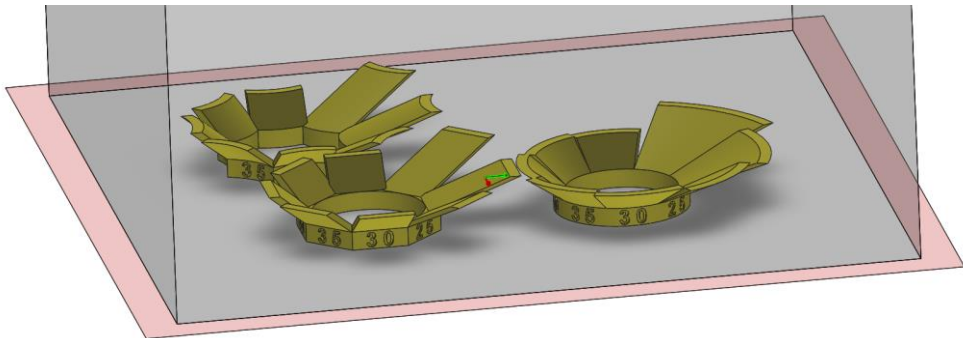


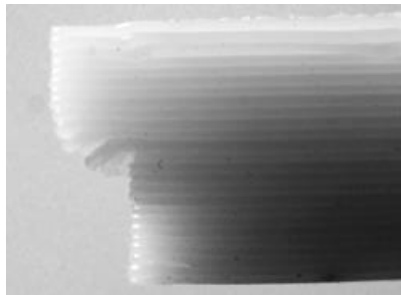
Figure 10.19. The three versions of the benchmark geometry for the overhanging angled wall feature.

This geometry provides overhanging geometries ranging between 15 and 50 degrees from the horizontal plane. Once these geometries are printed, the designer can annotate in the table the highest angle without defects as the

robust zone limit (e.g. as R) and the highest angle with defects but self-supporting as the compromised zone limit (e.g. as C)

## Overhangs

This feature refers to a characteristic overhanging angled wall: 0 degrees or horizontal overhanging walls. This design feature is very common in prismatic geometries, parts with embossed details, and assembled parts. Although the guidance from the overhanging angled wall is still valid, there are some key characteristics that the designer needs to understand to manufacture these features correctly.



*Figure 10.20. Deformation in a horizontal overhang.*

Characteristics – The overhanging beads profile is determined mainly by the Gravity as soon as the overhang length surpasses half of a bead thickness. A sagging deformation, which reduces the overhang's length, as shown in Figure 10.20, happens as a consequence. However, this deformation is reduced as the thickness of the overhanging feature increases.

Benchmark – The results from the study described in a previous chapter were considered for the GBTA design. Three versions of the benchmarking are provided, with 5, 10 and 15mm overhang width.

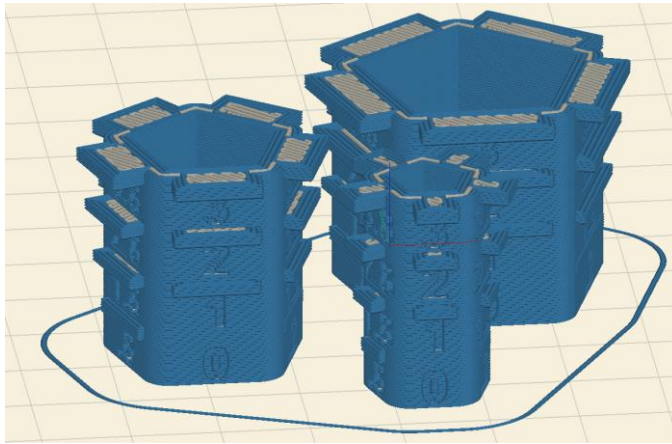


Figure 10.21. Toolpath simulation of the three overhang geometry test versions provided.

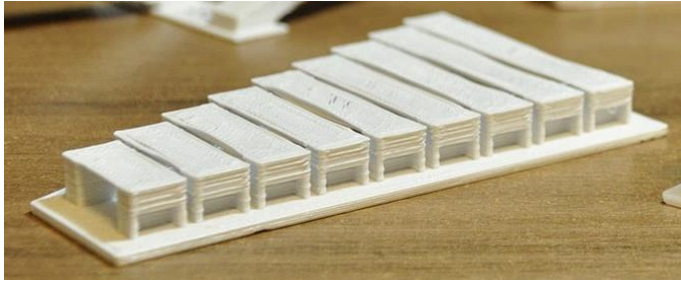
The designer can print one or all three versions shown in Figure 10.21 and identify the overhang length produced without failure.

**Best practice** – To avoid the failure of the overhangs, the designer can reduce the overhang by chamfering or rounding the overhang's corner or adding supports. The separation of the support with any vertical wall should be considered if the designer adds supports to an overhang feature.

## Bridges

The design feature *bridge* refers to a particular situation of the horizontal overhangs where there is material on both sides of the overhang. This feature was introduced in the general principles section, but as in the two features described before, the capability to produce this feature depends on the MMP set.

**Characteristics** – As described in a previous chapter, the rapid filament cooling & shrinkage in FFF allows depositing material that gets bonded to the below layer just by the ends of the bridge. The first layer of the bridge serves as a support for the subsequent layers and, therefore, reduces the amount of material in horizontal overhangs.



*Figure 10.22. Geometric benchmarking test artefact provided for bridges.*

**Benchmark** – As part of a study described in a previous chapter, a testing geometry was developed. This geometry, shown in Figure 10.22, is provided to the designer for this feature.

**Best practice** – The novel designer needs to be made aware that:

- This feature could be used to avoid larger support areas by designing a column on the extreme of an overhang.
- These are standard features that some of the toolpath generation software can identify and apply different parameters.
- The orientation of the first layer of the bridge is key to determining the bridge's maximum length.

### **Details & text**

Details and text refer to the positive and negative features embossed or engraved on the surface of a component. The engraved and embossed details are a common feature as these could be used to customise a design.

**Characteristics** – The designer needs to be aware that this specific feature mainly depends on the layer thickness and the nozzle diameter. E.g. If the feature is oriented mainly in the horizontal plane, the layer thickness determines the minimum height of the detail, while the nozzle diameter determines the width and height.

The limitation of non-being able to produce sharp corners is more visible in small details and text than in other features. The oval profile of the bead rounds the corners in parts manufactured by FFF.

Benchmark – Due to the large variability where these features can be represented, a testing geometry with various weights and sizes of the Arial font is provided. However, a recommendation is provided to observe as well the results in the engraved text from the other testing geometries and use this as reference.

Best practice – Design features with a width of at least two times the nozzle size and depth of two times the layer height for mainly vertical features. Invert the values for mainly horizontal features.

Engraved or embossed text is an inherent geometrically complex feature. It is recommended the usage of a font with uniform thickness. Otherwise, there is a risk of missing some of the sections of the characters.

## **Columns & pins**

Columns and pins are design features with the characteristic of having a small area vs height. These are very common in geometries with lattices or grids.

Characteristics – These features are limited to the minimal cross-section by the bead width. The cross-section profile definition is lost below a certain threshold due to the cylindrical profile of the bead, in a similar manner as described for the details.

When designed vertically, they are characterised by the reduced time required to produce. In columns and pins, the risk of deposition on a non-fully solid layer is higher without proper control of the temperature or speed of deposition.

The orientation of columns and pins is more critical than other features, as the contact area with previous layers is small. The downward force that the nozzle applies to deposit the filament could bend the column or pin, creating a non-uniform deposition, as shown in Figure 10.23.

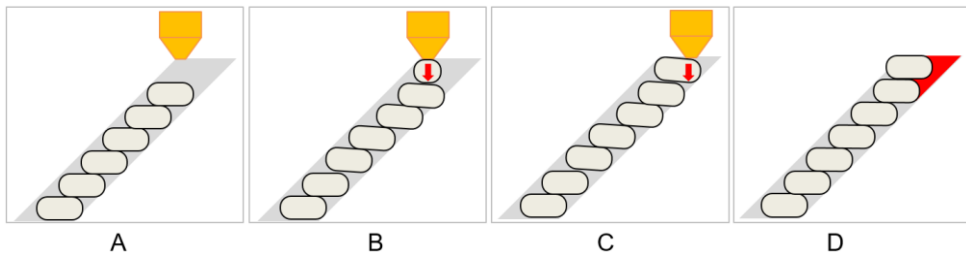


Figure 10.23. Distortion force in the deposition of columns in FFF. In B) and C), the column deforms while the new layer is deposited due to the pressure applied by the extrusion. D) This new layer is bonded in the wrong location and fails to follow the CAD design.

**Benchmark** – Columns and pins could have many different cross-sectional areas and orientations. A single geometry based on cylindrical columns is provided to simplify the analysis by the designer. Guidance needs to be provided to help the designer extrapolate the results to other geometries and orientations.

The two main parameters to capture in columns and pins in the *Design for FFF worksheet* table are the minimum diameter and estimated maximum length. These parameters reveal the two main characteristics, or limitations, described before: bead width and interlayer bonding.

**Best practice** – Due to the wide variety of loading conditions where columns and pins could be found, the values captured in the table could be understood only as a guide for a print without dimensional failure. However, a good practice is to produce a section with the columns and pins and test it under loading before manufacturing the final part.

Designing the columns as X times the bead width and rounding the corners of the columns' cross-section is recommended to improve the dimensional accuracy (Armillotta, 2006).

An additional tip is provided to make the designer think if the columns and pins could be avoided altogether, as these are inherently a high-risk feature in FFF. Replacement of these by continuous walls such as the ones used in the infill patterns could de-risk the failure.

## Walls

The walls refer to the design features where the side areas are larger than the cross-section.

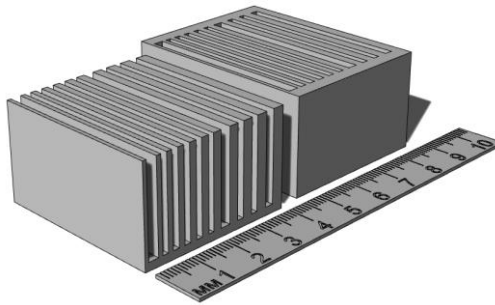


Figure 10.24. Walls benchmarking geometry provided.

**Characteristics** – The walls can have two types of structure: infill+contours (also called *thick walls*) and just contours (or *thin walls*). The structure depends on the thickness and the printing parameters. As the layer thickness determines the width of the beads deposited, the minimum wall thickness is determined by the layer thickness (Taşdemir, 2021). Walls thin enough to allow just contours are more prone to delamination than thicker walls due to heat dissipation and weak intralayer bonding strength. The cross-sectional thickness of angled walls is not the same as the thickness in the direction normal to the surface. The cross-sectional thickness is the characteristic that determines the structure.

**Benchmark** – The important feature to observe in walls is the system capability to deposit thin walls. The orientation, profile and MMP set determine the quality of a wall of a specific thickness. Therefore, the geometry provided comprises a set of thin walls with gradual thickness increase, as shown in Figure 10.24 in two configurations: with and without a solid supporting wall at the end. Indications are provided to look into the outcomes of other benchmarking geometries and get a value of minimum wall thickness.

**Best practice** – Changes in wall thickness could create hollow pockets inside walls, reducing the strength and water tightness (Taşdemir, 2021). It is then recommended to keep thin walls as uniform as possible and examine the structure where the thickness changes. A minimum of two beads thick is

commonly the recommended minimum wall thickness, as this allows the bonding of beads between layers and within layers.(Fernandez-Vicente et al., 2015)

## **Holes**

Due to the usual inclusion of parts within assemblies, negative features such as cylindrical holes are a ubiquitous feature.

Characteristics – Usually, the purpose of holes is to serve as a joining feature with hardware such as screws or bolts. Therefore, the main characteristics are that a tighter tolerance is usually required, as these are usually critical areas of mechanical load. Holes built parallel to the build platform (vertical) are commonly produced more accurately than in other orientations, and the alignment of the beads surrounding the holes increase its strength (Gómez-Gras et al., 2021). The profile of horizontal and angled holes, the ones with the axis not perpendicular to the build platform, is produced by a discrete number of planar layers. The dimensions are therefore less accurate as the hole size decreases.

Benchmark – The design limits are different between horizontal and vertical holes. For this reason, as shown in Figure 10.25, two testing geometries are provided:

- A vertical testing geometry with small holes to find the minimum diameter that can be manufactured,
- Another geometry with large horizontal holes, to find the largest dimension without distortion or failure. This one also serves the designer to identify the minimum diameter where the deviation from the dimension is not too large.



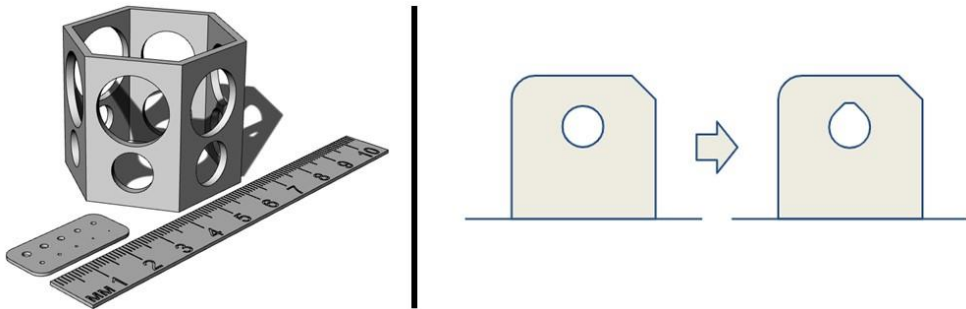


Figure 10.25. Testing parts provided to evaluate hole sizes (left) and illustration provided about hole modification (right). Ruler added for scale.

**Best practice** – Where possible, the holes should be aligned vertically as the precision and mechanical strength are higher than in other orientations. Holes should be designed holes where these are needed instead of drilling the components. The toolpath generation software generates beads surrounding the hole, and therefore increasing its strength. However, the material shrinkage should be considered as it alters the dimensions of the holes in this orientation (Yaman, 2018). Therefore, it is recommended to print a pilot hole and drill it to the nominal diameter. The recommendation to modify vertical holes into a truncated teardrop shape, as shown in Figure 10.25 (right), is provided.

### 10.6.3. ASSEMBLY CONSIDERATIONS.

One of the main benefits of using 3D Printing is the capability to create complex geometries that could replace various components into a single part (Tang et al., 2016). However, the components produced by 3D printing are usually part of an assembly through the interlocking with other components or bolted. This section provides the designer support when designing components that are part of assemblies. It should be noted that there is a wide range of types & designs of assemblies. Therefore, this section covers some of the most common.

When using this technology as the final production method, it is important to remind the designer that it can produce non-assembly mechanisms (Cuellar et al., 2018). These are functional just after coming out of the machine after some post-process (Wei et al., 2016).

## **Joints**

The Joints feature refers to components assembled with other 3D printed components or other components manufactured by other means. One of the standard joint designs is the lap joints, which keep a uniform wall thickness while avoiding the risk of a gap between components. Depending on the joint behaviour expected, with or without movement, some of the guidance provided in the next point should be considered here as well.

Characteristics – Three types of fit can happen between joined components: clearance fit (loose components), Interference fit (friction between components), transition fit (between the former two. Also called slip, lap joints, or push-fit) (Polini, 2014). Due to the layer-wise nature of the manufacturing method, the joint's orientation plays a big part in the result. For example, the profile of the layers increases the friction between components in a joint perpendicular to the layers. The best practice tips provided before for thin walls and small features should be considered in lap joints. Interference fits rely on the slight dimensional overlap between the hole and the inner components and a coupling force to fasten the joint. This results in the deformation of both parts (Troughton, 2008). However, this insertion under pressure seems to damage the coupling surface in many cases, creating delamination of filament. As a result, the disassembly forces are lower as the surface morphology is modified during the assembly (Bottini & Boschetto, 2019).

Benchmark – Due to the high dependence of the behaviour of the joint in the component geometry and configuration, a single value cannot be extracted for an MMP set. Advice is provided to produce a small section of the component(s) with the joint and identify the dimensions that need to be changed.

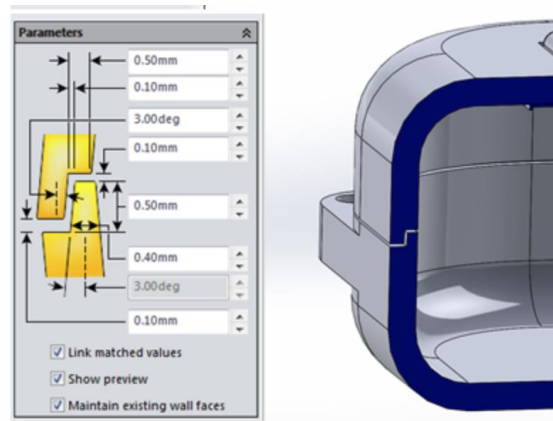


Figure 10.26. Tool for parametric automatic generation of lap joints in Solidworks (Dassault Systèmes, France).

**Best practice** – A good practice is to consider how the filaments are deposited in a joint and their expected mechanical behaviour, as explained in the overarching design considerations section. The staircase surface profile can be reduced by designing a rectangular prismatic joint or by reducing the angle of the overhang (Lussenburg et al., 2021). The joining of various components is a common practice in conventional manufacturing processes of polymer products. Therefore, many CAD software packages provide automatic generation tools for modifying the parameters of joints, as shown in Figure 10.26. It is recommended to use these tools for the design of joints.

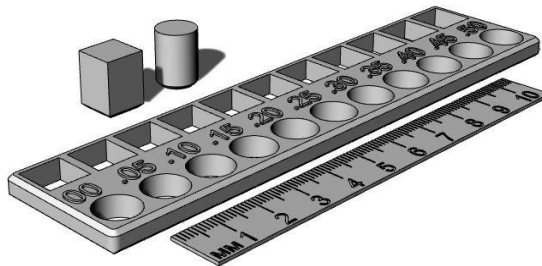
## Clearance

The clearance refers to the space between components produced together, either because they form part of the same assembly or because are printed close, to manufacture various parts simultaneously. The guidance provided in this section could also be applied to the space between surfaces of the same component, also called gaps.

**Characteristics** – The purpose of the clearance between surfaces determines the characteristics to consider. When the aim is to produce sliding surfaces, the staircase surface texture determines the best orientation for the sliding movement (Lussenburg et al., 2021). If the gap is too small, it bonds to the material deposited before when the filament is deposited. The radiating heat

from large parallel surfaces could create unwanted bonding between these. Overhanging unsupported overhanging walls can sag in clearance gaps, creating a bond between separated components. The manual removal of supports is complicated in these features unless these can be taken apart.

Benchmark – The MMP set determines the recommended clearance values between components and the geometry and purpose of the clearance. Therefore, the designer is advised to use the guidance provided before and produce a small feature section to determine the correct clearance value. A geometry with two typical geometries, straight and curved surfaces, is provided to ease the test of this feature. 10 mm square and round pegs and another body with square and cylindrical perforations with 0 to 0.5mm clearance are provided. The designer should test the pegs in each perforation and find the values that provide the fit required.



*Figure 10.27. Clearance and interference test geometry.*

Best practice – The designer should consider the printing configuration, build direction and accessibility to clearances to control the behaviour of the components printed together (Sossou et al., 2018). It is good practice to make the components self-supporting and keep a clearance that allows their movement when designing a joint that requires movement between parts, as shown in Figure 10.28.



*Figure 10.28. Top view of an example of clearance between moving components in a self-assembled mechanism. Source: (Clockspring3D, 2020a)*

The clearance between non-vertical surfaces could be controlled by considering the maximum unsupported overhang angle. For clearance in areas near the horizontal plane, using the guidance described in the bridges section is recommended.

### **Snap-fit joints**

The complexity provided by the technology allows embedding fastening features in the components. These types of joints prevent an assembly from separating without the use of glue. These are common in injection moulding components assembly, but the FFF characteristics require highlighting some of the considerations to be considered.

Characteristics – The most common types of locking features for FFF are the cantilever and annular snap-fit joints. The locking feature can be further divided into the deflection mechanism and the retention mechanism. The inclusion of fasteners requires good control of the tolerances of the components. A too loose fastener would not fix the components together, and a too tight one would not allow it to be assembled. The fastening between components relies on the material or design's inherent flexibility and usually comprises small details and thin walls. Therefore, the guidance provided for those aspects is applicable here.

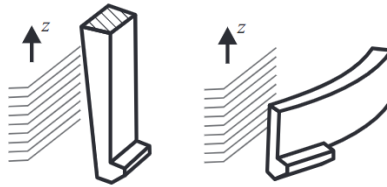


Figure 10.29. Bad (left) and good (right) orientations of a snap-fit joint. Adapted from Klahn et al. (2016)

One of the key characteristics to consider is the orientation of the fastener during manufacturing. The deposition of filaments along the beam of the snap-fit allows it to rely on the material bending characteristics instead of the interlayer bonding, which usually has a brittle behaviour (Klahn et al., 2016).

**Benchmark** – The behaviour of the snap-fit joints can be very different depending on the component’s geometry. Therefore, a benchmark geometry is not provided in this case. Instead, guidance is provided to produce a representative section of the component to validate the dimensions.

**Best practice** – The sharp edges of the hook of conventional snap-fit joints could be challenging to produce with FFF. Therefore, it is recommended to take into consideration the machine resolution. A common practice is aligning the snap-fit with the printing layers to use the inherent layer “bumps” (Ramírez et al., 2019). Locating features can be used to constrain the remaining degrees of freedom of the joint and establish a reference between the mating parts.

The use of fillets of a value of 50% of the snap-fit feature thickness is suggested for diminishing the effects of stress concentration. The stresses could build up as well if the joint is in a deformed state after assembly. Making sure that the joint is not under stress when assembled helps in avoiding failure. Another good practice to reinforce the design of the snap-fit features is to increase the width of the cantilever (Genc et al., 1998).

In terms of orientation, it is recommended to orient the bending in the orientation of the deposited filaments as shown in Figure 10.29, and not across layers, as the latter are more likely to shear and break (Ahn et al., 2002).

## Threads and inserts

The usage of threaded fasteners is one of the most common ways to join various components in an assembly. As shown in Figure 10.30, there are various methods to add these in FFF components: Self-tapping Screws, tapping, and inserts.

**Characteristics** – As explained in the holes section, a solid area is created around a hole. If a hole is not printed but drilled afterwards, the non-fully dense structure of the FFF components reduces the capability to transfer the load.

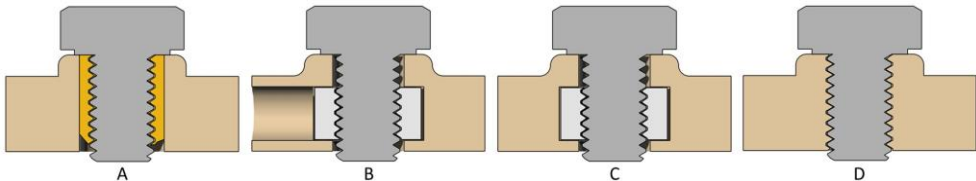


Figure 10.30. Some examples of methods to add threads to FFF components. Inserts (A), Nut with side pocket (B), in-print cavity (C), and threading (D).

The relatively low resolution of the FFF process restricts the capability to print the threads with enough detail unless the machine resolution is taken into consideration, as shown in Figure 10.31. By using self-tapping screws, the thread is created when inserting the screw, but if this is removed and inserted again, a risk exists of creating a different thread, weakening the union due to wear. Due to the relatively low stiffness of the materials used in FFF, the addition of fasteners by tapping the holes has a relatively low strength and the same risk explained before.

**Best practice** – Inserts could be added in two ways: adding an insert to the hole itself or adding a threaded insert in a cavity (e.g. a nut). Adding an insert in a hole by pressure or temperature creates compression stress that provides a better torque resistance and reduces the thread risk described before. The method of creating a cavity to fit an insert increases the area of load transfer for pull-out strength. However, a nut sliding pocket adds weakness to the joint. This weakness can be overcome by inserting the nut directly into the part during printing (Ahlers et al., 2021).



*Figure 10.31. Example of FFF printed threads. Note the large size of the thread. Source: (Clockspring3D, 2020b)*

### **Living hinges**

Living hinges are a feature that uses the relative flexibility of the materials used in FFF and the ability to change the thickness. These are part of a family of non-assembly mechanisms called compliant mechanisms (Gribbins, 2014). Although not an assembly itself, these enable the capability to manufacture various parts of a mechanism in just one component.

Characteristics – Living hinges gain their motion from the elastic deformation of an area thinner than the main body. The dimensions of a living hinge are derived by the material and type of application needed from the design. The thickness of the hinge determines its stiffness (Dirksen & Lammering, 2011). The material selected also determines the fatigue of the hinge and, therefore, the number of cycles the hinge is capable of withstanding.

Best practice – Printing living hinges in a vertical build orientation, aligning the beads along the hinge to increase durability. The thickness of the hinge should be a multiple of the bead thickness. If the hinge is produced horizontally, using a thickness with a value equal to a multiple of the layer thickness should provide reasonable control of the behaviour (Gribbins, 2014).

## **10.7. PROTOTYPE**

One of the significant benefits of AM is the capability to manufacture parts without long preparation. Furthermore, FFF is a relatively low-cost technology where most of the cost comes from the time required to operate the machine (Fernandez-Vicente et al., 2017). Therefore, one of the good practices to



manufacture successfully the final component is to produce preliminary prototypes of the most challenging features.

In this stage of the embodiment design process, the designer has already identified functional features, leveraged the design solutions available in the digital repositories, and created a preliminary design considering the features described earlier. At this stage, the designer is provided with guidance to de-risk the manufacture of the final component by the individual production of features that could fail. This practice helps understand whether the right solution has been selected or an alternative needs to be found. This is also useful to confirm that the digital design translates correctly into the physical component (Griffis, 2017).

The proposed workflow is as follows:

1. Design or separate the challenging geometric features – This refers to features that have been designed close to the limitations of the technology. E.g., thin walls, overhangs, joints, etc.
2. Print these features – The material, orientation, and parameters must be kept the same as the final part to represent the same conditions.
3. Evaluate the result – The designer is asked to evaluate if the output matches the design intent. Guidance on analysing the root cause of the failure is provided to the designer (e.g. using an Ishikawa diagram such as in Figure 10.1).
4. Modify the feature – If the feature does not comply with the design intent and the root cause has been identified, the designer is encouraged to redesign the feature and produce it again.

These preliminary prototypes could also be used to evaluate the post-processing methods selected and identify potential issues. This can be critical, especially in parts where off-the-shelf components are assembled with 3D printed parts. While most FFF materials could be sanded or heated up to fit together, this is usually not the case for non-3D printed components.

This iterative prototyping process is a common practice in product design (Laurel, 2003). For the scope of this guide, this gains an even higher meaning as the user is expected not to be an experienced engineer or designer, and therefore these methods might be unknown.

## **10.8. DELIVER**

In this stage, the designer is asked to apply the guidance provided and the learnings from the prototype stage and create the final design. This step is commonly understood as the detail design, where all the considerations have been previously clarified in the embodiment design (Griffis, 2017). This step output is the final design production, including the components post-processing according to what was identified previously.

In this section, the designer is invited to make a retrospective analysis of the learnings during the production to learn from reflection and reasoning (Diegel et al., 2019).

## **10.9. SUMMARY**

A design toolkit to support designers in the end-to-end design process was developed and described in this chapter. This design toolkit conveys the information gathered and developed by studies described in previous chapters of this document.

The method described provides support to leverage the capabilities of AM and the online open repositories of design solutions and produce a design considering the critical process characteristics for FFF.

The testing of this method and design guide with users is described in the next chapter.

# Chapter 11

## Evaluation of the toolkit & case studies

### 11.1. INTRODUCTION

The evaluation of new design tools is a common practice in design research. Most of the authors cited in the Design for Additive Manufacturing chapter evaluated their work through the application in case studies or user tests. Perez et al. (2019) evaluated the ideation quantity, quality, novelty, and utility when a group of engineering students used their design principle cards. Their method identified that a combination of representations (visual and textual) improves the overall output of ideation, helping to improve the quality and novelty of ideas. Laverne et al. (2015) developed a case study analysing the contribution of AM knowledge provision in the originality and manufacturability of the developed solutions. As shown in Figure 11.1, three multidisciplinary (engineering design, industrial design, and product ergonomics) groups of six participants were tasked to design an innovative product, providing three different levels of AM knowledge. Their findings highlighted the need to distinguish between restriction and opportunities and, therefore, provide the proper AM knowledge at the right time. Maidin et al. (2012) developed a series of user trials to test their database to support designers in the ideation stage. Their approach was to ask designers to sketch and redesign a familiar product, with and without their design solutions database. The test provided a sample

size and diversity not enough for statistical relevance but enabled the capture of insights on the tool's relevance and effectiveness.

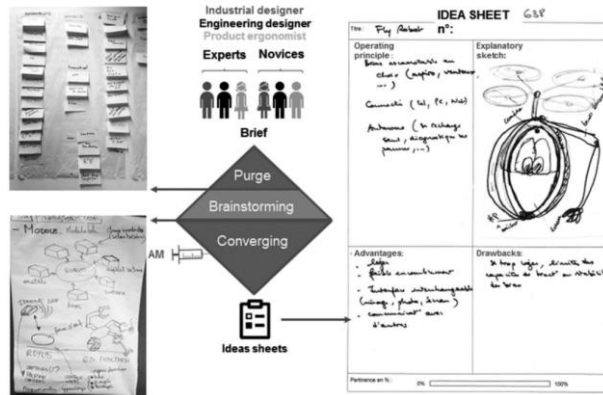


Figure 11.1. Protocol of the study developed by Laverne et al. (2015)

After applying their methodology to develop some conceptual case studies, Blösch-Paidosh and Shea validated it through a user study with 29 novice designers (Blösch-Paidosh & Shea, 2019) and another study with 27 product design students (Blösch-Paidosh et al., 2019) using the same methodology. All the participants were given an introductory lecture on AM technologies, their unique capabilities, and various examples before the experiment. Then the participants were divided into two groups, with and without provision of the design heuristics for AM cards, and tasked to redesign a product individually. The results were then evaluated on the novelty, the range of novel aspects, and utilisation of the information provided through statistical analysis. Their findings evidence the influence of the background of the participants in the detail and concepts generated quality and the usefulness of a mix of text and images to provide design support.

The previous chapter described the toolkit developed to support novel designers in creating functional components with FFF. This chapter examines the efficacy of the proposed toolkit discussed in the previous chapter by a qualitative study with inexperienced technology users.

## 11.2. METHODOLOGY. DESIGN OF THE TRIAL

The Design for FFF toolkit capability to assist in FFF product design was studied via a user study with novel designers.<sup>8</sup> This study was done with two different groups in two consecutive years, with a total of 40 participants in the experiment. Most of the participants were mechanical engineering or product design graduates with little to no experience with the technology.

The participants are introduced to the various Additive Manufacturing technologies characteristics in a series of sessions in the first half of this subject. Then in the second half, the scope is to develop a practical project utilising AM. The design for FFF toolkit was tested in the second half to support the novel designers in developing their product.

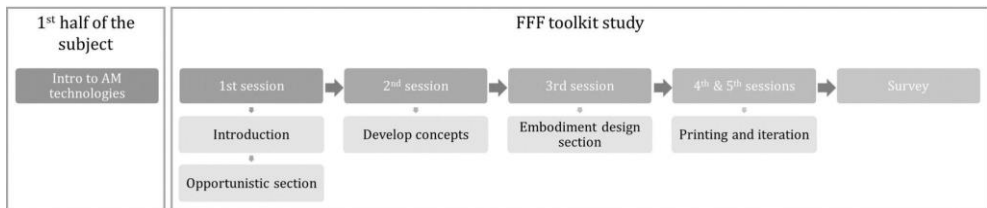


Figure 11.2. Experimental procedure.

As shown in Figure 11.2, the methodology and the design guide were introduced in the first session. The opportunistic design section of the guide, up to the section of design solutions extraction from databases, was described and made available to the participants at this stage. The aim was to reduce the risk of self-limitation in the ideation phase (Prabhu et al., 2021).

The participants were then divided into groups of three, encouraging the grouping with people from different backgrounds. Pahl et al. (2007) highlighted the importance of multidisciplinary work in early design stages to enable innovative products.

<sup>8</sup> The study was performed with the students of the Additive Manufacturing subject in the master's degree in Computer-Aided Integrated Manufacturing and Design at the Higher Technical School of Design Engineering (ETSID) of the Universitat Politècnica de València (UPV)

As design brief, the participants were asked to design a phone tripod produced mainly by polymer FFF. They were encouraged to leverage the capabilities of the technology and optimise their design for production where possible. This problem was chosen due to its likely familiarity with the participants and the large number of designs available.

The aforementioned opportunistic design section was provided, with an early version of the ideation cards as slides of examples as shown in Figure 11.3, as a stimulus to help generate new concepts.



Figure 11.3. The early version of the ideation cards that were provided in the study.

After this initial session, the participants were given another session to write or sketch ideas and asked to generate at least one concept. Once each group had a concept defined, the remaining sections of the toolkit were presented and provided to the participants. The optimum dimensions of characteristic features for the machine and materials were provided to the participants. Therefore, the designers did not need to print the provided testing geometries and capture the values in the *Design for FFF worksheet*.

The participants then developed their design through the embodiment phase and the prototyping of challenging features. The participants documented the activity in summary reports, allowing the author to capture their thought process and sources of inspiration. Following the design exercise, the designers were asked a series of questions about their perception of the design toolkit. Participants were asked to provide positive or negative responses and elaborate where possible. Some specific perception metrics were measured, following the model proposed by Paz et al. (2013). As shown in

Table 11.1, the metrics included in this study were usefulness, clarity, completeness, conciseness, and relevance.

Table 11.1 Questions of the toolkit evaluation survey.

Metric	Question
Usefulness	Was the guide a good reference for the process in general? Why?
Clarity	Were the guidelines clear and illustrative? Why?
Completeness	Regarding the overarching design considerations, did you miss any other element? Which ones?
Relevance	Is there any unnecessary section or rule? Which one?
Clarity	Was the guidance description clear or too complex? Why?
Conciseness	What is your perception about the length of the guide?

### 11.3. RESULTS & DISCUSSION

The structured approach of requirements capture seems to have helped the participants identify the critical elements to be considered during the design, such as freedom of rotation, part number reduction, foldability, and adaptability to a range of phones. Every participant mentions these as elements to develop their concepts around.

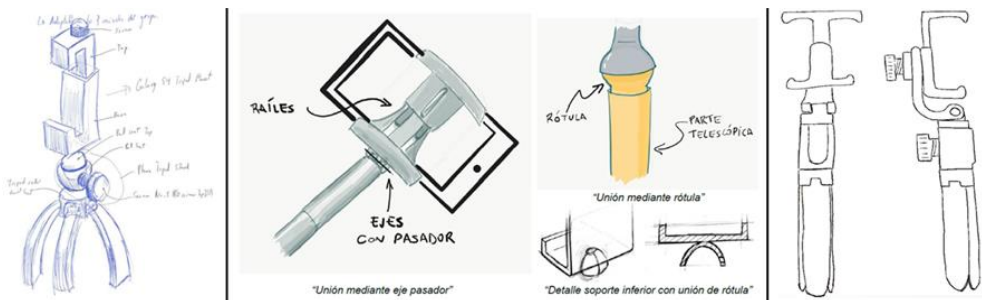


Figure 11.4. Examples of design concepts created by the participants.

The provision of examples to leverage the capabilities of the technology and the guidance to extract design solutions from digital repositories seems to

influence the quality of the concepts. Most of the participants identified design solutions in the digital repositories for each element in their design and evaluated the feasibility to implement these. It corroborates the findings of Bin Maidin et al. (2012), who demonstrated that their AM feature database was “*inspirational, useful, relevant, and helpful to support the conceptual design of parts and products.*”

However, there is some similarity between the designs. It seems that the participants focused their attention on finding design alternatives in the design repositories instead of implementing the ideation cards provided as digital slides. This could signify a potential interference in the variety of ideas by the medium used for this section. This finding is consistent with Yilmaz et al. (2012), who found that physical cards improve overall creativity and diversity of ideas. Therefore, the ideation cards in the newest version are provided as a physical element, as it has demonstrated to be a successful method to elicit creativity.

The background of the group members seemed to play a large part in terms of the creation of innovative ideas, as shown in Figure 11.5:

- The groups with all or most of their members with mechanical or engineering backgrounds used the digital repositories as the source to gather mechanical design solutions to be reused.
- Digital repositories were used instead to find inspiration to solve specific mechanical challenges by the groups of participants with mostly product-focused backgrounds.



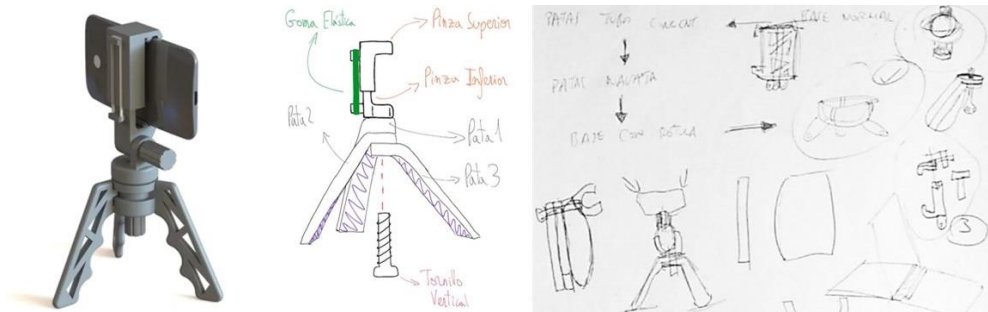


Figure 11.5. The design used as a reference in both cases (left) (Trentesous, 2018) and sketches from a group with mostly engineering background (centre) and product design (right).

It seems possible that this is an example of design fixation, as described by Sio et al. (2015) with the transfer of non-essential features from the designs from the digital repositories. For example, the first concept in Figure 11.5 transferred the printing of a threaded bolt instead of using off-the-shelf hardware, which would have been more reliable.

The participants successfully took into consideration the specific feature limitations and the machine and materials characteristics. The prototype phase helped in identifying unsuitable dimensions and potential improvements. E.g., one of the teams experienced the variance in properties from the first prototype in ABS to the final prototype material, HIPS. As shown in Figure 11.6, the areas with stress concentrations in the ball joints started to crack when testing the assembly. The design and orientation were modified, which improved the outcome.



Figure 11.6. Design iterations enabled by prototyping. Problem detected (left) and orientation of the parts in the print platform (centre) and reoriented in the second iteration (right).

### 11.3.1. CASE STUDY. TELESCOPIC PHONE HOLDER

One of the cases is analysed in detail below to study the application of each toolkit section in the participants' design.

#### Identify requirements

The participants identify the main requirements of the object: maximum range of rotation and orientation, maximum height and foldability, number of parts reduction, and adaptation to a range of smartphones. In terms of production objectives, they correctly identify the optimisation of production time and supports required.

#### Concept design. Ideation

After a search for ideas in commercial products and the digital repositories, the group opted for: (1) relying on a rubber band to allow a range of smartphone dimensions, (2) a telescopic main body to match the foldability requirements, and (3) A foldable tripod configuration of the legs. The designs used as inspiration are shown in Figure 11.7.



*Figure 11.7. Designs that were used as inspiration by the participants of this group.*

In terms of usage of the design principles, eight of the 15 design principles described earlier were leveraged by this group:

- Incorporate standard interfaces
- Hollow out parts to reduce weight and cost
- Embed off-the-shelf functional components
- Adjust the wall thickness to control the flexibility
- Consolidate components to incorporate multiple functions

- Design and print assemblies together
- Design modular elements
- Reuse component geometry

This large number of design principles used is a rather significant result. This result may partly be explained by the usage of examples already produced by FFF as inspiration.

### Concept design. Extract design solutions

The participants mainly identified two design solutions that could be leveraged in their designs: the telescopic element that locks in place when extended, and the clearance dimensions of the self-supporting hinge of the tripod legs, as shown in Figure 11.8.

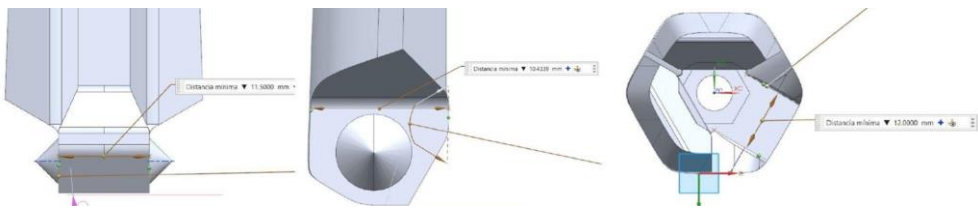


Figure 11.8. Self-supporting leg assembly design solution extracted.

Although the extraction of this design solution helped the team reduce the time of development of this non-assembly mechanism (Cuellar et al., 2018), it can be observed that this biased the design to reuse the profile of the reference design legs as well. This is a clear example of design fixation, as described by Sio et al. (2015).

### Embodiment design. Overarching considerations

It seems that the orientation, tolerances, resolution and material optimisation were considered for every component. The wall thicknesses of each component and the details were defined, considering the bead width of the system.

### Embodiment design. Post-processing

The participants seem to have considered the removal and avoidance of supports by creating self-supporting structures, as shown in Figure 11.9. The

components orientation also considered reducing the number of supports, as can be seen in the figure.

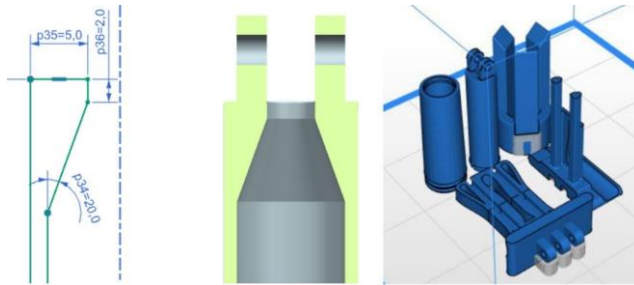


Figure 11.9. Post-processing considerations in the case study. Self-supporting feature in the telescopic feature (left) and print platform with most of the components without needing supports (right).

Due to the study's short length and being part of a subject, it was not expected to be considered any other post-processing method apart from support removal and some sanding of the support marks.

### Embodiment design. Design features

As described earlier, the angle of the walls was taken into consideration by the participant group. It seems that the wall thickness was optimised to the purpose of each section, and the maximum diameter of horizontal holes was taken into consideration, as shown in Figure 11.10.

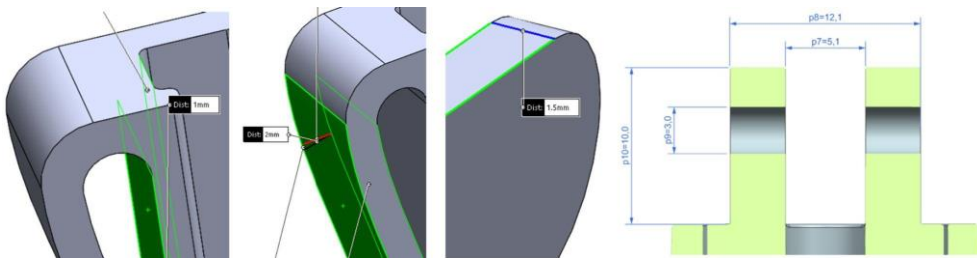


Figure 11.10. Dimensioning of the wall thickness in various features (left) and the size of the horizontal holes by the designers (right).

### Embodiment design. Assembly considerations

This group considered the assembly from the concept phase of the design and included a non-assembly mechanism for the legs, as described earlier., an

annular press-fit joint was included to assemble the two parts of the telescopic feature, as shown in Figure 11.11.

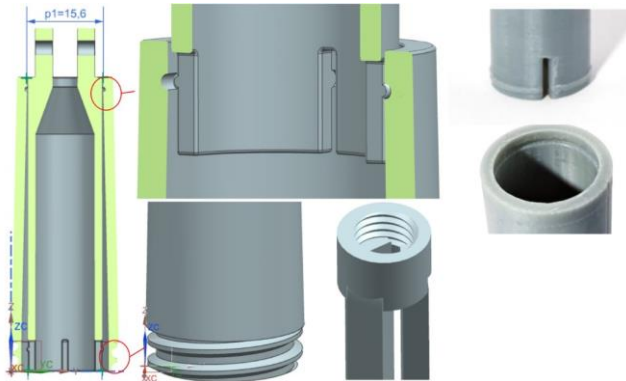


Figure 11.11. Assembly features in the design by the participant group. Annular press-fit joint (top) and printed thread (bottom).

To assemble the telescopic feature and the legs, a 19mm self-supporting printed thread was included. This reveals a consideration of the clearance required between components, produced already assembled, in case of the legs, and assembled afterwards, in the case of the telescopic feature.

### Prototype

It seems that the first iteration revealed some challenges in terms of tolerances, such as the fusion between the telescopic components due to the need to be produced in place or the lack of clearance between the thread components.

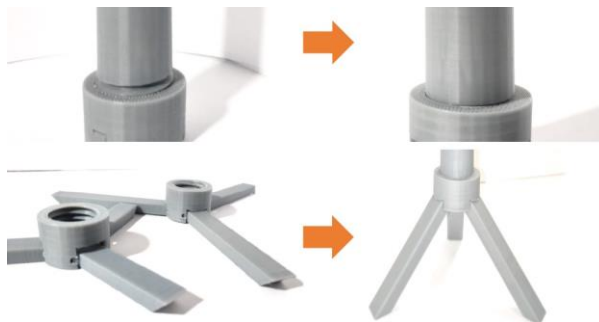
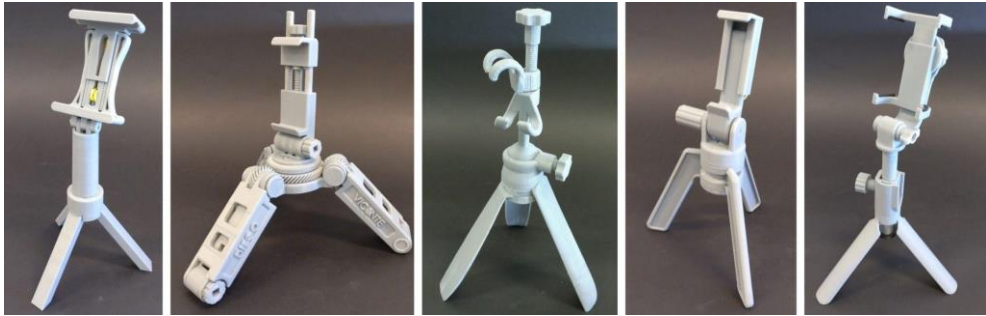


Figure 11.12. Some challenges that the designers identified in the prototyping step. Not enough clearance (top) and too large pocket to stop the tripod legs aperture (bottom).

Furthermore, the designers identified some areas where the product was not performing as expected, such as: (1) the lack of capability to fit large enough smartphones, so an elongation of that component was needed, or (2) the tripod legs lack of rotation restriction, as shown in Figure 11.12.

### Conclusion

The analysis of one of the examples reveals that most of the toolkit content was considered and applied by the participants in a successful manner. Although this was just one example, the designs developed by the other participants show the application of the guidance provided similarly, as shown in Figure 11.13.



*Figure 11.13. The case studied (left) and other example designs from the study.*

### 11.3.2. SURVEY

The participants' survey showed a consensus that the guidance provided was helpful, concise and clear, as shown in Figure 11.14. The main comments in one of the groups in terms of usefulness and clarity were about missing detailed parameters description and relationship between these.

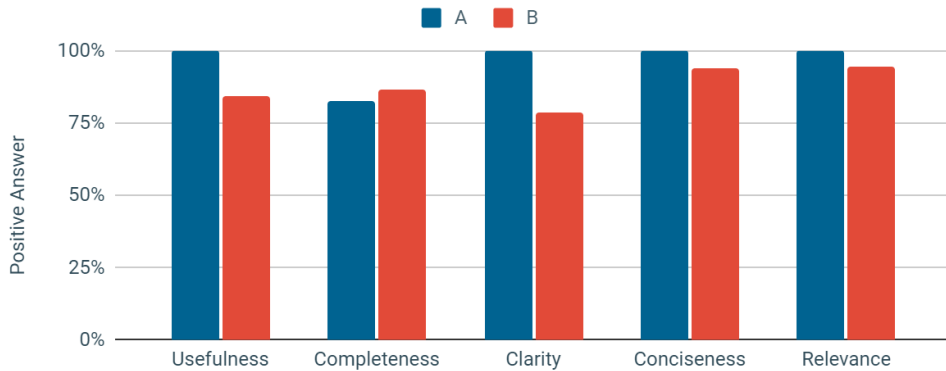


Figure 11.14. Chart with a summary of the survey results.

The second introductory session of the tool with the second year group (group B in Figure 11.14) was shorter than the first year. Some of the participants felt a bit confused with some of the characteristic geometries descriptions. Therefore, their perception of clarity of the toolkit was lower than the other group. This highlighted the need of structuring the information provided, which is already implemented in the newer version, by providing (1) *characteristics*, (2) *benchmark*, and (3) *best practices* sections for each characteristic geometry.

The perceived completeness scored lower than the other metrics. There were some suggestions to include features such as domes or living hinges in the first-year group. These features were included for the second year. This group had some manufacturing issues (due to the machines) and missed some details on potential issues and how to solve these. This was out of the current work scope but is included as potential further work complementary to other tools already available, such as Jennings (2021). The majority of participants agreed about the relevance of all the sections of the guide.

## 11.4. CONCLUSIONS & FUTURE WORK

The study described in this chapter has shown positive results in the efficacy of the proposed toolkit. The relatively inexperienced participants were capable of

understanding the guidance provided and applying this knowledge to improve their designs and develop successful prototypes.

The support in the concept stage, which was done by providing examples and methods to leverage the digital repositories and design principles, enabled the designers to increase the novelty of their designs. Various studies observed this previously (Blösch-Paidosh et al., 2019; Laverne et al., 2017; Perez, 2018). The digital repositories and the embodiment section of the toolkit enabled the participants to produce designs almost right the first time. Although the ideal values of the characteristic geometries were provided to the participants, the provision of benchmarking geometries in this section of the toolkit could enable the designers to understand the behaviour of their machine and produce a successful outcome.

This study was limited by the absence of an independent control group to observe the outcome without using the toolkit. A control group was not implemented to avoid hindering the participants' learning, as the study was developed as part of a master's subject. The trial of the toolkit with larger groups or with more diverse backgrounds could be a fruitful area for further work.

The toolkit received overall positive feedback and some suggestions for further development. Some of those suggestions have been already implemented in newer versions, while others could be addressed in further work.



# Chapter 12

## Discussion and Conclusions

### 12.1. INTRODUCTION

The final chapter of this thesis reflects upon the significance of this research and its potential impact on future design practice. The chapter also assesses the extent to which the aim and research objectives were addressed throughout the research. Finally, a comprehensive description of opportunities for future research is also provided.

This research has attempted to understand how novel users of extrusion-based desktop 3D printing can be supported to design components for this technology. In particular, it has investigated the elements to be considered and proposed a set of tools to support designers during the various stages of the design workflow. The research has not investigated how to optimise or calibrate the manufacturing parameters of the technology. Instead, it has studied the elements to be considered when designing, utilising the technology capabilities once the machine is calibrated.

In chapter 1, it was identified the need to develop a framework to help designers leverage extrusion-based desktop 3D printing capabilities and evaluate their suitability. The specification and design of a prototype design toolkit have provided an embodiment of this objective. However, this toolkit is by no means a fixed set of information as the technology, and the methods to leverage its capabilities, keep evolving at a fast pace. Instead, it provides

methods that could be customised and evolved, increasing its applicability even beyond desktop 3D printing.

## **12.2. ACHIEVEMENT OF RESEARCH OBJECTIVES**

Chapter 1 listed six objectives, based on the overall aim to DfAM support of novel users of extrusion-based desktop 3D printing technology, with or without a design engineering background. The extent to which these objectives have been addressed is now considered.

Research Objective 1 – *Understand the technology and social situation that define the ecosystem that frames this work.*

Chapter 2 looked at the history of 3D printing and the origin of desktop 3D printing. The seven categories of technologies and the design opportunities that these provide were also identified. Furthermore, the ecosystem that brought the rise in popularity of desktop 3D printing was evaluated, identifying the paradigm change in terms of user's profile.

Research Objective 2 – *Define the design and manufacturing criteria that need to be considered for this technology, and analyse the process elements and characteristics that define the outcome.*

Chapter 3 investigated the different system components and the physics involved in FFF systems. The characteristics of the typical design for manufacturing workflow with FFF was also identified. Finally, the process parameters and their implications were classified using the literature available. The literature review in chapter 4 also helped identify the main elements that designers need to consider when designing components to be produced with this technology.

Research Objective 3 – *Review the current tools and methods and define an approach suitable for the scope.*

Chapter 4 evaluated the approaches proposed in the literature, distinguishing the support provided in both the divergent and convergent phases of the design process. The benefits and limitations of the various

proposed tools were assessed. Chapter 10 proposes a methodology based on a set of tools in different formats, considering the literature approaches and the findings in previous chapters. The suitability of this methodology is evaluated with a positive outcome in chapter 11.

Research Objective 4 – *Identify the key common geometrical elements between components.*

Chapter 5 studied the approaches to understanding the geometrical behaviour of AM processes, identifying the provision of a set of Geometric Benchmark Test Artefacts (GBTAs) as the ideal method to support designers on this task. The most common design features were identified in a literature review, and the outcome of a set ofGBTAs for overhangs, bridges and angles was investigated. This study outcome served as the baseline for aGBTAs final set; these were proposed in chapters 5 and 10 as the tool to evaluate the geometrical behaviour.

Research Objective 5 – *Complement the information available in literature by addressing the research gaps in the main areas to produce functional components.*

The manufacturing of functional components requires matching a set of requirements with the component's physical or visual characteristics. Chapter 6 assesses the former by studying the literature and investigating the influence of three designer-led parameters in the mechanical behaviour.

Chapter 7 addresses both physical and visual characteristics by identifying the proposed methods in the literature for the components post-processing and developing various studies on this topic. Chapter 8 complements this knowledge by assessing the influence of the stepped surface and post-processing in components for aesthetic design evaluation.

Research Objective 6 – *Develop a set of design tools, adaptable to the variable performance of the wide range of machines, to leverage extrusion-based desktop 3D printing capabilities and evaluate their suitability.*

Building on the knowledge developed in previous chapters, chapter 10 proposes a new approach consisting of a set of tools in various formats. For the divergent phase, this research proposes a set of design innovation cards and methods to leverage the knowledge from these cards and the digital repositories.

A design guideline containing information from literature and the studies described in the previous chapters is proposed for the convergent phase. It provides general information about the best practices and characteristics for overarching design considerations and design features. However, it is complemented by a set of GBTA files and a worksheet to capture the specific behaviour in each design feature, allowing the user to customise the design guidance to his/her machine, material, and parameter set.

### **12.3. CONTRIBUTION TO KNOWLEDGE**

This thesis has made a number of original contributions to knowledge, as listed below:

1. This research investigated the impact of various infill patterns and density in the tensile and flexural behaviour of ABS FFF components. While the pattern seemed not to have a significant influence, various conclusions were extracted from the infill density change, including changes in fracture behaviour. The results of the tensile study were published and have already served as a source for other studies on the topic by multiple researchers (Fernandez-Vicente et al., 2016).
2. The adequate set of design features for geometrical assessment was investigated, and a set ofGBTAs suitable for material extrusion AM was proposed. These could be adopted in the next version of the ISO/ASTM 52902 standard. A study on the preliminary version of three of these features was published and cited several times by other studies (Fernandez-Vicente et al., 2015).

3. The influence of surface finish in the perception of 3D printed components for aesthetic design evaluation was investigated and published (Fernández-Vicente & Conejero, 2016). The findings highlight the need for post-processing to increase the suitability of desktop 3D printing as a method to create these components.
4. The various methods, including desktop 3D printing, to develop aesthetical models were classified and published. This publication also contained several methods for post-processing FFF components (Conejero et al., 2019).
5. The suitability of low-cost data acquisition, modelling software, desktop 3D printing and post-processing methods were investigated as potential tools for developing thumb orthoses. These were integrated into a novel design and manufactured workflow. This study was also published and cited by various studies (Fernandez-Vicente et al., 2017).
6. A novel framework to support designers in both divergent and convergent mindsets is proposed and evaluated. This framework builds upon proven methods such as the design heuristics (Blösch-Paidosh & Shea, 2019) and design guidelines with rules (Adam & Zimmer, 2014), but proposes novel characteristics:
  - a. Consideration of the potential non-professional background of the users.
  - b. Set of tools in various formats (Cards+CAD files+guideline+worksheet poster), instead of just a design guideline.
  - c. Integration of divergent and convergent design stages into a single framework.
  - d. Provides a methodology to leverage the vast amount of knowledge available in design repositories.
  - e. Allows customising the design rules to the user's material, machine, and parameters rather than providing average values, which keep continuously evolving thanks to the Open Source architecture of this technology and the wide range of systems.

## 12.4. LIMITATIONS OF THE RESEARCH

As with any research work, the research undertaken for this PhD has been limited in a number of ways, which should be acknowledged.

The most important limitation has been the fast development of this area in recent years. While some attention on FDM and design for AM was developed in the early 2000s, the desktop printers widespread availability from 2013, as described in chapter 2, accelerated the number of studies on these topics, as shown in Figure 12.1. Consequently, some of the studies literature review needed updating when finishing this dissertation. These were updated where possible, limited by the timeframe of this thesis.

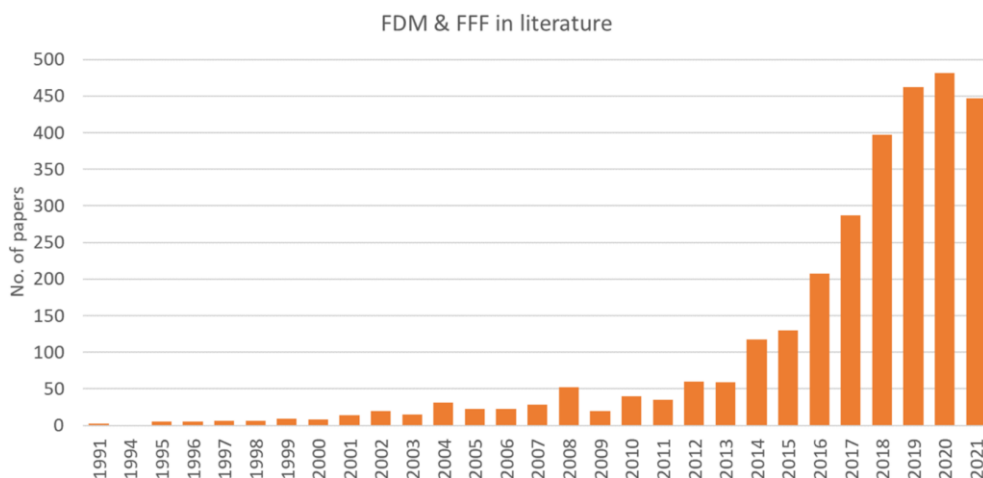


Figure 12.1. The number of papers by year with FDM & FFF in the title or abstract. Source: Scopus.

The increasing number of studies on the mechanical properties of FFF components and the wide range of materials and aspects to be covered limited the scope of the studies of mechanical assessment. These were areas with gaps in the knowledge when the studies were published, but the understanding of the topics has evolved since then.

Another limitation was the variety and quantity of participants evaluating the design toolkit. The author had the opportunity to test an early version of the toolkit with students with design and engineering backgrounds, but the final

version could not be tested with these or other types of participants. A larger number of professional and consumer designers may have led to further recommendations for improvement. Limitations on time precluded further research.

The wide range of materials and machine configurations limited some of the studies described in this thesis, such as in post-processing methods, applications or mechanical properties. It was decided to use one of the most widespread machines (Prusa i3), software and parameters (Slic3r) and materials (ABS). The results of these studies might differ if an alternative (or different) machine configuration is used. This limitation was considered when developing the design guideline to avoid restricting the user to this configuration.

## **12.5. FUTURE WORK**

Whilst this research has achieved the objectives listed at the beginning of this thesis, some recommendations could be implemented to develop the research on this topic further.

Chapter 6 presented the study of some mechanical properties for a specific configuration of machine, material and parameters. A linear correlation was identified between ABS's tensile strength and infill density. This approach could be developed in further work to help the designer make an educated guess of the mechanical behaviour of FFF components. This could be extended to other materials and parameters. Further research would therefore be required to integrate this knowledge in a methodology or tool that helps novel designers understand the behaviour of their components.

Concerning the development of the design toolkit, feedback from the preliminary version evaluation and reflection on the prototype have identified some areas that could be improved. Understanding the suitability of the newer multiformat version could be the focus of further research, identifying areas where this approach could be improved.

This thesis has argued that a design guideline with enhanced capabilities can be the best approach to support novel designers for this technology. Nonetheless, the study of the preferred methods and success with various methods of information (e.g., Youtube, users' knowledge sharing, forums, etc.) was not a focus of this research and therefore warrants further attention. Whilst this was not raised as an issue by any of the participants in the toolkit study, it is reasonable to question whether users might prefer other methods to obtain guidance.

Finally, this research has focused on supporting novel designers for desktop 3D printing technology. The methodology and tools developed could be applicable for other technologies, as professional engineers face similar challenges with industrial-grade AM processes. This could be an area for further investigation and development.



# Bibliography

- 3DDC. (n.d.). *Metal Plating Company* | 3DDC. Retrieved July 18, 2021, from <https://3ddc.eu/services-metal.html>
- 3D Hubs. (2016). *3D Printing Trends*. 3D Hubs. <https://www.3dhubs.com/trends>
- 3D Hubs. (2017). *3D Printing Trends. Q4 2017*. <https://f.3dhubs.com/tpeFNMnNBD83pKJYnSHpne.pdf>
- 3D Systems. (2016). *Sense 3D Scanner* | *Technical Specifications*. <http://www.3dsystems.com/shop/sense/techspecs>
- Abbott, A., Tandon, G., Bradford, R., Manufacturing, H. K.-..., & 2018, undefined. (2018). Process-structure-property effects on ABS bond strength in fused filament fabrication. *Additive Manufacturing*, 19, 29–38. <https://www.sciencedirect.com/science/article/pii/S2214860417300933>
- About Instructables*. (2011). <http://www.instructables.com/about/>
- ActivArmor. (2014). *ActivArmor* | *Watersafe, Breathable, Custom 3D Printed Splint*. <http://activarmor.com/>
- Adam, G. A. O., & Zimmer, D. (2014). Design for Additive Manufacturing—Element transitions and aggregated structures. *CIRP Journal of Manufacturing Science and Technology*, 7(1), 20–28. <https://doi.org//dx.doi.org/10.1016/j.cirpj.2013.10.001>
- Afrose, M. F., Masood, S. H., Iovenitti, P., Nikzad, M., & Sbarski, I. (2016). Effects of part build orientations on fatigue behaviour of FDM-processed PLA material. *Progress in Additive Manufacturing*, 1(1), 21–28. <https://doi.org/10.1007/s40964-015-0002-3>
- Agarwala, Jamalabad, Langrana, Safari, Whalen, & Danforth. (1996). Structural quality of parts processed by fused deposition. *Rapid Prototyping Journal*, 2(4), 4–19. <http://www.emeraldinsight.com/doi/abs/10.1108/13552549610732034>
- Ahlers, D., Wasserfall, F., Hendrich, N., Bungener, A. N., Butt, J.-T., & Zhang, J. (2021). Automated *In Situ* Placing of Metal Components Into 3-D Printed FFF Objects. *IEEE/ASME Transactions on Mechatronics*, 26(4), 1886–1894. <https://doi.org/10.1109/TMECH.2021.3078409>
- Ahn, D. K., Kwon, S. M., & Lee, S. H. (2008). Expression for surface roughness distribution of FDM processed parts. *ICSMA 2008 - International Conference on Smart Manufacturing Application*, 490–493. <https://doi.org/10.1109/ICSMA.2008.4505572>
- Ahn, Montero, Odell, Roundy, & Wright. (2002). Anisotropic material properties of fused deposition modeling ABS. *Rapid Prototyping Journal*, 8(4), 248–257. <https://doi.org/10.1108/13552540210441166>
- Akande, S. O., Dalgarno, K. W., & Munguia, J. (2015). Low-Cost QA Benchmark for Fused Filament Fabrication. *3D Printing and Additive Manufacturing*, 2(2), 78–84. <https://doi.org/10.1089/3dp.2015.0012>
- Akhouri, D., Banerjee, D., & Mishra, S. B. (2020). A review report on the plating process of fused deposition modelling (FDM) built parts. *Materials Today: Proceedings*, 26, 2140–2142. <https://doi.org/10.1016/J.MATPR.2020.02.461>

- Alafaghani, A., & Qattawi, A. (2018). Investigating the effect of fused deposition modeling processing parameters using Taguchi design of experiment method. *Journal of Manufacturing Processes*, 36, 164–174.  
<https://doi.org/10.1016/j.jmapro.2018.09.025>
- Altshuller, G., Shulyak, L., & Rodman, S. (1998). *40 Principles: TRIZ Keys to Technical Innovation (Triztools, V. 1)*. Technical Innovation Center, INC.; 1 edition.
- Anderson, C. (2010, January). In the next industrial revolution, atoms are the new bits. *Wired Magazine*.  
[https://www.wired.com/2010/01/ff\\_newrevolution/](https://www.wired.com/2010/01/ff_newrevolution/)
- Anderson, C. (2012). *Makers*. Crown Publishing Group.
- ANSI. (2018, June). *America Makes & ANSI Additive Manufacturing Standardization Collaborative – AMSC*. <https://www.ansi.org/standards-coordination/collaboratives-activities/additive-manufacturing-collaborative>
- Anthamatten, M., Letts, S. A., & Cook, R. C. (2004). Controlling Surface Roughness in Vapor-Deposited Poly(amic acid) Films by Solvent-Vapor Exposure. *Langmuir*, 20(15), 6288–6296.  
<https://doi.org/10.1021/LA0497797>
- Anthon, C. (1851). *A Classical Dictionary: Containing an Account of the Principal Proper Names Mentioned in Ancient Authors, and Intended to Elucidate All the Important Points Connected with the Geography, History, Biography, Mythology, and Fine Arts of the Greeks and Roman*. Harper.
- Arenas, J. M., Alía, C., Blaya, F., & Sanz, A. (2012). Multi-criteria selection of structural adhesives to bond ABS parts obtained by rapid prototyping. *International Journal of Adhesion and Adhesives*, 33, 67–74.  
<https://doi.org/10.1016/j.ijadhadh.2011.11.005>
- Ariadi, Y. (2016). *Facilitating consumer involvement in design for additive manufacturing/3D printing products* [Loughborough University].  
<https://dspace.lboro.ac.uk/2134/21763>
- Armillotta, A. (2006). Assessment of surface quality on textured FDM prototypes. *Rapid Prototyping Journal*, 12(1), 35–41.  
<https://doi.org/10.1108/13552540610637255>
- Armillotta, A., Cavallaro, M., & Minnella, S. (2013). A tool for computer-aided orientation selection in additive manufacturing processes. *High Value Manufacturing: Advanced Research in Virtual and Rapid Prototyping: Proceedings of the 6th International Conference on Advanced Research in Virtual and Rapid Prototyping*, 469–475.  
<https://doi.org/10.1201/b15961-86>
- Arun, K., Aravindh, K., Raja, K., Jeeva, P. A., & Karthikeyan, S. (2018). Metallization of PLA plastics prepared by FDM-RP process and evaluation of corrosion and hardness characteristics. *Materials Today: Proceedings*, 5(5), 13107–13110.  
<https://doi.org/10.1016/J.MATPR.2018.02.299>
- Asadollahi-Yazdi, E., Gardan, J., & Lafon, P. (2016). Integrated Design in Additive Manufacturing Based on Design for Manufacturing. *World Academy of Science, Engineering and Technology, International Journal of Mechanical, Aerospace, Industrial, Mechatronic and Manufacturing Engineering*, 10(6), 1044–1051.
- Atzeni, E., Iuliano, L., Minetola, P., & Salmi, A. (2010). Redesign and cost estimation of rapid manufactured plastic parts. *Rapid Prototyping Journal*, 16(5), 308–317.  
<https://doi.org/10.1108/13552541011065704>
- Azo materials. (2018, May 30). *Understanding Drawn Fibers*. AZO Materials.  
<https://www.azom.com/article.aspx?ArticleID=16014>
- Baese, C. (1904). *Photographic process for the reproduction of plastic objects*. (Patent No. US774549 A).  
<http://www.google.com/patents/US774549>
- Baich, L., & Manogharan, G. (2015). Study of infill print parameters on mechanical strength and production cost-time of 3d printed abs parts. *International Solid Freeform Fabrication Symposium*, 209–2018.
- Baichtal, J. (2008, November). *Thingiverse.com Launches A Library of Printable Objects*. Wired.Com.  
<https://www.wired.com/2008/11/thingiversecom/>
- Bakar, N. S. A., Alkahari, M. R., & Boejang, H. (2010). Analysis on fused deposition modelling performance. *Journal of Zhejiang University-SCIENCE A 2010 11:12*, 11(12), 972–977.  
<https://doi.org/10.1631/JZUS.A1001365>

- Bak, D. (2003). Rapid prototyping or rapid production? 3D printing processes move industry towards the latter. *Assembly Automation*, 23(4), 340–345. <https://doi.org/10.1108/01445150310501190>
- Barron, O. A., Glickel, S. Z., & Eaton, R. G. (2000). Basal joint arthritis of the thumb. *Journal of the American Academy of Orthopaedic Surgeons*, 8(5), 314–323.
- Bastian, A. (2013). *3D Print Finishing Technique for Improved Surface Quality*. Instructables. <http://www.instructables.com/id/3D-Print-Finishing-Technique-for-Improved-Surface-/>
- Bäumer, D., Bischofberger, W. R., Lichter, H., & Züllighoven, H. (1996). User interface prototyping—concepts, tools, and experience. *Proceedings of the 18th International Conference on Software Engineering*, 532–541.
- Baumers, M., Tuck, C., & Hague, R. (2015). Selective heat sintering versus laser sintering: comparison of deposition rate, process energy consumption and cost performance. *Proceedings of the Solid Freeform Fabrication Symposium*, 109–121.
- BCN3D. (2020). *IDEX Technology: Doubling Productivity While Halving Costs*. <https://3d.bcn3d.com/lp-bcn3d-signature-idex-technology>
- Becker, R., Grzesiak, A., & Henning, A. (2005). Rethink assembly design. *Assembly Automation*, 25(4), 262–266. <https://doi.org/10.1108/01445150510626370>
- Bell, C. (n.d.). *3D printing with Delta printers*.
- Bellehumeur, C., Li, L., Sun, Q., & Gu, P. (2004). Modeling of Bond Formation Between Polymer Filaments in the Fused Deposition Modeling Process. *Journal of Manufacturing Processes*, 6(2), 170–178. [https://doi.org/10.1016/S1526-6125\(04\)70071-7](https://doi.org/10.1016/S1526-6125(04)70071-7)
- Bellini, A. (2002). *Fused deposition of ceramics: a comprehensive experimental, analytical and computational study of material behavior, fabrication process and equipment*.
- Bellini, A., & Güçeri, S. (2003). Mechanical characterization of parts fabricated using fused deposition modeling. *Rapid Prototyping Journal*, 9(4), 252–264. <https://doi.org/10.1108/13552540310489631>
- Bellini, A., Güçeri, S., & Bertoldi, M. (2004). Liquefier Dynamics in Fused Deposition. *Journal of Manufacturing Science and Engineering*, 126(2), 237. <https://doi.org/10.1115/1.1688377>
- Bendsoe, M. P., & Sigmund, O. (2013). *Topology optimization: theory, methods, and applications*. Springer Science & Business Media.
- Bernier, S. N., Luyt, B., & Reinhard, T. (2015). *Design for 3D Printing: Scanning, Creating, Editing, Remixing, and Making in Three Dimensions*. Maker Media, Inc.
- Bhavsar, P., Sharma, B., Moscoso-Kingsley, W., & Madhavan, V. (2020). Detecting first layer bond quality during FDM 3D printing using a discrete wavelet energy approach. *Procedia Manufacturing*, 48, 718–724. <https://doi.org/10.1016/j.promfg.2020.05.104>
- Bhudolia, S. K., Gohel, G., Leong, K. F., & Islam, A. (2020). Advances in Ultrasonic Welding of Thermoplastic Composites: A Review. *Materials*, 13(6), 1284. <https://doi.org/10.3390/ma13061284>
- bin Maidin, S. (2011). *Development of a design feature database to support design for additive manufacturing (DfAM)*. <https://dSPACE.lboro.ac.uk/2134/9111>
- BJB Enterprises. (n.d.). *TC-1614 A/B Epoxy penetrating sealing and coating resin system*. Retrieved July 29, 2021, from <https://bjbenterprises.com/index.php/epoxy/3d-printed-part-sealer/tc-1614-a-b-582/>
- Blanther, J. E. (1892). *Manufacture of contour relief-maps* (Patent No. US473901 A). Google Patents. <http://www.google.com/patents/US473901>
- Blösch-Paidosh, A., Ahmed-Kristensen, S., & Shea, K. (2019). Evaluating the Potential of Design for Additive Manufacturing Heuristic Cards to Stimulate Novel Product Redesigns. *Volume 2A: 45th Design Automation Conference, 2A-2019*. <https://doi.org/10.1115/DETC2019-97865>
- Blösch-Paidosh, A., & Shea, K. (2019). Design Heuristics for Additive Manufacturing Validated Through a User Study1. *Journal of Mechanical Design*, 141(4). <https://doi.org/10.1115/1.4041051>
- Blösch-Paidosh, A., & Shea, K. (2017). Design Heuristics for Additive Manufacturing - Research Collection. In A. Maier, S. Škec, H. Kim, M. Kokkolaras, J. Oehmen, G. Fadel, F. Salustri, &

- M. van der Loos (Eds.), *Proceedings of the 21st International Conference on Engineering Design: Design for X, Design to X* (pp. 91–100). The Design Society. <https://www.research-collection.ethz.ch/handle/20.500.11850/182763>
- Booth, J. W., Alperovich, J., Chawla, P., Ma, J., Reid, T. N., & Ramani, K. (2017). The Design for Additive Manufacturing Worksheet. *Journal of Mechanical Design*, 139(10). <https://doi.org/10.1115/1.4037251>
- Boothroyd, G., Dewhurst, P., & Knight, W. (1998). *Product design for manufacture and assembly*, 1994. Marcel Dekker, New York.
- Boschetto, A., & Bottini, L. (2015). Surface improvement of fused deposition modeling parts by barrel finishing. *Rapid Prototyping Journal*, 21(6), 686–696. <https://doi.org/10.1108/RPJ-10-2013-0105>
- Boschetto, A., Bottini, L., & Veniali, F. (2016a). Integration of FDM surface quality modeling with process design. *Additive Manufacturing*, 12, 334–344. <https://doi.org/10.1016/j.addma.2016.05.008>
- Boschetto, A., Bottini, L., & Veniali, F. (2016b). Finishing of Fused Deposition Modeling parts by CNC machining. *Robotics and Computer-Integrated Manufacturing*, 41, 92–101. <https://doi.org/10.1016/j.rcim.2016.03.004>
- Boschetto, Giordano, & Veniali. (2013). 3D roughness profile model in fused deposition modelling. *Rapid Prototyping Journal*, 19(4), 240–252. <https://doi.org/10.1108/13552541311323254>
- Bosqué, C. (2015). What are you printing? Ambivalent emancipation by 3D printing. *Rapid Prototyping Journal*, 21(5), 572–581. <https://doi.org/10.1108/RPJ-09-2014-0128>
- Bottini, L., & Boschetto, A. (2019). Interference fit of material extrusion parts. *Additive Manufacturing*, 25, 335–346. <https://doi.org/10.1016/j.addma.2018.11.025>
- Bottini, L., Boschetto, A., & Veniali, F. (2014). Estimation of Material Removal by Profilometer Measurements in Mass Finishing. *Key Engineering Materials*, 611–612, 615–622. <https://doi.org/10.4028/WWW.SCIENTIFIC.NET/KEM.611-612.615>
- Bourell, D. L., Beaman, J. J., Leu, M. C., & Rosen, D. W. (2009). A brief history of additive manufacturing and the 2009 roadmap for additive manufacturing: looking back and looking ahead. *US – TURKEY Workshop On Rapid Technologies*, 24–25.
- Bourell, D. L., Leu, M. C., & Rosen, D. W. (2009). Roadmap for additive manufacturing: identifying the future of freeform processing. In *The University of Texas at Austin, Austin, TX*.
- Boyard, N., Rivette, M., Christmann, O., & Richir, S. (2013). A design methodology for parts using Additive Manufacturing. In *High Value Manufacturing: Advanced Research in Virtual and Rapid Prototyping* (pp. 399–404). CRC Press. <https://doi.org/10.1201/b15961-74>
- Brubaker, C. D., Newcome, K. N., Jennings, G. K., & Adams, D. E. (2019). 3D-Printed alternating current electroluminescent devices. *Journal of Materials Chemistry C*, 7(19), 5573–5578. <https://doi.org/10.1039/C9TC00619B>
- Bürenhaus, F., Moritzer, E., & Hirsch, A. (2019). Adhesive bonding of FDM-manufactured parts made of ULTEM 9085 considering surface treatment, surface structure, and joint design. *Welding in the World*, 63(6), 1819–1832. <https://doi.org/10.1007/s40194-019-00810-4>
- Burton, M. J. (2005). Design for rapid manufacture: developing an appropriate knowledge transfer tool for industrial designers. In *Design for rapid manufacture: developing an appropriate knowledge transfer tool for industrial designers*. Loughborough University.
- Byun, H. S., & Lee, K. H. (2006). Determination of optimal build direction in rapid prototyping with variable slicing. *The International Journal of Advanced Manufacturing Technology*, 28(3–4), 307–313. <https://doi.org/10.1007/s00170-004-2355-5>
- Camburn, B. A., Auernhammer, J. M., Sng, K. H. E., Mignone, P. J., Arlitt, R. M., Perez, K. B., Huang, Z., Basnet, S., Blessing, L. T., & Wood, K. L. (2017). Design Innovation: A Study of Integrated Practice. *Volume 7: 29th International Conference on Design Theory and Methodology*, 7. <https://doi.org/10.1115/DETC2017-68382>
- Campbell, I., Bourell, D., & Gibson, I. (2012). Additive manufacturing: rapid prototyping comes of age. *Rapid Prototyping Journal*, 18(4),

- 255–258.  
<https://doi.org/10.1108/13552541211231563>
- Campbell, I., Diegel, O., Kowen, J., & Wohlers, T. (2018). *Wohlers report 2018: 3D printing and additive manufacturing state of the industry: annual worldwide progress report*.
- Campbell, R. I., Martorelli, M., & Lee, H. S. (2002). Surface roughness visualisation for rapid prototyping models. *Computer-Aided Design*, 34(10), 717–725.  
[https://doi.org/10.1016/S0010-4485\(01\)00201-9](https://doi.org/10.1016/S0010-4485(01)00201-9)
- Canessa, E., Fonda, C., & Zennaro, M. (2013). *Low-cost 3D Printing for Science, Education and Sustainable Development* (Vol. 1). ICTP—The Abdus Salam International Centre for Theoretical Physics.
- Carmichael, J. (2013, August). *We'd happily break our wrist for this 3-d printed splint*. Popular Science.  
<http://www.popsci.com/technology/article/2013-08/intricate-3-d-printed-exoskeleton-splints>
- Castro-Casado, D. (2021). Chemical treatments to enhance surface quality of FFF manufactured parts: a systematic review. *Progress in Additive Manufacturing 2021 6:2*, 6(2), 307–319.  
<https://doi.org/10.1007/S40964-020-00163-1>
- Cavalcanti, D. K. K., Banea, M. D., & Queiroz, H. F. M. (2019). Mechanical Characterization of Bonded Joints Made of Additive Manufactured Adherends. *Annals of "Dunarea de Jos" University of Galati. Fascicle XII, Welding Equipment and Technology*, 30, 27–33.  
<https://doi.org/10.35219/AWET.2019.04>
- Cavalcanti, G. (2013, May 22). *Is it a Hackerspace, Makerspace, TechShop, or FabLab?* Makezine.Com.  
<http://makezine.com/2013/05/22/the-difference-between-hackerspaces-makerspaces-techshops-and-fablabs/>
- Cavallini, B., Ciurana, J., Reguant, C., & Delgado, J. (2009). Studying the repeatability in DMLS technology using a complete geometry test part. *International Conference on Advanced Research in Virtual and Rapid Prototyping*, 349–354.  
<https://doi.org/10.1201/9780203859476.ch54>
- Cazon, A., Aizpurua, J., Paterson, A., Bibb, R., & Campbell, R. I. (2014). Customised design and manufacture of protective face masks combining a practitioner-friendly modelling approach and low-cost devices for digitising and additive manufacturing. *Virtual and Physical Prototyping*, 9(4), 251–261.  
<https://doi.org/10.1080/17452759.2014.958648>
- Chaisson, C. E., Zhang, Y., McAlindon, T. E., Hannan, M. T., Aliabadi, P., Naimark, A., Levy, D., & Felson, D. T. (1997). Radiographic hand osteoarthritis: Incidence, patterns, and influence of pre-existing disease in a population based sample. *Journal of Rheumatology*, 24(7), 1337–1343.
- Chalasan, K., Jones, L., & Roscoe, L. (1995). Support Generation for Fused Deposition Modeling. *Solid Freeform Fabrication Symposium*.
- Chandra, A., Watson, J., Rowson, J. E., Holland, J., Harris, R. A., & Williams, D. J. (2005). Application of rapid manufacturing techniques in support of maxillofacial treatment: evidence of the requirements of clinical applications. *Proceedings of the Institution of Mechanical Engineers, Part B: Journal of Engineering Manufacture*, 219(6), 469–475.  
<https://doi.org/10.1243/095440505X32300>
- Chang, R. Y., & Tsaur, B. D. (1995). Experimental and theoretical studies of shrinkage, warpage, and sink marks of crystalline polymer injection molded parts. *Polymer Engineering & Science*, 35(15), 1222–1230.  
<https://doi.org/10.1002/pen.760351505>
- Chen, C., Lu, T. J., & Fleck, N. A. (1999). Effect of imperfections on the yielding of two-dimensional foams. *Journal of the Mechanics and Physics of Solids*, 47(11), 2235–2272.  
[https://doi.org/http://dx.doi.org/10.1016/S0022-5096\(99\)00030-7](https://doi.org/http://dx.doi.org/10.1016/S0022-5096(99)00030-7)
- Chen, X., Shao, F., Barnes, C., Childs, T., & Henson, B. (2009). Exploring relationships between touch perception and surface physical properties. *International Journal of Design*, 3(2), 67–77.  
<http://www.ijdesign.org/index.php/IJDesign/article/view/596/261>
- Chiu, Y. Y., & Liao, Y. S. (2003). Laser path planning of burn-out rule for LOM process. *Rapid Prototyping Journal*, 9(4), 201–211.  
<https://doi.org/10.1108/13552540310489587>
- Chohan, J. S., & Singh, R. (2017). Pre and post processing techniques to improve surface characteristics of FDM parts: a state of art review and future applications. *Rapid*

- Prototyping Journal*, 23(3), 495–513.  
<https://doi.org/10.1108/RPJ-05-2015-0059>
- Chua, C. K., & Leong, K. F. (2003). *Rapid prototyping: principles and applications* (Vol. 1). World Scientific.
- Chueca de Bruijn, A., Gómez-Gras, G., & Pérez, M. A. (2020). Mechanical study on the impact of an effective solvent support-removal methodology for FDM Ultem 9085 parts. *Polymer Testing*, 85, 106433.  
<https://doi.org/10.1016/j.polymertesting.2020.106433>
- Chulilla-Cano, J. L. (2011). The Cambrian Explosion of Popular 3D Printing. *International Journal of Interactive Multimedia and Artificial Intelligence*, 1(4), 30–32.  
<https://doi.org/10.9781/ijimai.2011.145>
- Ciraud, P. A. (1973). *Verfahren und vorrichtung zur herstellung beliebiger gegenstaende aus beliebigem schmelzbarem material* (Patent No. DE 2263777). German Patent and Trademark Office.  
<https://depatisnet.dpma.de/DepatisNet/depatisnet?action=bibdat&docid=DE000002263777A>
- Clark, E. C. (2019). *Using additive manufacturing techniques to increase the bearing strength of carbon fiber reinforced thermoplastics*.  
<http://dspace.calstate.edu/handle/10211.3/215086>
- Clifford, D. (2011). Project Nervi: Aesthetics and Technology. In P. Plowright & B. Gamper (Eds.), *ARCC 2011 | Considering Research: Reflecting upon current themes in Architecture Research* (pp. 73–83).
- Clockspring3D. (2020a). *Dice Dozer! | Clockspring 3D on Patreon*. Patreon.Com.  
<https://www.patreon.com/posts/dice-dozer-43317661>
- Clockspring3D. (2020b). *Square Flasks! | Clockspring 3D on Patreon*. Patreon.Com.  
<https://www.patreon.com/posts/square-flasks-36385478>
- Coldham, F. (2006). The Use of Splinting in the Non-Surgical Treatment of De Quervain's Disease: A Review of the Literature. *The British Journal of Hand Therapy*, 11(2), 48–55.  
<https://doi.org/10.1177/175899830601100203>
- Colpani, A., Fiorentino, A., & Ceretti, E. (2019). Characterization of chemical surface finishing with cold acetone vapours on ABS parts fabricated by FDM. *Production Engineering 2019* 13:3, 13(3), 437–447.  
<https://doi.org/10.1007/S11740-019-00894-3>
- Comb, J. W., Crump, S. S., Priedeman Jr, W. R., & Zinniel, R. L. (1996). Process of support removal for fused deposition modeling. In *U.S. Patent No. 5,503,785*. U.S. Patent and Trademark Office. Google Patents
- Conejero, A., Ayala López, P., Martínez, M., & Fernández Vicente, M. (2019). *PROTOTIPADO INDUSTRIAL. Guía para diseñadores* (1st ed.). Parramón.  
<https://parramon.com/collections/disenoproducto/products/prototipado-industrial-guia-para-disenadores>
- Conejero Rodilla, A. (2009). *Estudio de la utilización de modelos y prototipos en el diseño y desarrollo de producto. Casos de proyectos en pymes de la comunidad valenciana* [Universitat Politècnica de València].  
<https://dialnet.unirioja.es/servlet/tesis?codigo=250958&info=resumen&idioma=SPA>
- Conejero Rodilla, A. (2018). *3D Printed Speaker Design* (1st ed.).  
[https://issuu.com/etsid/docs/3d\\_printed\\_speaker\\_design](https://issuu.com/etsid/docs/3d_printed_speaker_design)
- Conner, B. P., Manogharan, G. P., Martof, A. N., Rodomsky, L. M., Rodomsky, C. M., Jordan, D. C., & Limperos, J. W. (2014). Making sense of 3-D printing: Creating a map of additive manufacturing products and services. *Additive Manufacturing*, 1, 64–76.  
<https://doi.org/10.1016/j.addma.2014.08.005>
- contributors, R. (2014). *J Head Nozzle - RepRapWiki*.  
[http://reprap.org/wiki/J\\_Head\\_Nozzle](http://reprap.org/wiki/J_Head_Nozzle)
- Coppard, B. M., & Lohman, H. (2008). *Introduction to splinting* (Third). Mosby. Elsevier Health Sciences.
- Costa, S. F., Duarte, F. M., & Covas, J. A. (2015). Thermal conditions affecting heat transfer in FDM/FFE: a contribution towards the numerical modelling of the process. *Virtual and Physical Prototyping*, 10(1), 35–46.  
<https://doi.org/10.1080/17452759.2014.984042>
- Costa, S. F., Duarte, F. M., & Covas, J. A. (2017). Estimation of filament temperature and

- adhesion development in fused deposition techniques. *Journal of Materials Processing Tech.*, 245, 167–179.  
<https://doi.org/10.1016/j.jmatprotec.2017.02.026>
- Cottalorda, J., Kohler, R., Garin, C., Genevois, P., Lecante, C., & Berge, B. (2005). Orthoses for Mild Scoliosis: A Prospective Study Comparing Traditional Plaster Mold Manufacturing With Fast, Noncontact, 3-Dimensional Acquisition. *Spine*, 30(4), 399–405.  
<https://doi.org/10.1097/01.brs.0000153346.40391.3b>
- Courtland, R. (2013). *Bre Pettis*. IEEE Spectrum.  
<http://spectrum.ieee.org/geek-life/profiles/bre-pettis>
- Cozmei, C., & Caloian, F. (2012). Additive Manufacturing Flickering at the Beginning of Existence. *Procedia Economics and Finance*, 3, 457–462. [https://doi.org/10.1016/S2212-5671\(12\)00180-3](https://doi.org/10.1016/S2212-5671(12)00180-3)
- Crocco, D., de Agostinis, M., & Olmi, G. (2013). Experimental characterization and analytical modelling of the mechanical behaviour of fused deposition processed parts made of ABS-M30. *Computational Materials Science*, 79, 506–518.  
<https://doi.org/10.1016/j.commatsci.2013.06.041>
- Crump, S. S. (1989). Apparatus and method for creating three-dimensional objects (Patent No. US5121329). In *June 9, 1992: Vol. US 07/429*, (No. US5121329). US Patent Office.
- Cruz Sanchez, F. A., Boudaoud, H., Muller, L., & Camargo, M. (2014). Towards a standard experimental protocol for open source additive manufacturing. *Virtual and Physical Prototyping*, 9(3), 151–167.  
<https://doi.org/10.1080/17452759.2014.919553>
- Cuan-Urquizo, E., Yang, S., & Bhaskar, A. (2015). Mechanical characterisation of additively manufactured material having lattice microstructure. *IOP Conference Series: Materials Science and Engineering*, 74(1), 012004.  
<https://doi.org/10.1088/1757-899X/74/1/012004>
- Cuellar, J. S., Smit, G., Plettenburg, D., & Zadpoor, A. (2018). Additive manufacturing of non-assembly mechanisms. In *Additive Manufacturing* (Vol. 21, pp. 150–158). Elsevier B.V.  
<https://doi.org/10.1016/j.addma.2018.02.004>
- Cumbicus, W. E., Estrems, M., Arizmendi, M., & Jiménez, A. (2021). Joining polymer parts with self-tapping screws: an improvement of the screw thread geometry. *International Journal of Material Forming*, 14(4), 777–798.  
<https://doi.org/10.1007/s12289-020-01593-6>
- Ćwikła, G., Grabowik, C., Kalinowski, K., Paprocka, I., & Ociepa, P. (2017). The influence of printing parameters on selected mechanical properties of FDM/FFF 3D-printed parts. *IOP Conference Series: Materials Science and Engineering*, 227(1), 012033. <https://doi.org/10.1088/1757-899X/227/1/012033>
- Dawoud, M., Taha, I., & Ebeid, S. J. (2016). Mechanical behaviour of ABS: An experimental study using FDM and injection moulding techniques. *Journal of Manufacturing Processes*, 21, 39–45.  
<https://doi.org/10.1016/j.jmappro.2015.11.002>
- de Bruijn, E. (2010). *On the viability of the open source development model for the design of physical objects. Lessons learned from the RepRap project*. University of Tilburg, The Netherlands.
- Deckard, C. R. (1986). *Method and apparatus for producing parts by selective sintering* (Patent No. US4863538). US Patent Office.
- Demir, İ., Aliaga, D. G., & Benes, B. (2018). Near-convex decomposition and layering for efficient 3D printing. *Additive Manufacturing*, 21, 383–394.  
<https://doi.org/10.1016/j.addma.2018.03.008>
- Design Council. (2005). *The 'double diamond' design process model*. Design Council.  
<https://www.designcouncil.org.uk/news-opinion/design-process-what-double-diamond>
- Dey, A., & Yodo, N. (2019). A Systematic Survey of FDM Process Parameter Optimization and Their Influence on Part Characteristics. *Journal of Manufacturing and Materials Processing*, 3(3), 64. <https://doi.org/10.3390/jmmp3030064>
- Lalegani Dezaki, M., Mohd Ariffin, M. K. A., & Baharuddin, B. T. H. T. (2021). Experimental Study of Drilling 3D Printed Polylactic Acid (PLA) in FDM Process. In H. K. Dave & J. P. Davim (Eds.), *Fused Deposition Modeling Based 3D Printing* (pp. 85–106). Springer Nature.  
[https://doi.org/10.1007/978-3-030-68024-4\\_5](https://doi.org/10.1007/978-3-030-68024-4_5)

- Diegel, O., Nordin, A., & Motte, D. (2019). Teaching Design for Additive Manufacturing Through Problem-Based Learning. In *Additive Manufacturing – Developments in Training and Education* (pp. 139–149). Springer International Publishing. [https://doi.org/10.1007/978-3-319-76084-1\\_10](https://doi.org/10.1007/978-3-319-76084-1_10)
- Dietz, A. (2019, March 5). Additive Fertigung mit Kunststoffen. *WOMag*. [https://www.wotech-technical-media.de/womag/ausgabe/2019/03/19\\_dietz\\_am\\_03j2019/19\\_dietz\\_am\\_03j2019.php](https://www.wotech-technical-media.de/womag/ausgabe/2019/03/19_dietz_am_03j2019/19_dietz_am_03j2019.php)
- Dirksen, F., & Lammering, R. (2011). On mechanical properties of planar flexure hinges of compliant mechanisms. *Mechanical Sciences*, 2(1), 109–117. <https://doi.org/10.5194/ms-2-109-2011>
- Dixit, N. K., Srivastava, R., & Narain, R. (2017). Improving surface roughness of the 3D printed part using electroless plating: *Proceedings of the Institution of Mechanical Engineers, Part L: Journal of Materials: Design and Applications*, 233(5), 942–954. <https://doi.org/10.1177/1464420717719920>
- Dobrovski, E. L., Verlinden, J. C., & Horvath, I. (2012). First steps towards collaboratively edited design for additive manufacturing knowledge. *Solid Freeform Fabrication Symposium*, 891–901.
- Drescher, P., Spath, S., & Seitz, H. (2014). Fabrication of biodegradable, porous scaffolds using a low-cost 3D printer. *International Journal of Rapid Manufacturing*, 4(2–4), 140–147.
- Dumas, J., Hergel, J., & Lefebvre, S. (2014). Bridging the gap. *ACM Transactions on Graphics*, 33(4), 1–10. <https://doi.org/10.1145/2601097.2601153>
- Duran, C., Subbian, V., Giovanetti, M. T., Simkins, J. R., & Beyette, F. R. (2015). Experimental desktop 3D printing using dual extrusion and water-soluble polyvinyl alcohol. *Rapid Prototyping Journal*, 21(5), 528–534. <https://doi.org/10.1108/RPJ-09-2014-0117>
- Edwards, K. L. (2003). Design for manufacturing: a structured approach. *Materials & Design*, 24(2), 157–158. [https://doi.org/10.1016/S0261-3069\(02\)00108-5](https://doi.org/10.1016/S0261-3069(02)00108-5)
- Effa, D., Nespoli, O., & Lambert, S. (2015). Using the case method to facilitate learning of design for manufacturing and cost. *Proceedings of the Canadian Engineering Education Association*, 0(0).
- Eggbeer, D., Bibb, R., Evans, P., & Ji, L. (2012). Evaluation of direct and indirect additive manufacture of maxillofacial prostheses. *Proceedings of the Institution of Mechanical Engineers. Part H, Journal of Engineering in Medicine*, 226(9), 718–728.
- Emmelmann, C., Herzog, D., & Kranz, J. (2017). Design for laser additive manufacturing. In *Laser Additive Manufacturing: Materials, Design, Technologies, and Applications* (pp. 259–279). Elsevier Inc. <https://doi.org/10.1016/B978-0-08-100433-3.00010-5>
- Emmelmann, C., Sander, P., Kranz, J., & Wycisk, E. (2011). Laser Additive Manufacturing and Bionics: Redefining Lightweight Design. *Physica Procedia*, 12(PART 1), 364–368. <https://doi.org/10.1016/j.phpro.2011.03.046>
- Equbal, A., & Sood, A. (2014). Metallization on FDM Parts Using the Chemical Deposition Technique. *Coatings*, 4(3), 574–586. <https://doi.org/10.3390/coatings4030574>
- Espalin, D., Medina, F., Arcaute, K., Zinniel, B., Hoppe, T., & Wicker, R. (2009). Effects of vapor smoothing on ABS part dimensions. *Proceedings from Rapid 2009 Conference & Exposition, TP09PUB14*, 1–17.
- Espert, A., Vilaplana, F., & Karlsson, S. (2004). Comparison of water absorption in natural cellulosic fibres from wood and one-year crops in polypropylene composites and its influence on their mechanical properties. *Composites Part A: Applied Science and Manufacturing*, 35(11), 1267–1276. <https://doi.org/10.1016/J.COMPOSITESA.2004.04.004>
- Es-Said, O., Foyos, J., Noorani, R., Mendelson, M., Marloth, R., & Pregar, B. A. (2000). Effect of Layer Orientation on Mechanical Properties of Rapid Prototyped Samples. *Materials and Manufacturing Processes*, 15(1), 107–122. <https://doi.org/10.1080/10426910008912976>
- Evans, M. A. (2002). *The integration of rapid prototyping within industrial design practice* [Loughborough University]. <https://hdl.handle.net/2134/5155>
- Evans, M. A., & Ian Campbell, R. (2003). A comparative evaluation of industrial design models produced using rapid prototyping and



- workshop-based fabrication techniques. *Rapid Prototyping Journal*, 9(5), 344–351.  
<https://doi.org/10.1108/13552540310502248>
- Evill, J. (2013). Cortex 3D-printed cast for fractured bones. *Dezeen Magazine*.
- e-Xstream engineering. (n.d.). *Digmat-AM*. e-Xstream engineering. Retrieved August 28, 2021, from <https://www.e-xstream.com/product/digmat-am>
- Fahad, M., & Hopkinson, N. (2012). A new benchmarking part for evaluating the accuracy and repeatability of Additive Manufacturing (AM) processes. *2nd International Conference on Mechanical, Production and Automobile Engineering (ICMPAE 2012)*, 234–238.
- Fernandez-Vicente, M. (2012). *Estudio e Integración de Sistemas de Bajo Coste para el Diseño Digital y el Prototipado Rápido*.  
<http://hdl.handle.net/10251/60485>
- Fernandez-Vicente, M., Armesto, L., & Conejero, A. (2014). Beneficios de la Integración de los Laboratorios de Fabricación Digital (FabLab) en la Educación Superior. In *Innovación educativa en las enseñanzas técnicas: Vol. II* (Vol. 144, pp. 1545–1554). Ediciones de la Universidad de Castilla La Mancha.
- Fernandez-Vicente, M., Calle, W., Ferrandiz, S., & Conejero, A. (2016). Effect of Infill Parameters on Tensile Mechanical Behavior in Desktop 3D Printing. *3D Printing and Additive Manufacturing*, 3(3), 183–192.  
<https://doi.org/10.1089/3dp.2015.0036>
- Fernandez-Vicente, M., Canyada, M., & Conejero, A. (2015). Identifying limitations for design for manufacturing with desktop FFF 3D printers. *International Journal of Rapid Manufacturing*, 5(1), 116–128.  
<https://doi.org/10.1504/IJRAPIDM.2015.073551>
- Fernandez-Vicente, M., Escario Chust, A., & Conejero, A. (2017). Low cost digital fabrication approach for thumb orthoses. *Rapid Prototyping Journal*, 23(6), 1020–1031.  
<https://doi.org/10.1108/RPJ-12-2015-0187>
- Fernández-Vicente, M., & Conejero, A. (2016). Suitability study of desktop 3d printing for concept design projects in engineering education. *10th International Technology, Education and Development Conference (INTED2016 Proceedings)*, 4485–4491.  
<https://doi.org/10.21125/inted.2016.2117>
- Fischer, M., & Schöppner, V. (2013). Some Investigations Regarding the Surface Treatment of Ultem\*9085 Parts Manufactured with Fused Deposition Modeling. *24th Annual International Solid Freeform Fabrication Symposium*, 805–8015.
- Fodran, E., Koch, M., & Menon, U. (1996). Mechanical and dimensional characteristics of fused deposition modeling build styles. *Solid Freeform Fabrication Proceedings*, 419–442.
- Frank, M., Joshi, S. B., & Wysk, R. A. (2003). Rapid Prototyping As An Integrated Product/Process Development Tool An Overview Of Issues And Economics. *Journal of the Chinese Institute of Industrial Engineers*, 20(3), 240–246.  
<https://doi.org/10.1080/10170660309509232>
- Fu, K. K., Yang, M. C., & Wood, K. L. (2015, August 2). Design Principles: The Foundation of Design. *Volume 7: 27th International Conference on Design Theory and Methodology*.  
<https://doi.org/10.1115/DETC2015-46157>
- Gajdoš, I., Spišák, E., Kaščák, L., & Krasinskyi, V. (2015). Surface Finish Techniques for FDM Parts. *Materials Science Forum*, 818, 45–48.  
<https://doi.org/10.4028/WWW.SCIENTIFIC.NET/MSF.818.45>
- Galantucci, L. M., Lavecchia, F., & Percoco, G. (2009). Experimental study aiming to enhance the surface finish of fused deposition modeled parts. *CIRP Annals - Manufacturing Technology*, 58(1), 189–192.  
<https://doi.org/10.1016/j.cirp.2009.03.071>
- Galantucci, L. M., Lavecchia, F., & Percoco, G. (2010). Quantitative analysis of a chemical treatment to reduce roughness of parts fabricated using fused deposition modeling. *CIRP Annals - Manufacturing Technology*, 59(1), 247–250.  
<https://doi.org/10.1016/j.cirp.2010.03.074>
- Gao, W., Zhang, Y., Ramanujan, D., Ramani, K., Chen, Y., Williams, C. B., Wang, C. C. L., Shin, Y. C., Zhang, S., & Zavattieri, P. D. (2015). The status, challenges, and future of additive manufacturing in engineering. *Computer-Aided Design*, 69, 65–89. <https://doi.org/10.1016/j.cad.2015.04.001>
- García-Guzmán, L., Távora, L., Reinoso, J., Justo, J., & París, F. (2018). Fracture resistance of 3D printed adhesively bonded DCB composite specimens using structured interfaces:

- Experimental and theoretical study. *Composite Structures*, 188, 173–184.  
<https://doi.org/10.1016/j.compstruct.2017.12.055>
- Garcia, R., & Prabhakar, P. (2017). Bond interface design for single lap joints using polymeric additive manufacturing. *Composite Structures*, 176, 547–555.  
<https://doi.org/10.1016/j.compstruct.2017.05.060>
- Garg, A., Bhattacharya, A., & Batish, A. (2015). On Surface Finish and Dimensional Accuracy of FDM Parts after Cold Vapor Treatment. *Materials and Manufacturing Processes*, 31(4), 522–529.  
<https://doi.org/10.1080/10426914.2015.1070425>
- Garg, A., Bhattacharya, A., & Batish, A. (2017). Chemical vapor treatment of ABS parts built by FDM: Analysis of surface finish and mechanical strength. *The International Journal of Advanced Manufacturing Technology*, 89(5–8), 2175–2191.  
<https://doi.org/10.1007/s00170-016-9257-1>
- Gaynor, A. T., Meisel, N. A., Williams, C. B., & Guest, J. K. (2014). Topology Optimization for Additive Manufacturing: Considering Maximum Overhang Constraint. *15th AIAA/ISSMO Multidisciplinary Analysis and Optimization Conference*, 1–8.  
<http://dx.doi.org/10.2514/6.2014-2036>
- Genc, S., Messler, R. W., & Gabriele, G. A. (1998). A Systematic Approach to Integral Snap-Fit Attachment Design. *Research in Engineering Design - Theory, Applications, and Concurrent Engineering*, 10(2), 84–93.  
<https://doi.org/10.1007/BF01616689>
- Gerber, G. (2008). *Designing for rapid manufacture* [Central University of Technology].  
<http://ir.cut.ac.za/handle/11462/42>
- Ghassemiparvin, B., & Ghalichechian, N. (2020). Design, fabrication, and testing of a helical antenna using 3D printing technology. *Microwave and Optical Technology Letters*, 62(4), 1577–1580.  
<https://doi.org/10.1002/MOP.32184>
- Gibson, I., Rosen, D., & Stucker, B. (2015a). *Additive Manufacturing Technologies*. Springer New York.  
<https://doi.org/10.1007/978-1-4939-2113-3>
- Gibson, I., Rosen, D., & Stucker, B. (2015b). Introduction and Basic Principles. In *Additive Manufacturing Technologies: 3D Printing, Rapid Prototyping, and Direct Digital Manufacturing* (pp. 1–18). Springer New York.  
[https://doi.org/10.1007/978-1-4939-2113-3\\_1](https://doi.org/10.1007/978-1-4939-2113-3_1)
- Gibson, L., Rosen, D. W., & Stucker, B. (2010). *Additive Manufacturing Technologies*. Springer-Verlag New York.
- Gibson, L. J., & Ashby, M. F. (1999). *Cellular solids: structure and properties*. Cambridge university press.
- Gibson, L. J., Ashby, M. F., & Harley, B. A. (2010). *Cellular materials in nature and medicine*. Cambridge University Press.
- Giller, W. (2021). *Ruthex threaded inserts | 3D CAD Model Library | GrabCAD*.  
<https://grabcad.com/library/ruthex-threaded-inserts-1>
- Gilloz, E. (2012). *RepRap Family Tree*. RepRapWiki.  
[http://reprap.org/wiki/RepRap\\_Family\\_Tree](http://reprap.org/wiki/RepRap_Family_Tree)
- Gómez-Gras, G., Pérez, M. A., Fábregas-Moreno, J., & Reyes-Pozo, G. (2021). Experimental study on the accuracy and surface quality of printed versus machined holes in PEI Ultem 9085 FDM specimens. *Rapid Prototyping Journal*, 27(11), 1–12.  
<https://doi.org/10.1108/RPJ-12-2019-0306>
- Gonzalez-Gomez, J., Valero-Gomez, A., Prieto-Moreno, A., & Abderrahim, M. (2012). A new open source 3d-printable mobile robotic platform for education. In *Advances in autonomous mini robots* (pp. 49–62). Springer.
- Gonzalez-Jorge, H., Riveiro, B., Vazquez-Fernandez, E., Martínez-Sánchez, J., & Arias, P. (2013). Metrological evaluation of Microsoft Kinect and Asus Xtion sensors. *Measurement*, 46(6), 1800–1806.  
<https://doi.org/10.1016/j.measurement.2013.01.011>
- Googler, A. (2012). A new home for SketchUp . *SketchUpdate*.  
<http://sketchupdate.blogspot.com/2012/04/new-home-for-sketchup.html>
- Gordon, E. R., Shokrani, A., Flynn, J. M., Goguelin, S., Barclay, J., & Dhokia, V. (2016). A Surface Modification Decision Tree to Influence Design in Additive Manufacturing. In *Sustainable Design and Manufacturing 2016. SDM 2016. Smart Innovation. Systems and Technologies* (pp. 423–434). Springer.  
[https://doi.org/10.1007/978-3-319-32098-4\\_36](https://doi.org/10.1007/978-3-319-32098-4_36)

- Gornet, T. (2015). History of Additive Manufacturing. In T. Wohlers (Ed.), *Wohlers Report 2015*.  
<http://wohlersassociates.com/history2015.pdf>
- Grauberger, P., Voß, K., & Matthiesen, S. (2019). Functional Analysis in Embodiment Design - An Investigation of Embodiment Function Relations in Testing Activities. *Proceedings of the Design Society: International Conference on Engineering Design*, 1(1), 1503–1512.  
<https://doi.org/10.1017/dsi.2019.156>
- Graybill, B. (2010). *Development of a predictive model for the design of parts fabricated by fused deposition modeling*. University of Missouri--Columbia.
- Green, R. (1984). *Formable orthopedic casts and splints* (Patent No. 4473671). USPTO.
- Gribbins, C. (2014). Investigation of Traditional and Alternate Living Hinge Designs for Fused Deposition Modeling Additive Manufacturing Process. In *PhD Dissertations and Master's Theses*. <https://commons.erau.edu/edt/213>
- Griffis, J. C. (2017). Design. In *Shape-Memory Polymer Device Design* (pp. 23–75). William Andrew Publishing.  
<https://doi.org/10.1016/B978-0-323-37797-3.00002-6>
- Guan, H. W., Savalani, M. M., Gibson, I., & Diegel, O. (2015). Influence of Fill Gap on Flexural Strength of Parts Fabricated by Curved Layer Fused Deposition Modeling. *Procedia Technology*, 20, 243–248.  
<https://doi.org/10.1016/j.protcy.2015.07.039>
- Gurralla, P. K., & Regalla, S. P. (2014). Part strength evolution with bonding between filaments in fused deposition modelling. *Virtual and Physical Prototyping*, 9(3), 141–149.  
<https://doi.org/10.1080/17452759.2014.913400>
- Gwamuri, J., Wittbrodt, B. T., Anzalone, N. C., & Pearce, J. M. (2014). Reversing the Trend of Large Scale and Centralization in Manufacturing: The Case of Distributed Manufacturing of Customizable 3-D-Printable Self-Adjustable Glasses. *Challenges in Sustainability*, 2(1), 30–40.
- Haefliger, S., von Krogh, G., & Spaeth, S. (2008). Code Reuse in Open Source Software. *Management Science*, 54(1), 180–193.  
<https://doi.org/10.1287/mnsc.1070.0748>
- Hague, R., Campbell, I., & Dickens, P. (2003). Implications on design of rapid manufacturing. *Proceedings of the Institution of Mechanical Engineers, Part C: Journal of Mechanical Engineering Science*, 217(1), 25–30.  
<https://doi.org/10.1243/095440603762554587>
- Haidiezul, A., Aiman, A., & Bakar, B. (2018). Surface Finish Effects Using Coating Method on 3D Printing (FDM) Parts. *IOP Conference Series: Materials Science and Engineering*, 318(1), 012065. <https://doi.org/10.1088/1757-899X/318/1/012065>
- Hallgrimsson, B. (IDSA C. U. (2011). *A Model for Every Purpose | Industrial Designers Society of America - IDSA*. <http://www-old.idsa.org/model-every-purpose>
- Hambali, R. H., Smith, P., & Rennie, A. E. W. (2012). Determination of the effect of part orientation to the strength value on additive manufacturing FDM for end-use parts by physical testing and validation via three-dimensional finite element analysis. *International Journal of Materials Engineering Innovation*, 3(3/4), 269.  
<https://doi.org/10.1504/IJMATEL.2012.049266>
- Han, W., Jafari, M. A., & Seyed, K. (2003). Process speeding up via deposition planning in fused deposition-based layered manufacturing processes. *Rapid Prototyping Journal*, 9(4), 212–218.  
<https://doi.org/10.1108/13552540310489596>
- Hart, K. R., & Wetzel, E. D. (2017). Fracture behavior of additively manufactured acrylonitrile butadiene styrene (ABS) materials. *Engineering Fracture Mechanics*, 177, 1–13.  
<https://doi.org/10.1016/J.ENGFRACMECH.2017.03.028>
- Havenga, S. P., de Beer, D. D., & van Tonder, P. J. M. (2014). Part finishing on entry level FDM models. *RAPDASA 2014*.
- Havenga, S. P., de Beer, D. J., van Tonder, P. J. M., & Campbell, R. I. (2018). The effect of acetone as a post-production finishing technique on entry-level material extrusion part quality. *South African Journal of Industrial Engineering*, 29(4), 53–64. <https://doi.org/10.7166/29-4-1934>
- Hayes, M. D., Edwards, D. B., & Shah, A. R. (2015). Fractography in Failure Analysis of Polymers. In *Fractography in Failure Analysis of Polymers*.

- Elsevier. <https://doi.org/10.1016/C2013-0-01392-8>
- Heaney, D. F. (2018). *Handbook of Metal Injection Molding* (2nd ed.). Woodhead Publishing.
- Heath, L. (2010). Wrist and hand injuries in sport. In P. Comfort & E. Abrahamson (Eds.), *Sports Rehabilitation and Injury Prevention* (p. 365). John Wiley & Sons.
- Hermann, S. (2020). *Testing the strength of 3D prints re-melted in salt. CNC Kitchen*. <https://www.cnckitchen.com/blog/testing-the-strength-of-3d-prints-re-melted-in-salt>
- Heskett, J. (1980). *Industrial design*. New York: Oxford University Press.
- He, Y., Xue, G., & Fu, J. (2015). Fabrication of low cost soft tissue prostheses with the desktop 3D printer. *Scientific Reports*, 4(1), 6973. <https://doi.org/10.1038/srep06973>
- Hodgson, G., Ranellucci, A., & Moe, J. (2014, May). *Slic3r Manual - Infill Patterns and Density*. <http://manual.slic3r.org/expert-mode/infill>
- Hong, J.-H., Yu, T., Chen, Z., Park, S.-J., & Kim, Y.-H. (2019). Improvement of flexural strength and compressive strength by heat treatment of PLA filament for 3D-printing. *Modern Physics Letters B*, 33(14n15), 1940025. <https://doi.org/10.1142/S0217984919400256>
- Hopkinson, N., Hague, R., & Dickens, P. (2006). *Rapid Manufacturing: An Industrial Revolution for the Digital Age*. Wiley. <http://books.google.es/books?id=JTEZPidytVsC>
- Housholder, R. F. (1979). *Molding process* (Patent No. US4247508A). US Patent Office. <https://patents.google.com/patent/US4247508A/en?q=us4247508>
- Howard, T. J., Culley, S. J., & Dekoninck, E. (2008). Describing the creative design process by the integration of engineering design and cognitive psychology literature. *Design Studies*, 29(2), 160–180. <https://doi.org/10.1016/j.destud.2008.01.001>
- HP. (2014). HP Multi Jet Fusion Technology: A Disruptive 3D Printing Technology for a New Era of Manufacturing [White paper]. In *HP Technical White Paper*. <https://www8.hp.com/h20195/v2/getpdf.aspx/4AA5-5472ENW.pdf?ver=4>
- Hsiao, W. (2018, February 20). *Sanding Block by walter. Thingiverse*. Thingiverse.Com. <https://www.thingiverse.com/thing:2798953>
- Huang, B., & Singamneni, S. (2012). Alternate slicing and deposition strategies for fused deposition modelling of light curved parts. *Journal of Achievements in Materials and Manufacturing Engineering*, 55(2), 511–517.
- Huang, B., & Singamneni, S. (2015). Raster angle mechanics in fused deposition modelling. *Journal of Composite Materials*, 49(3), 363–383. <https://doi.org/10.1177/0021998313519153>
- Huang, G. T. (2011, August). From Estonia to Boston: GrabCAD Looks to Play Big Role in New England's Tech Future. *Xconomy.Com*. <http://www.xconomy.com/boston/2011/08/23/from-estonia-to-boston-grabcad-looks-to-play-big-role-in-new-england%25E2%2580%2599s-tech-future/>
- Huang, P., Deng, D., & Chen, Y. (2013). Modeling and Fabrication of Heterogeneous Three-Dimensional Objects Based on Additive Manufacturing. *ASME 2013 International Mechanical Engineering Congress and Exposition. Volume 2A: Advanced Manufacturing, 2 A*. <https://doi.org/10.1115/IMECE2013-65724>
- Hudson, B. (n.d.). *How to design parts for FDM 3D Printing / 3D Hubs*. 3D Hubs Knowledge Base. Retrieved April 13, 2020, from <https://www.3dhubs.com/knowledge-base/how-design-parts-fdm-3d-printing/>
- Hull, C. W. (1984). *Method for production of three-dimensional objects by stereolithography* (Patent No. US4929402). US Patent Office. <https://patents.google.com/patent/US4929402A/en?q=3d+printing&country=US&before=priority:19900101>
- Hunt, E. J., Zhang, C., Anzalone, N., & Pearce, J. M. (2015). Polymer recycling codes for distributed manufacturing with 3-D printers. *Resources, Conservation and Recycling*, 97, 24–30. <https://doi.org/10.1016/j.resconrec.2015.02.004>
- Hur, J., Lee, K., Zhu-Hu, & Kim, J. (2002). Hybrid rapid prototyping system using machining and deposition. *Computer-Aided Design*, 34(10), 741–754. [https://doi.org/10.1016/S0010-4485\(01\)00203-2](https://doi.org/10.1016/S0010-4485(01)00203-2)

- Irwin, J. L., Pearce, J. M., Anza, Lone, G., & Oppliger, D. E. (2014). The RepRap 3-D Printer Revolution in STEM Education. *121st ASEE Annual Conference & Exposition*.
- ISO/ASTM. (2015). *ISO/ASTM 52900 Additive Manufacturing - General Principles - Terminology*.
- ISO/ASTM. (2018). *52910:2018 - Additive manufacturing — Design — Requirements, guidelines and recommendations*. <https://www.iso.org/standard/67289.html>
- ISO/ASTM. (2019). *52902:2019 - Additive manufacturing — Test artifacts — Geometric capability assessment of additive manufacturing systems*. ISO/ASTM. <https://www.iso.org/standard/67287.html>
- Austin, N. M. (2003). *Splinting the hand and upper extremity: principles and process* (M. A. Jacobs, N. Austin, & N. M. Austin, Eds.). Lippincott Williams & Wilkins.
- Jayanth, N., Senthil, P., & Prakash, C. (2018). Effect of chemical treatment on tensile strength and surface roughness of 3D-printed ABS using the FDM process. *Virtual and Physical Prototyping*, *13*(3), 155–163. <https://doi.org/10.1080/17452759.2018.1449565>
- Jee, H., & Witherell, P. (2017). A method for modularity in design rules for additive manufacturing. *Rapid Prototyping Journal*, *23*(6), 1107–1118. <https://doi.org/10.1108/RPJ-02-2016-0016>
- Jennings, A. (2021, March 20). *3D Printing Troubleshooting All Common Problems | All3DP*. <https://all3dp.com/1/common-3d-printing-problems-troubleshooting-3d-printer-issues/>
- Jin, Y., Wan, Y., Zhang, B., & Liu, Z. (2017). Modeling of the chemical finishing process for polylactic acid parts in fused deposition modeling and investigation of its tensile properties. *Journal of Materials Processing Technology*, *240*, 233–239. <https://doi.org/10.1016/j.JMATPROTEC.2016.10.003>
- Johnson, W. M., Rowell, M., Deason, B., & Eubanks, M. (2014). Comparative evaluation of an open-source FDM system. *Rapid Prototyping Journal*, *20*(3), 205–214. <https://doi.org/10.1108/RPJ-06-2012-0058>
- Jones, J. B., McNutt, P., Tosi, R., Perry, C., & Wimpenny, D. I. (2012). Remanufacture of turbine blades by laser cladding, machining and in-process scanning in a single machine. *23rd Annual International Solid Freeform Fabrication Symposium*, 821–827. <http://hdl.handle.net/2086/7552>
- Jones, R., Haufe, P., Sells, E., Irvani, P., Olliver, V., Palmer, C., & Bowyer, A. (2011). RepRap – the replicating rapid prototyper. *Robotica*, *29*(01), 177–191. <https://doi.org/10.1017/S026357471000069X>
- Jordá-Vilaplana, A., Fombuena, V., García-García, D., Samper, M. D., & Sánchez-Nácher, L. (2014). Surface modification of polylactic acid (PLA) by air atmospheric plasma treatment. *European Polymer Journal*, *58*, 23–33. <https://doi.org/10.1016/j.eurpolymj.2014.06.020>
- Jumani, M. S. (2013). *Cost modelling of rapid manufacturing based mass customisation system for fabrication of custom foot orthoses*. <http://hdl.handle.net/10443/2193>
- Kah, P., Suoranta, R., Martikainen, J., & Magnus, C. (2014). Techniques for joining dissimilar materials: Metals and polymers. *Reviews on Advanced Materials Science*, *36*(2).
- Kalpajian, S., & Schmid, S. (2013). Manufacturing engineering and technology, SI 6th Edition. In *Pearson*. Pearson.
- Kannan, S., & Senthilkumaran, D. (2014). Investigating the influence of electroplating layer thickness on the tensile strength for fused deposition processed ABS thermoplastics. *International Journal of Engineering and Technology*, *6*(2), 1047–1052.
- Kannan, T. R. (2017). *Design for Additive Manufacturing*. <https://dfmpro.geometricglobal.com/files/2017/05/Whitepaper-Design-for-Additive-Manufacturing.pdf>
- Karasahin, D. (2013). *Osteoid Medical cast, attachable bone stimulator*. A Design Award and Competition. <https://competition.adesignaward.com/design.php?ID=34151>
- Karasik, E., Fattal, R., & Werman, M. (2019). Object Partitioning for Support-Free 3D-Printing. *Computer Graphics Forum*, *38*(2), 305–316. <https://doi.org/10.1111/CGF.13639>

- Kelly, S., Paterson, A., & Bibb, R. J. (2015). A review of wrist splint designs for additive manufacture. *Proceedings of 2015 14th Rapid Design, Prototyping and Manufacture Conference (RDPM 14)*.
- Kentzer, J., Koch, B., Thiim, M., Jones, R. W., & Villumsen, E. (2011). An open source hardware-based mechatronics project: The replicating rapid 3-D printer. *2011 4th International Conference on Mechatronics: Integrated Engineering for Industrial and Societal Development, ICOM'11 - Conference Proceedings*. <https://doi.org/10.1109/ICOM.2011.5937174>
- Keough, M., McLeod, J. F., Salomons, T., Hillen, P., Pei, Y., Gibson, G., McEleney, K., Oleschuk, R., & She, Z. (2021). Realizing new designs of multiplexed electrode chips by 3-D printed masks. *RSC Advances*, *11*(35), 21600–21606. <https://doi.org/10.1039/D1RA03482K>
- Khan, M. S., & Mishra, S. B. (2020). Minimizing surface roughness of ABS-FDM build parts: An experimental approach. *Materials Today: Proceedings*, *26*, 1557–1566. <https://doi.org/10.1016/J.MATPR.2020.02.320>
- Khan, M. S., Mishra, S. B., Kumar, M. A., & Banerjee, D. (2018). Optimizing Surface Texture and Coating Thickness of Nickel Coated ABS-3D Parts. *Materials Today: Proceedings*, *5*(9), 19011–19018. <https://doi.org/10.1016/J.MATPR.2018.06.252>
- Kinnear, W. A., van der Walt, J. G., Rossouw, V., & Booysen, G. J. (2016). *Benchmarking of FDM printed replacement parts for rural wheelchairs*. <http://ir.cut.ac.za/handle/11462/1685>
- Klahn, C., Leutenecker, B., & Meboldt, M. (2014). Design for additive manufacturing - Supporting the substitution of components in series products. *Procedia CIRP*, *21*, 138–143. <https://doi.org/10.1016/j.procir.2014.03.145>
- Klahn, C., Singer, D., & Meboldt, M. (2016). Design Guidelines for Additive Manufactured Snap-Fit Joints. *Procedia CIRP*, *50*, 264–269. <https://doi.org/10.1016/j.procir.2016.04.130>
- Kočí, J. (2019a). *How to improve your 3D prints with annealing*. *Prusa Printers*. [https://blog.prusaprinters.org/how-to-improve-your-3d-prints-with-annealing\\_31088/](https://blog.prusaprinters.org/how-to-improve-your-3d-prints-with-annealing_31088/)
- Kočí, J. (2019b). *How to print on a powder-coated sheet - Prusa Printers*. <https://blog.prusaprinters.org/how-to-print-on-a-powder-coated-sheet/>
- Kodama, H. (1981). Automatic method for fabricating a three-dimensional plastic model with photo-hardening polymer. *Review of Scientific Instruments*, *52*(11), 1770–1773. <https://doi.org/10.1063/1.1136492>
- Ko, H., Yi, H., & Jeong, H. E. (2017). Wall and ceiling climbing quadruped robot with superior water repellency manufactured using 3D printing (UNIClimb). *International Journal of Precision Engineering and Manufacturing - Green Technology*, *4*(3), 273–280. <https://doi.org/10.1007/s40684-017-0033-y>
- Kovan, V., Altan, G., & Topal, E. S. (2017). Effect of layer thickness and print orientation on strength of 3D printed and adhesively bonded single lap joints. *Journal of Mechanical Science and Technology*, *31*(5), 2197–2201. <https://doi.org/10.1007/s12206-017-0415-7>
- Kruth, (1998). Progress in Additive Manufacturing and Rapid Prototyping. *CIRP Annals*, *47*(2), 525–540. [https://doi.org/10.1016/S0007-8506\(07\)63240-5](https://doi.org/10.1016/S0007-8506(07)63240-5)
- Kulkarni, P., & Dutta, D. (1998). On the Integration of Layered Manufacturing and Material Removal Processes. *Volume 2: 24th Design Automation Conference*, *2*. <https://doi.org/10.1115/DETC98/DAC-5623>
- Kumar, A., Choudhary, A., Tiwari, A., James, C., Kumar, H., Kumar Arora, P., & Akhtar Khan, S. (2021). An investigation on wear characteristics of additive manufacturing materials. *Materials Today: Proceedings*, *47*, 3654–3660. <https://doi.org/10.1016/j.matpr.2021.01.263>
- Kumar, R., Singh, R., & Ahuja, I. P. S. (2019). Mechanical, thermal and micrographic investigations of friction stir welded: 3D printed melt flow compatible dissimilar thermoplastics. *Journal of Manufacturing Processes*, *38*, 387–395. <https://doi.org/10.1016/j.jmappro.2019.01.043>
- Kumke, M., Watschke, H., & Vietor, T. (2016). A new methodological framework for design for additive manufacturing. *Virtual and Physical Prototyping*, *11*(1), 3–19. <https://doi.org/10.1080/17452759.2016.1139377>
- Kuo, C.-C., & Su, S.-J. (2013). A simple method for improving surface quality of rapid prototype. *Indian Journal of Engineering and Materials*

- Sciences (IJEMS)*, 20(6), 465–470.  
<http://nopr.niscair.res.in/handle/123456789/25583>
- Kuo, C.-C., Tsou, Y.-C., & Chen, B.-C. (2012). Enhancing the efficiency of removing support material from rapid prototype parts. *Materialwissenschaft Und Werkstofftechnik*, 43(3), 234–240.  
<https://doi.org/10.1002/mawe.201200841>
- Labs / FabLabs. (n.d.). Www.Fablabs.Io. Retrieved October 31, 2016, from <https://www.fablabs.io/labs>
- Langeveld, L. H. (2006). Design with X is new in product design education. *DS 36: Proceedings DESIGN 2006, the 9th International Design Conference*, 1179–1186.
- Lanzotti, A., Grasso, M., Staiano, G., & Martorelli, M. (2015). The impact of process parameters on mechanical properties of parts fabricated in PLA with an open-source 3-D printer. *Rapid Prototyping Journal*, 21(5), 604–617.  
<https://doi.org/10.1108/RPJ-09-2014-0135>
- Lanzotti, A., Martorelli, M., & Staiano, G. (2015). Understanding Process Parameter Effects of RepRap Open-Source Three-Dimensional Printers Through a Design of Experiments Approach. *Journal of Manufacturing Science and Engineering*, 137(1), 11017.  
<https://doi.org/10.1115/1.4029045>
- Lauff, C. A., Perez, K. B., Camburn, B. A., & Wood, K. L. (2019). Design Principle Cards: Toolset to Support Innovations With Additive Manufacturing. *Volume 4: 24th Design for Manufacturing and the Life Cycle Conference; 13th International Conference on Micro- and Nanosystems*, 4.  
<https://doi.org/10.1115/DETC2019-97231>
- Laurel, B. (2003). *Design research: Methods and perspectives*. MIT press.
- Lavecchia, F., Percoco, G., Pei, E., & Galantucci, L. M. (2018). Computer Numerical Controlled Grinding and Physical Vapor Deposition for Fused Deposition Modelled Workpieces. *Advances in Materials Science and Engineering*, 2018, 1–7.  
<https://doi.org/10.1155/2018/9037490>
- Laverne, F., Segonds, F., Anwer, N., & le Coq, M. (2014). DFAM in the design process: A proposal of classification to foster early design stages. *CONFERE*.
- Laverne, F., Segonds, F., Anwer, N., & le Coq, M. (2015). Assembly Based Methods to Support Product Innovation in Design for Additive Manufacturing: An Exploratory Case Study. *Journal of Mechanical Design*, 137(12), 121701.  
<https://doi.org/10.1115/1.4031589>
- Laverne, F., Segonds, F., D'Antonio Gianluca, & le Coq, M. (2017). Enriching design with X through tailored additive manufacturing knowledge: a methodological proposal. *International Journal on Interactive Design and Manufacturing*, 11(2), 279–288. <https://doi.org/10.1007/s12008-016-0314-7>
- Leary, M., Babae, M., Brandt, M., & Subic, A. (2013). Feasible Build Orientations for Self-Supporting Fused Deposition Manufacture: A Novel Approach to Space-Filling Tesselated Geometries. *Advanced Materials Research*, 633, 148–168.  
<https://doi.org/10.4028/www.scientific.net/AMR.633.148>
- Leary, M., Merli, L., Torti, F., Mazur, M., & Brandt, M. (2014a). Optimal topology for additive manufacture: A method for enabling additive manufacture of support-free optimal structures. *Materials & Design*, 63, 678–690.  
<https://doi.org/10.1016/j.matdes.2014.06.015>
- Leary, M., Merli, L., Torti, F., Mazur, M., & Brandt, M. (2014b). Optimal topology for additive manufacture: A method for enabling additive manufacture of support-free optimal structures. *Materials and Design*, 63, 678–690.  
<https://doi.org/10.1016/j.matdes.2014.06.015>
- Lederle, F., Meyer, F., Brunotte, G.-P., Kaldun, C., & Hübner, E. G. (2016). Improved mechanical properties of 3D-printed parts by fused deposition modeling processed under the exclusion of oxygen. *Progress in Additive Manufacturing 2016 1:1*, 1(1), 3–7.  
<https://doi.org/10.1007/S40964-016-0010-Y>
- Lee, J., & Huang, A. (2013). Fatigue analysis of FDM materials. *Rapid Prototyping Journal*, 19(4), 291–299.  
<https://doi.org/10.1108/13552541311323290>
- Lee, J.-Y., Nagalingam, A. P., & Yeo, S. H. (2020). A review on the state-of-the-art of surface finishing processes and related ISO/ASTM standards for metal additive manufactured components. *Virtual and Physical Prototyping*, 16(1), 68–96.

- <https://doi.org/10.1080/17452759.2020.1830346>
- Lee, K. M., Park, H., Kim, J., & Chun, D. M. (2019). Fabrication of a superhydrophobic surface using a fused deposition modeling (FDM) 3D printer with poly lactic acid (PLA) filament and dip coating with silica nanoparticles. *Applied Surface Science*, 467–468. <https://doi.org/10.1016/j.apsusc.2018.10.205>
- Le, H. P. (1998). Progress and trends in ink-jet printing technology. *Journal of Imaging Science and Technology*, 42(1), 49–62.
- Leigh, S. J., Bradley, R. J., Pursell, C. P., Billson, D. R., & Hutchins, D. A. (2012). A Simple, Low-Cost Conductive Composite Material for 3D Printing of Electronic Sensors. *PLoS ONE*, 7(11), e49365. <https://doi.org/10.1371/journal.pone.0049365>
- Leite, M., Varanda, A., Ribeiro, A. R., Silva, A., & Vaz, M. F. (2018). Mechanical properties and water absorption of surface modified ABS 3D printed by fused deposition modelling. *Rapid Prototyping Journal*, 24(1), 195–203. <https://doi.org/10.1108/RPJ-04-2016-0057>
- Lessig, L. (2005). *Free culture: The nature and future of creativity*. The penguin press.
- Leutenecker-Twelsiek, B., Klahn, C., & Meboldt, M. (2016). Designing a Power Tool to Show the Potentials of Additive Manufacturing - Effects of Additive Manufacturing on the Product Development Process. *Solid Freeform Fabrication Symposium*, 1900–1909.
- Liao, Y. S., Chiu, L. C., & Chiu, Y. Y. (2003). A new approach of online waste removal process for laminated object manufacturing (LOM). *Journal of Materials Processing Technology*, 140(1-3 SPEC.), 136–140. [https://doi.org/10.1016/S0924-0136\(03\)00690-3](https://doi.org/10.1016/S0924-0136(03)00690-3)
- Likert, R. (1932). A technique for the measurement of attitudes. *Archives of Psychology*, 140.
- Lindwall, A., & Törlind, P. (2018). Evaluating design heuristics for additive manufacturing as an explorative workshop method. *Proceedings of International Design Conference, DESIGN*, 3, 1221–1232. <https://doi.org/10.21278/idc.2018.0310>
- Lipina, J., & Kryś, V. (2016). Application of rapid prototyping technology in designing robots and peripheral devices. *MM Science Journal*, 2016(01), 856–861. [https://doi.org/10.17973/MMSJ.2016\\_03\\_201544](https://doi.org/10.17973/MMSJ.2016_03_201544)
- Lipina, J., Kryś, V., & Sedlák, J. (2014). Shaped Glued Connection of Two Parts Made by Rapid Prototyping Technology. *Applied Mechanics and Materials*, 555, 541–548. <https://doi.org/10.4028/www.scientific.net/AMM.555.541>
- Lipina, J., Marek, J., & Kryś, V. (2014). Screw connection and its load capacity in components made by rapid prototyping technology. *SAMI 2014 - IEEE 12th International Symposium on Applied Machine Intelligence and Informatics, Proceedings*, 201–204. <https://doi.org/10.1109/SAMI.2014.6822407>
- Lipson, H., & Kurman, M. (2010). *Factory@Home: The Emerging Economy of Personal Fabrication*. <http://www.mae.cornell.edu/lipson/FactoryAtHome.pdf>
- Liu, J. (2016). Guidelines for AM part consolidation. *Virtual and Physical Prototyping*, 11(2), 133–141. <https://doi.org/10.1080/17452759.2016.1175154>
- Livesu, M., Ellero, S., Martínez, J., Lefebvre, S., & Attene, M. (2017). From 3D models to 3D prints: an overview of the processing pipeline. *Computer Graphics Forum*, 36(2), 537–564. <https://doi.org/10.1111/cgf.13147>
- Loh, G. H., Pei, E., Harrison, D., & Monzón, M. D. (2018). An overview of functionally graded additive manufacturing. *Additive Manufacturing*, 23, 34–44. <https://doi.org/10.1016/j.ADDMA.2018.06.023>
- Lonardo, P. M., Lucca, D. A., & de Chiffre, L. (2002). Emerging Trends in Surface Metrology. *CIRP Annals*, 51(2), 701–723. [https://doi.org/10.1016/S0007-8506\(07\)61708-9](https://doi.org/10.1016/S0007-8506(07)61708-9)
- Luo, L., Baran, I., Rusinkiewicz, S., & Matusik, W. (2012). Chopper: Partitioning models into 3D-printable parts. *ACM Transactions on Graphics*, 31(6). <https://doi.org/10.1145/2366145.2366148>
- Lusardi, M. M., Jorge, M., & Nielsen, C. C. (2013). *Orthotics and prosthetics in rehabilitation* (Third). Elsevier Health Sciences.



- Lussenburg, K., Sakes, A., & Breedveld, P. (2021). Design of non-assembly mechanisms: A state-of-the-art review. *Additive Manufacturing*, 39, 101846. <https://doi.org/10.1016/j.addma.2021.101846>
- Maidin, S. bin, Campbell, I., & Pei, E. (2012). Development of a design feature database to support design for additive manufacturing. *Assembly Automation*, 32(3), 235–244. <https://doi.org/10.1108/01445151211244375>
- Maidin, S. bin, & Campbell, R. I. (2010). Development of a repository to support design for additive manufacturing (DFAM). *Annals of DAAAM & Proceedings*, 1559–1561.
- Malone, E., & Lipson, H. (2007). Fab@Home: the personal desktop fabricator kit. *Rapid Prototyping Journal*, 13(4), 245–255. <https://doi.org/10.1108/13552540710776197>
- Mardani-Kivi, M., Karimi Mobarakeh, M., Bahrami, F., Hashemi-Motlagh, K., Saheb-Ekhtiari, K., & Akhondzadeh, N. (2014). Corticosteroid Injection With or Without Thumb Spica Cast for de Quervain Tenosynovitis. *The Journal of Hand Surgery*, 39(1), 37–41. <https://doi.org/10.1016/j.jhsa.2013.10.013>
- Markillie, P. (2012). A third industrial revolution. *The Economist*, 21. <http://www.economist.com/node/21552901>
- Martínez Abellán, V. (2016). *Planteamiento de integración de bajo coste entre tecnologías de fabricación aditiva y sustractiva* [Universitat Politècnica de València]. <https://riunet.upv.es/handle/10251/59661>
- Martin, J. H., Ashby, D. S., & Schaedler, T. A. (2017). Thin-walled high temperature alloy structures fabricated from additively manufactured polymer templates. *Materials & Design*, 120, 291–297. <https://doi.org/10.1016/j.MATDES.2017.02.023>
- Matsubara, K. (1976). Molding method of casting using photocurable substance (Patent No. 51.10813). In *Japanese Kokai Patent Application, Sho* (51.10813).
- Mattox, D. M. (2010). Handbook of Physical Vapor Deposition (PVD) Processing. In *Handbook of Physical Vapor Deposition (PVD) Processing*. Elsevier. <https://doi.org/10.1016/C2009-0-18800-1>
- Mcor. (n.d.). *Mcor Technologies*. Retrieved January 1, 2012, from <http://www.mcor technologies.com>
- Mediprint. (2016). *NovaCast de MediPrint*. <http://mediprint3d.com.mx/>
- Melgoza, E. L., Serenó, L., Rosell, A., & Ciurana, J. (2012). An integrated parameterized tool for designing a customized tracheal stent. *Computer-Aided Design*, 44(12), 1173–1181.
- Mellis, D., Banzi, M., Cuartielles, D., & Igoe, T. (2007). Arduino: An open electronic prototyping platform. *Proceedings of the Conference on Human Factors in Computing (Alt.Chi) (CHI'07)*, 1, 1–11.
- Menichinelli, M. (2011). Business Models for Fab Labs. *Openp2Pdesign.Org*. <http://www.openp2pdesign.org/2011/fabbing/business-models-for-fab-labs/>
- Merklein, M., Junker, D., Schaub, A., & Neubauer, F. (2016). Hybrid Additive Manufacturing Technologies – An Analysis Regarding Potentials and Applications. *Physics Procedia*, 83, 549–559. <https://doi.org/10.1016/j.PHPRO.2016.08.057>
- Meshmixer. (2016). *Meshmixer - health*. <http://www.meshmixer.com/health.html>
- Micallef, J. (2015). Beginning Design for 3D Printing. In *Beginning Design for 3D Printing*. Apress. <https://doi.org/10.1007/978-1-4842-0946-2>
- Michaeli, W., & Hopmann, C. (2016). *Extrusion dies for plastics and rubber*. [https://extrusion.4spe.org/wp-content/uploads/2019/01/Extrusion\\_Dies\\_for\\_Plastics\\_and\\_Rubber.pdf](https://extrusion.4spe.org/wp-content/uploads/2019/01/Extrusion_Dies_for_Plastics_and_Rubber.pdf)
- mifervi. (2021). *Benchmark - Collections*. Thingiverse.Com. <https://www.thingiverse.com/mifervi/collections/benchmark>
- Minetola, P., Iuliano, L., & Marchiandi, G. (2016). Benchmarking of FDM Machines through Part Quality Using IT Grades. *Procedia CIRP*, 41, 1027–1032. <https://doi.org/10.1016/j.PROCIR.2015.12.075>
- Minetur Spain. (2016). *Precio neto de la electricidad para uso doméstico y uso industrial*. [http://www.minetur.gob.es/ES/IndicadoresyEstadisticas/DatosEstadisticos/IV.Energ%25C3%25Adayemisiones/IV\\_12.pdf](http://www.minetur.gob.es/ES/IndicadoresyEstadisticas/DatosEstadisticos/IV.Energ%25C3%25Adayemisiones/IV_12.pdf)

- Mireles, J., Adame, A., Espalin, D., Medina, F., Winker, R., Hoppe, T., Zinniel, B., & Wicker, R. (2011). Analysis of sealing methods for FDM-fabricated parts. *Solid Freeform Fabrication Symposium*.
- Mohamed, O., Masood, S., & Bhowmik, J. (2015). Optimization of fused deposition modeling process parameters: a review of current research and future prospects. *Advances in Manufacturing*, 3(1), 42–53. <https://doi.org/10.1007/s40436-014-0097-7>
- Moilanen, J. (2012). Emerging Hackerspaces – Peer-Production Generation. In I. Hammouda, B. Lundell, T. Mikkonen, & W. Scacchi (Eds.), *Open Source Systems: Long-Term Sustainability* (pp. 94–111). Springer Berlin Heidelberg. [https://doi.org/10.1007/978-3-642-33442-9\\_7](https://doi.org/10.1007/978-3-642-33442-9_7)
- Moilanen, J., Daly, A., Lobato, R., & Allen, D. (2015). Cultures of sharing in 3D printing: What can we learn from the licence choices of Thingiverse users? *Journal of Peer Production*, 6. <https://ssrn.com/abstract=2440027>
- Moilanen, J., & Vadén, T. (2013). 3D printing community and emerging practices of peer production. *First Monday*, 18(8). <https://doi.org/10.5210/fm.v18i8.4271>
- Montero, M., Roundy, S., Odell, D., Ahn, S.-H., & Wright, P. K. (2001). Material characterization of fused deposition modeling (FDM) ABS by designed experiments. *Proceedings of Rapid Prototyping and Manufacturing Conference, SME*, 1–21.
- Monzon, M. D., Diaz, N., Benitez, A. N., Marrero, M. D., & Hernandez, P. M. (2010). Advantages of Fused Deposition Modeling for Making Electrically Conductive Plastic Patterns. *2010 International Conference on Manufacturing Automation*, 37–43. <https://doi.org/10.1109/ICMA.2010.18>
- Moreno Nieto, D., & Molina, S. I. (2020). Large-format fused deposition additive manufacturing: a review. *Rapid Prototyping Journal*, 26(5), 793–799. <https://doi.org/10.1108/RPJ-05-2018-0126>
- Morioka, I. (1935). *Process for Manufacturing a Relief by the Aid of Photography* (Patent No. US2015457 A). US Patent Office. <http://www.google.com/patents/US2015457>
- Morris, R. (2016). The Fundamentals of Product Design. In *The Fundamentals of Product Design*. Bloomsbury Publishing Plc. <https://doi.org/10.5040/9781474221634>
- Mota, C., & Catarina. (2011). The rise of personal fabrication. *Proceedings of the 8th ACM Conference on Creativity and Cognition - C&C '11*, 279. <https://doi.org/10.1145/2069618.2069665>
- Moylan, S., Slotwinski, J., Cooke, A., Jurrens, K., & Donmez, M. A. (2012). Proposal for a standardized test artifact for additive manufacturing machines and processes. *Solid Freeform Fabrication Symposium*, 902–920.
- MPL S.R.L. (2016). *Ficha Tecnica acetona SPB*. <https://www.mpl.es/wp-content/uploads/2016/08/300339-300800-Acetona-SPB.pdf>
- Msallem, B., Sharma, N., Cao, S., Halbeisen, F. S., Zeilhofer, H.-F., & Thieringer, F. M. (2020). Evaluation of the Dimensional Accuracy of 3D-Printed Anatomical Mandibular Models Using FFF, SLA, SLS, MJ, and BJ Printing Technology. *Journal of Clinical Medicine*, 9(3), 817. <https://doi.org/10.3390/jcm9030817>
- Mueller, B., & Kochan, D. (1999). Laminated object manufacturing for rapid tooling and patternmaking in foundry industry. *Computers in Industry*, 39(1), 47–53. [https://doi.org/10.1016/S0166-3615\(98\)00127-4](https://doi.org/10.1016/S0166-3615(98)00127-4)
- Mueller, T., Elkaseer, A., Charles, A., Fauth, J., Rabsch, D., Scholz, A., Marquardt, C., Nau, K., & Scholz, S. G. (2020). Eight Weeks Later—The Unprecedented Rise of 3D Printing during the COVID-19 Pandemic—A Case Study, Lessons Learned, and Implications on the Future of Global Decentralized Manufacturing. *Applied Sciences*, 10(12), 4135. <https://doi.org/10.3390/app10124135>
- Muller, P., Hascoet, J.-Y., & Mognol, P. (2014). Toolpaths for additive manufacturing of functionally graded materials (FGM) parts. *Rapid Prototyping Journal*, 20(6), 511–522. <http://dx.doi.org/10.1108/RPJ-01-2013-0011>
- Munz, O. J. (1951). *Photo-glyph recording* (Patent No. US2775758A). <https://patents.google.com/patent/US2775758A/en?q=Photo-Glyph+Recording&oq=Photo-Glyph+Recording>
- Mwema, F. M., & Akinlabi, E. T. (2020). Basics of Fused Deposition Modelling (FDM). In

- SpringerBriefs in Applied Sciences and Technology*. [https://doi.org/10.1007/978-3-030-48259-6\\_1](https://doi.org/10.1007/978-3-030-48259-6_1)
- Myminifactory. (n.d.). *MyMiniFactory.com*. Retrieved November 24, 2021, from <https://www.myminifactory.com/>
- Nancharaiah, T., Raju, D. R., & Raju, V. R. (2010). An experimental investigation on surface quality and dimensional accuracy of FDM components. *International Journal on Emerging Technologies*, 1(2), 106–111.
- Nickel, A. H., Barnett, D. M., & Prinz, F. B. (2001). Thermal stresses and deposition patterns in layered manufacturing. *Materials Science and Engineering: A*, 317(1–2), 59–64. [https://doi.org/10.1016/S0921-5093\(01\)01179-0](https://doi.org/10.1016/S0921-5093(01)01179-0)
- Niewengłowski, G. H. (1897). La photosculpture. In *La Science française : revue populaire illustrée*. <http://gallica.bnf.fr/ark:/12148/bpt6k116378f/f295.image.r>
- Oehlberg, L., Willett, W., & Mackay, W. E. (2015). Patterns of Physical Design Remixing in Online Maker Communities. *Proceedings of the 33rd Annual ACM Conference on Human Factors in Computing Systems - CHI '15*, 639–648. <https://doi.org/10.1145/2702123.2702175>
- Oh, Y., Ko, H., Sprock, T., Bernstein, W. Z., & Kwon, S. (2021). Part decomposition and evaluation based on standard design guidelines for additive manufacturability and assemblability. *Additive Manufacturing*, 37, 101702. <https://doi.org/10.1016/j.addma.2020.101702>
- Oh, Y., Zhou, C., & Behdad, S. (2018). Part decomposition and assembly-based (Re) design for additive manufacturing: A review. *Additive Manufacturing*, 22, 230–242. <https://doi.org/10.1016/j.ADDMA.2018.04.018>
- Olivera, S., Muralidhara, H. B., Venkatesh, K., Gopalakrishna, K., & Vivek, C. S. (2016). Plating on acrylonitrile–butadiene–styrene (ABS) plastic: a review. *Journal of Materials Science*, 8(51), 3657–3674. <https://doi.org/10.1007/S10853-015-9668-7>
- Open Bionics. (2015). *Open Bionics. 3D Printed, Dual Material, Medical Splint*. Open Bionics Blog. <http://www.openbionics.com/blog>
- Oxman, N. (2011). Variable property rapid prototyping. *Virtual and Physical Prototyping*, 6(1), 3–31. <https://doi.org/10.1080/17452759.2011.558588>
- Pahl, G., Beitz, W., Feldhusen, J., & Grote, K.-H. (2007). Engineering Design. In *Engineering Design: A Systematic Approach*. Springer London. <https://doi.org/10.1007/978-1-84628-319-2>
- Palousek, D., Rosicky, J., Koutny, D., Stoklásek, P., & Navrat, T. (2014). Pilot study of the wrist orthosis design process. *Rapid Prototyping Journal*, 20(1), 27–32. <https://doi.org/10.1108/RPJ-03-2012-0027>
- Panda, S. S., Chabra, R., Kapil, S., & Patel, V. (2020). Chemical vapour treatment for enhancing the surface finish of PLA object produced by fused deposition method using the Taguchi optimization method. *SN Applied Sciences* 2020 2:5, 2(5), 1–13. <https://doi.org/10.1007/S42452-020-2740-1>
- Pandey, P. M., Reddy, N. V., & Dhande, S. G. (2003). Improvement of surface finish by staircase machining in fused deposition modeling. *Journal of Materials Processing Technology*, 132(1–3), 323–331. [https://doi.org/10.1016/S0924-0136\(02\)00953-6](https://doi.org/10.1016/S0924-0136(02)00953-6)
- Pandzic, A., Hodzic, D., 30th, A. M.-P. of the, & 2019, undefined. (2019). Influence of Material Colour on Mechanical Properties of PLA Material in FDM Technology. *Proceedings of the 30th DAAAM International Symposium on Intelligent Manufacturing and Automation*. <https://doi.org/10.2507/30th.daaam.proceedings.075>
- Papadimitriou, S., Papalexakis, E., Liu, B., & Xiong, H. (2015). Remix in 3D Printing. *Proceedings of the 24th International Conference on World Wide Web - WWW '15 Companion*, 367–368. <https://doi.org/10.1145/2740908.2745943>
- Patel, Y. (2008). *The Machining of Polymers*. <https://spiral.imperial.ac.uk/handle/10044/1/4435>
- Paterson, A. (2013). *Digitisation of the splinting process: exploration and evaluation of a computer aided design approach to support additive manufacture*. Loughborough University.
- Paterson, A. M., Bibb, R., Campbell, R. I., & Bingham, G. (2015). Comparing additive manufacturing technologies for customised wrist splints. *Rapid Prototyping Journal*, 21(3), 230–243. <https://doi.org/10.1108/RPJ-10-2013-0099>

- Paterson, A. M., Bibb, R. J., & Campbell, R. I. (2012a). Evaluation of a digitised splinting approach with multiple-material functionality using Additive Manufacturing technologies. *Proceedings of the Solid Freeform Fabrication Symposium*, 656–672.
- Paterson, A. M., Bibb, R. J., & Campbell, R. I. (2012b). Evaluation of a three-dimensional Computer Aided Design Workflow for Upper Extremity Splint Design to Support Additive Manufacture. *Proceedings of the 13th National Conference on Rapid Design, Prototyping and Manufacturing*. 22nd July, Lancaster., 71–80.
- Paterson, A. M., Donnison, E., Bibb, R. J., & Ian Campbell, R. (2014). Computer-aided design to support fabrication of wrist splints using 3D printing: A feasibility study. *Hand Therapy*, 19(4), 102–113.  
<https://doi.org/10.1177/1758998314544802>
- Paterson, A. M. J., Bibb, R. J., & Campbell, R. I. (2010). A review of existing anatomical data capture methods to support the mass customisation of wrist splints. *Virtual and Physical Prototyping*, 5(4), 201–207.  
<https://doi.org/10.1080/17452759.2010.528183>
- Paz, F., Villanueva, D., Rusu, C., Roncagliolo, S., & Pow-Sang, J. A. (2013). Experimental evaluation of usability heuristics. *Proceedings of the 2013 10th International Conference on Information Technology: New Generations, ITNG 2013*.  
<https://doi.org/10.1109/ITNG.2013.23>
- Pearce, J. M. (2012). Materials science. Building research equipment with free, open-source hardware. *Science (New York, N.Y.)*, 337(6100), 1303–1304.  
<https://doi.org/10.1126/science.1228183>
- Pearce, J. M., Blair, C. M., Laciak, K. J., Andrews, R., Nosrat, A., & Zelenika-Zovko, I. (2010). 3-D Printing of Open Source Appropriate Technologies for Self-Directed Sustainable Development. *Journal of Sustainable Development*, 3(4), 17.
- Pei, E., Campbell, I., & Evans, M. (2011). A Taxonomic Classification of Visual Design Representations Used by Industrial Designers and Engineering Designers. *The Design Journal*, 14(1), 64–91.  
<https://doi.org/10.2752/175630610X12877385838803>
- Percoco, G., Lavecchia, F., & Galantucci, L. M. (2012). Compressive Properties of FDM Rapid Prototypes Treated with a Low Cost Chemical Finishing. *Research Journal of Applied Sciences, Engineering and Technology*, 4(19), 3838–3842.
- Perez, K. B. (2018). Design Innovation with Additive Manufacturing (AM): An AM-centric Design Innovation Process. In *Singapore University of Technology and Design*.
- Perez, K. B., Anderson, D. S., Hölltä-Otto, K., & Wood, K. L. (2015). Crowdsourced Design Principles for Leveraging the Capabilities of Additive Manufacturing. *Proceedings of the 20th International Conference on Engineering Design (ICED 15)*, 291–300.
- Perez, K. B., Hilburn, S., Jensen, D., & Wood, K. L. (2019). Design principle-based stimuli for improving creativity during ideation. *Proceedings of the Institution of Mechanical Engineers, Part C: Journal of Mechanical Engineering Science*, 233(2), 493–503.  
<https://doi.org/10.1177/0954406218809117>
- Petrie, C. (2013). The age of DIY. *IEEE Internet Computing*, 17(6), 93–94.  
<https://doi.org/10.1109/MIC.2013.120>
- Petrovic, V., Vicente, H. G., Jordá Ferrando, O., Delgado Gordillo, J., Ramón, B. P., & Portolés Griñan, L. (2011). Additive layered manufacturing: sectors of industrial application shown through case studies. *International Journal of Production Research*, 49(4), 1061–1079.  
<https://doi.org/10.1080/00207540903479786>
- Pettis, B., France, A. K., & Shergill, J. (2012). *Getting Started with MakerBot*. O'Reilly Media.  
[https://books.google.com/books/about/Getting\\_Started\\_with\\_MakerBot.html?id=PIYn88TqqRC](https://books.google.com/books/about/Getting_Started_with_MakerBot.html?id=PIYn88TqqRC)
- Pham, D. T. (1998). A comparison of rapid prototyping technologies. *International Journal of Machine Tools Manufacture*, 38(10–11), 1257.
- piuLAB. (2014). *Wrist brace*. Thingiverse.Com.  
<http://www.thingiverse.com/thing:403001>
- Polini, W. (2014). To model joints with clearance for tolerance analysis. *Proceedings of the Institution of Mechanical Engineers, Part B: Journal of Engineering Manufacture*, 228(12), 1689–1700.  
<https://doi.org/10.1177/0954405414522610>

- Ponche, R., Hascoet, J. Y., Kerbrat, O., & Mognol, P. (2012). A new global approach to design for additive manufacturing. *Virtual and Physical Prototyping*, 7(2), 93–105. <https://doi.org/10.1080/17452759.2012.679499>
- Ponche, R., Kerbrat, O., Mognol, P., & Hascoet, J.-Y. (2014). A novel methodology of design for Additive Manufacturing applied to Additive Laser Manufacturing process. *Robotics and Computer-Integrated Manufacturing*, 30(4), 389–398. <https://doi.org/10.1016/j.rcim.2013.12.001>
- Popescu, D., Zapciu, A., Amza, C., Baci, F., & Marinescu, R. (2018). FDM process parameters influence over the mechanical properties of polymer specimens: A review. *Polymer Testing*, 69, 157–166. <https://doi.org/10.1016/j.polymertesting.2018.05.020>
- Prabhu, R., Simpson, T. W., Miller, S. R., & Meisel, N. A. (2021). Fresh in My Mind! Investigating the effects of the order of presenting opportunistic and restrictive design for additive manufacturing content on students' creativity. *Journal of Engineering Design*, 32(4), 187–212. <https://doi.org/10.1080/09544828.2021.1876843>
- Priedeman, W., & Brosch, A. (2004). Soluble material and process for three-dimensional modeling (Patent No. US6790403B1). In *Google Patents* (US6790403B1). <https://patents.google.com/patent/US6790403B1/en>
- Priedeman, W. R. Jr., & Smith, D. T. (2003). *Smoothing method for layered deposition modeling* (Patent No. US8123999B2).
- Prusa Research. (2020). *3D printed face shields for medics and professionals - Prusa3D - 3D Printers from Josef Průša*. Prusa3D.Com. <https://www.prusa3d.com/covid19/>
- Qureshi, A. J., Mahmood, S., Wong, W. L. E., & Talamona, D. (2015). Design for Scalability and Strength Optimisation for components created through FDM process. In C. Weber & S. Husung (Eds.), *Proceedings of the 20th International Conference on Engineering Design (ICED 15) Volume 6: Design Methods and Tools - Part 2* (pp. 255–266).
- Raju, K. V. M. K., Janardhana, G. R., Kumar, P. N., & Rao, V. D. P. (2011). Optimization of cutting conditions for surface roughness in CNC end milling. *International Journal of Precision Engineering and Manufacturing*, 12(3), 383–391. <https://doi.org/10.1007/s12541-011-0050-7>
- Ramaswamy, S., & Lesser, A. J. (2002). Microscopic damage and macroscopic yield in acrylonitrile-butadiene-styrene (ABS) resins tested under multi-axial stress states. *Polymer*, 43(13), 3743–3752. [https://doi.org/10.1016/S0032-3861\(02\)00181-7](https://doi.org/10.1016/S0032-3861(02)00181-7)
- Ramírez, E. A., Caicedo, F., Hurel, J., Helguero, C. G., & Amaya, J. L. (2019). Methodology for design process of a snap-fit joint made by additive manufacturing. *Procedia CIRP*, 79, 113–118. <https://doi.org/10.1016/j.procir.2019.02.021>
- Ranellucci, A. (n.d.). *Slic3r - G-code generator for 3D printers*. <http://slic3r.org/>
- Ranellucci, A. (2013). Reprap, Slic3r and the Future of 3D Printing. In E. Canessa, C. Fonda, & M. Zennaro (Eds.), *Low-cost 3D Printing for Science, Education & Sustainable Development* (pp. 75–82). ICTP.
- Rankouhi, B., Javadpour, S., Delfanian, F., & Letcher, T. (2016). Failure Analysis and Mechanical Characterization of 3D Printed ABS With Respect to Layer Thickness and Orientation. *Journal of Failure Analysis and Prevention*, 16(3), 467–481. <https://doi.org/10.1007/s11668-016-0113-2>
- Rayna, T., Striukova, L., & Darlington, J. (2014). Open Innovation, Co-Creation and Mass Customisation: What Role for 3D Printing Platforms? *Proceedings of the 7th World Conference on Mass Customization, Personalization, and Co-Creation (MCPC 2014)*, 425–435. [https://doi.org/10.1007/978-3-319-04271-8\\_36](https://doi.org/10.1007/978-3-319-04271-8_36)
- Redwood, B., Schffer, F., & Garret, B. (2017). *The 3D Printing Handbook: Technologies, Design and Applications* (1st ed.).
- RepRap. (n.d.). *Marlin - RepRapWiki*. <http://reprap.org/wiki/Marlin>
- Rezayat, H., Zhou, W., Siriruk, A., Penumadu, D., & Babu, S. S. (2015). Structure–mechanical property relationship in fused deposition modelling. *Materials Science and Technology*, 31(8), 895–903.

- <https://doi.org/10.1179/1743284715Y.000000010>
- Riddick, J. C., Haile, M. A., Wahldt, R. von, Cole, D. P., Bamiduro, O., & Johnson, T. E. (2016). Fractographic analysis of tensile failure of acrylonitrile-butadiene-styrene fabricated by fused deposition modeling. *Additive Manufacturing*, 11, 49–59. <https://doi.org/10.1016/j.addma.2016.03.007>
- Rifkin, J. (2011). *The third industrial revolution: how lateral power is transforming energy, the economy, and the world*. Macmillan.
- Roberson, D. A., Torrado Perez, A. R., Shemelya, C. M., Rivera, A., MacDonald, E., & Wicker, R. B. (2015). Comparison of stress concentrator fabrication for 3D printed polymeric izod impact test specimens. *Additive Manufacturing*, 7, 1–11. <https://doi.org/10.1016/j.addma.2015.05.002>
- Rodrigo Corbaton, C., Fernández-Vicente, M., & Conejero, A. (2016). Design and 3d printing of custom-fit products with free online software and low cost technologies. A study of viability for product design student projects. *10th International Technology, Education and Development Conference (INTED2016 Proceedings)*, 3906–3910. <https://doi.org/10.21125/inted.2016.1955>
- Fischer, X., & Nadeau, J.-P. (2011). Research in Interactive Design Vol. 3. In X. Fischer & J.-P. Nadeau (Eds.), *IDMME-Virtual Concept Research in Interactive Design Vol. 3*. Springer Paris. <https://doi.org/10.1007/978-2-8178-0169-8>
- Rodriguez, J. F., Thomas, J. P., & Renaud, J. E. (2000). Characterization of the mesostructure of fused-deposition acrylonitrile-butadiene-styrene materials. *Rapid Prototyping Journal*, 6(3), 175–186. <https://doi.org/10.1108/13552540010337056>
- Rodríguez, J. F., Thomas, J. P., & Renaud, J. E. (2001). Mechanical behavior of acrylonitrile butadiene styrene (ABS) fused deposition materials. Experimental investigation. *Rapid Prototyping Journal*, 7(3), 148–158. <https://doi.org/10.1108/13552540110395547>
- Rodríguez, J. F., Thomas, J. P., & Renaud, J. E. (2003). Mechanical behavior of acrylonitrile butadiene styrene fused deposition materials modeling. *Rapid Prototyping Journal*, 9(4), 219–230. <https://doi.org/10.1108/13552540310489604>
- Rodríguez-Panes, A., Claver, J., & Camacho, A. M. (2018). The influence of manufacturing parameters on the mechanical behaviour of PLA and ABS pieces manufactured by FDM: A comparative analysis. *Materials*, 11(8), 1333. <https://doi.org/10.3390/ma11081333>
- Romani, A., Mantelli, A., Tralli, P., Turri, S., Levi, M., & Suriano, R. (2021). Metallization of Thermoplastic Polymers and Composites 3D Printed by Fused Filament Fabrication. *Technologies*, 9(3), 49. <https://doi.org/10.3390/technologies9030049>
- Rosales, S., Ferrándiz, S., Reig, M. J., & Seguí, J. (2017). Study of soluble supports generation in 3d printed part. *Procedia Manufacturing*, 13, 833–839. <https://doi.org/10.1016/j.promfg.2017.09.188>
- Rosato, D. v., Rosato, D. v., & Rosato, M. G. (2000). Fundamentals of Designing Products. In *Injection Molding Handbook* (pp. 415–478). Springer US. [https://doi.org/10.1007/978-1-4615-4597-2\\_5](https://doi.org/10.1007/978-1-4615-4597-2_5)
- Rosen, D. W. (2007). Design for additive manufacturing: a method to explore unexplored regions of the design space. *Solid Freeform Fabrication Symposium Proceedings 2007*.
- Rosen, D. W., Seepersad, C. C., Simpson, T. W., & Williams, C. B. (2015). Special Issue: Design for Additive Manufacturing: A Paradigm Shift in Design, Fabrication, and Qualification. *Journal of Mechanical Design*, 137(11), 110301. <https://doi.org/10.1115/1.4031470>
- Roxas, M. (2008). *Fluid dynamics analysis of desktop-based fused deposition modeling rapid prototyping*. University of Toronto.
- Royeen, L. (2015). The style evolution of glasses: acknowledging well-being for wearable medical device. *The Open Journal of Occupational Therapy*, 3(4), 12. <https://doi.org/10.15453/2168-6408.1224>
- Rupal, B. S., Ahmad, R., & Qureshi, A. J. (2018). Feature-Based Methodology for Design of Geometric Benchmark Test Artifacts for Additive Manufacturing Processes. *Procedia CIRP*, 70, 84–89. <https://doi.org/10.1016/J.PROCIR.2018.02.012>
- Sabourin, E., Houser, S. A., & Bøhn, J. H. (1996). Adaptive slicing using stepwise uniform refinement. *Rapid Prototyping Journal*, 2(4), 20–

26.  
<https://doi.org/10.1108/13552549610153370>
- Sachs, E. M., Hadjiloucas, C., Allen, S., & Yoo, H. J. (2003). *Metal and ceramic containing parts produced from powder using binders derived from salt* (Patent No. 6,508,980). USPTO.
- Sachs, E. M., Haggerty, J. S., Cima, M. J., & Williams, P. A. (1989). *Three-dimensional printing techniques* (Patent No. US5204055). US Patent Office.
- Sadoski, M., Goetz, E. T., & Fritz, J. B. (1993). Impact of Concreteness on Comprehensibility, Interest, and Memory for Text: Implications for Dual Coding Theory and Text Design. *Journal of Educational Psychology*, 85(2), 291–304.  
<https://doi.org/10.1037/0022-0663.85.2.291>
- Sanabria Aguirre, J. G. (2016). *Estudio del acabado superficial en piezas fabricadas por deposición fundida tras ser sometidas a un baño de acetona* [Universitat Politècnica de València].  
<https://riUNET.upv.es/handle/10251/62249>
- Sanchez, C., Boudaoud, Muller, & Camargo. (2014). Towards a standard experimental protocol for open source additive manufacturing. *Virtual and Physical Prototyping*, 9(3), 151–167.  
<http://www.tandfonline.com/doi/abs/10.1080/17452759.2014.919553>
- Sass, L., & Oxman, R. (2006). Materializing design: the implications of rapid prototyping in digital design. *Digital Design Digital Design*, 27(3), 325–355.  
<https://doi.org/10.1016/j.destud.2005.11.009>
- Schmidt, R., & Umetani, N. (2014). Branching support structures for 3D printing. *ACM SIGGRAPH 2014 Studio on - SIGGRAPH '14*, 1–1.  
<https://doi.org/10.1145/2619195.2656293>
- Schneider, S. (2019). *Vibratory Tumbling 3D Printed Plastic and Metal Parts | Kramer Industries, Inc.*  
<https://www.kramerindustriesonline.com/tumbling-3d-printed-plastic-parts/>
- Seepersad, C. C., Govett, T., Kim, K., Lundin, M., & Pinerio, D. (2012). A designer's guide for dimensioning and tolerancing SLS parts. *Solid Freeform Fabrication Symposium*.  
<http://sffsymposium.engr.utexas.edu/Manuscripts/2012/2012-70-Seepersad.pdf>
- Sells, E., Smith, Z., Bailard, S., Bowyer, A., & Olliver, V. (2010). RepRap: The Replicating Rapid Prototyper: Maximizing Customizability by Breeding the Means of Production. *Handbook of Research in Mass Customization and Personalization, Forthcoming*.  
<http://papers.ssrn.com/abstract=1594475>
- Sever, P., Drstvensek, I., Campbell, R., & Maidin, S. (2009). Design for rapid manufacturing – capturing designers' knowledge. In *Innovative Developments in Design and Manufacturing*. CRC Press.  
<https://doi.org/10.1201/9780203859476.ch48>
- Sher, D. (2015, June). Bracing for a Revolution, Exovite Envisions a Connected 3D Printed Splint. *3dprintingindustry.Com*.
- Shofner, M. L., Lozano, K., Rodríguez-Macías, F. J., & Barrera, E. v. (2003). Nanofiber-reinforced polymers prepared by fused deposition modeling. *Journal of Applied Polymer Science*, 89(11), 3081–3090.  
<https://doi.org/10.1002/app.12496>
- Sinclair, M. (2012). *The specification of a consumer design toolkit to support personalised production via additive manufacturing*.  
<https://dSPACE.lboro.ac.uk/dspace-jspui/handle/2134/11051>
- Singh, R., & Singh, M. (2015). Surface roughness improvement of cast components in vacuum moulding by intermediate barrel finishing of fused deposition modelling patterns: *Proceedings of the Institution of Mechanical Engineers, Part E: Journal of Process Mechanical Engineering*, 231(2), 309–316.  
<https://doi.org/10.1177/0954408915595576>
- Singh, S., Singh, M., Prakash, C., Gupta, M. K., Mia, M., & Singh, R. (2019). Optimization and reliability analysis to improve surface quality and mechanical characteristics of heat-treated fused filament fabricated parts. *The International Journal of Advanced Manufacturing Technology* 2019 102:5, 102(5), 1521–1536.  
<https://doi.org/10.1007/S00170-018-03276-8>
- Singh, S., & Singh, R. (2016). Effect of annealing on surface roughness of additively manufactured plastic parts: A case study. *Proceedings of the National Conference on Production Engineering (COPE-2016), Guru Nanak Dev Engineering College, Ludhiana, India*, 7–8.
- Sinha, S., Chen, H. E., Meisel, N. A., & Miller, S. R. (2017). Does designing for additive manufacturing help us be more creative? an exploration in engineering design education.

- Proceedings of the ASME Design Engineering Technical Conference*, 3.  
<https://doi.org/10.1115/DETC2017-68274>
- Sio, U. N., Kotovsky, K., & Cagan, J. (2015). Fixation or inspiration? A meta-analytic review of the role of examples on design processes. *Design Studies*, 39, 70–99.  
<https://doi.org/10.1016/j.DESTUD.2015.04.004>
- Smith, A. G., Hielscher, S., Dickel, S., Soderberg, J., & van Oost, E. (2013). Grassroots Digital Fabrication and Makerspaces: Reconfiguring, Relocating and Recalibrating Innovation? *SSRN Electronic Journal*.  
<https://doi.org/10.2139/ssrn.2731835>
- Smith, Z. (2008). *RepRap: Blog: Announcing Thingiverse.com*.  
<http://blog.reprap.org/2008/11/announcing-thingiversecom.html?showComment=1227090960000>
- Smyth, C. T. (2015). *Functional Design for 3D Printing: Designing 3d printed things for everyday use*. Clifford Smyth.
- Solon, O. (2013). *Digital fabrication is so much more than 3D printing*. Wired Magazine.  
<http://www.wired.co.uk/article/digital-fabrication>
- Sood, A. K., Ohdar, R. K., & Mahapatra, S. S. (2010). Parametric appraisal of mechanical property of fused deposition modelling processed parts. *Materials & Design*, 31(1), 287–295.  
<https://doi.org/10.1016/j.matdes.2009.06.016>
- Sood, A. K., Ohdar, R. K., & Mahapatra, S. S. (2012). Experimental investigation and empirical modelling of FDM process for compressive strength improvement. *Journal of Advanced Research*, 3(1), 81–90.  
<https://doi.org/10.1016/j.jare.2011.05.001>
- Sossou, G., Demoly, F., Montavon, G., & Gomes, S. (2018). An additive manufacturing oriented design approach to mechanical assemblies. *Journal of Computational Design and Engineering*, 5(1), 3–18.  
<https://doi.org/10.1016/j.jcde.2017.11.005>
- Spiller, Q., & Fleischer, J. (2018). Additive manufacturing of metal components with the ARBURG plastic freeforming process. *CIRP Annals*, 67(1), 225–228.  
<https://doi.org/10.1016/j.cirp.2018.04.104>
- Stoll, H. W. (1986). Design for manufacture: An overview. *Applied Mechanics Reviews*, 39(9), 1359–1364.  
<https://doi.org/10.1115/1.3149526>
- Stratasys. (2010). *Stratasys (SSYS) - Description of business*.  
<http://www.hotstocked.com/companies/s/stratasys-SSYS-description-56002.html>
- Stratasys. (2014). *Comparison of Sealing Methods for FDM Materials*. [https://www.stratasys.com/-/media/files/education-f123/tags/tag\\_fdm\\_sealing\\_en\\_1015\\_web.pdf](https://www.stratasys.com/-/media/files/education-f123/tags/tag_fdm_sealing_en_1015_web.pdf)
- Stratasys. (2015a). *Embedding Hardware*.  
[https://www.stratasys.com/-/media/files/Best-Practices/BP\\_FDM\\_EmbeddingHardware\\_1115](https://www.stratasys.com/-/media/files/Best-Practices/BP_FDM_EmbeddingHardware_1115)
- Stratasys. (2015b). *Inserting Hardware Post-Build*.  
[https://www.stratasys.com/-/media/files/Best-Practices/BP\\_FDM\\_InsertingHardwarePostBuild\\_1115](https://www.stratasys.com/-/media/files/Best-Practices/BP_FDM_InsertingHardwarePostBuild_1115)
- Stratasys. (2017a). *Composite Tooling Design Guide*.  
<https://www.stratasys.com/campaign/resource-guide/composite-tooling>
- Stratasys. (2017b). *ULTEM 9085. Production-Grade Thermoplastic for Fortus 3D Printers: Technical Report*.
- Stratasys Co. (2013). *Technical application guide: FDM for End-Use Parts*.  
<http://usglobalimages.stratasys.com/Main/Secure/Applications/End Use Parts/SSYS-TAG-End-UseParts-11-13.pdf>
- Stratasys Direct. (2015). *Fused Deposition Modeling (FDM) Design Guidelines*.  
<https://www.stratasysdirect.com/resources/design-guidelines/fused-deposition-modeling>
- Stratasys Ltd. (n.d.). *PolyJet Technology*. Retrieved September 2, 2016, from <http://www.stratasys.com/3d-printers/technologies/polyjet-technology>
- Strömshed, E. (2016). *The Perfect Fit - Development process for the use of 3D technology in the manufacturing of custom-made prosthetic arm sockets*. <http://lup.lub.lu.se/student-papers/record/8875364>
- Stucker, B. E., & Janaki Ram, G. D. (2007). Layer-based additive manufacturing technologies. In J. R. Groza, J. F. Shackelford, E. J. Lavernia, & M. T.



- Powers (Eds.), *CRC materials processing handbook* (pp. 21–26). CRC Press.
- Studio Fathom. (2014). *3D Printer Cast, Advanced 3D Printing - Studio Fathom Cast Project*. <http://studiofathom.com/hashcast/>
- Suder, J., Vocetka, M., Kot, T., Fojtík, F., & Fusek, M. (2020). Testing of glued joints on plastic parts manufactured using FFF technology. *Acta Polytechnica*, *60*(6). <https://doi.org/10.14311/AP.2020.60.0512>
- Sun, Q., Rizvi, G. M., Bellehumeur, C. T., & Gu, P. (2008). Effect of processing conditions on the bonding quality of FDM polymer filaments. *Rapid Prototyping Journal*, *14*(2), 72–80. <https://doi.org/10.1108/13552540810862028>
- Surendran, N. K., Xu, X. W., Stead, O., & Silyn-Roberts, H. (2009). Contemporary technologies for 3D digitization of Maori and Pacific Island artifacts. *International Journal of Imaging Systems and Technology*, *19*(3), 244–259.
- Swanson, W. J., Turley, P. W., Leavitt, P. J., Karwoski, P. J., Labossiere, J. E., & Skubic, R. L. (2004). *High temperature modeling apparatus* (Patent No. US6722872B1). <https://patents.google.com/patent/US6722872B1/en>
- Swift, K. G., & Booker, J. D. (2013a). Guidelines for Design for Manufacture (DFM). In *Manufacturing Process Selection Handbook* (pp. 411–417). Elsevier. <https://doi.org/10.1016/B978-0-08-099360-7.15001-3>
- Swift, K. G., & Booker, J. D. (2013b). Manufacturing Process Selection Handbook. In *Manufacturing Process Selection Handbook*. Elsevier. <https://doi.org/10.1016/C2011-0-07343-X>
- Tamburrino, F., Barone, S., Paoli, A., & Rationale, A. v. (2021). Post-processing treatments to enhance additively manufactured polymeric parts: a review. *Virtual and Physical Prototyping*, *16*(2), 221–254. <https://doi.org/10.1080/17452759.2021.1917039>
- Tang, Y., Yang, S., & Zhao, Y. F. (2016). Sustainable Design for Additive Manufacturing Through Functionality Integration and Part Consolidation. *Handbook of Sustainability in Additive Manufacturing*, *1*, 101–144.
- Tanikella, N. G., Wittbrodt, B., & Pearce, J. M. (2017). Tensile strength of commercial polymer materials for fused filament fabrication 3D printing. *Additive Manufacturing*, *15*, 40–47. <https://doi.org/10.1016/j.addma.2017.03.005>
- Tapscott, D., & Williams, A. D. (2008). *Wikinomics: How mass collaboration changes everything*. Penguin Publishing Group.
- Taşdemir, V. (2021). Investigation of Dimensional Integrity and Surface Quality of Different Thin-Walled Geometric Parts Produced via Fused Deposition Modeling 3D Printing. *Journal of Materials Engineering and Performance* *2021* *30*:5, *30*(5), 3381–3387. <https://doi.org/10.1007/S11665-021-05809-X>
- Teich, M., & Porter, R. (1996). *The industrial revolution in national context: Europe and the USA*. Cambridge University Press.
- Thingiverse. (n.d.). *Thingiverse - Digital Designs for Physical Objects*. Retrieved July 5, 2016, from <http://www.thingiverse.com/about/>
- Thomas, D. (2009). The development of design rules for selective laser melting. In *The development of design rules for selective laser melting*. University of Wales.
- Thompson, M. K., Moroni, G., Vaneker, T., Fadel, G., Campbell, R. I., Gibson, I., Bernard, A., Schulz, J., Graf, P., Ahuja, B., & Martina, F. (2016). Design for Additive Manufacturing: Trends, opportunities, considerations, and constraints. *CIRP Annals - Manufacturing Technology*, *65*(2), 737–760. <https://doi.org/10.1016/j.cirp.2016.05.004>
- Tiwary, V. K., P. A., & Malik, V. R. (2021). An overview on joining/welding as post-processing technique to circumvent the build volume limitation of an FDM-3D printer. *Rapid Prototyping Journal*, *27*(4), 808–821. <https://doi.org/10.1108/RPJ-10-2020-0265>
- Tiwary, V. K., Ravi, N. J., Arunkumar, P., Shivakumar, S., Deshpande, A. S., & Malik, V. R. (2020). Investigations on friction stir joining of 3D printed parts to overcome bed size limitation and enhance joint quality for unmanned aircraft systems. *Proceedings of the Institution of Mechanical Engineers, Part C: Journal of Mechanical Engineering Science*, *234*(24), 4857–4871. <https://doi.org/10.1177/0954406220930049>

- Torrado, A. R., & Roberson, D. A. (2016). Failure Analysis and Anisotropy Evaluation of 3D-Printed Tensile Test Specimens of Different Geometries and Print Raster Patterns. *Journal of Failure Analysis and Prevention*, 16(1), 154–164. <https://doi.org/10.1007/s11668-016-0067-4>
- Torres, J., Cotelo, J., Karl, J., & Gordon, A. P. (2015). Mechanical Property Optimization of FDM PLA in Shear with Multiple Objectives. *JOM 2015* 67:5, 67(5), 1183–1193. <https://doi.org/10.1007/S11837-015-1367-Y>
- Tosto, C., Tirillò, J., Sarasini, F., & Cicala, G. (2021). Hybrid metal/polymer filaments for fused filament fabrication (FFF) to print metal parts. *Applied Sciences (Switzerland)*, 11(4), 1444. <https://doi.org/10.3390/app11041444>
- Townsend, V., & Urbanic, R. J. (2011). A Systems Approach to Hybrid Design: Fused Deposition Modeling and CNC Machining. In *Global Product Development* (pp. 711–720). Springer Berlin Heidelberg. [https://doi.org/10.1007/978-3-642-15973-2\\_72](https://doi.org/10.1007/978-3-642-15973-2_72)
- Trentesous. (2018). *Tripod Folding Version 2 by trentesous - Thingiverse*. Thingiverse. <https://www.thingiverse.com/thing:2862445>
- Troughton, M. J. (2008). Handbook of Plastics Joining: A Practical Guide. In A. William (Ed.), *Handbook of Plastics Joining: A Practical Guide* (2nd ed.). TWI.
- Troxler, P. (2010, October 8). Commons-Based Peer-Production of Physical Goods: Is There Room for a Hybrid Innovation Ecology? *3rd Free Culture Research Conference*. <https://doi.org/10.2139/ssrn.1692617>
- Tsouknidas, A., Pantazopoulos, M., Katsoulis, I., Fasinakis, D., Maropoulos, S., & Michailidis, N. (2016). Impact absorption capacity of 3D-printed components fabricated by fused deposition modelling. *Materials & Design*, 102(15), 41–44. <https://doi.org/10.1016/j.matdes.2016.03.154>
- Turner, & Gold. (2015). A review of melt extrusion additive manufacturing processes: II. Materials, dimensional accuracy, and surface roughness. *Rapid Prototyping Journal*, 21(3), 250–261. <http://www.emeraldinsight.com/doi/abs/10.1108/RPJ-02-2013-0017>
- Turner, N., Strong, & Gold, A. (2014). A review of melt extrusion additive manufacturing processes: I. Process design and modeling. *Rapid Prototyping Journal*, 20(3), 192–204. <http://www.emeraldinsight.com/doi/abs/10.1108/RPJ-01-2013-0012>
- Tymrak, B. M., Kreiger, M., & Pearce, J. M. (2014). Mechanical properties of components fabricated with open-source 3-D printers under realistic environmental conditions. *Materials & Design*, 58, 242–246. <https://doi.org/10.1016/j.matdes.2014.02.038>
- UK, D. C. (2019). The Design Process: What is the Double Diamond? *Design Council*.
- UK's MHRA. (n.d.). *3D printing (additive manufacturing) of medical devices or component parts during the coronavirus (COVID-19) pandemic - GOV.UK*. Retrieved July 22, 2021, from <https://www.gov.uk/guidance/3d-printing-additive-manufacturing-of-medical-devices-or-component-parts-during-the-coronavirus-covid-19-pandemic>
- Ulrich, K. T. (2003). *Product design and development*. Tata McGraw-Hill Education.
- Ultimaker. (n.d.). *Using glue | Professional 3D printing made accessible*. Retrieved October 20, 2019, from <https://ultimaker.com/en/resources/16968-using-glue>
- U.S. NIH & FDA. (n.d.). *COVID 3D TRUST: Trusted Repository for Users and Suppliers through Testing*. Retrieved July 22, 2021, from <https://3dprint.nih.gov/collections/covid-19-response>
- Valerga, A. P., Batista, M., Fernandez-Vidal, S. R., & Gamez, A. J. (2019). Impact of Chemical Post-Processing in Fused Deposition Modelling (FDM) on Polylactic Acid (PLA) Surface Quality and Structure. *Polymers 2019, Vol. 11, Page 566*, 11(3), 566. <https://doi.org/10.3390/POLYM11030566>
- Valjak, F., & Bojčetić, N. (2019). Conception of design principles for additive manufacturing. *Proceedings of the International Conference on Engineering Design, ICED, 2019-August*. <https://doi.org/10.1017/dsi.2019.73>
- Vanek, J., Galicia, J. A. G., & Benes, B. (2014). Clever Support: Efficient Support Structure Generation for Digital Fabrication. *Computer Graphics Forum*, 33(5), 117–125. <https://doi.org/10.1111/CGF.12437>

- van Holm, E. J. (2012). What are Makerspaces, Hackerspaces, and Fab Labs? *SSRN Electronic Journal*. <https://doi.org/10.2139/ssrn.2548211>
- Vayre, B., Vignat, F., & Villeneuve, F. (2012). Designing for Additive Manufacturing. *Procedia CIRP*, 3, 632–637. <https://doi.org/10.1016/j.procir.2012.07.108>
- Veehof, M. M., Taal, E., Willems, M. J., & van de Laar, M. A. F. J. (2008). Determinants of the use of wrist working splints in rheumatoid arthritis. *Arthritis & Rheumatism*, 59(4), 531–536. <https://doi.org/10.1002/art.23531>
- Vicente, C., Fernandes, J., Deus, A., Vaz, M., Leite, M., & Reis, L. (2019). Effect of protective coatings on the water absorption and mechanical properties of 3D printed PLA. *Frattura Ed Integrità Strutturale*, 13(48), 748–756. <https://doi.org/10.3221/IGF-ESIS.48.68>
- Viseur, R. (2012). From Open Source Software to Open Source Hardware. In I. Hammouda, B. Lundell, T. Mikkonen, & W. Scacchi (Eds.), *Open Source Systems: Long-Term Sustainability* (Vol. 378, pp. 286–291). Springer Boston. [https://doi.org/10.1007/978-3-642-33442-9\\_23](https://doi.org/10.1007/978-3-642-33442-9_23)
- von Hippel, E. A. (2005). *Democratizing innovation*. MIT Press.
- von Krogh, G., & von Hippel, E. (2006). The Promise of Research on Open Source Software. *Management Science*, 52(7), 975–983. <https://doi.org/10.1287/mnsc.1060.0560>
- Voodoo Manufacturing. (n.d.). *Voodoo Manufacturing: Fast, Affordable, High-Volume 3D Printing*. Retrieved July 4, 2016, from <https://www.voodoomfg.com/>
- Wachsmuth, J. P. (2008). Multiple Independent Extrusion Heads for Fused Deposition Modeling. In *Mechanical Engineering: Vol. Master of*.
- Wang, T.-M., Xi, J.-T., & Jin, Y. (2007). A model research for prototype warp deformation in the FDM process. *The International Journal of Advanced Manufacturing Technology*, 33(11–12), 1087–1096. <https://doi.org/10.1007/s00170-006-0556-9>
- WASP. (2015). *WASP collaborates with Rizzoli's Orthopedic Institute*. <http://www.wasproject.it/w/en/wasp-collaborates-with-rizzolis-orthopedic-institute/>
- Weiss, S., LaStayo, P., Mills, A., & Bramlet, D. (2004). Splinting the degenerative basal joint: Custom-made or prefabricated neoprene? *Journal of Hand Therapy*, 17(4), 401–406. <https://doi.org/10.1197/j.jht.2004.07.002>
- Wei, Y., Chen, Y., Yang, Y., & Li, Y. (2016). Novel design and 3-D printing of nonassembly controllable pneumatic robots. *IEEE/ASME Transactions on Mechatronics*, 21(2), 649–659. <https://doi.org/10.1109/TMECH.2015.2492623>
- Wellborn, W. W. (1995). Fundamentals of mass finishing. *Products Finishing (Cincinnati)*, 60(3).
- White, J., Tenore, C., Pavich, A., Scherzer, R., & Stagon, S. (2018). Environmentally benign metallization of material extrusion technology 3D printed acrylonitrile butadiene styrene parts using physical vapor deposition. *Additive Manufacturing*, 22, 279–285. <https://doi.org/10.1016/j.addma.2018.05.016>
- Wickramasinghe, S., Do, T., & Tran, P. (2020). FDM-Based 3D printing of polymer and associated composite: A review on mechanical properties, defects and treatments. *Polymers*, 12(7), 1529. <https://doi.org/10.3390/polym12071529>
- Willème, F. (1864). *Photo-sculpture* (Patent No. US43822). US Patent Office. <https://patents.google.com/patent/US43822A/en?q=photographing+sculpture&before=priority:18650101>
- Wilson, J. M., Piya, C., Shin, Y. C., Zhao, F., & Ramani, K. (2014). Remanufacturing of turbine blades by laser direct deposition with its energy and environmental impact analysis. *Journal of Cleaner Production*, 80, 170–178. <https://doi.org/10.1016/j.jclepro.2014.05.084>
- Wittbrodt, B., & Pearce, J. M. (2015). The Effects of PLA Color on Material Properties of 3-D Printed Components. *Additive Manufacturing*, 8, 110–116. <https://doi.org/10.1016/j.addma.2015.09.006>
- Wittbrodt, B. T., Glover, A. G., Laureto, J., Anzalone, G. C., Oppliger, D., Irwin, J. L., & Pearce, J. M. (2013). Life-cycle economic analysis of distributed manufacturing with open-source 3-D printers. *Mechatronics*, 23(6), 713–726. <https://doi.org/10.1016/j.mechatronics.2013.06.002>
- Wohlers, T. (2015). *Wohlers Report 2015*.

- Wohlers, T. (2016a). *Popularity of FDM*. Wohlers Talk. <http://wohlersassociates.com/blog/2016/01/popularity-of-fdm/>
- Wohlers, T. (2016b). *Wohlers Associates Publishes 20th Anniversary Edition of Its 3D Printing and Additive Manufacturing Industry Report*. <http://wohlersassociates.com/press71.html>
- Wohlers, T., & Caffrey, T. (2015). *Wohlers Report 2015: 3D Printing and Additive Manufacturing State of the Industry Annual Worldwide Progress Report*. Wohlers Associates.
- Wong, Y. S., Fuh, J. Y. H., Loh, H. T., & Mahesh, M. (2002). Rapid prototyping and manufacturing (RP&M) benchmarking. In *Software Solutions for RP* (pp. 57–94). PEP Ltd, UK.
- Wu, W., Jiang, J., Jiang, H., Liu, W., Li, G., Wang, B., Tang, M., & Zhao, J. (2018). Improving bending and dynamic mechanics performance of 3D printing through ultrasonic strengthening. *Materials Letters*, 220, 317–320. <https://doi.org/10.1016/j.matlet.2018.03.048>
- Xu, Y., Unkovskiy, A., Klaua, F., Rupp, F., Geis-Gerstorfer, J., & Spintzyk, S. (2018). Compatibility of a silicone impression/adhesive system to FDM-printed tray materials—a laboratory peel-off study. *Materials*, 11(10). <https://doi.org/10.3390/ma11101905>
- Yaman, U. (2018). Shrinkage compensation of holes via shrinkage of interior structure in FDM process. *International Journal of Advanced Manufacturing Technology*, 94(5–8), 2187–2197. <https://doi.org/10.1007/s00170-017-1018-2>
- Yang, L., & Anam, M. A. (2014). An investigation of standard test part design for additive manufacturing. *International Solid Freeform Fabrication Symposium*, 901–922.
- Yang, M. C. (2005). A study of prototypes, design activity, and design outcome. *Design Studies*, 26(6), 649–669. <https://doi.org/10.1016/j.destud.2005.04.005>
- Yang, S., Tang, Y., & Zhao, Y. F. (2015). A new part consolidation method to embrace the design freedom of additive manufacturing. *Journal of Manufacturing Processes*, 20, 444–449. <https://doi.org/10.1016/j.jmapro.2015.06.024>
- Yap, Y. L., Toh, W., Koneru, R., Lin, R., Chan, K. I., Guang, H., Chan, W. Y. B., Teong, S. S., Zheng, G., & Ng, T. Y. (2020). Evaluation of structural epoxy and cyanoacrylate adhesives on jointed 3D printed polymeric materials. *International Journal of Adhesion and Adhesives*, 100, 102602. <https://doi.org/10.1016/j.ijadhadh.2020.102602>
- Yilmaz, S., Christian, J. L., Daly, S. R., Seifert, C., & Gonzalez, R. (2012). How Do Design Heuristics Affects Outcomes? In *DS 70: Proceedings of DESIGN 2012, the 12th International Design Conference, Dubrovnik, Croatia*. <https://www.designsociety.org/publication/32088/HOW+DO+DESIGN+HEURISTICS+AFFECTS+OUTCOMES%3F>
- Zagidullin, R., Antipov, D., Dmitriev, A., & Zezin, N. (2021). Development of a methodology for eliminating failures of an FDM 3D printer using a “failure tree” and FMEA analysis. *Journal of Physics: Conference Series*, 1925(1). <https://doi.org/10.1088/1742-6596/1925/1/012085>
- Zdravprint. (n.d.). *Zdravprint. Orthoses, 3D models, 3D Printing*. Zdravprint.Ru. Retrieved July 4, 2016, from <http://zdravprint.ru/>
- Zhang, W., Doherty, M., Leeb, B. F., Alekseeva, L., Arden, N. K., Bijlsma, J. W., Dinçer, F., Dziedzic, K., Häuselmann, H. J., & Herrero-Beaumont, G. (2007). EULAR evidence based recommendations for the management of hand osteoarthritis: report of a Task Force of the EULAR Standing Committee for International Clinical Studies Including Therapeutics (ESCISIT). *Annals of the Rheumatic Diseases*, 66(3), 377–388.
- Zhang, Y., & Chou, K. (2008). A parametric study of part distortions in fused deposition modelling using three-dimensional finite element analysis. *Proceedings of the Institution of Mechanical Engineers, Part B: Journal of Engineering Manufacture*, 222(8), 959–968. <https://doi.org/10.1243/09544054JEM990>
- Zhou, Q., Panetta, J., & Zorin, D. (2013). Worst-case structural analysis. *ACM Transactions on Graphics*, 32(4). <https://doi.org/10.1145/2461912.2461967>
- Zhu, J., Chen, J. L., Lade, R. K., Suszynski, W. J., & Francis, L. F. (2015). Water-based coatings for 3D printed parts. *Journal of Coatings Technology and Research*, 12(5), 889–897. <https://doi.org/10.1007/s11998-015-9710-3>

- Ziemian, C. W., Sharma, M. M., & Ziemian, S. N. (2012). Anisotropic Mechanical Properties of ABS Parts Fabricated by Fused Deposition Modelling. In M. Gokcek (Ed.), *Mechanical Engineering* (pp. 159–180). InTech. <https://doi.org/10.5772/34233>
- Ziemian, S., Okwara, M., & Ziemian, C. W. (2015). Tensile and fatigue behavior of layered acrylonitrile butadiene styrene. *Rapid Prototyping Journal*, 21(3), 270–278.
- Zinniel, R. L. (2009). *Surface-treatment method for rapid-manufactured three-dimensional objects*.
- Zortrax. (n.d.). *Platform Maintenance of Zortrax M200 3D Printer | Zortrax Support Center*. Retrieved October 20, 2019, from <https://support.zortrax.com/m200-platform-maintenance/>



# Appendix

In this printed version, the *Design for Additive Manufacturing with desktop 3D printing* toolkit guide, the *AM design ideation cards*, the benchmarking geometries and the *DfAM for FFF worksheet* are provided separately.

These can also be found in:

<p>Toolkit guide</p>  <p><a href="https://bit.ly/DfAMtool">https://bit.ly/DfAMtool</a></p>	<p>Ideation cards</p>  <p><a href="https://bit.ly/AMdesignCards">https://bit.ly/AMdesignCards</a></p>
<p>Benchmarking geometries</p>  <p><a href="https://bit.ly/FFFbench">https://bit.ly/FFFbench</a></p>	<p>Worksheet</p>  <p><a href="https://bit.ly/DfFFFsheet">https://bit.ly/DfFFFsheet</a></p>